Sample Entropy as a tool for quantifying human gait complexity: the effect of age and walking velocity

Jeroen P. Vermeulen
Delft University of Technology, Biomedical Engineering

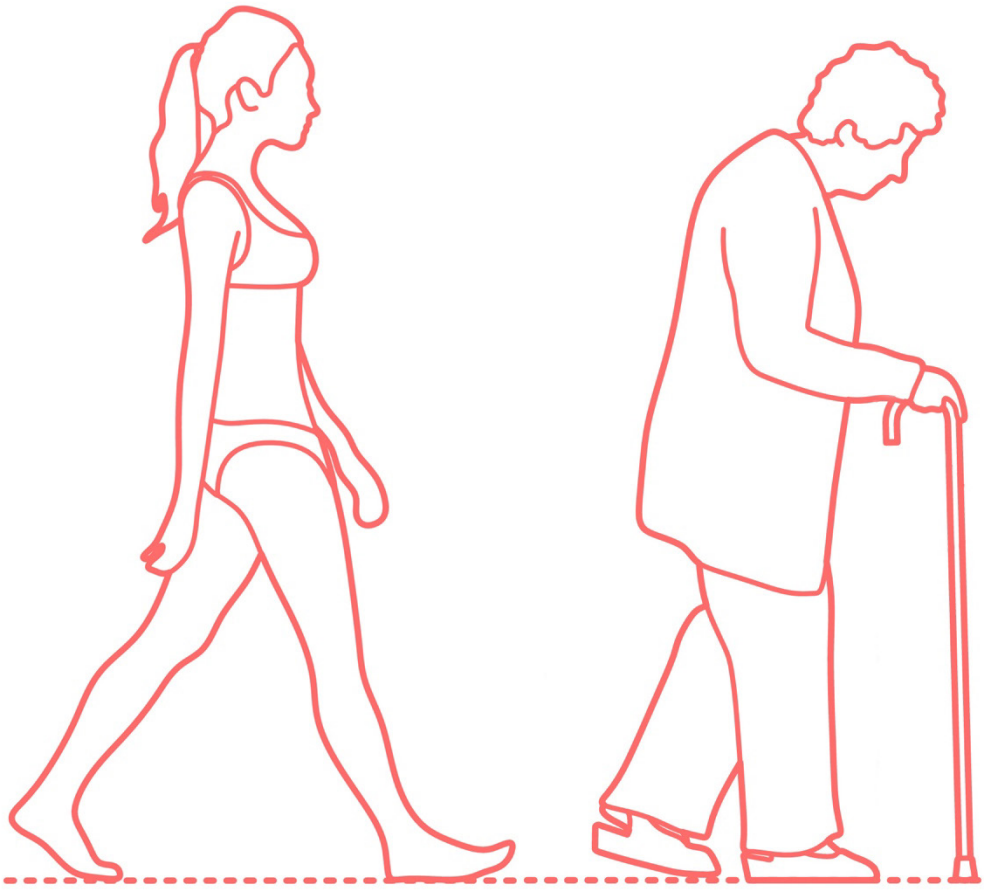

TU Delft

LUMC Leids Universitair Medisch Centrum

VUmc

Sample entropy as a tool for quantifying human gait complexity: the effect of age and walking velocity

Jeroen P. Vermeulen
Delft University of Technology, Biomedical Engineering

To obtain the Master of Science degree in Biomedical Engineering
at Delft University of Technology

Supervisors

Dr.ir. Alfred Schouten,	TUDelft
Dr.ir. Winfred Mugge,	TUDelft
Dr.ir. Jurriaan de Groot,	LUMC
Dr. Marjon Stijntjes,	LUMC

Dataset

MSc. Marjolein Booij,	VUmc

January 2020

Preface

The first part of my master thesis project started at the onset of May 2019, I started exploring my topics of interest. I was unsure about the focus of my master thesis project, until I visited Alfred Schouten and Winfred Mugge. Here, I gained interest in researching a topic that involved signal analysis. Alfred and Winfred introduced me to a few possible subjects for my research. As a result, I chose to do a literature study on the topic of Long Latency Reflex modulation. Thirteen weeks later, I was satisfied with my literature study results. I handed in my work and received a positive response of Alfred and Winfred. This motivated me for the rest of the research period that was about to follow.

Next, I started my internship at the Leiden University Medical Center (LUMC). Here, I was supervised by Jurriaan de Groot and Marjon Stijntjes. Jurriaan introduced me to shoulder kinematics research that portrayed *entropy* as sensitive measure to quantify changes with age (Overbeek et al., 2020). Subsequently, rehabilitation medicine proposed signal entropy may be a useful ambulatory biomarker as predictor for functional decline. When I was introduced to this topic, I explored some of the original studies that introduced entropy algorithms to medical data (Lipsitz et al., 1992; Pincus et al., 1991a; Pincus et al., 1994; Pincus et al., 1996). I discovered neurology research that portrayed entropy algorithms as a possible useful tool for detecting early onset of dementia (Bertrand et al., 2016). Consecutively, I wanted to make my own contribution by researching the application of *entropy* in human gait data. Therefore, I conducted an additional literature study on the topic of entropy algorithms in medical data.

After finishing the literature study, I proposed to research entropy in gait data of healthy patients versus Parkinson's patients. These patients would walk at different walking velocities, to expose complexity changes with walking velocity and with disease in electromyography (EMG) and accelerometry data. Results would indicate if signal entropy was a convenient measure for healthy gait function. Consecutively, after a discussion with Alfred and Winfred, we adjusted this proposal. We discussed to research the algorithm in EMG and accelerometry data of young versus old healthy subjects. Here, the entropy algorithm could quantify complexity changes with age and with walking velocity. We proposed to assess the effects of age and of walking velocity, since both independent variables were known to alter gait function (Bisi et al., 2016; Hamill et al., 199; Kang et al., 2008)

In March 2020, I applied to the Human Research Ethical Committee (HREC) of the TUDelft and my research proposal got approved. However, the approval coincided with the onset of COVID-19 in the Netherlands. As a result, we had to make an alternative plan for my research. Together with Jurriaan de Groot and Marjon Stijntjes, we approached a PhD student of the Amsterdam VU University Medical Center (VUmc), Marjolein Booij. Marjolein recorded data of young and old subjects that performed asymmetrical step tasks on a treadmill. The recorded data included EMGs, ground reaction forces (GRFs) and joint angles (GAs). We concluded that this dataset would be suitable for my proposed research. Finally, in the second week of June 2020, I received Marjolein's data and I started my research.

Jeroen Vermeulen – January 2020

Table of content

Thesis Introduction

Traditional methods in biomechanics and motor control often have focused on linear relations in time series of human locomotor system components. However, behaviors in these components are generally non-linear. Therefore, linear methods often lack the fidelity to fully explore the complexity found in these components. The latter has caused research to investigate a non-linear system approach. To evaluate non-linearities in human movement, we can analyze complexity. Research proposed that quantification of signal complexity can serve as a convenient tool to identify healthy gait function, to evaluate outcomes of physical therapies and to monitor the progression of disease. In the present study, our objective was to display that *Sample Entropy (SaEn)* is a sensitive measure to quantify changes in human gait function. We analyzed complexity changes with age, since healthy gait function is known to deteriorate with age. Subsequently, we analyzed complexity changes with walking velocity, since walking velocity is known to alter gait function. Here, we quantified signal complexity changes with *SaEn* in electromyography, ground reaction force and joint angle time series of asymmetrical stepping tasks.

In the first section of this document, the scientific paper of the research is presented. Subsequently, in the second section, the appendices are presented. The interested reader is referred to these appendices. The appendices entail the definition, the parameter choosing, current applications and limitations of the *SaEn* algorithm. Finally, detailed results of our experiments are presented.

Part I:
Scientific paper

Nomenclature

Abbreviations

AP	Anterior-Posterior / Flexion-Extension
ApEn	Approximate Entropy
AFS	Asymmetrical targets at Fast Speed (130%*PWS)
ANS	Asymmetrical targets at Normal Speed (PWS)
CTC	Center-To-Center distance
CV	Coefficient of Variation
DOF	Degrees of Freedom
ECG	Electrocardiography
EEG	Electroencephalography
EMG	Elecromyography
F1	Fixed speed 1: 70%*PWS
F2	Fixed speed 2: 160%*PWS
GA	Joint Angle / Gait Angle
GRF	Ground Reaction Force
IC	Initial Contact
LG	Lateral Gastrocnemius
LH	Lateral Hamstrings
ls	Long step
MG	Medial Gastrocnemius
MH	Medial Hamstrings
ML	Medial-Lateral / Abduction-Adduction
MSE	Multiscale (Sample) Entropy
PDF	Probability Density Function
PWS	Preferred Walking Speed
RF	Rectus Femoris
SaEn	Sample Entropy
SD	Standard Deviation
sEMG	Surface Electromyography
ss	Short Step
TO	Toe-off
VE	Vertical
VL	Vastus Lateralis
VM	Vastus Medialis

Symbols

m	Embedding dimension
N	Dataset length
σ	Standard deviation
r	Tolerance
τ	Scale factor
μ	Mean

Abstract

Purpose – The entropy algorithm is a recently developed statistic for quantifying the complexity of time series data. To date, research of biomechanics and motor control discussed whether entropy algorithms could be used as a convenient tool to identify healthy gait function, to evaluate outcomes of physical therapies and to monitor the progression of disease. Here, we show that *Sample Entropy (SaEn)* is a sensitive measure for exposing complexity changes in human gait function.

Methods – We analyzed signal complexity changes in electromyography (EMG), ground reaction force (GRF) and joint angle (GA) time series data of asymmetrical step tasks. We used the *coarse-grained time series* method and the *SaEn* algorithm, to determine the temporal resolution that contained most complex structures per datatype. Subsequently, we analyzed complexity changes with age and with walking velocity in the selected resolution. We analyzed complexity changes with age, since healthy gait function is known to deteriorate with age. In turn, we analyzed complexity changes with walking velocity, since walking velocity is known to alter gait function. Eighteen young (mean age 23.27 +/- 1.79 years) and nineteen old (mean age 66.37 +/- 5.26 years) subjects were analyzed for an equal number of strides, described by an equal number of samples, to account for the *SaEn* dataset length bias.

Results – Age increased entropy in EMG signals. Consecutively, age decreased GRF entropy in the medial-lateral (ML) component for short steps and increased entropy for long steps. Lastly, age decreased entropy in GA signals. Furthermore, walking velocity decreased entropy in EMG signals. Consecutively, walking velocity increased GRF entropy in anterior-posterior (AP) and vertical (VE) components and decreased entropy in the medial-lateral (ML) component. Lastly, walking velocity increased entropy in GA signals.

Conclusions – We portrayed that EMG, GRF and GA signals of human gait altered in entropy with walking velocity and with age. Therefore, our results demonstrate the feasibility of *SaEn* to quantify changes in healthy gait function. Additional research should confirm possible future clinical applications for entropy algorithms.

Introduction

The improvement of human gait function is a major goal of many surgical and rehabilitative orthopedic treatments. In these treatments, age is typically marked as a factor that progressively impairs healthy gait function (Lipsitz et al., 1992). To quantify healthy gait function, previous research used models that assessed joint kinematics, joint accelerations and muscle activation patterns (EMG) by means of the mean and standard deviation (SD) (Sosnoff et al., 2012), the coefficient of variation (CV) (Hausdorff et al., 2015) and the Lyapunov exponent (Terrier et al., 2015). However, it is becoming increasingly clear that these models might not be optimal for evaluating information that motor complexity conveys (Harbourne et al., 2009).

To quantify healthy gait function, we can use entropy algorithms that quantify signal complexity. Consecutively, decreased complexity in joint kinematics and GRFs is linked to increased risk of falling (Kang et al., 2008; Liang et al., 2016; Yu et al., 2009). We typically find this system instability when parts of the neuromotor system lose function with aging or disease (Hamill et al., 1999; Masani et al., 2002). Therefore, the identification of altered physiological complexity, might prove to be a clinically useful biomarker to expose gait cycle changes with aging or disease (Kang et al., 2016; Kaplanis et al., 2010; Lipsitz et al., 1992; Pincus et al., 2006; Pincus et al., 1991b; Pincus et al., 1994; Smith et al., 2011). Moreover, quantifying altered physiological complexity might prove to be useful in identifying disabilities in early stages (Bertrand et al., 2016; McIntosh et al., 2018). In the human gait cycle, the physiological complexity can be defined as healthy function, characterized by an interaction of control mechanisms that adapt to unpredictable changes in the environment. An altered physiological complexity is then regarded as a pathological condition (Lipsitz et al., 1992).

Biomedical research previously identified altered physiological complexity in system outputs as a useful biomarker in endocrinology, cardiology and neurology (Goldberger et al., 2002; Pincus et al., 2006; Pincus et al., 2000; Pincus et al., 1996). In endocrinology, irregular human hormonal secretion processes were exposed with entropy algorithms, that models including means and SDs failed to expose (Pincus et al., 1996). Additionally, in cardiology, entropy algorithms exposed subtle shifts in time series data of the heart, that corresponded to compromised physiological setting (Pincus et al., 2000). In neurology, entropy algorithms were displayed as a possible useful tool for detecting early onset of dementia (Bertrand et al., 2016) and for detecting individuals at risk for cognitive decline (McIntosh et al., 2018). Other studies included athletes, in which electroencephalograph (EEG) complexity analysis determined the athlete's readiness to resume competitive activity after cerebral concussion (Cavanaugh et al., 2005; Stergiou et al., 2006). Conducting more research on these topics could lead to compelling future clinical applications for entropy algorithms.

Most interestingly, studies of human gait analysis covered compelling topics of signal complexity analysis. These topics included: increased stride-to-stride complexity with aging and with disease (Hausdorff et al., 2005; Yu et al., 2009), increased complexity of ground reaction forces with walking instability and with age (Masani et al., 2002; Zhang et al., 2019), increased joint complexity with age and with movement disfunction (Coates et al., 2020; Qiao et al., 2018), prosthesis movement complexity evaluation of femoral amputees (Bogen et al., 2019; Lammoth et al., 2010) and decreased electromyography complexity with walking speed and with age (Kang et al., 2016; Xie et al., 2010). However, there remains considerable debate on the application of signal complexity analysis in the human gait cycle.

To date, research proposed that quantification of signal complexity can serve as a convenient tool to identify healthy gait function and to evaluate outcomes of physical therapies (Bisi et al., 2016; Georgoulis et al., 2006; Kang et al., 2016; Morrison et al., 2012). Therefore, in the present study, we showed that *Sample Entropy (SaEn)* is a sensitive measure for quantifying changes in human gait function. We investigated the effects of two independent variables on human gait outputs. We analyzed complexity changes with *age*, since healthy gait function is known to deteriorate with age (Bisi et al., 2016; Hamill et al., 1999; Masani et al., 2002). Subsequently, we analyzed complexity changes with *walking velocity*, since walking velocity is known to alter gait function (Georgoulis et al., 2006; Kang et al., 2016). We quantified the effects of age on the complexity outcomes of EMG, ground reaction force (GRF) and joint angle (GA) time series in asymmetrical step tasks. Consecutively, complexity outcomes were quantified for 'comfortable' and 'fast' walking velocities in the asymmetrical tasks. Additionally, for these tasks, we assessed whether entropy differed with independent variable 'left or right leg' and with 'short or long step'. Lastly, we investigated the effects of 'slow' and 'fast' walking velocities on EMG complexity of symmetrical step tasks of old subjects, with step targets excluded.

The primary objective of the present study was to answer the following research question: 'Which complexity changes are found with walking velocity and with age in human motion and electromyography signals of asymmetrical step tasks?' Additionally, as a secondary objective, we investigated in which of the measured data types complexity changes with age were most prominently expressed. This secondary objective formed basis for motivating future rehabilitation studies and reemphasized what we know about the topic today. In the present study, complexity effects were quantified using the *Sample Entropy* algorithm *(SaEn)*. This algorithm is defined in ***Appendix A1,*** based on previous literature (Delgado et al., 2019; Yentes et al., 2013). The algorithm was applied on EMG responses of muscles involved in hip and knee flexion and extension, and of muscles involved in plantarflexion. Consecutively, complexity effects were studied in anterior-posterior (AP), vertical (VE) and medial-lateral (ML) GRF components. Lastly, we studied these effects in flexion-extension and abduction-adduction GA components of the hip, knee and foot. We hypothesized that older adults exhibit more signal complexity in EMGs, but less signal complexity in GRFs and GAs, in contrast with younger adults. In turn, this may be caused by slower walking speed and increased neuromotor noise (Bisi et al., 2016; Kang et al., 2016; Kang et al., 2008; Liant et al., 2016; Masani et al., 2002; Pavei et al., 2019; Qiao et al., 2018; Zhang et al., 2019). Consecutively, we hypothesized that walking velocity decreases complexity in EMGs, but increases complexity in GRFs and GAs (Kang et al., 2016; Kwon et al., 2005; Pietraszewski et al., 2012)

Methods

Subjects and evaluation protocol

We used a dataset that was recorded by the Amsterdam VU University Medical Center (VUmc). Eighteen young adults and nineteen old adults participated in the study. Subjects provided written informed consent as approved by the VUmc ethical committee. Characteristics of the test subjects are shown in *Table 1*. When subject reported they did not suffer from health issues that affect their movement in daily life activities, they were enrolled in the experiments. Subjects were asked to wear their own comfortable sports shoes, since providing them with standard shoes would likely introduce perturbations in complexity outcomes (Zhang et al., 2017).

	Young adults	Old adults	*p*-value
Gender (M/F)	9/10	13/7	0.3406*
Age (y)	23.27 +/- 1.79	66.37 +/- 5.26	4.73e-30
Height (m)	1.76 +/- 0.11	1.76 +/- 0.10	0.9638
Body mass (kg)	70.42 +/- 10.22	79.42 +/- 12.88	0.0198
PWS (m/s)	1.32 +/- 0.18	1.22 +/- 0.17	0.0645

Table 1) Subject characteristics – Gender, age, height, body mass and PWS for young and old subject groups are given in μ +/- σ. *p*-values of a paired t-test are given to display the significance of difference between the two groups. *Asterisk* denotes *p*-value for fisher's exact test. Subjects significantly differed in body mass. A repeated measures ANOVA with within-subject factor 'EMG', 'GRF', 'GA' and between subject factor 'body mass' revealed that body mass did not alter entropy outcomes of EMG ($F_{(1,35)}$=.751, p=.744), GRF ($F_{(1,35)}$=.515, p=.827) and GA ($F_{(1,34)}$=1.157 , p=.641) outputs.

Treadmill and virtual environment

All subject data was collected on a self-paced Motek C-Mill treadmill (Aarts et al., 2018). The treadmill was provided with a virtual environment (*Figure 1)*. The virtual environment displayed a straight walking trajectory in a forest, that gave subject visual feedback of their walking velocity. In step target trials, targets were first briefly displayed on the walking trajectory of the virtual environment. Successively, the targets appeared on the treadmill belt. When subjects stepped in a step target, they were facilitated with an auditory 'beep'. Subjects walked with their head straight looking at the virtual environment. This way, subjects would walk in a similar fashion as in overground walking.

Walking trajectory familiarization

In the *familiarization trial,* subjects were asked to familiarize on the treadmill by walking trials in a straight line at preferred walking speed (PWS) for 360 seconds. The experimental set-up of walking trials is presented in *Table 2*. During familiarization, the treadmill's 'self-paced' setting was switched on, so that the treadmill's velocity could be freely adjusted until the subject reached PWS. This would exclude treadmill boundary conditions as much as possible, that could affect complexity outcomes in the recordings (Papegaaij et al., 2017; Sloot et al., 2014). The fixed speed setting was switched on during the walking trials, so that subjects would yield gait outputs at a constant gait speed.

Walking trials and experimental conditions

In *trial 0 (Baseline Stepping – BS),* subjects were asked to walk at PWS and step in the symmetrically displayed block-shaped step targets as accurate as possible. The center-to-center distance (CTC) of these step targets matched the known mean step length *(μ_{step})* of the subject. The mean step length was derived from joint kinematics of the *familiarization trial*. Consecutively, the configuration of the step targets per trial, is shown in ***Figure 2*** and ***Table 2***. The *BS trial* was solely used to expose whether EMG responses in asymmetrical stepping statistically differed with the independent variables: 'left or right leg' and 'short or long step'. These outcomes determined whether we separated our final statistics per these components.

In *trial 1 (Asymmetric Normal Stepping – ANS),* subjects were asked to walk at PWS and step in the displayed asymmetrical block-shaped step targets as accurate as possible. Step targets were displayed on the treadmill at an increased CTC of 130%*μ_{step} (long step) at one leg and a decreased CTC of 70%*μ_{step} (short step) at the other leg. This way, step targets appeared in asymmetrical fashion towards the walking direction of the belt. Here, subjects were randomly assigned to either *Group 1* or *Group 2.* Subjects assigned to *Group 1* were required to make long steps with the left leg and short steps with the right leg. Subjects assigned to *Group 2* were required to make short steps with the left leg and long steps with the right leg (***Figure 2***).

In *trial 2 (Asymmetric Fast Stepping – AFS)*, subjects were again presented with asymmetrical step targets. For both groups, left and right leg step targets switched respective to *trial 1*. Here, the walking velocity was increased with 130%*PWS, to assess the effect of walking velocity on the complexity outcomes in both age groups.

Lastly, in *trial 3 (Fixed speed 1 – F1)* and in *trial 4 (Fixed speed 2 – F2),* we analyzed the effect of walking velocity on symmetrical step tasks of older subjects. Here, we assessed complexity changes in EMG with walking velocity, while step targets were excluded. In *F1*, subjects were required to walk at a low fixed walking speed of 70%*PWS. In *F2,* subjects were required to walk at a high fixed walking speed of 160%*PWS (Kang et al., 2016; Kang et al., 2008; Qiao et al., 2018). For these trials the entropy analysis of GRFs and GAs was excluded, since these datatypes violated the mimimum required dataset length for accurate entropy outcomes *(N > 100)* (Pincus et al., 1991b; Yentes et al., 2013).

Figure 1) Motek C-Mill treadmill with virtual environment – Step targets were presented on the Motek C-Mill treadmill band for the left and right foot. Targets first appeared in the virtual environment, sequentially, they appeared on the treadmill band. Subjects walked with their head straight, looking at the virtual environment. This way, the walking task would resemble overground walking. When subjects stepped in a target, the target turned green and an auditory 'beep' was presented. When subjects missed a target, the target turned red. Ground reaction force plates were integrated in the treadmill band (f_{GRF} = *100 Hz*). The weight bearing mechanism and the handrails of the C-Mill were not used in our study.

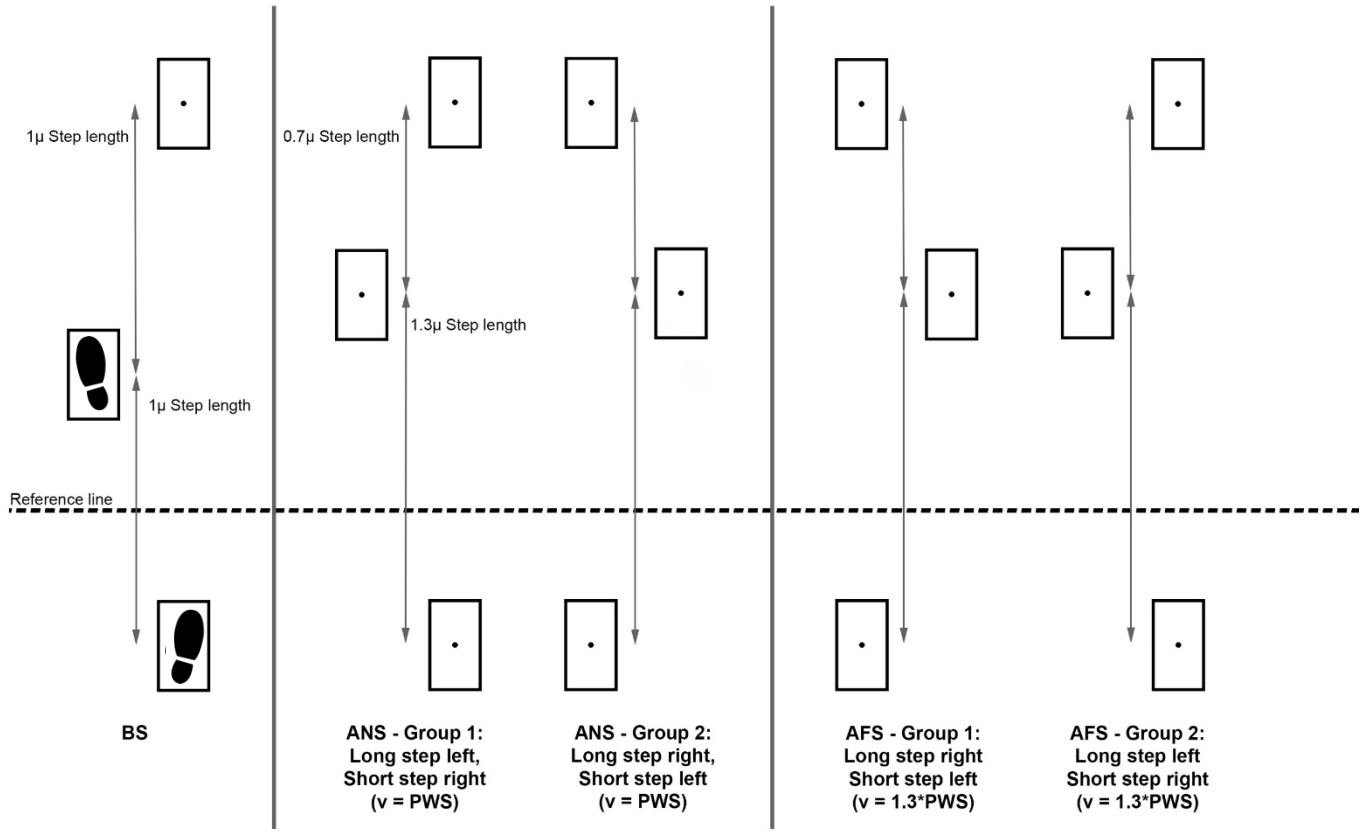

Figure 2) Configuration of the step targets per trial – For *baseline stepping (BS)*, the mean step length was determined with joint kinematics of the *familiarization trial*. In the *BS* trial, subjects were asked to walk at PWS and step in the symmetrically displayed block-shaped step targets as accurate as possible. The center-to-center distance matched the mean step length of the subject. In *trial 1 (Asymmetric Normal Speed – ANS),* stepping blocks were displayed on the treadmill at an increased center to center distance of 130%*(μ_step) at one leg and a decreased center to center distance of 70%*(μ_step) at the other leg. This way, step targets appeared in an asymmetrical fashion in the walking direction of the belt. Per subject, it was randomly selected whether long and short steps appeared left or right of the midline of the treadmill band. Therefore, subjects were assigned to either *Group 1* or *Group 2*. In *trial 2 (Asymmetric Fast Speed – AFS)*, for both groups left and right leg step targets switched respective to *trial 1*. In this trial, the walking velocity was increased with 130%*PWS.

Experimental condition	**Walking velocity**	**Step targets**	**Included subjects**	**Recording duration**	**Included datatype(s)**	**Purpose**
Familiarization trial	PWS (Self-paced)	Deactivated	N_{young} = 18 N_{old} = 19	360 seconds	Kinematics	Mean step length PWS Step targets
Trial 0: *Baseline stepping (BS)*	PWS	Left, right leg: center to center distance (CTC) matched with mean step length	N_{young} = 18 N_{old} = 19	30 seconds	EMG	*SaEn* with *left, right leg* *SaEn* with *short, long step*
Break	-	-	-	-	-	-
Trial 1: *Asymmetrical stepping normal speed (ANS)*	PWS	Subjects randomly assigned to: <u>Group 1</u> Left leg – 130%*CTC (*long step*) Right leg – 70%*CTC (*short step)* <u>Group 2</u> Left leg – 70%*CTC (*short step*) Right leg – 130%*CTC (*long step)*	<u>EMG:</u> N_{young} = 18 N_{old} = 19 <u>GRF, GA:</u> N_{young} = 18 N_{old} = 18	180 seconds	EMG, GRF, GA	*Coarse-grained time series* *SaEn* with *Age* *SaEn* with $V_{walking}$
Break	-	-	-	-	-	-
Trial 2: *Asymmetrical stepping fast speed* *(AFS)*	130% * PWS	Left, right leg step targets switched for both groups	<u>EMG:</u> N_{young} = 18 N_{old} = 19 <u>GRF, GA:</u> N_{young} = 18 N_{old} = 18	180 seconds	EMG, GRF, GA	*Coarse-grained time series* *SaEn* with *Age* *SaEn* with $V_{walking}$
Break	-	-	-	-	-	-
Trial 3: *Fixed speed 1* *(F1)*	70% * PWS	Deactivated	Old N_{old} = 17	30 seconds	EMG	*Coarse-grained time series* *SaEn with* $V_{walking}$
Trial 4: *Fixed speed 2* *(F2)*	160% * PWS	Deactivated	Old N_{old} = 17	30 seconds	EMG	*Coarse-grained time series* *SaEn* with $V_{walking}$

Table 2) Experimental set-up of trials – Walking velocities, step targets, included subjects, recording durations, included datatypes and purpose of the trials are given. Every subject was first familiarized with the treadmill (*familiarization trial).* Joint kinematics of this trial were in turn used to determine the step targets for trials *BS, ANS* and *AFS.* Trial *BS* was used to assess whether EMG responses differed with the 'left or right leg' and with the displayed step target, 'short or long step'. Trials *ANS*, *AFS* assessed the effect of walking velocity and of age on entropy outcomes. Here, short steps were configured to match a center-to-center distance (CTC) of 70%*(μ_step), while long steps matched a CTC of 130%*(μ_step). Trial *F1* assessed if a slow fixed walking speed of 70%*PWS, was an important factor for an increased EMG complexity in older subjects. These results were contrasted with results of *F2.* In *F2*, walking speed was increased to 160% of PWS. Consecutively, for all trials, entropy analysis was conducted on datatypes with sufficient dataset length (*N > 100*).

Data acquisition and pre-processing

Three dependent variables were recorded during the trials, surface electromyography (sEMG), ground reaction forces (GRFs) and joint angles (GAs). Fourteen 'Covidien Kendall' sEMG sensors recorded muscle activation patterns of muscles involved in hip and knee flexion and extension, and of muscles involved in plantarflexion ($f_{s,EMG}$= *1000 Hz)*. Quadriceps, lateral and medial hamstrings and lateral and medial calf muscles were measured during walking trials (*Table 3*). In the recordings, the left and right lateral hamstrings were measured as the combination of the left and right semimembranosus and semitendinosus, respectively. This choice was made by the dataset recorder. To decrease resistance in electrodes, skin sites overlying each muscle belly were cleaned and prepared before connection. The sEMG electrodes were connected to the center of each muscle belly to reduce crosstalk (De Luca, 1997). After data acquisition, max raw EMG power was identified in the *10-300 Hz* range (*Appendix E1)*. Subsequently, raw sEMG signals were filtered according to the SENIAM guidelines (Stegeman et al., 2007). Signals were demeaned, high-pass filtered using a 4th order Butterworth filter (1 Hz), low pass filtered using a 2nd order Butterworth filter (450 Hz), full wave rectified and low-pass filtered using a 2nd order Butterworth filter (450 Hz), respectively. The corner frequencies of the filters were chosen so that frequency content of muscle movement and activation would be represented in the filtered signal. Filtering procedures were applied in Matlab 2018a (Mathworks, Natick MA).

Muscle number	Muscle name	Abbreviation
1.	Vastus lateralis (right)	rVL
2.	Rectus femoris (right)	rRF
3.	Vastus medialis (right)	rVM
4.	Biceps femoris (right lateral hamstrings)	rLH
5.	Semimembranosus, Semitendinosus (right medial hamstrings)	rMH
6.	Lateral gastrocnemius (right)	rLG
7.	Medial gastrocnemius (right)	rMG
8.	Vastus lateralis (left)	lVL
9.	Rectus femoris (left)	lRF
10.	Vastus medialis (left)	lVM
11.	Biceps femoris (left lateral hamstrings)	lLH
12.	Semimembranosus, Semitendinosus (left medial hamstrings)	lMH
13.	Lateral gastrocnemius (left)	lLG
14.	Medial gastrocnemius (left)	lMG

Table 3) Recorded muscle responses with sEMG – Recorded muscles are displayed in the order of connection for signal acquisition. EMG data was collected with 14 'Covidien Kendall' sEMG electrodes. The left, right lateral hamstrings were measured as the combination of the left, right semimembranosus and semitendinosus, respectively. Abbreviations of the muscles are displayed for reference to the matlab coding environment (Mathworks, Natick MA).

Tri-dimensional GRFs were recorded using force sensors integrated in the Motek C-Mill (Aarts et al., 2018). The force sensors registered GRFs in the following directions: anterior-posterior (F_x), mediolateral (F_y) and vertical (F_z). Force plates recorded with a sample frequency of f_{GRF} = *100 Hz*. Max raw GRF power was identified in the *5-20 Hz* range. Subsequently, GRFs were low-pass filtered using a 2nd order zero-lag butterworth filter (f_c=*20 Hz*). The corner frequency of the filters was chosen, so that higher frequency content of foot forces would be present in the filtered GRF signal (Gruber et al., 2017).

The treadmill was enclosed by 10 'Vicon Vantage' marker tracking cameras, that measured joint kinematics of the subject. Marker tracking cameras were configured in 360 degrees around the subject, to account for possible NaN values in marker tracking data (*Figure 3)*. Cameras recorded at a sample frequency $f_{s,vicon}$ = *100 Hz* and captured 38 reflective markers (*Figure 4)*. Consecutively, with joint kinematics, we derived flexion-extension (AP) and abduction-adduction (ML) GA time series of the hip, knee and ankle. These joint angles were suitable for complexity analysis. Max GA power was identified in the *0-20 Hz* range. Consecutively, marker data was low-pass filtered using a 2nd order zero-lag butterworth filter (f_c=*20 Hz*).

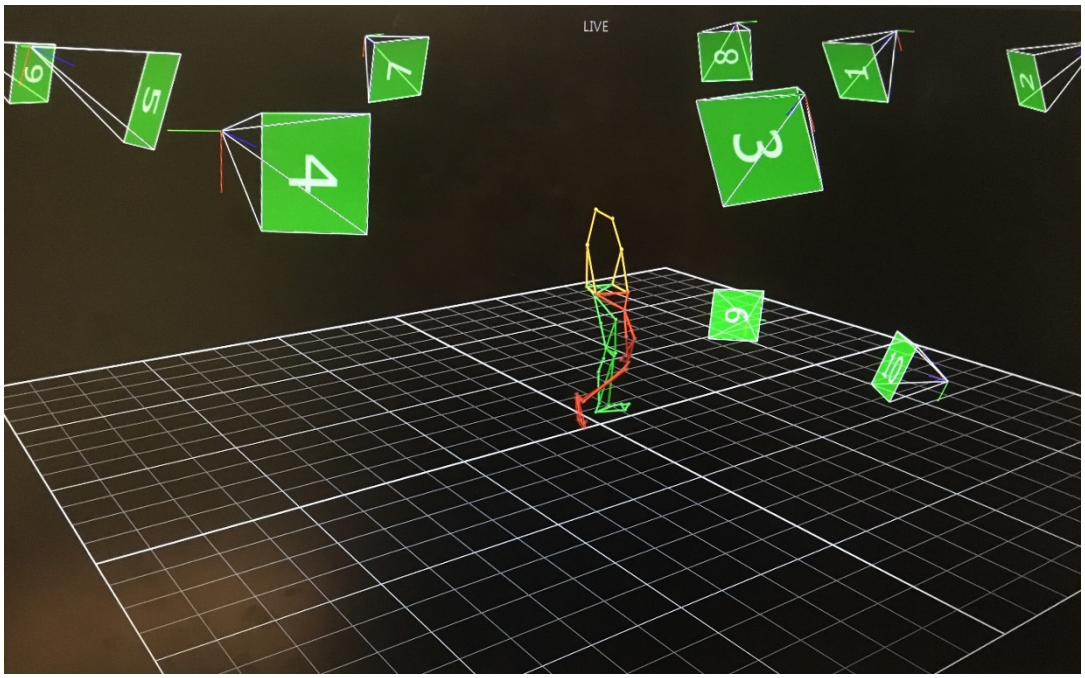

Figure 3) Kinematics: marker tracking camera placement – The self-paced treadmill was enclosed by 10 'Vicon Vantage' marker tracking cameras, that captured movement kinematics of the subject. Vicon marker tracking cameras were set-up in 360 degrees around the subject, to exclude NaN values in marker tracking data. The cameras operated at a sample frequency $f_{s,vicon}$ = *100 Hz* and captured 38 reflective markers that were connected to the subject. The environment depicted is part of 'Vicon Nexus' marker tracking software.

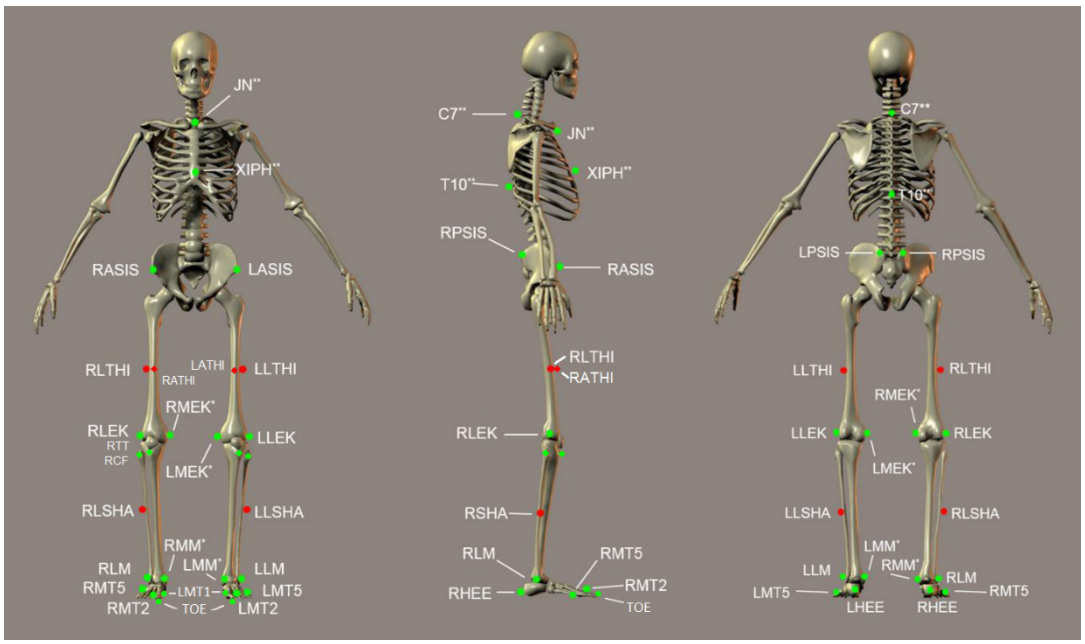

Figure 4) Kinematics: marker locations – The marker locations for the lower extremity in anterior, medial and posterior view are displayed, respectively. Marker locations of the lower extremity were tracked with Vicon Vantage motion tracking cameras and used for entropy analysis. Marker movements of the upper extremity were not used for analysis. Marker positions were connected to the boney landmarks as depicted in *Appendix D.*

Data processing: Normalizing the data

To account for differences in dataset length between subjects, we used toe-off (TO) and initial contact (IC) identifiers of GRF data to extract an equal amount of stance and swing phases for every subject. For EMG data, we extracted 13 gait phases per subject, whereas for GRFs and GAs, we extracted 110 gait phases per subject. One should note, that EMGs were recorded at $f_{s,EMG}$*=1000 Hz*, whereas GRFs and GAs were recorded at f_s*=100 Hz.* Therefore, EMG data satisfied the minimum required dataset length for accurate *SaEn* outcomes with ten times less gait phases than GRF and GA data (Pincus et al., 1991b; Pincus et al., 2000; Pincus et al., 1992; Yentes et al., 2013). In EMGs, 13 gait phases amply reached the minimum required dataset length ($N \gg 100$). In turn, we could not extract 130 gait phases of GRFs and GAs, due to subjects with insufficient gait identifiers. Therefore, we extracted 110 gait phases per subject in these datatypes, that reached the minimum required dataset length ($N > 100$). However, analysis of GRFs and GAs was excluded from *trial 0 (BS), trial 3 (F1)* and *trial 4 (F2),* due to insufficient dataset length (*Table 2*). More information about the entropy bias for short datasets can be found in previous literature (Kibushi et al., 2018; McCrum et al., 2019; Yentes et al., 2013).

Consecutively, we normalized EMG, GRF and GA data to the number of samples. Per datatype, data was resampled to the subject that described gait phases with the least number of samples. Here, we used a shape preserving *spline* algorithm for resampling. Literature approved that resampling with spline preserved the frequency content of joint kinematics, EMGs and EEGs (Coutinho et al., 2017; Eng et al., 2007; Lencioni et al., 2017; Marateb et al., 2016; Unser et al., 1999). We displayed the effect of resampling with a spline algorithm on entropy outcomes, by interpreting results of a regular signal and of exemplar EMG data. Subsequently, we explored the entropy dataset length bias for a regular signal and for the experimental EMG data *(Appendix A3).* Data resampling was executed in Matlab 2018a (Mathworks, Natick MA), using function *resample.*

Data analysis: Signal complexity

The complexity of a time series can be quantified with entropy algorithms. Entropy algorithms divide time series into non-overlapping segments and calculate the conditional probability that a segment is repeated during the time series. The first non-linear complexity algorithm *Approximate Entropy (ApEn)* and its successor *Sample Entropy (SaEn)* are defined and compared in *Appendix A1* (Pincus et al., 1991a; Richman & Moorman, 2000). Both *ApEn [0-2]* and *SaEn [0-3]* outputs are maximized for random sequences (e.g.: white noise function) and minimized for periodic sequences (e.g.: sinusoid function). It is generally accepted that both maximally ordered, and maximally disordered systems possess no complex structures. Therefore, a meaningful physiologic complexity measure can be defined between these two extreme states (Smith et al., 2011).

ApEn and *SaEn* are single-scale methods by definition, that quantify complexity in a single temporal resolution of the time series. Therefore, to quantify complexity in multiple temporal resolutions, an additional procedure is required that derives the resolutions: *coarse-graining time series* (Bisi et al., 2016). For accurate entropy outcomes, *ApEn* requires a dataset length of at least 200 datapoints, while *SaEn* requires just 100 datapoints. Furthermore, *ApEn* includes self-matches of segments, while *SaEn* excludes self-matches. Excluding self-matches eliminates the bias towards regularity. Therefore, *SaEn* yields more accurate complexity outcomes for short and noisy non-uniform time series than *ApEn* (Yentes et al., 2013). Here, we quantified complexity with *SaEn. SaEn* calculations were conducted with inputs $m=2$ and $r=0.1*SD$, as recommended by literature *(Appendix A3)* (Chen et al., 2018; Montesinos et al., 2018; Pincus et al., 1991b; Yentes et al., 2013).

Data analysis: Temporal resolutions – Coarse-graining time series

To account for short,- and long-range correlations in biological time series, recent literature proposed to take *SaEn* values of multiple temporal resolutions of the signal into account (Bisi et al., 2016; Costa et al., 2005; Tao et al., 2015). Here, we derived these resolutions with the *coarse-graining time series* procedure. In this procedure, from a one dimensional discrete time series $\{x_1, \dots, x_i, \dots, x_N\}$, a *coarse-grained time series* $\{y^\tau\}$ is constructed, corresponding to a scale factor τ. Consecutively, the data points inside each window are averaged.

Each element of the *coarse-grained time series* is then calculated according to the following equation:

$$y_j^{\tau} = \frac{1}{\tau} \sum_{i=(j-1)\tau+1}^{j\tau} x_i, \ 1 \leq j \leq \frac{N}{\tau}.$$

For scale one, the time series *{y¹}* is equal to the original time series. In turn, the length of each *coarse-grained time series* is equal to the length of the original time series divided by scale factor τ. Subsequently, we calculated *SaEn* values for the *coarse-grained time series*, that exposed the temporal resolution of the signal that contained most complex structures (Ahmed et al., 2011a; Costa et al., 2005; Costa et al., 2003; Qumar et al., 2013). Consecutively, we followed previous literature, that suggested complexity changes with age and with disease are most prominently expressed in the selected resolution (Kang et al., 2006; McIntosh et al., 2018; McIntosh et al., 2010; Kaplanis et al., 2012). Therefore, we analyzed entropy changes with walking velocity and with age in the temporal resolution that maximized complexity. Here, it was of great importance to analyze *SaEn* changes in a fixed scale per datatype, since *SaEn* outcomes change with scales (Ahmed et al., 2011a; Costa et al., 2005).

The procedure of calculating *SaEn* outcomes over multiple temporal resolutions is called *Multiscale Entropy (MSE)* in literature (Costa et al., 2005). In the supplementary material, we determine *MSE* outcomes for regular and irregular data, to portray the working principle of the procedure (*Appendix A2*).

Statistical analysis

In the ***preliminary test***, we determined whether independent variables 'left or right leg' and 'short or long step' changed entropy in dependent variables 'EMG', 'GRF' and 'GA'. Results of the preliminary test determined whether we separated final statistics in our main test per these independent variables. We subtracted EMG baseline entropy outcomes of symmetric stepping (*trial BS)* from entropy outcomes of asymmetrical stepping (*trial ANS).* Subsequently, we conducted a repeated measures ANOVA to test the effects of the independent variables on the dependent variable 'EMG'. The ANOVA design included: within subject factor one 'EMG' (7 levels), within subject factor two 'short or long step' (2 levels) and between subject factor 'left or right leg' (2 levels). Consecutively, we conducted two repeated measures ANOVAs to confirm the effect of the independent variables on the dependent variables 'GRF' (3 levels) and 'GA' (6 levels). Here, baseline GRF and GA *SaEn* outcomes were excluded, because the minimum required dataset length was violated in the *BS trial* for these datatypes.

Finally, in the ***main test****,* we answered the research question. We determined whether independent variables 'age' and 'walking velocity' changed entropy in dependent variables 'EMG', 'GRF' and 'GA'. We conducted one repeated measures ANOVA per datatype. The design for trial *ANS* and *AFS* included: within-subject factor one 'EMG', 'GRF' or 'GA', within-factor two 'velocity' (2 levels) and between subject factor 'age' (2 levels). An additional repeated measures ANOVA was conducted for trials *F1* and *F2.* This test assessed whether independent variable 'walking velocity' changed entropy in the dependent variable 'EMG' of older subjects. This test included: within-subject factor one 'muscle' (7 levels) and within-subject factor two 'velocity' (2 levels).

For the above-mentioned tests, we corrected confidence intervals for multiple testing using the Bonferroni correction. Shapiro-Wilk tests (*p>0.05)* and visual inspection of histograms and normal Q-Q plots confirmed that EMG, GRF and GA data were normally distributed for both young and old subjects. The level of statistical significance of repeated measures tests was set to *p<0.05*. In our graphs, *p*-values of <0.05 were denoted as '*', *p*-values of <0.01 as '**', *p*-values of <0.001 as '***' and *p*-values of <0.0001 as '****', respectively. When *p*-values just did not reach significance ($0.05 < p < 0.055$), we denoted them as '~'. Statistical analyses were carried out using SPSS software (version 25.0, SPSS Inc. Chicago, IL USA). Graphs were plotted in Matlab 2018a (Mathworks, Natick MA).

Results

Here, we investigate entropy changes with walking velocity and with age in EMG, GRF and GA signals of asymmetrical step tasks. Additionally, we assess whether entropy changed with the 'left or right leg' and with the step target, 'short or long step' (*preliminary test)*. Lastly, we investigate entropy changes with 'slow' and 'fast' walking velocities for symmetrical step tasks of old subjects, with step targets excluded. These results will show whether *SaEn* is a sensitive measure for quantifying changes in human gait function.

First, we calculated *SaEn* outcomes for the EMG response of an exemplar old subject. For this subject, we plot EMGs and corresponding *SaEn* values of the right VL muscle. These results are plotted for a low fixed walking velocity (*Trial F1*) and for a high fixed walking velocity (*Trial F2*) in contrast to PWS (*Figure 5)*.

Second, we determined *SaEn* outcomes of *coarse-grained time series* of EMG, GRF and GA data. This identified which temporal resolution maximized complexity (Ahmed et al., 2011a; Costa et al., 2005; Costa et al., 2003). For GRF and GA data, *coarse-grained time series* at scale factor $\tau = 20$ reached the dataset length requirement of $N > 100$. Coarser scales of the data did not satisfy this requirement. Therefore, we analyzed the first 20 temporal scales for all datatypes. We plot exemplar *coarse-grained time series* and its *SaEn* results of RF EMG data *(Figure 6)*, of VE GRF data *(Figure 7)* and of AP hip GA data *(Figure 8)*, respectively. Outcomes of additional data components are displayed in the supplementary material (*Appendix E2).* EMG *SaEn* outputs were maximized for all muscles in *scale 1*. GRF *SaEn* outputs of AP and VE components were maximized in *scale 12,* while outputs of the ML component were maximized in *scale 13*. Lastly, GA *SaEn* outputs were maximized in *scale 14*, except short step AP (ssAP) components, that were elevated with +/- 8% in a coarser scale. *SaEn* values of ssAP hip and knee components were elevated in *scale 19*, while the ssAP ankle component was elevated in *scale 20*.

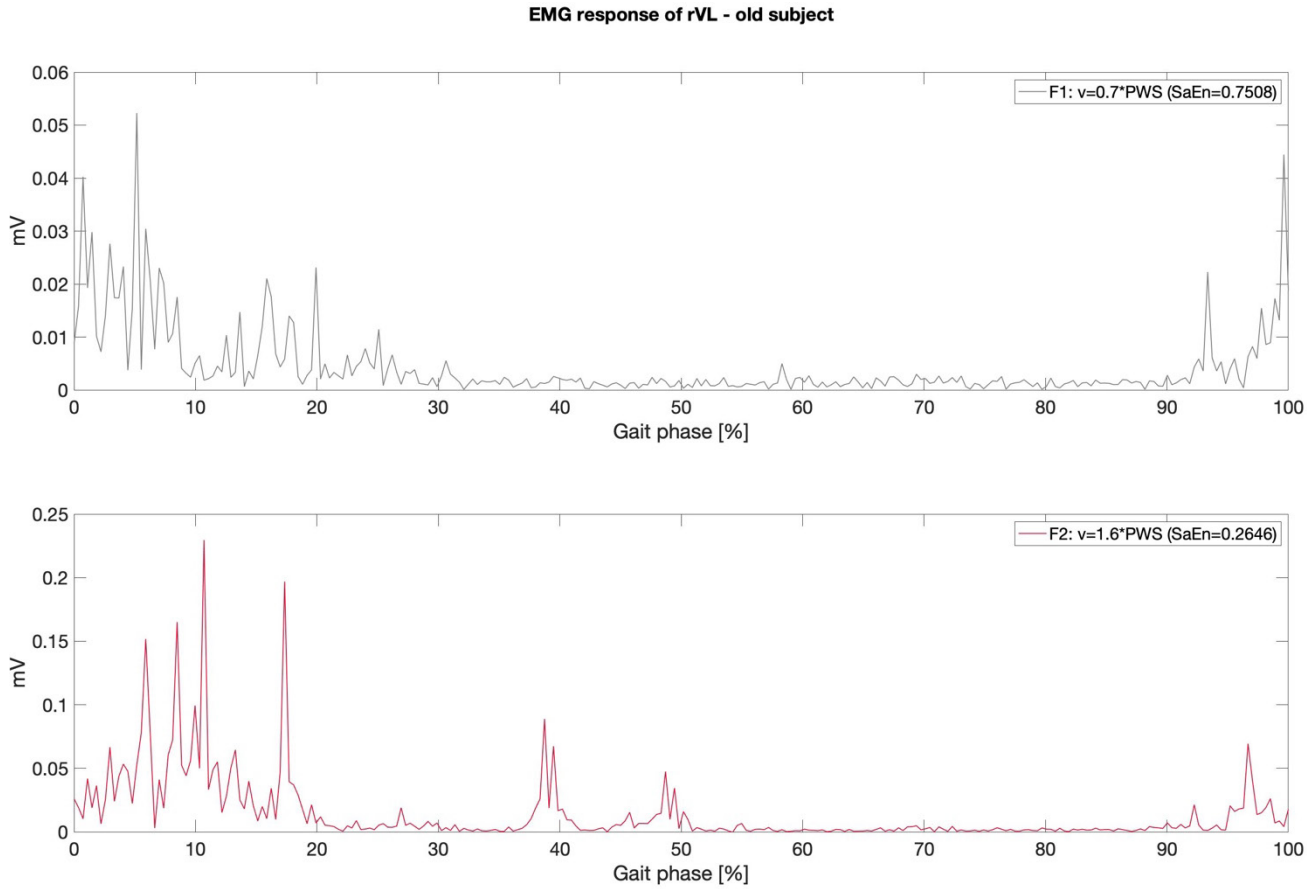

Figure 5) EMG responses at fixed speeds for rVL muscle of exemplar old subject – rVL muscle responses are shown for a consecutive stance and swing phase at two fixed walking velocities. The x-axis displays the percentage of the gait cycle, starting with the stance phase and ending with the swing phase. In turn, *SaEn* outcomes of the responses are given in *right upper corners*. EMG data was recorded at fixed speed lower than PWS (*trial F1*: 0.7*PWS), and at fixed speed higher than PWS (*trial F2:* 1.6*PWS), plotted in *gray* and *red,* respectively. For low walking velocity, EMG complexity of rVL significantly increased, in contrast with high walking velocity.

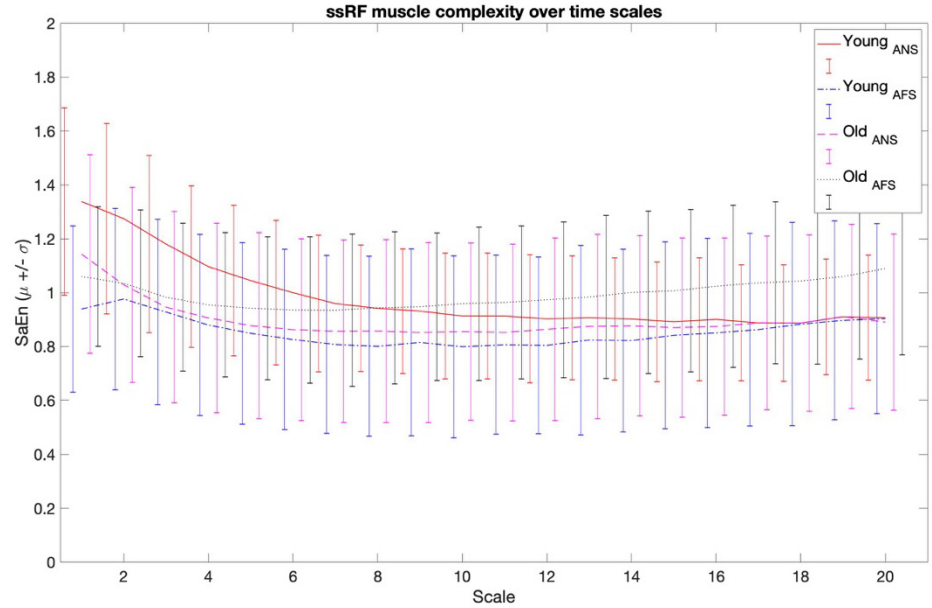

Figure 6) Coarse-grained time series and *SaEn* of EMG data – *SaEn* outcomes (μ +/- σ) of asymmetrical step tasks are given for the EMG response of the RF muscle subjected to short steps (ssRF). *SaEn* values are plotted for temporal resolutions of the data, *scale 1-20*. *SaEn* values are plotted for young *ANS* (*red)* and *AFS* trials *(blue dash-dotted)* and for old *ANS (purple dashed)* and *AFS* trials *(black dotted),* respectively. *SaEn* outputs were maximized in the original temporal resolution of the data, *scale 1*. Results of additional EMG data components are given in *Appendix E2.*

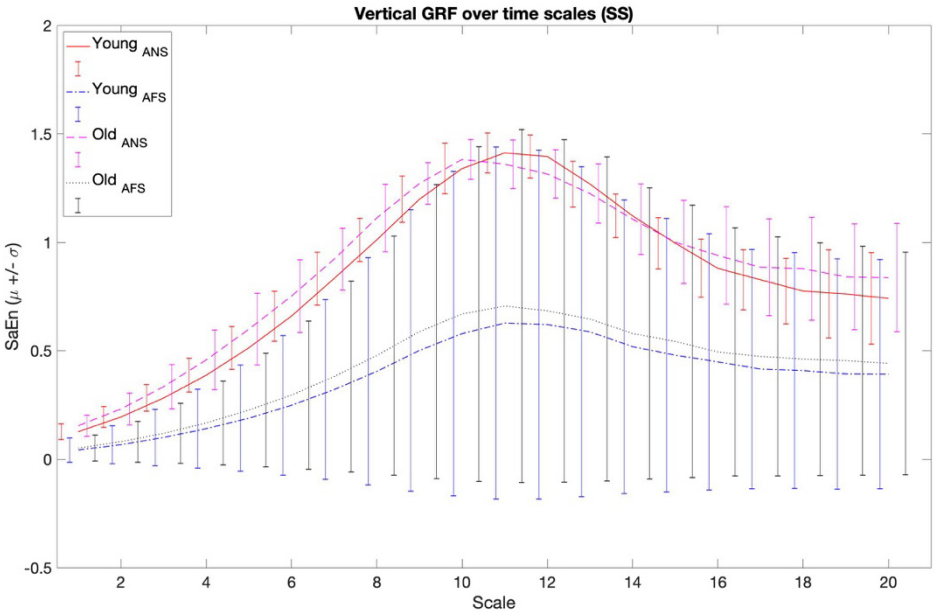

Figure 7) Coarse-grained time series and *SaEn* of GRF data – *SaEn* outcomes (μ +/- σ) of asymmetrical step tasks are given for the VE GRF component subjected to short steps. *SaEn* values are plotted for temporal resolutions of the data, *scale 1-20*. We plotted *SaEn* values for young *ANS* (*red)* and *AFS* trials *(blue dash-dotted)* and for old *ANS (purple dashed)* and *AFS* trials *(black dotted),* respectively. *SaEn* outputs were maximized in the 12th temporal resolution of the data, *scale 12*. Results of additional GRF data components are given in *Appendix E2.*

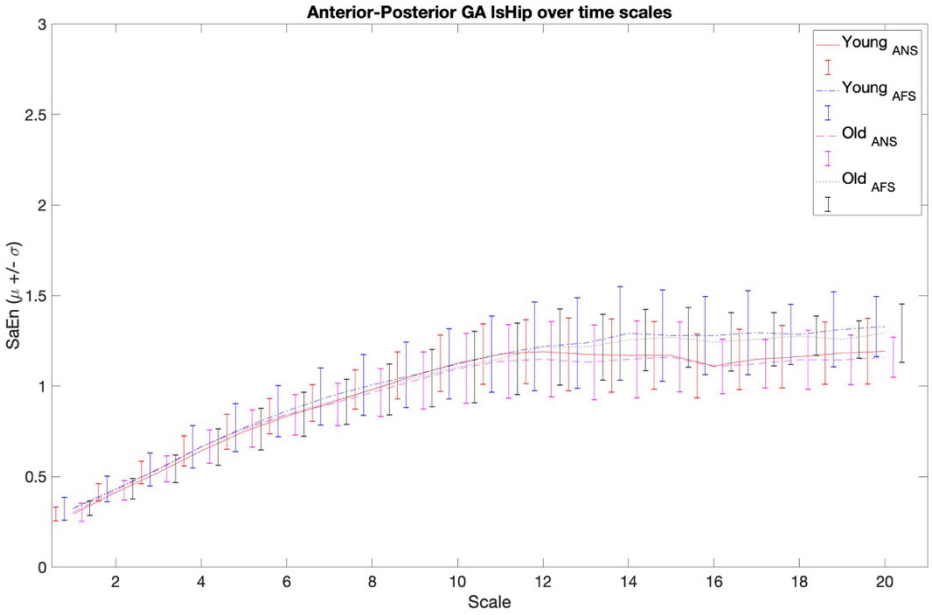

Figure 8) Coarse-grained time series and *SaEn* of GA data – *SaEn* outcomes (μ +/- σ) of asymmetrical step tasks are given for the AP Hip component subjected to long steps. *SaEn* values are plotted for temporal resolutions of the data, *scale 1-20*. We plotted *SaEn* values for young *ANS* (*red)* and *AFS* trials *(blue dash-dotted)* and for old *ANS (purple dashed)* and *AFS* trials *(black dotted),* respectively. *SaEn* outputs were maximized in the 14th temporal resolution of the data, *scale 14*. Results of additional GRF data components are given in *Appendix E2.*

In the *preliminary test*, the repeated measures ANOVA of EMG data revealed no significant main effect of 'left or right leg' ($F_{(1,35)}$=.313 , p=.580) and no significant main effect of 'short or long step' ($F_{(1,35)}$=.540 , p=.468). However, contrasts for the main effect of 'short or long step' displayed significant effects for RF ($F_{(1,35)}$=5.461 , p=.025), VM ($F_{(1,35)}$=4.838 , p=.035), LG ($F_{(1,35)}$=32.612 , p<.0001) and MG ($F_{(1,35)}$=9.861 , p=.003) muscles. Two subsequent repeated measures tests revealed no significant main effect of 'left or right leg' on entropy of GRFs ($F_{(1,34)}$=.005 , p=.944) and of GAs ($F_{(1,34)}$=1.906, p=.176). Subsequently, no significant main effect of 'short or long step' was found in GRFs ($F_{(1,34)}$=.295, p=.590), while a significant main effect was found in GAs ($F_{(1,34)}$=24.509 p<.0001). These results suggested to separate short and long step data components in our *main test* below. Left and right leg components were combined by averaging.

EMG responses: complexity alteration with walking velocity and with age (Trials ANS, AFS)

In *scale 1* of EMG data, we assessed the main effect of the within-subject factor 'walking velocity'. Maulchy's test of sphericity was not violated for the main effects of this factor. Therefore, sphericity could be assumed. Here, all subject data was included (N_{young} = 18, N_{old} = 19). The repeated measures ANOVA revealed a highly significant main effect of walking velocity on *SaEn* of EMG responses (*Table 4a*). In turn, contrasts revealed that walking velocity decreased *SaEn* of EMG for short steps in RF, VM and LH. Subsequently, walking velocity decreased *SaEn* for long steps in VL, RF, VM, LH and MH. Elevating walking velocity to 130%*PWS resulted in significant decreased entropy in the mentioned muscle responses. The mean *SaEn* outcomes with walking velocity are plotted per muscles involved in hip flexion and knee extension (*Figure 9a*), hip extension and knee flexion (*Figure 9b*) and plantarflexion (*Figure 9c*), respectively.

The main effect of the between-subject factor 'age' was not significant on *SaEn* outcomes of EMG responses. However, contrasts revealed age increased *SaEn* in the MH subjected to short and long steps. Subsequently, age increased *SaEn* in the MG subjected to short and long steps (*Figure 10a-c*). Old subjects exhibited highly significant increased entropy in medial hamstrings and gastrocnemius muscles compared to young subjects.

Main effects of the two-way interaction 'age*velocity' were significant. Contrasts of this effect revealed that walking velocity caused larger decreases in entropy of EMG for young subjects than for old subjects. These components included short step Vastus Lateralis (ssVL), ssRF, ssVM and ssLH.

EMG responses: complexity alteration with walking velocity in old subjects (Trials F1, F2)

Finally, the main effect of 'walking velocity' was assessed for symmetrical step tasks of older subjects *(trial F1, F2).* Here, two older subjects were excluded (N_{old} = 17) due to the lack of sufficient stride identifiers. Highly significant results were found for the main effect of walking velocity on *SaEn* outcomes of EMG (*Table 4b*). Contrasts revealed that low walking velocity (70%*PWS) caused increased entropy in VL, RF, VM, LH, MH and LG muscles, in contrast with high walking velocity (160%*PWS) (*Figure 11a-c*).

a)

EMG (*SaEn)*	**Main effect 'velocity'**	**Main effect 'age'**	**Interaction 'vel*age'**
	$F_{(1,35)}$=38.690, p<.0001	$F_{(1,35)}$=2.665, p=.112	$F_{(1,35)}$=6.171, p=.018
Muscle	**Conditions: ANS vs. AFS**	**Subjects: Young vs. Old**	
ssVL	$F_{(1,35)}$= 2.895, p=.98	$F_{(1,35)}$= .277, p=.602	**$F_{(1,35)}$= 4.285, p=.046**
ssRF	**$F_{(1,35)}$=24.227, p<.0001**	$F_{(1,35)}$= .097, p=.758	**$F_{(1,35)}$=12.907, p=.001**
ssVM	**$F_{(1,35)}$=16.778, p<.001**	$F_{(1,35)}$= .406, p=.528	**$F_{(1,35)}$= 5.690, p=.023**
ssLH	**$F_{(1,35)}$= 7.060, p=.012**	$F_{(1,35)}$= .523, p=.474	**$F_{(1,35)}$= 7.536, p=.009**
ssMH	$F_{(1,35)}$= .267, p=.609	**$F_{(1,35)}$=16.719, p<.001**	$F_{(1,35)}$= 3.404, p=.074
ssLG	$F_{(1,35)}$= .999, p=.324	$F_{(1,35)}$= 1.736, p=.196	$F_{(1,35)}$= .530, p=.472
ssMG	$F_{(1,35)}$= .245, p=.624	**$F_{(1,35)}$= 8.072, p=.007**	$F_{(1,35)}$= .068, p=.796
lsVL	**$F_{(1,35)}$= 5.610, p=.024**	$F_{(1,35)}$= .554, p=.461	$F_{(1,35)}$= 1.905, p=.176
lsRF	**$F_{(1,35)}$=24.937, p<.0001**	$F_{(1,35)}$= .122, p=.729	$F_{(1,35)}$= .062, p=.804
lsVM	**$F_{(1,35)}$=15.718, p<.001**	$F_{(1,35)}$= .208, p=.651	$F_{(1,35)}$= .230, p=.634
lsLH	**$F_{(1,35)}$=28.923, p<.0001**	$F_{(1,35)}$= .233, p=.632	$F_{(1,35)}$= .209, p=.650
lsMH	**$F_{(1,35)}$=11.026, p=.002**	**$F_{(1,35)}$=18.913, p<.001**	$F_{(1,35)}$= .248, p=.622
lsLG	$F_{(1,35)}$= 1.237, p=.274	$F_{(1,35)}$= .820, p=.371	$F_{(1,35)}$= .068, p=.796
lsMG	$F_{(1,35)}$= .126, p=.725	**$F_{(1,35)}$= 8.917, p=.005**	$F_{(1,35)}$= .138, p=.713

b)

EMG *(SaEn)*	**Main effect 'velocity'**
	$F_{(1,16)}$=86.063, p<.0001
Muscle	**Conditions: F1 vs. F2**
VL	**$F_{(1,16)}$=14.643, p=.001**
RF	**$F_{(1,16)}$=21.048, p<.001**
VM	**$F_{(1,16)}$=55.243, p<.0001**
LH	**$F_{(1,16)}$=14.551, p=.002**
MH	**$F_{(1,16)}$=16.107, p=.001**
LG	**$F_{(1,16)}$=18.711, p=.001**
MG	$F_{(1,16)}$=1.072, p=.316

Table 4ab) EMG: main and interaction effects of velocity and age on entropy of asymmetrical and symmetrical step tasks – **a)** Main effects and contrasts of velocity, age and velocity*age on *SaEn* of EMG signals are given for trials *ANS, AFS* (N_{young} = 18, N_{old} = 19). Data components are separated per short step (ss) and per long step (ls), since ss and ls components were statistically different. Left and right muscle *SaEn* outcomes were averaged. **b)** Main effect and contrasts of walking velocity on *SaEn* EMG outputs of older individuals in trials *F1, F2* are given (N_{old} = 17). Left and right muscle *SaEn* outcomes were averaged. For a) and b), significant contrast effects are displayed in *bold.* Each table represents one repeated measures ANOVA test.

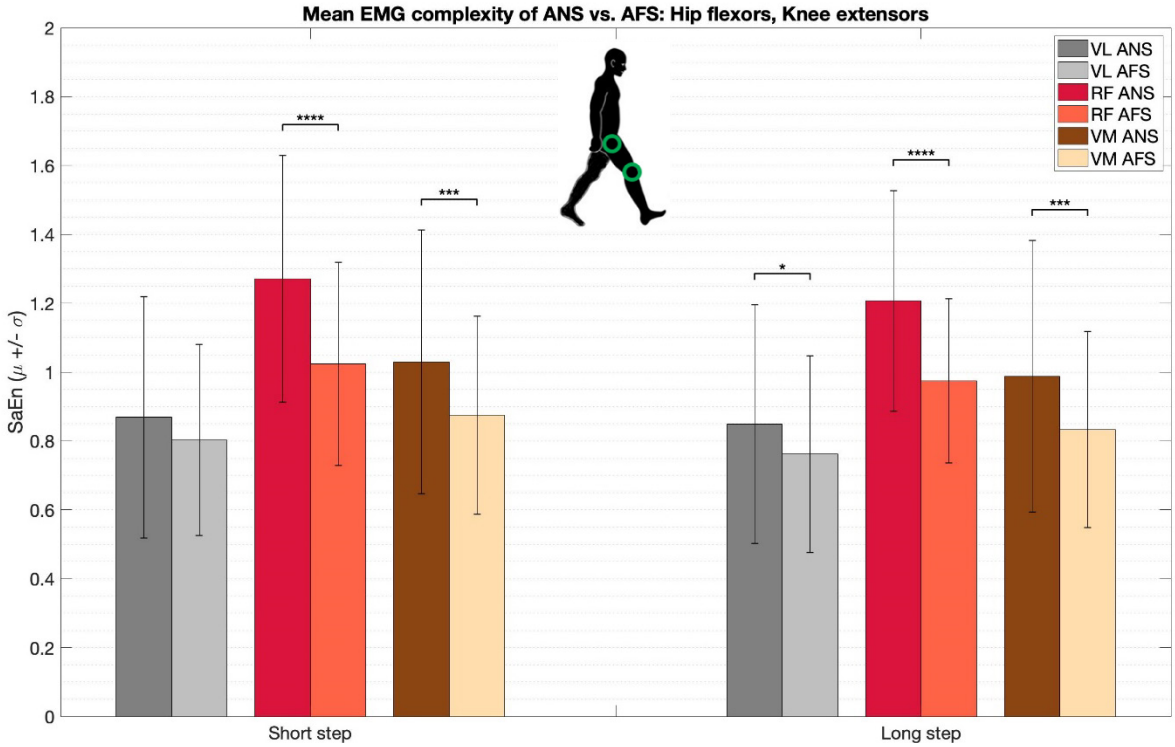

Figure 9a) Main effect velocity on entropy of hip flexor and knee extensor muscles (ANS, AFS) – *Adjacent bars* display *SaEn* values ($\mu \pm \sigma$) at PWS (*ANS*) vs. 1.3*PWS (*AFS*) in asymmetrical step tasks. Data of all young and old subjects were included in this analysis (N_{young} = 18, N_{old} = 19). Results of muscles VL, RF and VM with short steps (*left*) and with long steps (*right*) are displayed, respectively. RF and VM muscles displayed highly significant entropy decrease with walking velocity for both short and long steps.

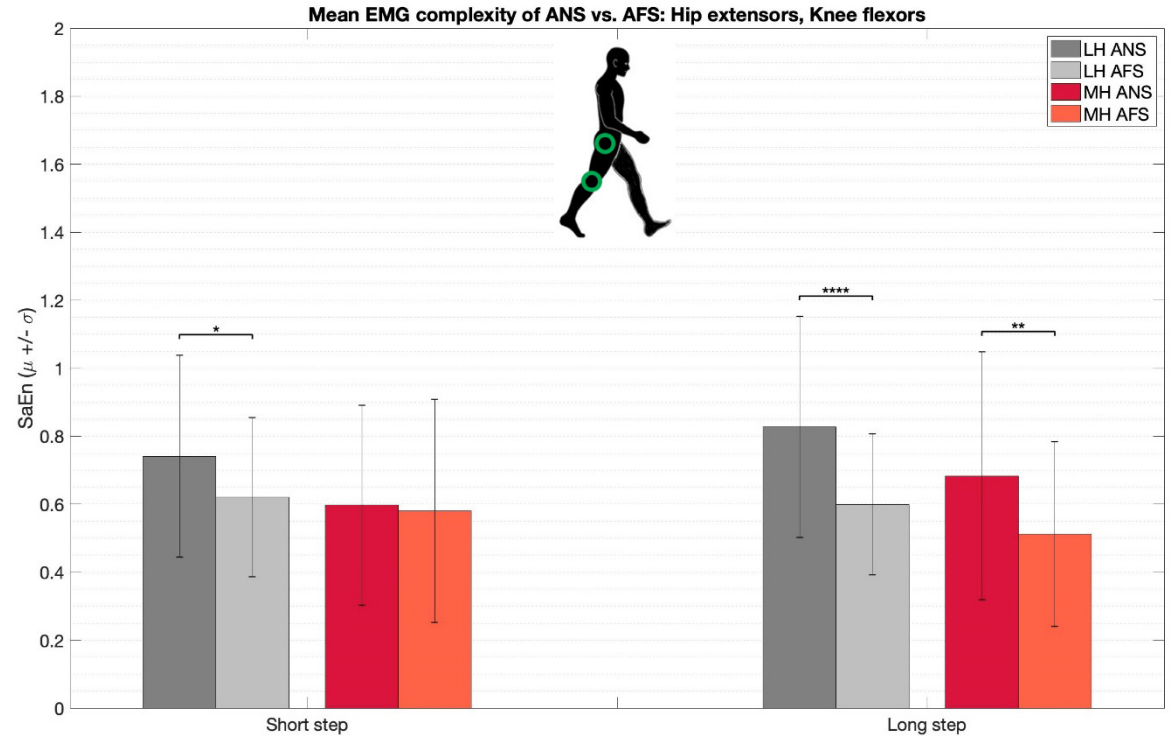

Figure 9b) Main effect velocity on entropy of hip extensor and knee flexor muscles (ANS, AFS) – *Adjacent bars* display *SaEn* values ($\mu \pm \sigma$) at PWS (*ANS*) vs. 1.3*PWS (*AFS*) in asymmetrical step tasks. Data of all young and old subjects were included in the statistical analysis (N_{young} = 18, N_{old} = 19). Results of muscles LH and MH with short steps (*left*) and with long steps (*right*) are displayed, respectively. The MH muscle displayed highly significant entropy decrease with walking velocity for long steps.

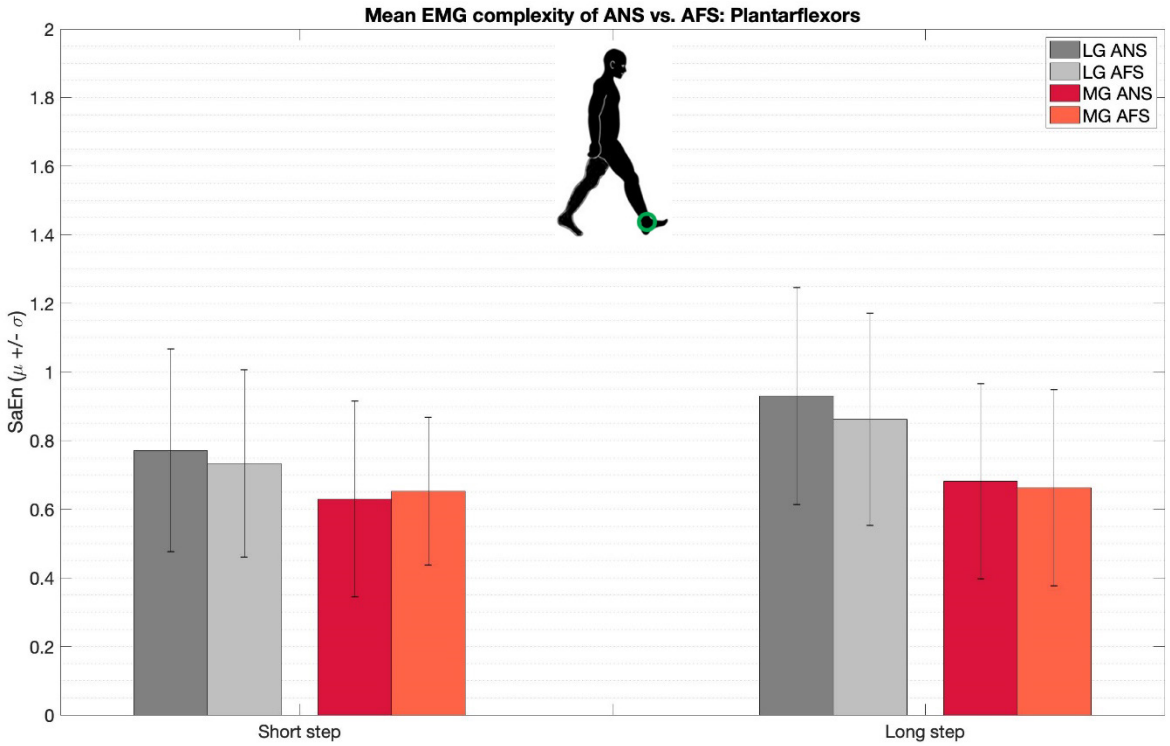

Figure 9c) Main effect velocity on entropy of plantar flexor muscles (ANS, AFS) – *Adjacent bars* display *SaEn* values ($\mu \pm \sigma$) at PWS (*ANS*) vs. 1.3*PWS (*AFS*) in asymmetrical step tasks. Data of all young and old subjects were included in the statistical analysis ($N_{young} = 18$, $N_{old} = 19$). Results of muscles LG and MG with short steps (*left*) and with long steps (*right*) are displayed, respectively. These muscles displayed no significant entropy alteration with walking velocity.

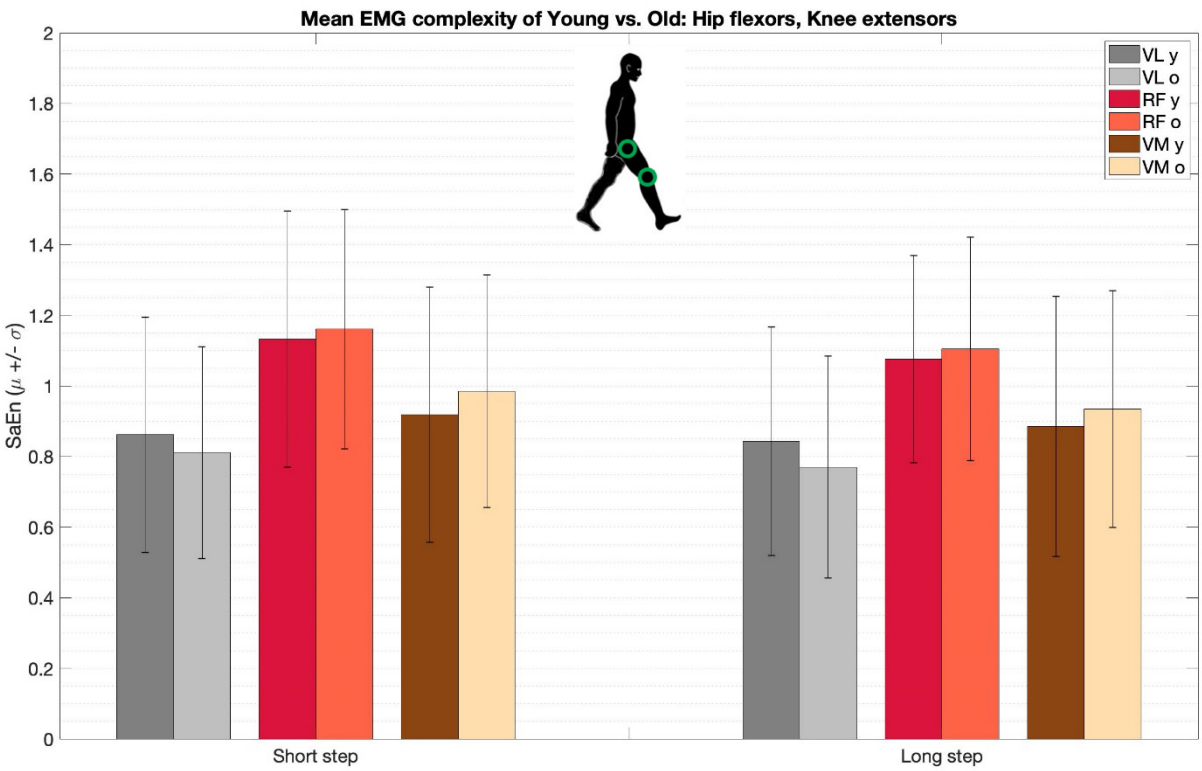

Figure 10a) Main effect age on entropy of hip flexor and knee extensor muscles (ANS, AFS) – *Adjacent bars* display *SaEn* values ($\mu \pm \sigma$) of young vs. old subjects in asymmetrical step tasks. Data of trials *ANS* and *AFS* were included in the statistical analysis. Results of muscles VL, RF and VM with short steps (*left*) and with long steps (*right*) are displayed, respectively. These muscles displayed no significant entropy alteration with age.

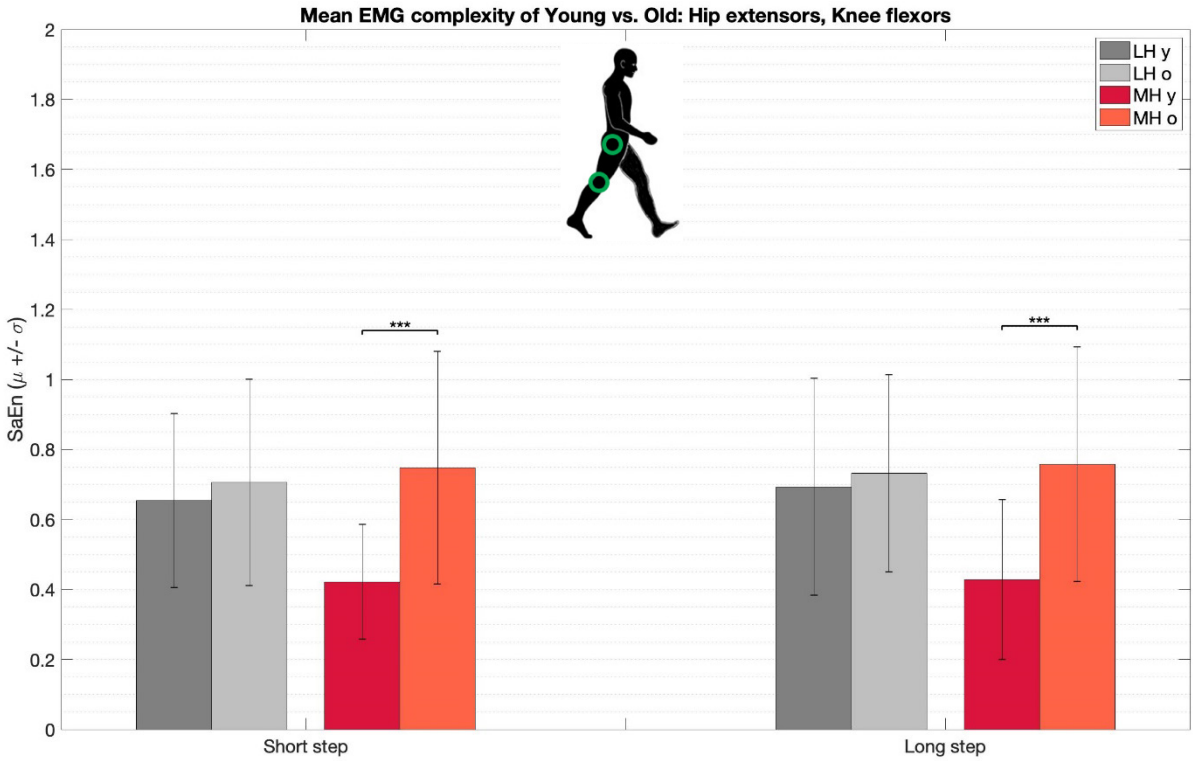

Figure 10b) Main effect age on entropy of hip extensor and knee flexor muscles (ANS, AFS) – *Adjacent bars* display *SaEn* values (μ ± σ) of young vs. old subjects in asymmetrical step tasks. Data of trials *ANS* and *AFS* were included in the statistical analysis. Results of muscles LH and MH with short steps (*left*) and with long steps (*right*) are displayed, respectively. The MH muscle displayed highly significant entropy increase with age for short and long steps.

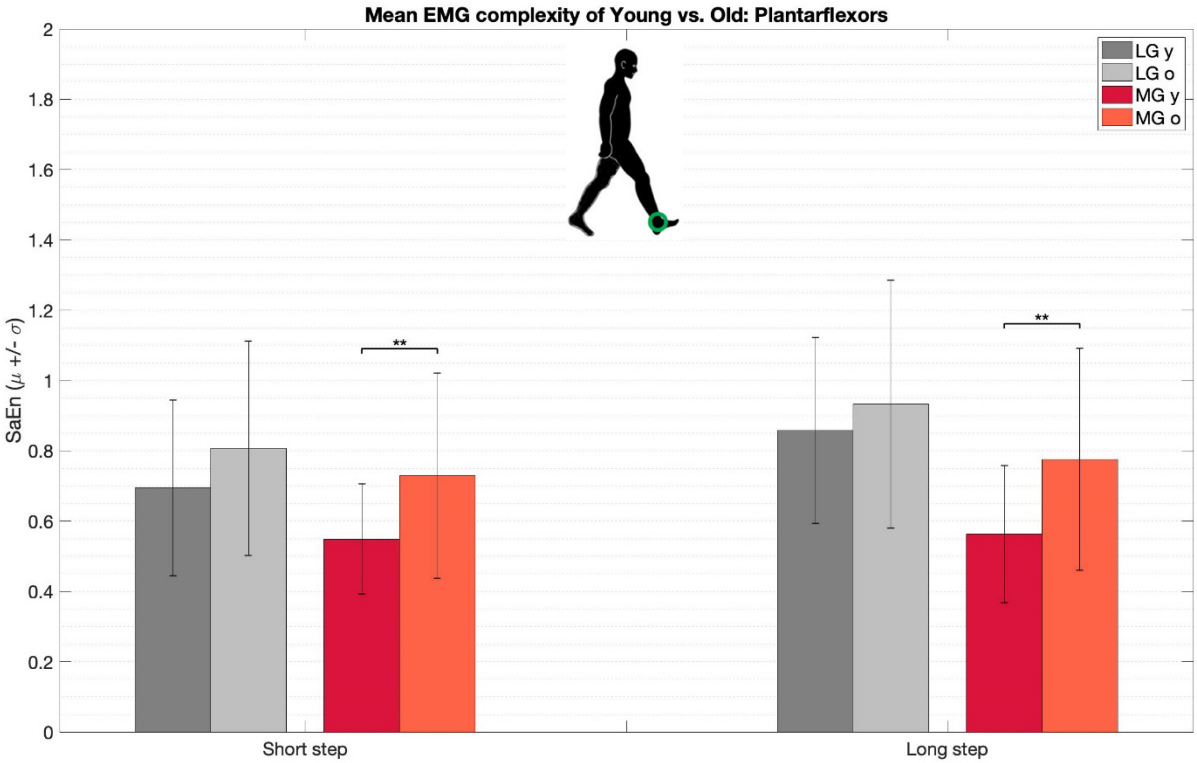

Figure 10c) Main effect age on entropy of plantar flexor muscles (ANS, AFS) – *Adjacent bars* display *SaEn* values (μ ± σ) of young vs. old subjects in asymmetrical step tasks. Data of trials *ANS* and *AFS* were included in the statistical analysis. Results of muscles LH and MH with short steps (*left*) and with long steps (*right*) are displayed, respectively. The MG muscle displayed significant entropy increase with age for short and long steps.

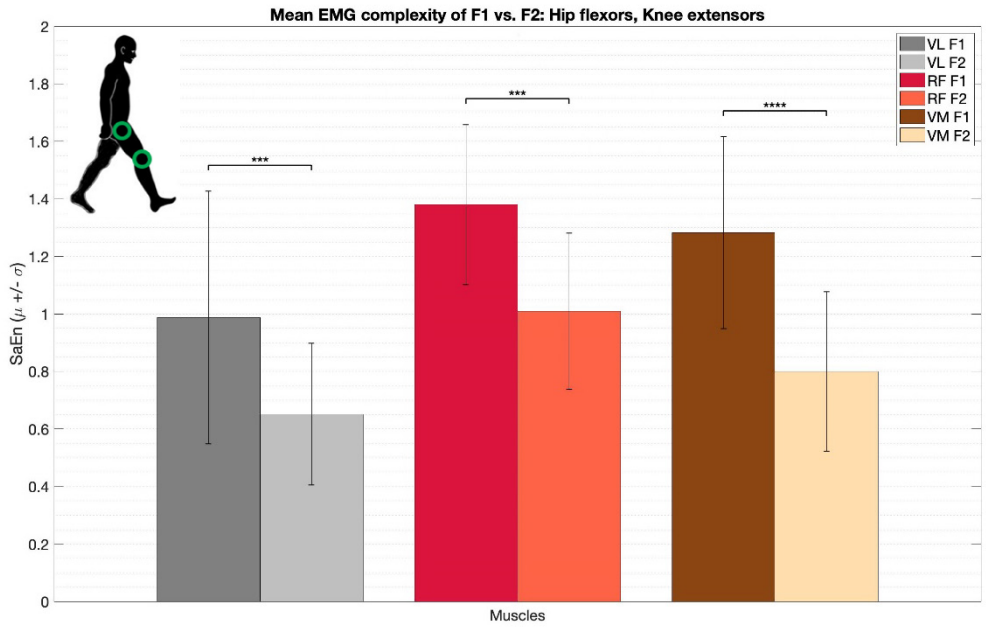

Figure 11a) Main effect velocity on entropy of hip flexor and knee extensor muscles (F1, F2) – *Adjacent bars* display *SaEn* values ($\mu \pm \sigma$) at 0.7*PWS (*F1*) vs. 1.6*PWS (*F2*) in symmetrical step tasks. Only old subjects were measured in *trials F1, F2* (N_{old} = 17). Results of muscles VL, RF and VM are displayed, respectively. Highly significant entropy decreases with walking velocity were found in these muscles.

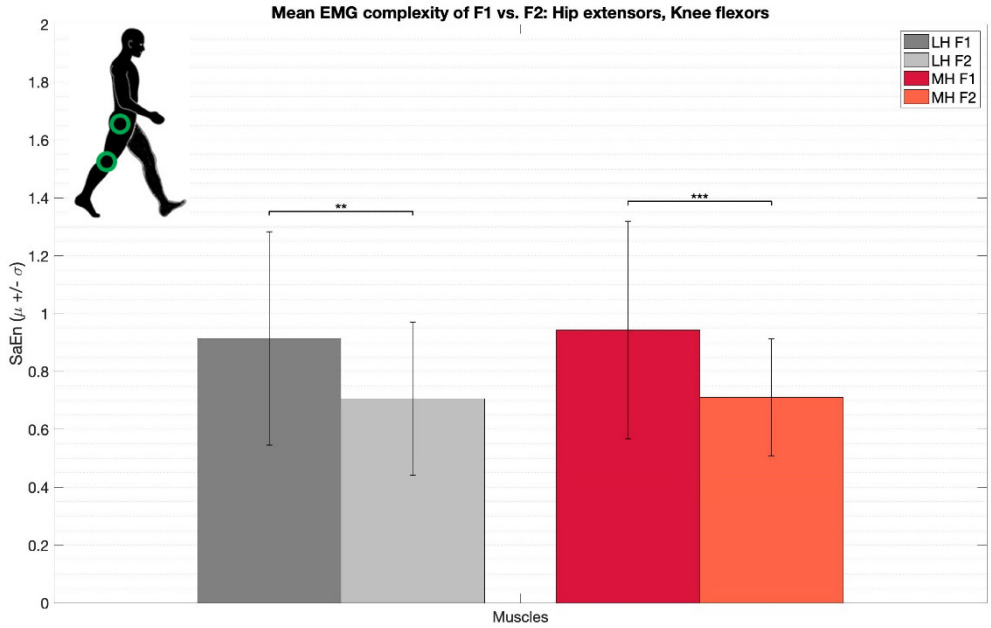

Figure 11b) Main effect velocity on entropy of hip extensor and knee flexor muscles (F1, F2) – *Adjacent bars* display *SaEn* values ($\mu \pm \sigma$) at 0.7*PWS (*F1*) vs. 1.6*PWS (*F2*) in symmetrical step tasks. Only old subjects were measured in *trials F1, F2* (N_{old} = 17). Results of muscles LH and MH are displayed, respectively. Significant entropy decreases with walking velocity were found in these muscles.

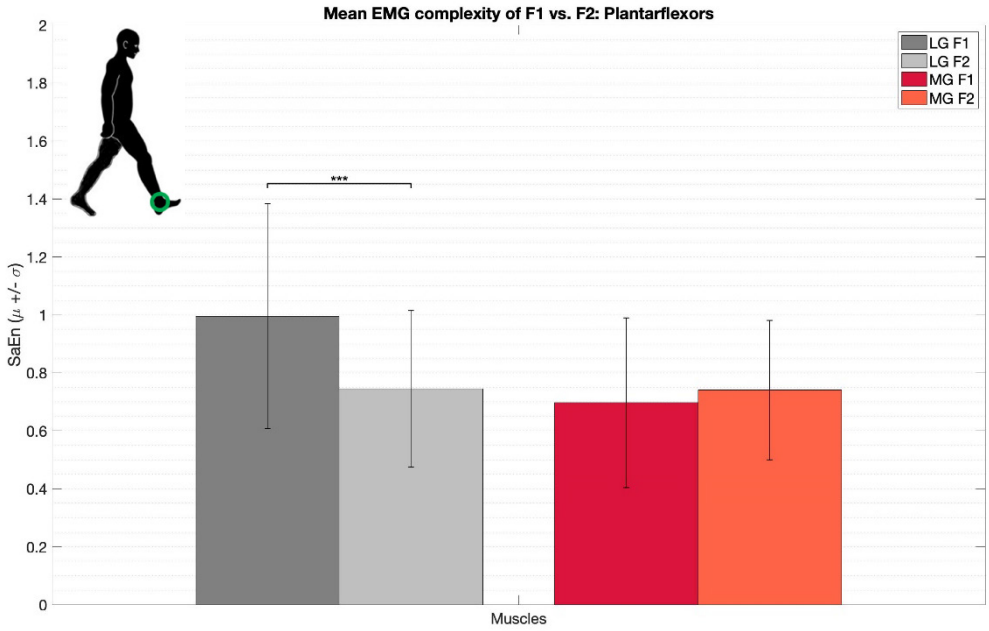

Figure 11c) Main effect velocity on entropy of plantar flexor muscles (F1, F2) – *Adjacent bars* display *SaEn* values ($\mu \pm \sigma$) at 0.7*PWS (*F1*) vs. 1.6*PWS (*F2*) in symmetrical step tasks. Only old subjects were measured in *trials F1, F2* (N_{old} = 17). Results of muscles LG and MG are displayed, respectively. Highly significant entropy decrease with walking velocity was found in the LG muscle.

GRF responses: complexity alteration with walking velocity and with age (Trials ANS, AFS)

In *scale 12* of GRF data, we assessed the main effect of the within-subject factor 'walking velocity'. Maulchy's test of sphericity was not violated for the main effects of this factor. Therefore, sphericity could be assumed. Here, one old subject was excluded from our analysis due to the lack of sufficient stride identifiers (N_{young} = 18, N_{old} = 18). The repeated measures ANOVA revealed a significant main effect of walking velocity on *SaEn* outcomes of GRF responses (*Table 5*). In turn, contrasts revealed that walking velocity increased GRF entropy in AP and VE components, while ML entropy decreased *(Figure 12)*. Entropy outcomes of AP, VE and ML GRF components altered with walking velocity with a high level of significance.

Consecutively, the main effect of the between-subject factor 'age' was not significant on *SaEn* outcomes of GRF responses. However, contrasts revealed age decreased ML entropy for short steps, while age increased ML entropy for long steps *(Figure 13)*.

Finally, the main effect for the interaction 'age*velocity' was not significant. In turn, contrasts revealed significant effects of the interaction per GRF component. Walking velocity caused larger decreases in GRF entropy for young subjects than for old subjects. This effect was found in long step VE (lsVE) and lsML components.

GRF (*SaEn*)	**Main effect 'velocity'**	**Main effect 'age'**	**Interaction 'vel*age'**
	$F_{(1,34)}$=4.841, p=.035	$F_{(1,34)}$=1.195, p=.282	$F_{(1,34)}$=.993, p=.326
Component	**Conditions: ANS vs. AFS**	**Subjects: Young vs. Old**	
ssAP	**$F_{(1,34)}$=16.376, p<.001**	$F_{(1,34)}$= .019, p=.891	$F_{(1,34)}$= .146, p=.705
ssVE	**$F_{(1,34)}$=13.176, p=.001**	$F_{(1,34)}$= .653, p=.425	$F_{(1,34)}$=1.616, p=.212
ssML	**$F_{(1,34)}$= 7.703, p=.009**	**$F_{(1,34)}$=8.626, p=.006**	**$F_{(1,34)}$=8.441, p=.006**
lsAP	**$F_{(1,34)}$=10.848, p=.002**	$F_{(1,34)}$= .000, p=.999	$F_{(1,34)}$=2.167, p=.150
lsVE	**$F_{(1,34)}$=10.286, p=.003**	$F_{(1,34)}$= .727, p=.400	**$F_{(1,34)}$=4.856, p=.034**
lsML	**$F_{(1,34)}$=21.996, p<.0001**	**$F_{(1,34)}$=5.525, p=.025**	**$F_{(1,34)}$=4.601, p=.039**

Table 5) GRF: main and interaction effects of velocity and age on entropy of asymmetrical step tasks – Main effects and contrasts of velocity, age and velocity*age on *SaEn* of GRF signals are given for trials *ANS, AFS* (N_{young} = 18, N_{old} = 18). Data components were separated per short step (ss) and per long step (ls), since ss and ls components were statistically different. Significant contrast effects are displayed in *bold.* The table represents one repeated measures ANOVA test.

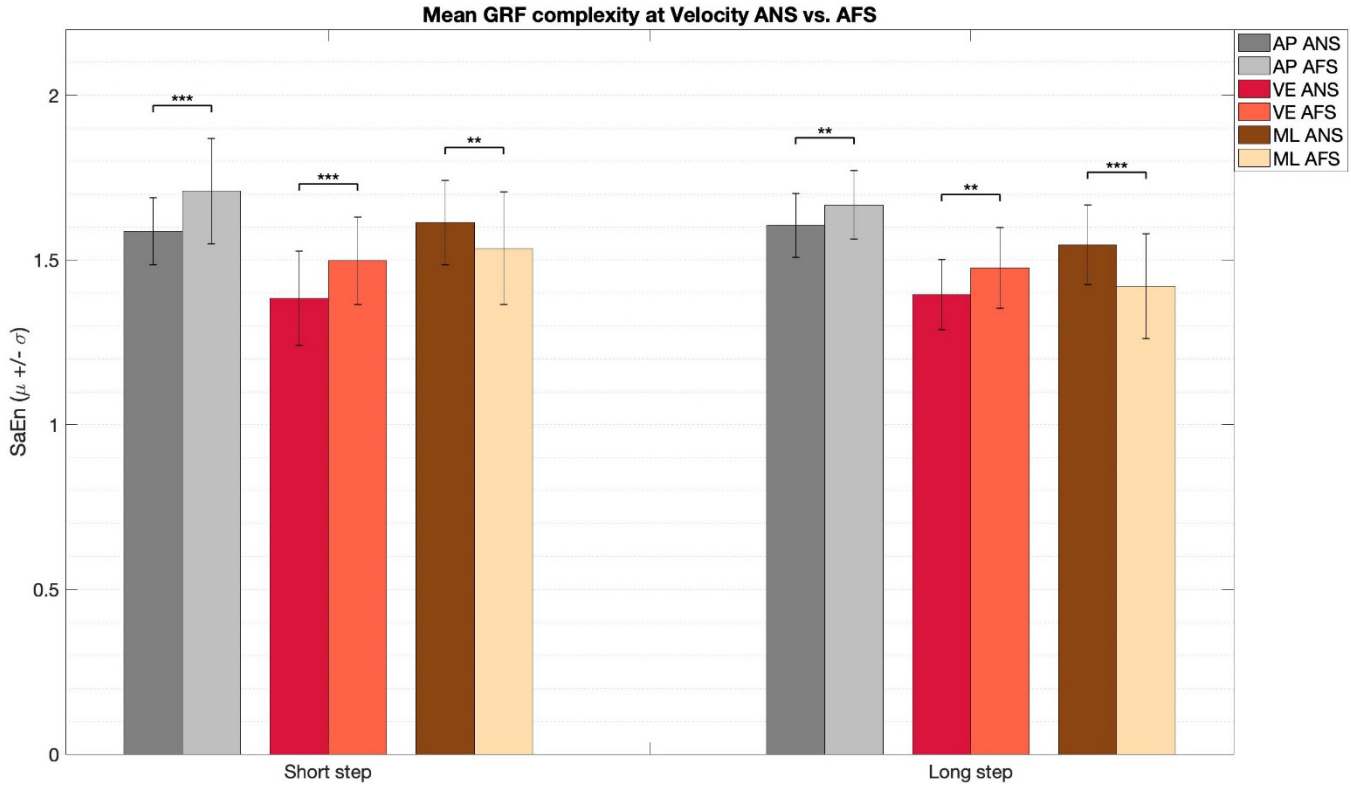

Figure 12) Main effect velocity on entropy of GRF components (ANS, AFS) – *Adjacent bars* display *SaEn* values ($\mu \pm \sigma$) at PWS (*ANS*) vs. 1.3*PWS (*AFS*) in asymmetrical step tasks. Data of young and old subjects were included in this analysis (N_{young} = 18, N_{old} = 18). Results of GRF components AP, VE and ML with short steps (*left*) and with long steps (*right*) are displayed, respectively. Short an long step AP and VE components displayed significant complexity increase with walking velocity, while the ML component displayed a significant decrease with walking velocity.

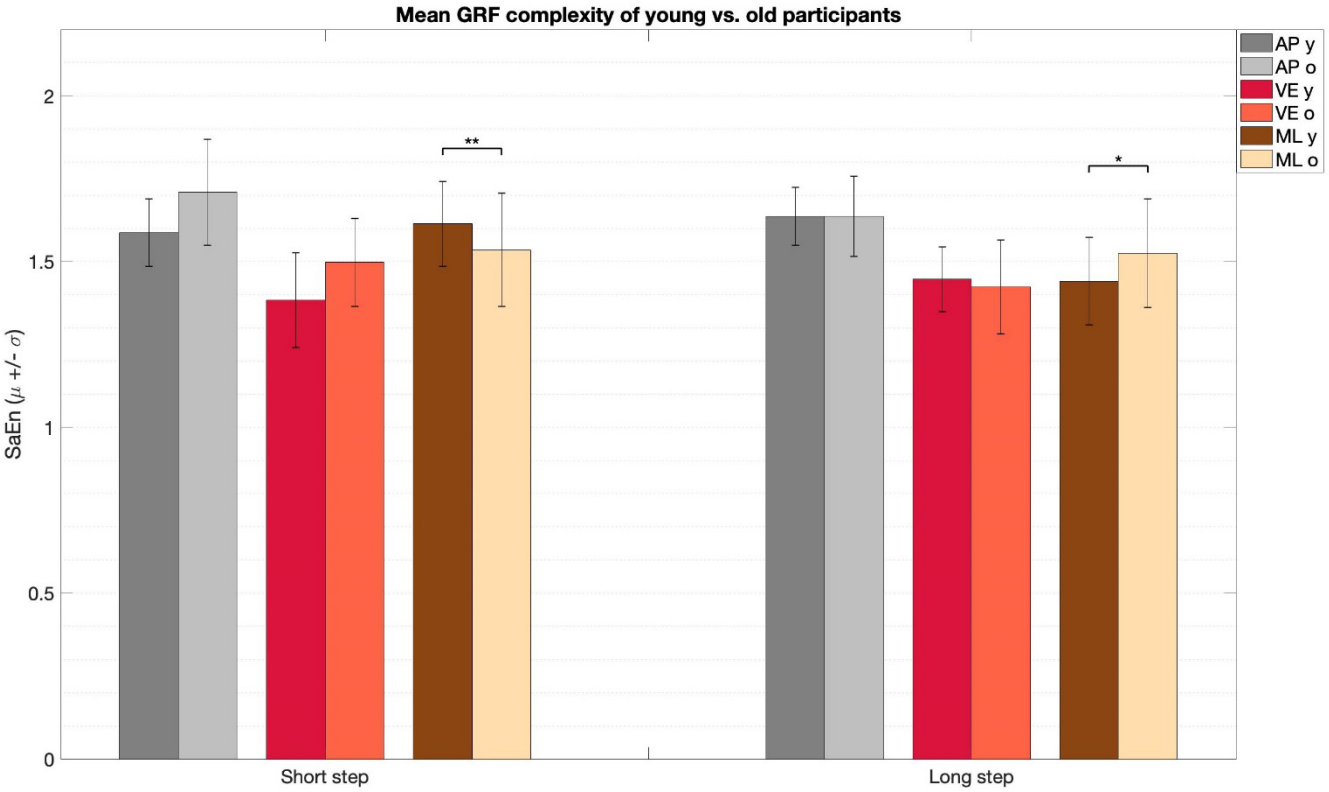

Figure 13) Main effect age on entropy of GRF components (ANS, AFS) – *Adjacent bars* display SaEn values ($\mu \pm \sigma$) of young vs. old subjects in asymmetrical step tasks. Data of trials *ANS* and *AFS* were included in the statistical analysis. Results of components AP, VE and ML with short steps (*left*) and with long steps (*right*) are displayed, respectively. ML components displayed significant decrease with age for short steps, and significant decrease with age for long steps.

GA responses: complexity alteration with walking velocity and with age (Trials ANS, AFS)

In *scale 14* of GA data, we assessed the main effect of within-subject factor 'walking velocity'. Maulchy's test of sphericity was not violated for the main effects of this factor. Therefore, sphericity was assumed. One old subject was excluded due to the lack of sufficient stride identifiers (N_{young} = 18, N_{old} = 18). The repeated measures ANOVA revealed a significant main effect of walking velocity on *SaEn* outcomes of GAs (*Table 6*). Contrasts revealed that walking velocity increased *SaEn* of short step AP components of the hip, knee and ankle. Subsequently, walking velocity increased long step AP components of the hip and knee *(Figure 14)*. Elevating walking velocity to 130%*PWS resulted in significant increased entropy in flexion-extension movements of the hip, knee and ankle. Entropy of abduction-adduction movements was unaffected.

Consecutively, the main effect of the between-subject factor 'age' was significant on *SaEn* outcomes of GAs. Contrasts revealed that age decreased *SaEn* for knee components lsAP, ssML, lsML and for ankle component lsAP *(Figure 15)*. Old subjects exhibited decreased entropy in flexion-extension and medial-lateral movements of the knee and in flexion-extension movements of the ankle.

Finally, main effects of the interaction 'age*velocity' were not significant. However, contrasts revealed significant effects of the interaction in the AP knee component for short steps, while the AP hip component for short steps just did not reach significance. Young subjects displayed equal entropy values with walking velocity in knee flexion-extension movements, while old subjects displayed increased entropy with walking velocity in this component.

GA (*SaEn*)	**Main effect 'velocity'**	**Main effect 'age'**	**Interaction 'vel*age'**
	$F_{(1,34)}$=10.201, p=.003	$F_{(1,34)}$=6.253, p=.017	$F_{(1,34)}$=.049, p=.827
Component	**Conditions: ANS vs. AFS**	**Subjects: Young vs. Old**	
AP ssHip	**$F_{(1,34)}$= 4.532, p=.041**	$F_{(1,34)}$= .845, p=.365	$F_{(1,34)}$=3.994, p=.054
AP ssKnee	**$F_{(1,34)}$= 5.405, p=.026**	$F_{(1,34)}$=3.826, p=.059	**$F_{(1,34)}$=5.707, p=.023**
AP ssAnkle	**$F_{(1,34)}$=15.144, p<.001**	$F_{(1,34)}$= .508, p=.481	$F_{(1,34)}$= .938, p=.340
AP lsHip	**$F_{(1,34)}$= 4.836, p=.035**	$F_{(1,34)}$= .361, p=.552	$F_{(1,34)}$= .024, p=.877
AP lsKnee	**$F_{(1,34)}$= 5.372, p=.027**	**$F_{(1,34)}$=7.157, p=.011**	$F_{(1,34)}$= .039, p=.845
AP lsAnkle	$F_{(1,34)}$= .541, p=.467	**$F_{(1,34)}$=4.836, p=.035**	$F_{(1,34)}$= .028, p=.869
ML ssHip	$F_{(1,34)}$= .906, p=.348	$F_{(1,34)}$=1.632, p=.210	$F_{(1,34)}$= .342, p=.563
ML ssKnee	$F_{(1,34)}$= 3.579, p=.067	**$F_{(1,34)}$=7.224, p=.011**	$F_{(1,34)}$=1.237, p=.274
ML ssAnkle	$F_{(1,34)}$= .079, p=.780	$F_{(1,34)}$= .008, p=.930	$F_{(1,34)}$= .348, p=.559
ML lsHip	$F_{(1,34)}$= .235, p=.631	$F_{(1,34)}$=1.780, p=.191	$F_{(1,34)}$= .016, p=.901
ML lsKnee	$F_{(1,34)}$= .159, p=.692	**$F_{(1,34)}$=7.096, p=.012**	$F_{(1,34)}$=2.282, p=.140
ML lsAnkle	$F_{(1,34)}$= .111, p=.741	$F_{(1,34)}$=1.592, p=.216	$F_{(1,34)}$=2.222, p=.145

Table 6) GA: main and interaction effects of velocity and age on entropy of asymmetrical step tasks – Main effects and contrasts of velocity, age and velocity*age on *SaEn* outcomes of GA signals are given for trials *ANS, AFS* (N_{young} = 18, N_{old} = 18). Data components were separated per short, long step, since results displayed that short and long step components were statistically different. Significant contrast effects are displayed in *bold.* The table represents one repeated measures ANOVA test.

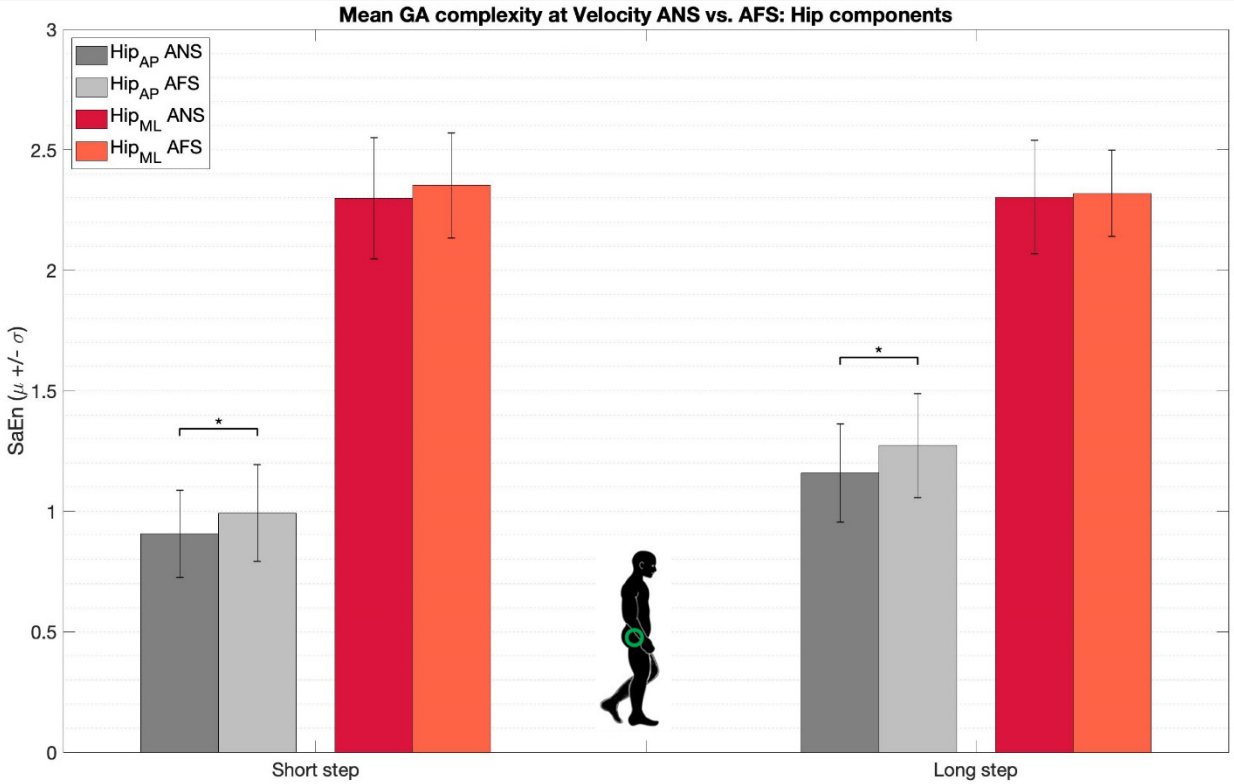

Figure 14a) Main effect velocity on entropy of hip GA components (ANS, AFS) – *Adjacent bars* display SaEn values ($\mu \pm \sigma$) at PWS (*ANS*) vs. 1.3*PWS (*AFS*) in asymmetrical step tasks. Data of young and old subjects was included in this analysis (N_{young} = 18, N_{old} = 18). Results of hip AP and ML components with short steps (*left*) and with long steps (*right*) are displayed, respectively. The hip AP component displayed significant entropy increase with walking velocity for both short and long steps.

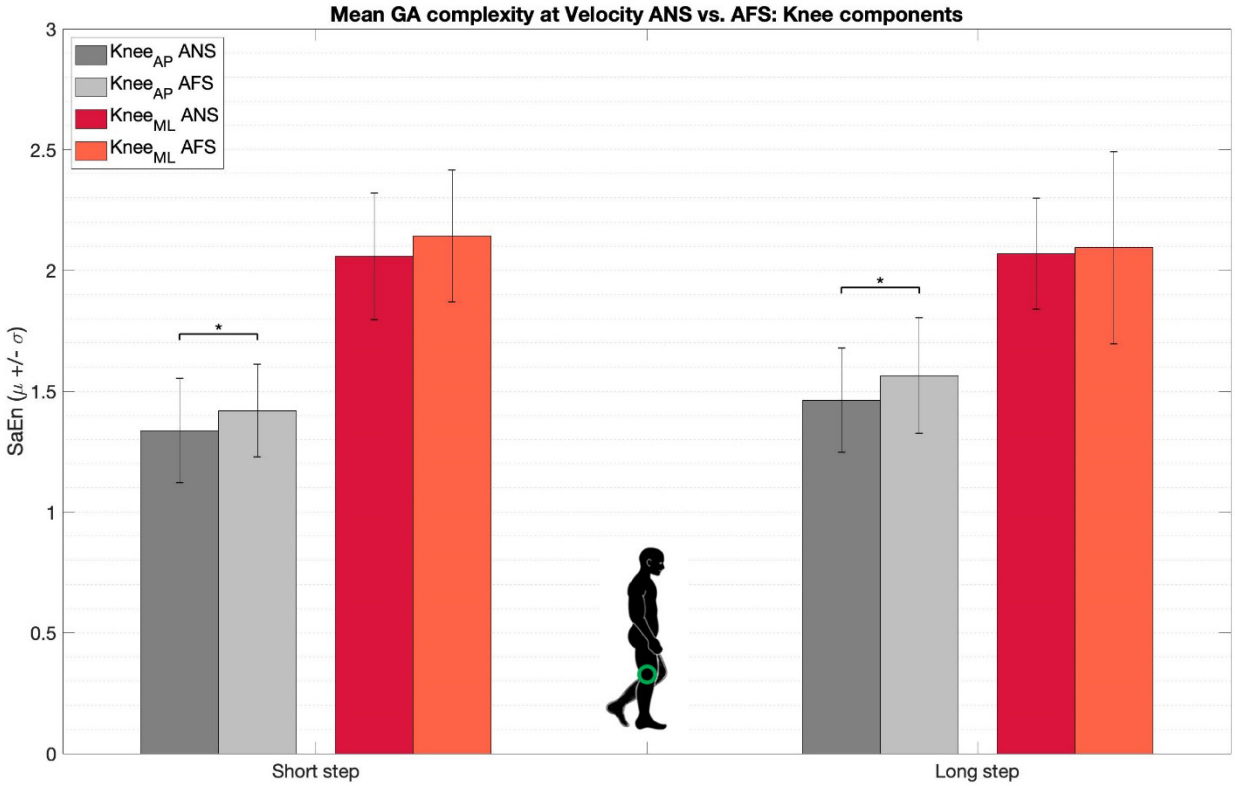

Figure 14b) Main effect velocity on entropy of knee GA components (ANS, AFS) – *Adjacent bars* display SaEn values ($\mu \pm \sigma$) at PWS (*ANS*) vs. 1.3*PWS (*AFS*) in asymmetrical step tasks. Data of young and old subjects was included in this analysis (N_{young} = 18, N_{old} = 18). Results of knee AP and ML components with short steps (*left*) and with long steps (*right*) are displayed, respectively. The knee AP component displayed significant entropy increase with walking velocity for both short and long steps.

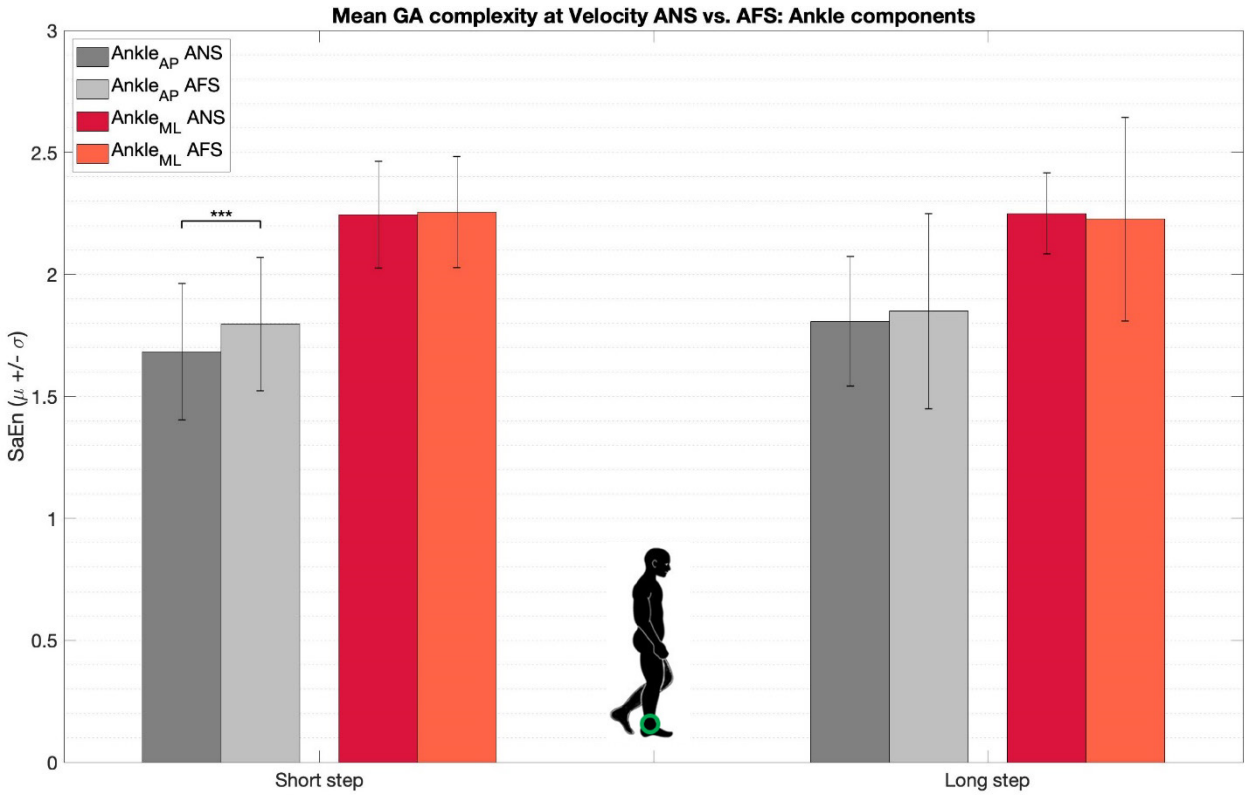

Figure 14c) Main effect velocity on entropy of ankle GA components (ANS, AFS) – *Adjacent bars* display SaEn values ($\mu \pm \sigma$) at PWS (*ANS*) vs. 1.3*PWS (*AFS*) in asymmetrical step tasks. Data of young and old subjects was included in this analysis (N_{young} = 18, N_{old} = 18). Results of ankle AP and ML components with short steps (*left*) and with long steps (*right*) are displayed, respectively. The ankle AP component displayed highly significant entropy increase with walking velocity for short step targets.

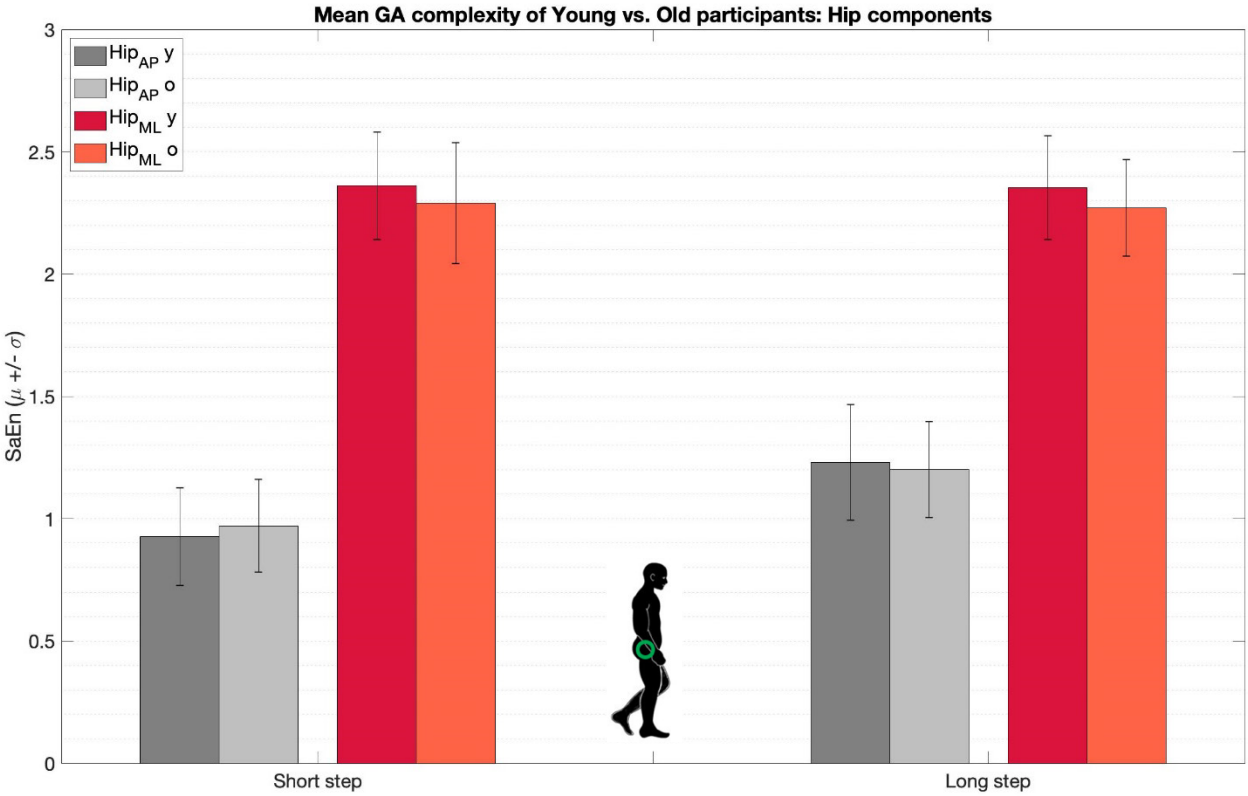

Figure 15a) Main effect age on entropy of hip GA components (ANS, AFS) – *Adjacent bars* display SaEn values ($\mu \pm \sigma$) of young vs. old subjects in asymmetrical step tasks. Data of trials *ANS* and *AFS* was included in the statistical analysis. Results of hip AP and ML components with short steps (*left*) and with long steps (*right*) are displayed, respectively. These GA components displayed no significant entropy alteration with age.

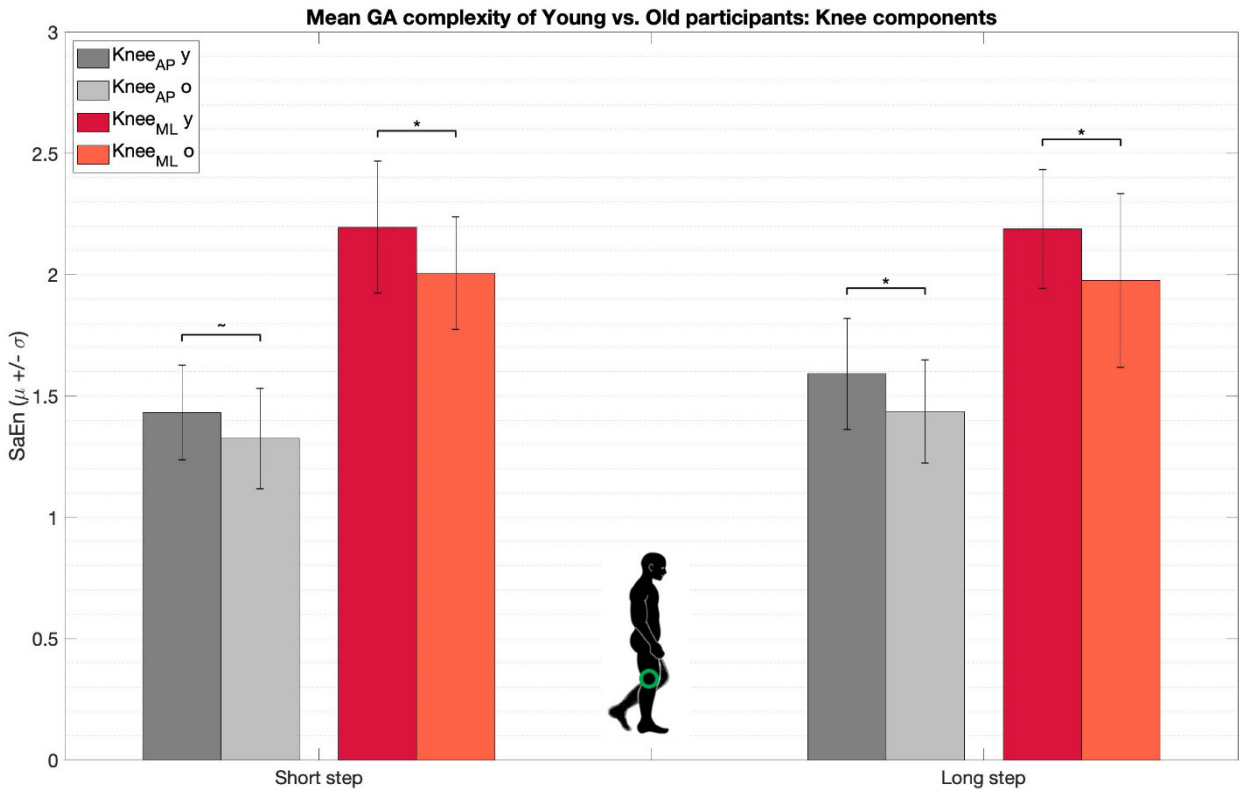

Figure 15b) Main effect age on entropy of knee GA components (ANS, AFS) – *Adjacent bars* display SaEn values ($\mu \pm \sigma$) of young vs. old subjects in asymmetrical step tasks. Data of trials *ANS* and *AFS* was included in the statistical analysis. Results of knee AP and ML components with short steps (*left*) and with long steps (*right*) are displayed, respectively. Knee ssML, lsAP and lsML components displayed significant entropy decrease with age. The knee ssAP component just did not reach significance.

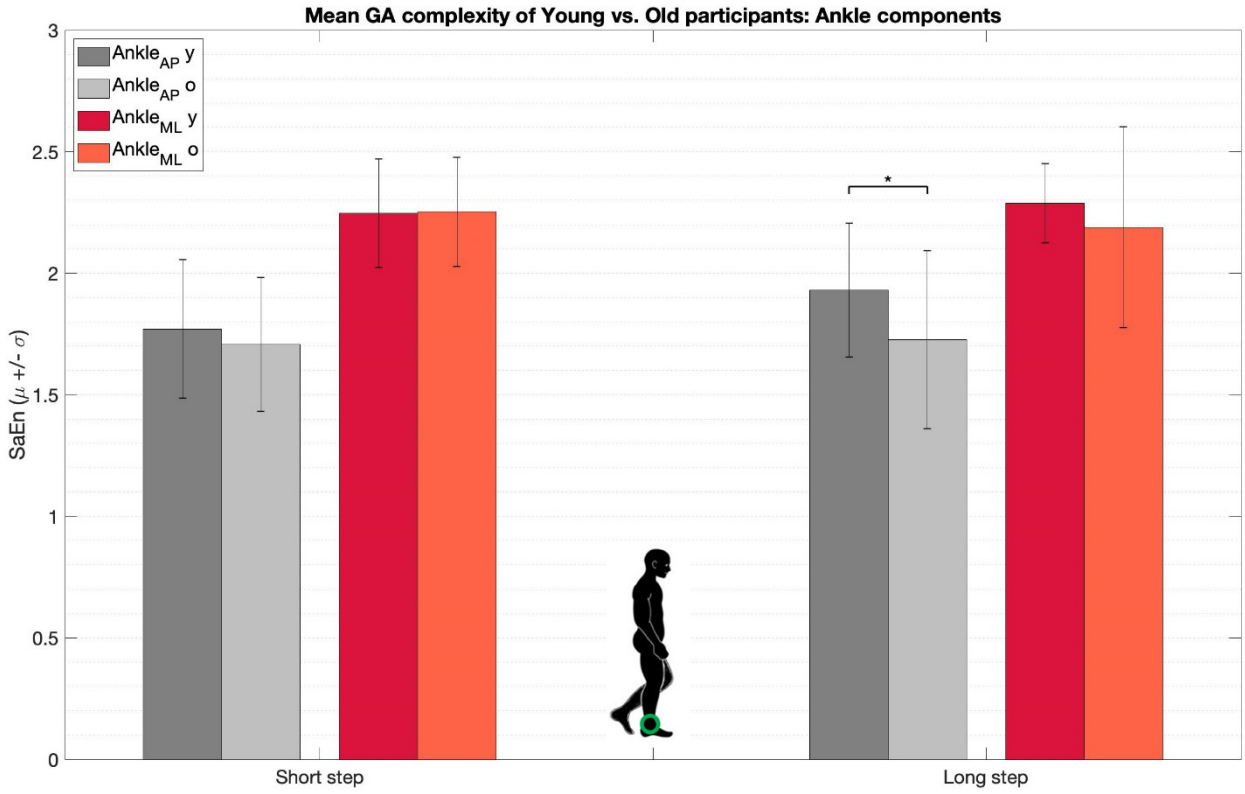

Figure 15c) Main effect age on entropy of ankle GA components (ANS, AFS) – *Adjacent bars* display SaEn values ($\mu \pm \sigma$) of young vs. old subjects in asymmetrical step tasks. Data of trials *ANS* and *AFS* was included in the statistical analysis. Results of knee AP and ML components with short steps (*left*) and with long steps (*right*) are displayed, respectively. The ankle AP component displayed significant entropy alteration with age for long step targets.

Discussion

In the present study, we showed that *Sample Entropy (SaEn)* is a sensitive measure for quantifying changes in human gait function. We investigated entropy changes in electromyography (EMG), ground reaction force (GRF) and joint angle (GA) time series of asymmetrical step tasks. We found that age increased EMG entropy in the medial hamstrings (MH) and medial gastrocnemius (MG). Consecutively, age decreased GRF entropy in the medial-lateral (ML) component for short steps and increased entropy for long steps. Lastly, age decreased GA entropy in knee and ankle components. Furthermore, we found that walking velocity decreased entropy in EMG signals. Consecutively, walking velocity increased GRF entropy in anterior-posterior (AP) and vertical (VE) components and decreased entropy in the medial-lateral (ML) component. Lastly, walking velocity increased entropy in GA signals. Additionally, we found that walking velocity decreased entropy in EMGs of older subjects, that performed symmetrical step tasks with step targets excluded.

EMG complexity alteration with walking velocity

EMG complexity of asymmetrical step tasks decreased with walking velocity for quadriceps and hamstring muscles subjected to short steps (ssRF, ssVM and ssLH). Similarly, complexity decreased for quadriceps and hamstrings muscles subjected to long steps (lsVL, lsRF, lsVM, lsLH and lsMH). Here, the gastrocnemius muscle did not display these changes. To substantiate on these findings, we identified literature that found complexity decreases in EMGs with walking velocity. These changes were exposed in quadriceps, hamstrings (Den Otter et al., 2004) and medial gastrocnemius muscles (Kang et al., 2016; Kang et al., 2006). However, these studies used symmetrical step tasks to assess these changes. For accurate asymmetrical stepping at different walking velocities, we speculate that appropriate flexion and extension movements of the hip and knee were crucial. This could explain the complexity changes found in the quadriceps and hamstrings muscles. In turn, the gastrocnemius is proposed to be mainly involved in foot lift off (Hamner et al., 2010). Decreased complexity in EMGs could be linked to optimization of the neuromotor system. In system theory, high complexity in system driver components (i.e.: EMG) is typically linked to system instability (Hamill et al., 1999; Masani et al., 2002). We speculate that high walking velocity introduced increased risk of system instability. Therefore, it can be reasoned that the hamstrings and quadriceps muscles optimally adapt to walking velocity and minimize complexity of muscle responses at high walking velocity. This leads to system stability and would eliminate the risk of falling while reaching task success (Kang et al., 2008; Liang et al., 2016; Yu et al., 2009).

To substantiate on the latter speculation, results of symmetrical step tasks of older subjects displayed that walking velocity lower than PWS led to high muscle complexity. Subsequently, walking velocity higher than PWS led to low muscle complexity (Hamill et al., 1999; Masani et al., 2002). Here, the medial head of the gastrocnemius did not display these changes. This stood in agreement with literature, that too showed these effects in EMGs of symmetrical step tasks (Kang et al., 2016; Kang et al., 2006). We suggest that walking at lower velocity than PWS allows for more muscle complexity while system stability is maintained. Subsequently, walking at high velocity allows for less muscle complexity. Fortunately, we identified a study that related system instability to signal complexity. This study showed that decreased GRF complexity is an indicator for fall risk in older subjects (Liang et al., 2016).

EMG complexity alteration with age

Medial hamstrings (MH) and medial gastrocnemius (MG) muscle responses increased in complexity with age for asymmetrical step tasks. Previous research by Kang and colleagues found a significant increase of MG EMG complexity with age, for symmetrical stepping (Kang et al., 2016). In literature, complexity changes with age are typically proposed to be caused by lower walking speed and increased neuromotor noise (Bisi et al., 2016; Kang et al., 2016; Kang et al., 2008; Liant et al., 2016; Masani et al., 2002; Pavei et al., 2019; Qiao et al., 2018; Zhang et al., 2019). Additional literature substantiates on this proposal, that displays complexity changes with age were found independent of walking velocity. Therefore, age-related factors other than walking velocity seem to contribute to the increased gait complexity (Kang et al., 2006). In turn, literature displays aged muscles introduce system instability (Bisi et al., 2016). In our case, we propose that greater EMG complexity with aging, may be a sign of muscle deterioration. High complexity found in the MH may be indicative of instability in knee flexion and hip extension movements. Similarly, high complexity in the MG may reflect instability of the propulsion movement of the foot.

Unfortunately, literature that assessed EMG complexity changes with age is still scarce. Therefore, we identified subsequent literature that assessed these changes with diseased states. We identified an exemplar study that contrasted complexity in leg muscle responses of cerebral palsy (CP) patients with healthy patients. Their study exposed increased complexity with disease in hamstrings muscles for normal walking (Tao et al., 2015). This complexity increase likely reflects substantial over-activation, abnormal synchronization and spasticity, as a result of brain injury following CP. In the study by Tao and colleagues, an increased complexity reflected system instability.

Additionally, we identified a study that contrasted lower extremity EMG responses of post-stroke patients with healthy adults (Chen et al., 2018). In the study by Chen and colleagues, subjects performed obstacle step tasks. Their results reported a complexity increase with stroke in the RF muscle. This increase was proposed to be linked to a reduced number of motor units, caused by stroke. In turn, the stepping task likely introduced these changes specifically in the RF muscle, because the stepping task required subjects to strongly flex the knee to pass obstacle tests.

Lastly, we identified literature that included healthy and Parkinson's disease (PD) patients, who performed isometric contractions. Results showed significant decreased complexity with PD in quadriceps and hamstrings muscles (Flood et al., 2019). Considering the above-mentioned results, we suggest that complexity changes in EMG responses can be linked to muscle health and to the task requirement. Therefore, we propose that evaluating EMG complexity information could be of particular interest to evaluate outcomes of medical interventions.

GRF complexity alteration with walking velocity

GRF complexity increased with walking velocity in anterior-posterior (AP), vertical (VE) and medial-lateral (ML) components subjected to short and long steps. Fortunately, these results stand in accordance with literature that assessed GRF complexity with walking velocity. In a study by Masani and colleagues, complexity of AP, VE and ML components was minimized for PWS (Masani et al., 2002). In turn, complexity increased when walking velocity was increased or decreased in contrast to PWS. These optimization phenomena suggest that we choose the most energetically efficient velocity when we walk. Subsequently, at PWS, the gait system seems to be most stable.

Additionally, we identified a study that measured AP and VE GRF components for skilled versus unskilled race-walking athletes. A study by Preatoni and colleagues found increased entropy in VE components for skilled race walkers (Preatoni et al., 2010). Typically, GRF outputs may be considered as the final outcome of the whole movement. Subsequently, we suspect that the complexity found in these outputs likely consists of random fluctuations and functional changes that are associated with properties of the neuromotor system. In our study and the study by Masani and colleagues, an increase in GRF complexity likely reflected energy expenditure, that seems to be minimized at PWS. In turn, in the study by Preatoni and colleagues, an increase in complexity reflected athletic performance. Therefore, we suggest that the physiological meaning assigned to complexity outcomes of GRFs, is strongly dependent on the experimental set-up.

GRF complexity alteration with age

ML GRF complexity decreased with age for short steps and increased with age for long steps. To understand the meaning of these results, we propose to connect GRF complexity results to results found in EMG responses. We found research that shows the MG muscle output is strongly related to inversion-eversion torques of the foot (Vieira et al., 2013). Consecutively, for asymmetrical step tasks, we speculate that foot torques were used to stabilize the leg. This stabilization was likely applied while the other leg was in swing phase to reach the next step target. We propose that the age effect found in complexity outcomes of the MG muscle, could explain the age effect found in the ML GRF component. These results indicate possible stepping strategies that were used by the subject. Subsequently, age is proposed as a factor that deteriorated this stepping strategy.

Additionally, a study by Zhang and colleagues assessed GRF complexity changes with age in running tasks. In these tasks, the complexity of AP and VE components was increased with age (Zhang et al., 2019). This study proposed that low GRF complexity reflected a controlled and well-coordinated running pattern. In turn, increased GRF complexity was linked to a loss of inter-segmental coordination and loss of smoothness of force production in running. Considering the above-mentioned GRF results, one could suggest that GRFs can be used to quantify healthy gait function. However, evaluating GRF information will not gain insights in the source of gait disabilities. Nevertheless, including analysis of GRF entropy could possibly be convenient for rehabilitation procedures, for example, to expose the movement outcome of disability (Liang et al., 2016; Masani et al., 2002).

GA complexity alteration with velocity

GA AP complexity increased with walking velocity in hip, knee and ankle components subjected to short steps. Subsequently, GA AP complexity increased with walking velocity in hip and knee components subjected to long steps. Here, the ML component did not alter with walking velocity. These complexity changes are likely correlated to the task requirement. The asymmetrical stepping tasks typically required subjects to make well-coordinated flexion-extension movements with their lower extremity joints. In particular, for short steps, it was crucial to stabilize the leg with the ankle. The other leg could then make a long swing phase motion that reached the long step target. As a consequence, ankle AP complexity increased with walking velocity for short steps. This is supported by our GRF results, that showed increased complexity in AP, ML and VE components. Subsequently, hip and knee AP complexities are increased with walking velocity for both short and long steps. This result can be explained by the larger forward leg propulsion, that was required to reach the step target at increased walking velocity. As for GRFs, we propose that GAs may be considered as the final outcome of the whole movement. Therefore, we expected some of their results could be linked.

To elaborate on the latter speculation, we identified additional studies that assessed complexity alteration of GAs. Firstly, a study by Georgoulis and colleagues measured healthy versus anterior cruciate ligament deficient (ACL) patients for normal walking tasks (Georgoulis et al., 2006). Their study displayed decreased complexity in the deficient knee, in contrast with the healthy knee. Here, low complexity reflected limited degrees of freedom (DOF) of knee motion. Consecutively, a study by Preatoni and colleagues measured skilled versus unskilled running athletes for running tasks (Preatoni et al., 2010). In their study, skilled athletes displayed increased entropy values at hip and ankle AP angles, in contrast with unskilled athletes. When we consider the results of GAs, we propose the physiological meaning of GA complexity strongly depends on the application. When disabilities are compared with healthy states, decreased complexity reflects limited DOF (Georgoulis et al., 2006). Consecutively, when race-walking is assessed, increased complexity in GAs reflects athletic performance (Preatoni et al., 2010).

GA complexity alteration with age

We found that complexity decreased with age in knee and ankle AP components for long steps. Subsequently, complexity decreased with age in the ML ankle component for short and long steps. Literature on this topic typically displays MH and MG muscles are crucial for coordinated knee and ankle flexion and extension movements (Beyer et al., 2019; Vieira et al., 2013). Therefore, we propose that the knee and ankle AP complexity decrease with age, could be linked to the increase found in MH and MG muscles. Similarly, complexity decrease with age in the knee ML component could be linked to changes found in the ML GRF component. Here, we speculate that decreased complexity of knee and ankle GA components, reflects limited DOF of older subjects. In turn, limited DOF is quantified by more regular GA outputs.

Unfortunately, literature on GA complexity alteration with aging is still scarce. We identified one exemplar study that applied perturbations to the hip during normal walking of young and old subjects. Results of the study by Qiao and colleagues found increased complexity for old subjects as a response to perturbations, in contrast with young subjects (Qiao et al., 2018). This characterized that the locomotor system of old subjects was more prone to destabilization by external disturbances. Collecting these results, proposes that complexity analysis of GA outputs could be convenient to expose physiological changes of joint movements with aging. Moreover, the results of GAs can be linked to the results found in EMGs and GRFs. In fact, including complexity analysis of these three datatypes in physical therapies, might help in unveiling functional changes in gait with aging or disease. Moreover, contrasting complexity outcomes of diseased states to healthy states in these data outputs, might help to optimize future physical therapies to improve gait function in an efficient manner.

Limitations

Firstly, we only analyzed changes with age and with walking velocity in the temporal resolution of EMGs, GRFs and GAs that maximized complexity. Here, we followed literature that suggested complexity changes with age and with disease are most prominently expressed in the selected temporal resolution (Kang et al., 2006; McIntosh et al., 2018; McIntosh et al., 2010; Kaplanis et al., 2012). Unfortunately, human gait studies that assess *SaEn* changes with age over a broad temporal resolution range are still limited. In our study, EMG, GRF and GA frequency power was maximized in the *[10-300] Hz*, *[5-20] Hz* and *[0-20] Hz* range, respectively. Evaluating *SaEn* changes with age in temporal resolutions that represent these frequencies, would help to approve a possible optimal data scale range to expose changes in healthy gait function with age and with disease. In fact, investigating this scale range could be of particular interest for clinicians. For example, knowing which frequencies to target with *SaEn,* could help in monitoring the improvement of gait function after stroke in an efficient manner (Harbourne et al., 2009). Alternatively, to investigate changes in human movement, *SaEn* might be evaluated in temporal scales that reflect human motion. For example, in the *[0-10] Hz* frequency range of GRFs and GAs. We therefore suggest that future gait studies should investigate entropy changes with age and with disease for additional temporal resolutions, that could help define possible future clinical applications for the *SaEn* algorithm.

Secondly, our study is limited in that we only considered *SaEn* values of the first 20 scales of the passband of the analyzed signals. We considered EMG frequencies *25-500 Hz*, GRF frequencies *1-20 Hz* and GA frequencies of *0.5-10 Hz*. This limitation was introduced by the limited available stride identifiers in many subjects. To overcome the entropy dataset length bias, we analyzed an equal amount of gait phases and data samples for all subjects. In turn, we excluded data that had insufficient identifiers available per condition. In trials *ANS* and *AFS,* EMG, GRF and GA data satisfied the minimum amount of dataset length *(N > 100)*. However, in trials *F1* and *F2*, GRF and GA data did not satisfy the requirement (Yentes et al., 2013). Therefore, we excluded these datatypes from entropy analysis in these trials. To counter the entropy dataset length bias, we therefore recommend that future entropy studies check the sample frequencies of the equipment beforehand. Subsequently, the minimum required dataset length of the entropy algorithm should be checked. Finally, sufficient recording times should be selected.

Thirdly, in our complexity analyses we used input parameter *r=0.1* for *SaEn*. This parameter determined the criterion for finding similarity in complexity calculations *(Appendix A3)*. Here, we followed literature that suggested that the *r* that maximized entropy outcomes, defined as r_{max}, is the best *r* value to choose. The value of entropy obtained by r_{max} would then quantify the highest information difference between segments. More importantly, this r_{max} would allow to account for more of the signal complexity than other values of *r* (Chen et al., 2018; Castiglioni et al., 2008). Important to note, however, is that the correct choosing of *r* is still discussed in literature. Recent studies propose the *r*-value should lie in the range of *0.01-0.25*. These studies include human hormonal processes (Pincus et al., 1991b; Pincus et al., 1992), ECG data (Castiglioni et al., 2008), respiratory signals (Chen et al., 2018) and gait data (Yentes et al., 2013). Our results are limited in that we only evaluated results for the range of *r = [0.1-0.2]*. Subsequently, we found an increased level of statistical significance with age for r_{max} (*r=0.1),* in contrast with other values of *r* in this range. In this document we only included the data generated by r_{max}.

Lastly, our results might be limited in that we determined *SaEn* of EMGs, GRFs and GAs that were recorded on a treadmill in the 'fixed speed' setting *(trial 0-4).* Here, literature identified that the natural complexity found in kinematics might be slightly biased towards regularity in a 'fixed speed' treadmill setting, when compared to a 'self-paced' setting. Fortunately, differences in kinematics between the two settings were small and were proposed to be clinically irrelevant (Sloot et al., 2014). Additional research should confirm whether EMGs and GRFs are found indifferent in the two treadmill settings. Subsequently, treadmills can alter the natural complexity of gait outputs when compared to gait outputs of overground walking. Literature proposed that after 6 minutes of treadmill familiarization, joint kinematics are found indifferent from overground walking (Papegaaij et al., 2017). Fortunately, this requirement was satisfied in the recordings of our dataset. However, we suggest that future studies should investigate this phenomenon in EMGs and GRFs. Therefore, our results might be limited, in that we analyzed treadmill gait data instead of overground gait data. Last but not least, subjects that performed walking tasks with step targets included in *trial 1-2*, were provided with auditory feedback. Here, our results are limited, in that auditory feedback might have distorted gait outputs. In literature, we found that gait outputs are altered with visual feedback (Kim et al., 2012). Therefore, we suggest future studies should investigate gait outputs without feedback (open-loop) versus with feedback (closed-loop), to confirm this limitation.

Strength of our data and future directions

To date, research of biomechanics and motor control discussed whether entropy algorithms could be used to characterize healthy gait function and to evaluate outcomes of physical therapies (Lipsitz et al., 1992; Morrison et al., 2012; Stergiou et al., 2006). Therefore, conducting the present study was useful. We exhibited entropy changes with age and with walking velocity in EMGs, GRFs and GAs of asymmetrical step tasks. As a secondary goal, we showed which datatype most prominently expressed entropy changes with age. In EMG data, MH and MG muscles showed increased entropy with age with a high level of significance. These complexity changes were likely linked to muscle health and to the task requirement (Kang et al., 2016; Lipsitz et al., 1996). In GRFs and GAs, we found decreased entropy with age with a lower level of significance. Our results, and results of others (Lipsitz et al., 1992; Pincus et al., 2006; Smith et al., 2011), demonstrate the feasibility of entropy algorithms for quantifying healthy gait function in medical interventions. We suggest additional research should add on these results, that could help define a possible physiological entropy standard for healthy gait function. Subsequently, we suggest that future gait rehabilitation therapies could use entropy of EMGs to investigate the source of gait disabilities and to monitor the progression of rehabilitation. Additionally, GRFs and GAs could be included in the analysis, to help identify the movement outcome of the disability.

Secondly, the present study made a difference in entropy analysis. We showed that *SaEn* has its limits. In our supplementary material, we assessed *SaEn*'s dependency on the number of samples of the interpreted dataset. We portrayed these effects for regular and erratic data (*Appendix A3*). As a result, we accounted for the entropy dataset length bias by extracting an equal amount of gait phases per subject. We normalized all subjects to a fixed number of samples with a shape preserving spline algorithm (Coutinho et al., 2017; Eng et al., 2007; Lencioni et al., 2017; Marateb et al., 2016; Unser et al., 1999). Subsequently, we discovered literature that did not account for the entropy dataset length bias. These studies considered entropy analysis of EMG (Kang et al., 2016; Rathleff et al., 2011; Tao et al., 2015), of accelerometry (Bisi et al., 2016; Clermont et al., 2016; Lammoth et al., 2010; Lee et al., 2010; Tochigi et al., 2012), of GRFs (Preatoni et al., 2010; Zhang et al., 2019) and of EEG data (Chung et al., 2013; McIntosh et al., 2018; McIntosh 2010). Therefore, we suggest future entropy studies should account for the dataset length bias.

At the current stage of entropy research in medical interventions, we suspect a promising future lies ahead. An elegant example of promising research can be found in current neurology studies. These studies exhibited increased entropy of EEGs in patients with dementia in contrast with patients who remained dementia-free. Consecutively, these studies suggested that entropy algorithms could help to identify individuals at risk for dementia in early stages of the disease (Bertrand et al., 2016; McIntosh et al., 2018). Additional research exposed neural disturbances in EEGs with entropy, that were associated with the development of Alzheimer's (Maturana-Candelas et al., 2019). Lasty, entropy research exhibited an effective non-invasive discrimination technique, that separated healthy patients from neuromuscular disorder patients (Kaplanis et al., 2010, Vallejo et al., 2018). Conducting additional research on these subjects could confirm interesting future clinical applications for entropy algorithms.

Acknowledgements

I would like to thank Dr.ir. Alfred Schouten, Dr.ir. Winfred Mugge, Dr.ir. Jurriaan de Groot and Dr. Marjon Stijntjes for their supervision and for their help in finding the dataset for this research. Especially during the ongoing COVID-19 pandemic, I sincerely appreciate their invested time and their encouraging attitude. Their help guided me through this challenging period. Moreover, I sincerely thank Marjolein Booij for recording the dataset and for her help in the process of this research. This research was supported by the TUDelft, LUMC and VUmc.

References

Ahmad, S., Tejuja, A., Newman, K. D., Zarychanski, R., & Seely, A. J. (2009). Clinical review: a review and analysis of heart rate complexity and the diagnosis and prognosis of infection. *Critical Care*, *13*(6), 232.

Ahmed, M. U., & Mandic, D. P. (2011a). Multivariate multiscale entropy analysis. *IEEE Signal Processing Letters*, *19*(2), 91-94.

Ahmed, M. U., & Mandic, D. P. (2011b). Multivariate multiscale entropy: A tool for complexity analysis of multichannel data. *Physical Review E*, *84*(6), 061918

Aarts, L., Papegaaij, S., Steenbrink, F., & Martens, P. (2018). Quality of treadmill embedded force plates for gait analysis.

Bertrand, J. A., McIntosh, A. R., Postuma, R. B., Kovacevic, N., Latreille, V., Panisset, M., ... & Gagnon, J. F. (2016). Brain Connectivity Alterations Are Associated with the Development of Dementia in Parkinson's Disease. *Brain connectivity*, *6*(3), 216-224.

Beyer, E. B., Lunden, J. B., & Giveans, M. R. (2019). Medial and lateral hamstrings response and force production at varying degrees of knee flexion and tibial rotation in healthy individuals. *International journal of sports physical therapy*, *14*(3), 376.

Bisi, M. C., & Stagni, R. (2016). Complexity of human gait pattern at different ages assessed using multiscale entropy: from development to decline. *Gait & posture*, *47*, 37-42.

Busa, M. A., & van Emmerik, R. E. (2016). Multiscale entropy: A tool for understanding the complexity of postural control. *Journal of Sport and Health Science*, *5*(1), 44-51.

Bogen, B., Aaslund, M. K., Ranhoff, A. H., & Moe-Nilssen, R. (2019). Two-year changes in gait complexity in community-living older adults. *Gait & posture*.

Castiglioni, P., & Di Rienzo, M. (2008, September). How the threshold “r” influences approximate entropy analysis of heart-rate complexity. In *2008 Computers in Cardiology* (pp. 561-564). IEEE.

Cavanaugh, J. T., Guskiewicz, K. M., Giuliani, C., Marshall, S., Mercer, V., & Stergiou, N. (2005). Detecting altered postural control after cerebral concussion in athletes with normal postural stability. *British journal of sports medicine*, *39*(11), 805-811.

Chen, Y., Hu, H., Ma, C., Zhan, Y., Chen, N., Li, L., & Song, R. (2018). Stroke-related changes in the complexity of muscle activation during obstacle crossing using fuzzy approximate entropy analysis. *Frontiers in neurology*, *9*, 131.

Chen, X., Solomon, I. C., & Chon, K. H. (2008). Parameter selection criteria in approximate entropy and sample entropy with application to neural respiratory signals. *Am. J. Physiol. Regul. Integr. Comp. Physiol., to be published*.

Chung, C. C., Kang, J. H., Yuan, R. Y., Wu, D., Chen, C. C., Chi, N. F., ... & Hu, C. J. (2013). Multiscale entropy analysis of electroencephalography during sleep in patients with Parkinson disease. *Clinical EEG and neuroscience*, *44*(3), 221-226.

Clermont, C. A., & Barden, J. M. (2016). Accelerometer-based determination of gait complexity in older adults with knee osteoarthritis. *Gait & posture*, *50*, 126-130.

Coates, L., Shi, J., Rochester, L., Del Din, S., & Pantall, A. (2020). Entropy of Real-World Gait in Parkinson’s Disease Determined from Wearable Sensors as a Digital Marker of Altered Ambulatory Behavior. *Sensors*, *20*(9), 2631.

Costa, M., Goldberger, A. L., & Peng, C. K. (2005). Multiscale entropy analysis of biological signals. *Physical review E*, *71*(2), 021906.

Costa, M., Goldberger, A. L., & Peng, C. K. (2002). Multiscale entropy analysis of complex physiologic time series. *Physical review letters*, *89*(6), 068102.

Costa, M., Peng, C. K., Goldberger, A. L., & Hausdorff, J. M. (2003). Multiscale entropy analysis of human gait dynamics. *Physica A: Statistical Mechanics and its applications*, *330*(1-2), 53-60.

Coutinho, E., van Peer, J., Grandjean, D., & Scherer, K. R. (2017). Emotion-Antecedent Appraisal Checks: EEG and EMG datasets for Novelty and Pleasantness [Data set].

De David, A. C., Carpes, F. P., & Stefanyshyn, D. (2015). Effects of changing speed on knee and ankle joint load during walking and running. *Journal of sports sciences*, *33*(4), 391-397.

Delgado-Bonal, A., & Marshak, A. (2019). Approximate entropy and sample entropy: A comprehensive tutorial. *Entropy*, *21*(6), 541.

De Luca, C. J. (1997). The use of surface electromyography in biomechanics. *Journal of applied biomechanics*, *13*(2), 135-163.

Den Otter, A. R., Geurts, A. C. H., Mulder, T., & Duysens, J. (2004). Speed related changes in muscle activity from normal to very slow walking speeds. *Gait & posture*, *19*(3), 270-278.

Eng, F., & Gustafsson, F. (2007, September). Algorithms for downsampling non-uniformly sampled data. In *2007 15th European Signal Processing Conference* (pp. 1965-1969). IEEE.

Flood, M. W., Jensen, B. R., Malling, A. S., & Lowery, M. M. (2019). Increased EMG intermuscular coherence and reduced signal complexity in Parkinson's disease. *Clinical neurophysiology*, *130*(2), 259-269.

Georgoulis, A. D., Moraiti, C., Ristanis, S., & Stergiou, N. (2006). A novel approach to measure complexity in the anterior cruciate ligament deficient knee during walking: the use of the approximate entropy in orthopaedics. *Journal of clinical monitoring and computing*, *20*(1), 11-18.

Goldberger, A. L., Peng, C. K., & Lipsitz, L. A. (2002). What is physiologic complexity and how does it change with aging and disease?. *Neurobiology of aging*, *23*(1), 23-26.

Gruber, A. H., Edwards, W. B., Hamill, J., Derrick, T. R., & Boyer, K. A. (2017). A comparison of the ground reaction force frequency content during rearfoot and non-rearfoot running patterns. *Gait & posture*, *56*, 54-59.

Hamill, J., van Emmerik, R. E., Heiderscheit, B. C., & Li, L. (1999). A dynamical systems approach to lower extremity running injuries. *Clinical biomechanics*, *14*(5), 297-308.

Hamner, S. R., Seth, A., & Delp, S. L. (2010). Muscle contributions to propulsion and support during running. *Journal of biomechanics*, *43*(14), 2709-2716.

Harbourne, R. T., & Stergiou, N. (2009). Movement complexity and the use of nonlinear tools: principles to guide physical therapist practice. *Physical therapy*, *89*(3), 267-282.

Hausdorff, J. M. (2005). Gait complexity: methods, modeling and meaning. *Journal of neuroengineering and rehabilitation*, *2*(1), 19.

Hof, A. L., Elzinga, H., Grimmius, W., & Halbertsma, J. P. K. (2002). Speed dependence of averaged EMG profiles in walking. *Gait & posture*, *16*(1), 78-86.

Jordan, K., Challis, J. H., & Newell, K. M. (2007). Walking speed influences on gait cycle complexity. *Gait & posture*, *26*(1), 128-134.

Kang, H. G., & Dingwell, J. B. (2016). Differential changes with age in multiscale entropy of electromyography signals from leg muscles during treadmill walking. *PloS one*, *11*(8), e0162034.

Kang, H. G., & Dingwell, J. B. (2009). Dynamics and stability of muscle activations during walking in healthy young and older adults. *Journal of biomechanics*, *42*(14), 2231-2237.

Kang, H. G., & Dingwell, J. B. (2008). Separating the effects of age and walking speed on gait complexity. *Gait & posture*, *27*(4), 572-577.

Kaplanis, P. A., Pattichis, C. S., & Zazula, D. (2010). Multiscale entropy-based approach to automated surface EMG classification of neuromuscular disorders. *Medical & biological engineering & computing*, *48*(8), 773-781.

Kavanagh, J. J. (2009). Lower trunk motion and speed-dependence during walking. *Journal of neuroengineering and rehabilitation*, *6*(1), 9.

Kibushi, B., Hagio, S., Moritani, T., & Kouzaki, M. (2018). Speed-dependent modulation of muscle activity based on muscle synergies during treadmill walking. *Frontiers in human neuroscience*, *12*, 4.

Kim, S. J., & Krebs, H. I. (2012). Effects of implicit visual feedback distortion on human gait. *Experimental brain research*, *218*(3), 495-502.

Kwon, J. W., Son, S. M., & Lee, N. K. (2015). Changes of kinematic parameters of lower extremities with gait speed: a 3D motion analysis study. *Journal of Physical Therapy Science*, *27*(2), 477-479.

Lamoth, C. J., Ainsworth, E., Polomski, W., & Houdijk, H. (2010). Complexity and stability analysis of walking of transfemoral amputees. *Medical engineering & physics*, *32*(9), 1009-1014

Lee, J. B., Sutter, K. J., Askew, C. D., & Burkett, B. J. (2010). Identifying symmetry in running gait using a single inertial sensor. *Journal of Science and Medicine in Sport*, *13*(5), 559-563.

Lencioni, T., Carpinella, I., Rabuffetti, M., Marzegan, A., & Ferrarin, M. (2019). Human kinematic, kinetic and EMG data during different walking and stair ascending and descending tasks. *Scientific data*, *6*(1), 1-10.

Liang, S., Jia, H., Li, Z., Li, H., Gao, X., Ma, Z., ... & Zhao, G. (2016, August). Fall risk factors analysis based on sample entropy of plantar kinematic signal during stance phase. In *2016 38th Annual International Conference of the IEEE Engineering in Medicine and Biology Society (EMBC)* (pp. 4832-4836). IEEE.

Lipsitz, L. A., & Goldberger, A. L. (1992). Loss of 'complexity' and aging: potential applications of fractals and chaos theory to senescence. *Jama*, *267*(13), 1806-1809.

Lu, S., Chen, X., Kanters, J. K., Solomon, I. C., & Chon, K. H. (2008). Automatic selection of the threshold value $ r $ for approximate entropy. *IEEE Transactions on Biomedical Engineering*, *55*(8), 1966-1972.

Madeleine, P., & Madsen, T. M. T. (2009). Changes in the amount and structure of motor complexity during a deboning process are associated with work experience and neck–shoulder discomfort. *Applied Ergonomics*, *40*(5), 887-894.

Marateb, H. R., Farahi, M., Rojas, M., Mañanas, M. A., & Farina, D. (2016). Detection of multiple innervation zones from multi-channel surface EMG recordings with low signal-to-noise ratio using graph-cut segmentation. *PLoS One*, *11*(12), e0167954.

Masani, K., Kouzaki, M., & Fukunaga, T. (2002). Complexity of ground reaction forces during treadmill walking. *Journal of Applied Physiology*, *92*(5), 1885-1890.

Maturana-Candelas, A., Gómez, C., Poza, J., Pinto, N., & Hornero, R. (2019). EEG characterization of the Alzheimer's disease continuum by means of multiscale entropies. *Entropy*, *21*(6), 544.

McCamley, J. D., Denton, W., Arnold, A., Raffalt, P. C., & Yentes, J. M. (2018). On the calculation of sample entropy using continuous and discrete human gait data. *Entropy*, *20*(10), 764.

McCrum, C., Lucieer, F., van de Berg, R., Willems, P., Fornos, A. P., Guinand, N., ... & Meijer, K. (2019). The walking speed-dependency of gait complexity in bilateral vestibulopathy and its association with clinical tests of vestibular function. *Scientific Reports*, *9*(1), 1-12.

McGregor, S. J., Busa, M. A., Skufca, J., Yaggie, J. A., & Bollt, E. M. (2009). Control entropy identifies differential changes in complexity of walking and running gait patterns with increasing speed in highly trained runners. *Chaos: An Interdisciplinary Journal of Nonlinear Science*, *19*(2), 026109.

McIntosh, A. R. (2018). Neurocognitive aging and brain signal complexity. *bioRxiv*, 259713.

McIntosh, A. R., Kovacevic, N., Lippe, S., Garrett, D., Grady, C., & Jirsa, V. (2010). The development of a noisy brain. *Archives italiennes de biologie*, *148*(3), 323-337.

McIntosh, A. R., Vakorin, V., Kovacevic, N., Wang, H., Diaconescu, A., & Protzner, A. B. (2014). Spatiotemporal dependency of age-related changes in brain signal complexity. *Cerebral Cortex*, *24*(7), 1806-1817.

Monaco, V., Rinaldi, L. A., Macrì, G., & Micera, S. (2009). During walking elders increase efforts at proximal joints and keep low kinetics at the ankle. *Clinical biomechanics*, *24*(6), 493-498.

Montesinos, L., Castaldo, R., & Pecchia, L. (2018). On the use of approximate entropy and sample entropy with centre of pressure time-series. *Journal of neuroengineering and rehabilitation*, *15*(1), 116.

Morrison, S., & Newell, K. M. (2012). Aging, neuromuscular decline, and the change in physiological and behavioral complexity of upper-limb movement dynamics. *Journal of aging research*, *2012*.

Murray, M. P., Mollinger, L. A., Gardner, G. M., & Sepic, S. B. (1984). Kinematic and EMG patterns during slow, free, and fast walking. *Journal of Orthopaedic Research*, *2*(3), 272-280

Overbeek, C. L., Geurkink, T. H., de Groot, F. A., Klop, I., Nagels, J., Nelissen, R. G., & de Groot, J. H. (2020). Shoulder movement complexity in the ageing shoulder: a cross-sectional analysis and reliability assessment. *Journal of Orthopaedic Research®*.

Papegaaij, S., & Steenbrink, F. (2017). Clinical gait analysis: Treadmill-based vs overground. *Motek Inc.: Amsterdam, The Netherlands*.

Pavei, G., Cazzola, D., Torre, A. L., & Minetti, A. E. (2019). Race Walking Ground Reaction Forces at Increasing Speeds: A Comparison with Walking and Running. *Symmetry*, *11*(7), 873.

Pietraszewski, B., Winiarski, S., & Jaroszczuk, S. (2012). Three-dimensional human gait pattern–reference data for normal men. *Acta of Bioengineering and Biomechanics*, *14*(3), 9-16.

Pincus, S. M. (2006). Approximate entropy as a measure of irregularity for psychiatric serial metrics. *Bipolar disorders*, *8*(5p1), 430-440.

Pincus, S. M. (1991b). Approximate entropy as a measure of system complexity. *Proceedings of the National Academy of Sciences*, *88*(6), 2297-2301.

Pincus, S. M. (2000). Approximate entropy in cardiology. *Herzschrittmachertherapie und Elektrophysiologie*, *11*(3), 139-150.

Pincus, S. M., & Goldberger, A. L. (1994). Physiological time-series analysis: what does regularity quantify?. *American Journal of Physiology-Heart and Circulatory Physiology*, *266*(4), H1643-H1656.

Pincus, S. M., & Keefe, D. L. (1992). Quantification of hormone pulsatility via an approximate entropy algorithm. *American Journal of Physiology-Endocrinology And Metabolism*, *262*(5), E741-E754.

Pincus, S. M., Gladstone, I. M., & Ehrenkranz, R. A. (1991a). A regularity statistic for medical data analysis. *Journal of clinical monitoring*, *7*(4), 335-345.

Pincus, S. M., Mulligan, T., Iranmanesh, A., Gheorghiu, S., Godschalk, M., & Veldhuis, J. D. (1996). Older males secrete luteinizing hormone and testosterone more irregularly, and jointly more asynchronously, than younger males. *Proceedings of the National Academy of Sciences*, *93*(24), 14100-14105.

Preatoni, E., Ferrario, M., Donà, G., Hamill, J., & Rodano, R. (2010). Motor complexity in sports: a non-linear analysis of race walking. *Journal of sports sciences*, *28*(12), 1327-1336.

Raffalt, P. C., McCamley, J., Denton, W., & Yentes, J. M. (2019). Sampling frequency influences sample entropy of kinematics during walking. *Medical & biological engineering & computing*, *57*(4), 759-764.

Raffalt, P. C., Vallabhajosula, S., Renz, J. J., Mukherjee, M., & Stergiou, N. (2018). Lower limb joint angle complexity and dimensionality are different in stairmill climbing and treadmill walking. *Royal Society open science*, *5*(12), 180996.

Rathleff, M. S., Samani, A., Olesen, C. G., Kersting, U. G., & Madeleine, P. (2011). Inverse relationship between the complexity of midfoot kinematics and muscle activation in patients with medial tibial stress syndrome. *Journal of Electromyography and Kinesiology*, *21*(4), 638-644.

Richman, J. S., & Moorman, J. R. (2000). Physiological time-series analysis using approximate entropy and sample entropy. *American Journal of Physiology-Heart and Circulatory Physiology*, *278*(6), H2039-H2049.

Schniepp, R., Wuehr, M., Neuhaeusser, M., Kamenova, M., Dimitriadis, K., Klopstock, T., ... & Jahn, K. (2012). Locomotion speed determines gait complexity in cerebellar ataxia and vestibular failure. *Movement disorders*, *27*(1), 125-131.

Sloot, L. H., Van der Krogt, M. M., & Harlaar, J. (2014). Self-paced versus fixed speed treadmill walking. *Gait & posture*, *39*(1), 478-484.

Smith, B. A., Teulier, C., Sansom, J., Stergiou, N., & Ulrich, B. D. (2011). Approximate entropy values demonstrate impaired neuromotor control of spontaneous leg activity in infants with myelomeningocele. *Pediatric physical therapy: the official publication of the Section on Pediatrics of the American Physical Therapy Association*, *23*(3), 241.

Sosnoff, J. J., Sandroff, B. M., & Motl, R. W. (2012). Quantifying gait abnormalities in persons with multiple sclerosis with minimal disability. *Gait & posture*, *36*(1), 154-156.

Srinivasan, D., & Mathiassen, S. E. (2012). Motor complexity in occupational health and performance. *Clinical biomechanics*, *27*(10), 979-993.

Stegeman, D., & Hermens, H. (2007). Standards for surface electromyography: The European project Surface EMG for non-invasive assessment of muscles (SENIAM).

Stergiou, N., Harbourne, R. T., & Cavanaugh, J. T. (2006). Optimal movement complexity: a new theoretical perspective for neurologic physical therapy. *Journal of Neurologic Physical Therapy*, *30*(3), 120-129.

Qiao, M., Feld, J. A., & Franz, J. R. (2018). Aging effects on leg joint complexity during walking with balance perturbations. *Gait & posture*, *62*, 27-33.

Qumar, A., Aziz, W., Saeed, S., Ahmed, I., & Hussain, L. (2013, December). Comparative study of multiscale entropy analysis and symbolic time series analysis when applied to human gait dynamics. In *2013 International Conference on Open Source Systems and Technologies* (pp. 126-132). IEEE.

Tao, W., Zhang, X., Chen, X., Wu, D., & Zhou, P. (2015). Multi-scale complexity analysis of muscle coactivation during gait in children with cerebral palsy. *Frontiers in human neuroscience*, *9*, 367.

Terrier, P., & Reynard, F. (2015). Effect of age on the variability and stability of gait: a cross-sectional treadmill study in healthy individuals between 20 and 69 years of age. *Gait & posture*, *41*(1), 170-174.

Tochigi, Y., Segal, N. A., Vaseenon, T., & Brown, T. D. (2012). Entropy analysis of tri-axial leg acceleration signal waveforms for measurement of decrease of physiological complexity in human gait. *Journal of Orthopaedic Research*, *30*(6), 897-904.

Unser, M. (1999). Splines: A perfect fit for signal and image processing. *IEEE Signal processing magazine*, *16*(6), 22-38.

Vallejo, M., Gallego, C. J., Duque-Muñoz, L., & Delgado-Trejos, E. (2018). Neuromuscular disease detection by neural networks and fuzzy entropy on time-frequency analysis of electromyography signals. *Expert systems*, *35*(4), e12274.

Vieira, T. M., Minetto, M. A., Hodson-Tole, E. F., & Botter, A. (2013). How much does the human medial gastrocnemius muscle contribute to ankle torques outside the sagittal plane?. *Human movement science*, *32*(4), 753-767.

Wang, X., Ma, Y., Hou, B. Y., & Lam, W. K. (2017). Influence of gait speeds on contact forces of lower limbs. *Journal of healthcare engineering*, *2017*.

Wu, S. D., Wu, C. W., Lin, S. G., Lee, K. Y., & Peng, C. K. (2014). Analysis of complex time series using refined composite multiscale entropy. *Physics Letters A*, *378*(20), 1369-1374.

Xie, H. B., Guo, J. Y., & Zheng, Y. P. (2010). Fuzzy approximate entropy analysis of chaotic and natural complex systems: detecting muscle fatigue using electromyography signals. *Annals of biomedical engineering*, *38*(4), 1483-1496.

Yakhdani, H. R. F., Bafghi, H. A., Meijer, O. G., Bruijn, S. M., van den Dikkenberg, N., Stibbe, A. B., ... & van Dieën, J. H. (2010). Stability and complexity of knee kinematics during gait in knee osteoarthritis before and after replacement surgery. *Clinical biomechanics*, *25*(3), 230-236.

Yang, A. C., Wang, S. J., Lai, K. L., Tsai, C. F., Yang, C. H., Hwang, J. P., ... & Fuh, J. L. (2013). Cognitive and neuropsychiatric correlates of EEG dynamic complexity in patients with Alzheimer's disease. *Progress in Neuro-Psychopharmacology and Biological Psychiatry*, *47*, 52-61.

Yentes, J. M., Hunt, N., Schmid, K. K., Kaipust, J. P., McGrath, D., & Stergiou, N. (2013). The appropriate use of approximate entropy and sample entropy with short data sets. *Annals of biomedical engineering*, *41*(2), 349-365.

Yu, H., Riskowski, J., Brower, R., & Sarkodie-Gyan, T. (2009, June). Gait complexity while walking with three different speeds. In *2009 IEEE International Conference on Rehabilitation Robotics* (pp. 823-827). IEEE.

Zhang, S., Li, Y., & Li, L. (2017). The Differential Effects of Footwear on Sample Entropy of Ground Reaction Force during Running: 487 Board# 308 May 31 9: 30 AM-11: 00 AM. *Medicine & Science in Sports & Exercise*, *49*(5S), 135.

Zhang, S., Li, Y., & Li, L. (2019). Running ground reaction force complexity at the initial stance phase increased with ageing. *Sports biomechanics*, 1-10.

Part II: Appendices

Appendices – Overview

In *Appendix A*, we give the definition of the *Approximate Entropy* algorithm *(ApEn)*. *ApEn* was derived by Steven Pincus (Pincus et al., 1991ab). In turn, *ApEn* is contrasted to its successor, the *Sample Entropy* algorithm *(SaEn)*. *SaEn* was used to quantify signal complexity in the present research. Finally, details are presented on the parameter choosing and the dataset length dependency of the *SaEn* algorithm.

In *Appendix B*, we collect results of medical research that quantified signal complexity with *SaEn* in human EMGs, GRFs, accelerometry and EEGs. Subsequently, we identify limitations in these studies. Finally, we present a solution to these limitations.

In *Appendix C*, the application to the Human Research Ethical Committee (HREC – TUDelft) is presented. However, the proposed research could not be conducted because of the ongoing COVID-19 pandemic.

In *Appendix D,* we display the joint maker placement. These markers measured joint kinematics in the experiments.

Finally, in *Appendix E*, we present detailed results of the experiments.

Appendix A – Entropy algorithms explained

Introduction

Time series data generated by biological systems often contain deterministic and stochastic components (Costa et al., 2005). Subsequently, the stochastic components of these time series are often considered as 'noise' of the biological system. Chaotic structures are typically challenging to quantify with conventional measures as the mean and standard deviation (SD) (Sosnoff et al., 2012), the coefficient of variation (CV) (Hausdorff et al., 2015) and the Lyapunov exponent (Terrier et al., 2015). However, chaotic structures of biological systems are proposed to strongly relate to motor learning and health (Pincus et al., 1991a; McIntosh et al., 2010). Therefore, Steven Pincus proposed to encapsulate properties of the changing complexity of a biological system with *Approximate Entropy* (*ApEn*). The *ApEn* algorithm quantifies signal complexity non-linearly (Pincus et al., 1991a; Pincus et al., 1991b). Consecutively, endocrinology, cardiology and neurology considered the quantification of signal complexity in biological system outputs as a useful biomarker (Goldberger et al., 2002; Pincus et al., 2006; Pincus et al., 2000; Pincus et al., 1996).

Cardiology has an increasing recognition for entropy algorithms to evaluate electrocardiograms (ECGs) and beat-to-beat differences (BBDs) in heart rate data. Here, signal complexity analysis could identify high-risk patients for congestive heart failure, atrial fibrillation or cardiac arrhythmia in early stages of the disease (Costa et al., 2005; Pincus et al., 1991a). Previously, the physician was trained to recognize these abnormalities by hand. Here, entropy algorithms could likely help to optimize the training procedure of the physician.

Consecutively, research of human gait analysis investigated the clinical application of analyzing signal complexity. However, there remains debate on the topic (Bisi et al., 2016; Georgoulis et al., 2006; Kang et al., 2016). This ongoing debate inspired the present research to investigate whether entropy is a sensitive measure for quantifying complexity changes in human gait function. In the present appendix, we select the complexity algorithm suitable for our analysis (*Appendix A1, Appendix A2*). Furthermore, we discuss the choosing of its parameters and its dependency on dataset length (*Appendix A3*).

A1) Approximate Entropy and Sample Entropy

⁎ Approximate Entropy (ApEn) – definition and explanation

Approximate Entropy (*ApEn*) was derived by Steven M. Pincus. *ApEn* quantifies a measure of complexity or regularity of a time series *x(i)* (Pincus et al., 1991b). The algorithm calculates the logarithmic probability that segments of the data fall within a distance *r* of the standard deviation of the dataset. This is derived via the correlation function *C(r).* First, the time series *x(i),* with *i=1, … ,N,* is divided into segments:

u(i)=[x(i), x(i+τ), x(i+2τ), … , x(i+(m-1)τ)]

Here, *m* is the segment length or embedding dimension, and τ is the time lag, set to 1. Subsequently, we calculate whether segment x_i is similar to the rest of the *m*-segments. The distance *d* is then expressed as the maximal distance between two *m*-dimensional points:

d[u(i),u(j)] = max(|u(i+k) – u(j+k)|), with *1 ≤ j ≤ N-m+1* and *0 ≤ k ≤ m -1*

Consecutively, the correlation function $C_i^m(r)$ is the number of vectors *u(j)* within the distance *r* from the template vector *u(i)*. If the distance is more than the threshold *r*, the algorithm counts '1'. If the distance is less than *r*, the algorithm counts '0', respectively. Here, '1' counts lead to a higher complexity value and '0' counts lead to a lower complexity value. This is derived as follows:

$C_i^m(r) = (N - m + 1)^{-1} = \sum_{i=1}^{N-m+1}\left(H(r * \sigma - |d(u(i), u(j))|\right)$

In the latter formula, *H(…)* is expressed as the Heaviside step function. Here *H* is *'1'* if $(r * \sigma - |d(u(i), u(j)) \geq 0$ and '0' otherwise. Then, $\varnothing^m(r)$ is representing the average of the natural logarithm of C_i^m. Note here, that the logarithm computes the fraction (Nr. of segments similar to block x_i / Nr. of segments). This way, small fractions won't skew the distribution. This is formulated as:

$\varnothing^m(r) = (N - m + 1)^{-1} \sum_{i=1}^{N-m+1}(\ln (C_i^m(r))$

Finally, *ApEn* is expressed as the difference between the logarithmic probability that vectors which are close for *m* points, are also close if lengthened to *m + 1* points. This way, higher regularity would mean less difference between '*m*' and '*m+1*' segment lengths:

$ApEn(m,r,N) = \varnothing^m(r) - \varnothing^{m+1}(r)$

The *ApEn* algorithm depends on the embedding dimension *m,* the criterion for similarity *r* and the number of data points *N.* In general, *m* is set to 1 or 2 to ensure statistical validity, *r* is set to 10% or 20% of the standard deviation of the time series. *N* should exceed 200 data points. *ApEn* gives an output of '2.0' if the analyzed signal is completely random and gives an output of '0.0' if the signal is periodic (e.g.: sinusoid function) (Pincus, 1991b; Lipsitz et al., 1992; Yentes et al., 2013).

⁎ Sample Entropy (SaEn) – definition and explanation

Sample Entropy (SaEn) is a modification on *ApEn. SaEn* quantifies the complexity of structure or complexity of a time series *x(i)*. In contrast with *ApEn*, *SaEn* excludes self-matches in the distance vector *d* (Pincus et al., 1991b; Yentes et al., 2013). When self matches are excluded, the bias towards regularity is eliminated. This means that when distance *d* between *u(i)* and *u(j)* is computed, *i* is never equal to *j* (Delgado et al., 2019). In *SaEn,* the exclusion of self-matches is written in the distance function as:

$d[u(i),u(j)] = max(|u(i+k) - u(j+k)|)$, with $1 \leq j \leq N-m$ and $i \neq j$

Now, $\varnothing' ^{m}(r)$ represents the average of the probability of matches $C'_i{}^{m}(r)$. Here, $C'_i{}^{m}(r)$ is computed as $C_i{}^{m}(r)$, only now for the distance vector excludes self-matches. This is formulated as:

$$\varnothing' ^{m}(r) = (N-m)^{-1} \sum_{i=1}^{N-m} (C_i'^{m}(r))$$

Finally, *SaEn* represents the negative logarithm of the relationship between the probability that two sequences coincide for *m+1* and *m* points. This is formulated as:

$$SaEn(m,r,N) = -ln(\varnothing' ^{m+1}(r) / \varnothing' ^{m}(r))$$

SaEn depends on the embedding dimension *m* and the criterion for similarity *r.* In general, *m* is set to 1 or 2 to ensure statistical validity. Subsequently, *r* is set to 10% or 20% times the standard deviation of the time series. *N* should be at least 100 data points (Richman & Moorman, 2000). *SaEn* yields an output of '3.0' if the analyzed signal is completely random and yields an output of '0.0' if the signal is periodic (e.g.: sinusoid function) (Pincus, 1991; Lipsitz et al., 1992; Richman & Moorman, 2000; Yentes et al., 2013). Consecutively, we explain the parameter choosing and the dataset length dependency of the *SaEn* algorithm in *Appendix A3*.

⁎ Contrasting ApEn and SaEn for time series data

ApEn and *SaEn* are algorithms that determine the complexity of time series data based on non-linear analysis. Despite their similarities, the theory behind these techniques is different. This is sometimes ignored in literature (Delgado-Bonal et al., 2019). *SaEn* is largely independent on the dataset length *N* and shows more consistent behavior for different input parameters in time series data than *ApEn* (Yentes et al., 2013). This makes *SaEn* more effective for short and noisy time series (Delgado et al., 2018; Richman & Moorman 2000). The latter property is a useful property of *SaEn*, since studies of human gait often favor to require maximally short recording times of the subject. In fact, experimental set-ups are often limited by recording devices with a low sampling frequency (e.g.: $f_s = 100$ *Hz*). In turn, a low sample frequency requires long recording times of the subject to reach the minimum amount of dataset length for *ApEn*. Moreover, *SaEn* excludes the bias towards regularity by excluding self-matches (Delgado-Bonal et al., 2019). Therefore, the present research quantified signal complexity in EMGs, GRFs and GAs using the *SaEn* algorithm, that stood in agreement with previous literature (Ahmed et al., 2011a; Chung et al., 2013; Costa et al., 2003; Delgado et al., 2019; Yentes et al., 2013).

A2) Multiscale Entropy

⁎ Multiscale Entropy (MSE) – definition and explanation

The *Multiscale Entropy (MSE)* method is used to display the complexity of time series data over multiple timescales or temporal resolutions of the data. First, the temporal resolutions are determined with the *coarse-grained time series* procedure. Consecutively, *SaEn* values are calculated for these temporal resolutions. To account for both short, - and long-range correlations in biological systems, literature proposed to calculate *SaEn* values over multiple scales of the time series (Costa et al., 2005; Tao et al., 2015; Bisi et al., 2016; Maturana-Candelas et al., 2019; Yang et al., 2013). In heart rate data, it was generally difficult to distinguish inter-beat interval time series of different diseased and healthy states with only a single-scale *SaEn* value. Therefore, the original time series $\{x_i\}$ is divided into multiple time scales of the dataset. The *coarse-grained time series* is then $\{y_j\}$:

$$y_j^{\tau} = \frac{1}{\tau} \sum_{i=(j-1)\tau+1}^{j\tau} x_i, \ 1 \le j \le \frac{N}{\tau}.$$

The original time series is divided into non-overlapping windows of length τ and the data points inside each window are averaged *(Figure A.1)*. Subsequently, *SaEn* values are used to quantify the complexity of the *coarse-grained time series*. When we plot entropy outcomes over multiple scales, the *MSE* curves can be contrasted, based on the following guideline:

- If for the majority of scales, the entropy values are higher in one time series than for the other time series, the former time series is considered as more complex than the latter.
- A monotonic decrease of entropy values indicates the original time series only contains information at the smallest time scale, *scale 1*.

We give a visual representation of the *coarse-graining time series* procedure for a completely regular signal and for the experimental EMG data on the next pages.

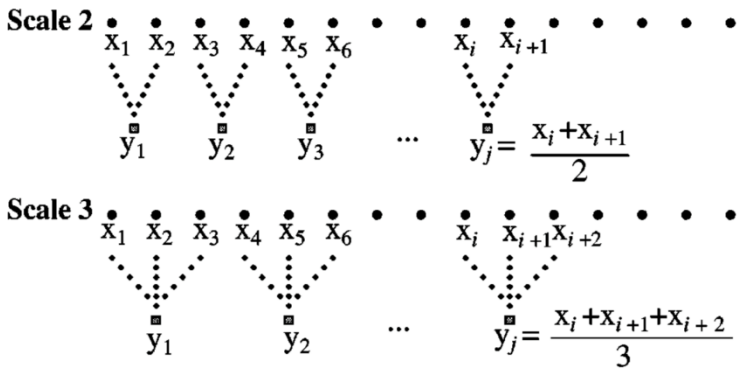

Figure A.1) Coarse-grained time series – The MSE method calculates sample entropy outcomes of coarse-grained time series, in which the original dataset is divided into multiple time-scales, as displayed above. *Coarse-grained* time series are implemented in Matlab 2018a (Mathworks, Natick MA).

For more information, see (Costa et al., 2002)

⁎ Coarse-grained time series – sinusoid

Here, we give a simple explanation of the definition of a *coarse-grained time series*. We interpret a completely regular signal, a sinusoid. Subsequently, we represent this signal for different resolutions. First, we analyze the experimental gait data of young (*N*=18; μ_{age} = 25) and old (*N*=19; μ_{age} = 65) subjects at comfortable walking speed. From the subject data, we determined the mean frequency and the mean duration of a single stride:

$$Single\ stride\ (Young) \quad : f = 1.00\ Hz\ ;\ T = 1.0s$$
$$Single\ stride\ (Old) \quad : f = 0.83\ Hz\ ;\ T = 1.2s$$

We plot the regular signal for these eigenfrequencies and sample times with f_s = *1000 Hz*. Subsequently, we plot the *coarse-grained time series* at *scale 10* and *scale 20* of the signals. When we plot the signal for different temporal resolutions, the sample time and frequency vector change. For example, the time and frequency vectors at *scale 10* would yield:

$dt_{scale10} = dt_{original} * 10$
$f_{scale10} = f_{original} / 10$

The sinusoid signal and its coarse-grained time series are plotted in *Figure A.2a*. Subsequently, *Figure A.2b* is zoomed in on the first peak of the signal. The latter figure displays the sinusoid function is described with less points in the *coarse-grained time series* than in the original time scale.

⁎ Coarse-grained time series – EMG of right VL muscle

Next, we interpret the EMG response of the right VL muscle of an exemplar old subject. We extract a single stance and swing phases for this subject. In turn, we determined the *coarse-grained time series* of *scale 5, 10, 15* and *20* of the data. The number of datapoints in the *coarse-grained time series* are modified. In *scale 10* this would yield:

$N_{scale10} = N_{original} / 10$

Consecutively, we plot the EMG signal and its *coarse-grained time series* of the right VL muscle in *Figure A.3*.

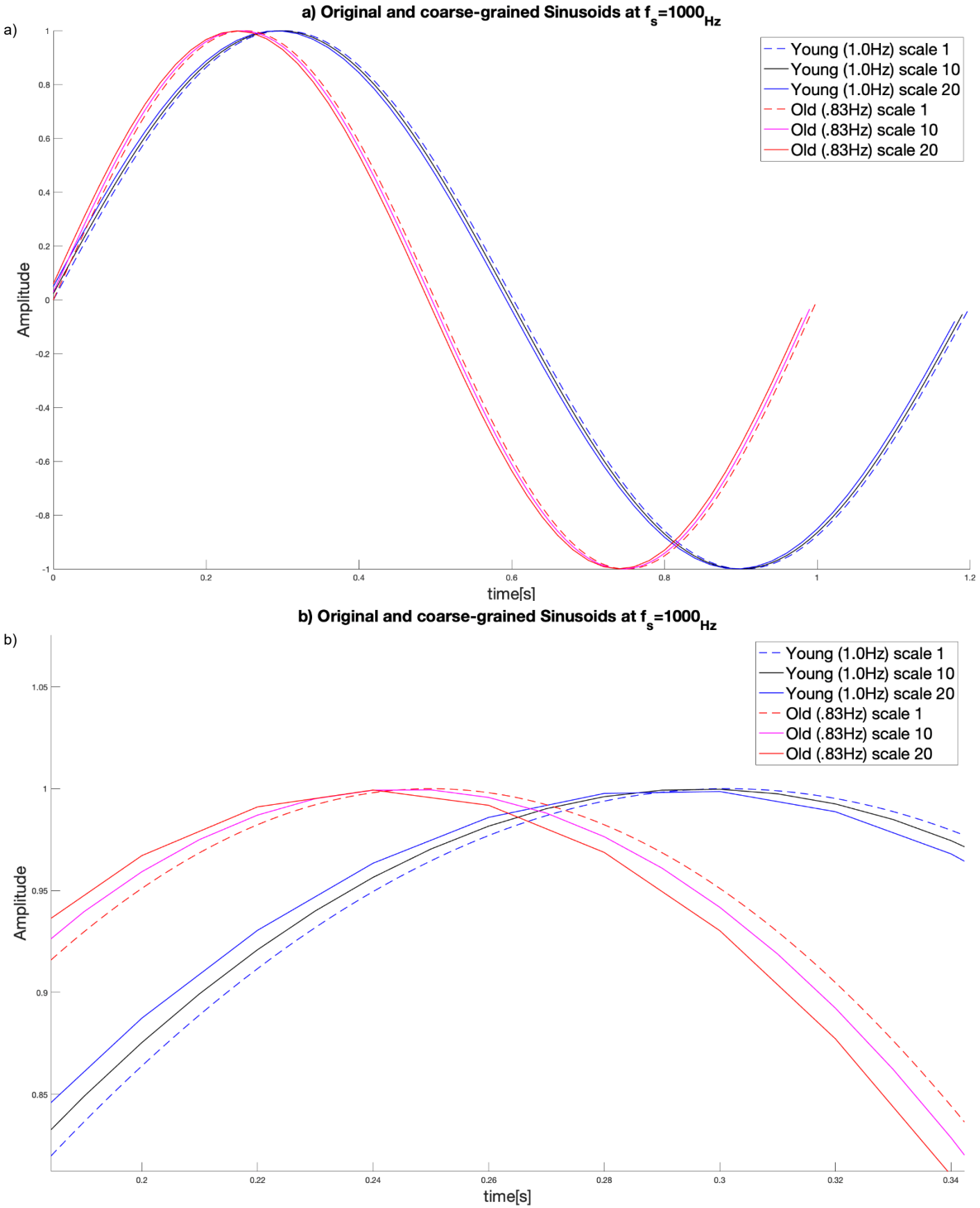

Figure A.2ab) Coarse-grained time series of a sinusoid signal – **a)** 1.0 Hz and 0.83 Hz sinusoids representing the gait frequency of young and old subjects, respectively. Both sinusoids are plotted for *fs=1000 Hz*. The coarse-grained time series are plotted for scale 10 and 20. **b)** Same as in a). The plots of scale 10 and 20 show the original signal is described with less points, and thus displayed at lower temporal resolution. Coarse-grained time series were implemented in Matlab 2018a (Mathworks, Natick MA).

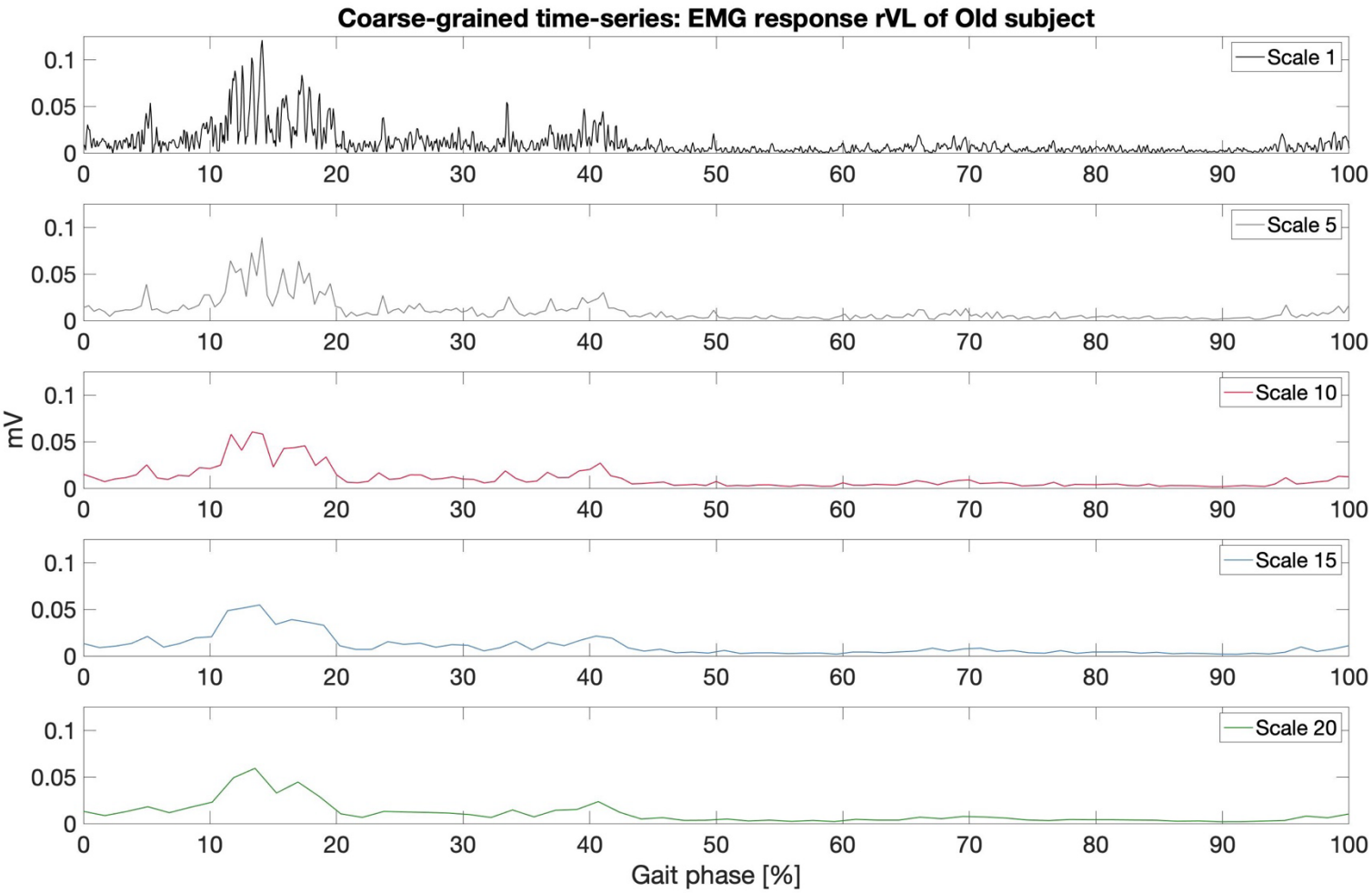

Figure A.3) Coarse-grained time series of EMG response right Vastus Lateralis muscle - The original the EMG response of the right VL muscle of an exemplar old subject of trial *ANS* is displayed (*black*). The x-axis displays the percentage of the gait cycle, starting with the stance phase and ending with the swing phase. Temporal resolutions of the signal are represented by coarse-grained time series of *Scale 5* (*gray*), *Scale 10* (crimson red), *Scale 15* (steel blue) and *Scale 20* (*forest green*), respectively. The dataset lengths are normalized, to display the effects of the coarse-graining procedure on the signal. Dataset lengths are modifier according to: ($N_{scale\ nr.}$ = $N_{original}$ / *Scale nr.). Scale 1* of the EMG signal only contains frequencies < 450 Hz. In the consecutive scales of this data, the frequency content represented is limited to: (450 Hz / *Scale nr.*).

A3) Parameters *m*, *r* and *N*

Entropy calculations are dependent on input parameters *m, r* and the dataset length *N*. We identified exemplar studies of human heart rate data (Castiglioni et al., 2008; Pincus et al., 1991b) and human gait data (Montesinos et al., 2018; Yentes et al., 2013) that investigated the influence of these parameters on entropy outcomes.

∗ The embedding dimension parameter: m

The embedding dimension cuts the analyzed time series data into segments with length *m.* Consecutively, all *m*-length segments of the time series data are compared to the rest of the dataset. Parameter *m* determines the sensitivity of the *number of correlations* that can be found within the given time series (Yentes et al., 2013; Pincus et al., 1991b). In fast varying data like heart rate data and EMG, a greater segment distance means less comparisons. In turn, this will decrease the maximum complexity that can be found. Research in human foot center-of-pressure data (Ahmed et al., 2011a; Montesinos), EMG data (Kang et al., 2013) and ECG data (Costa et al., 2005) suggests that an *m*-value of 2 is most effective to quantify complexity for healthy and diseased states. In turn, choosing a higher *m* decreases the max value of entropy that can be found (Montesinos et al., 2018). We approved this effect in the present research for the measured data types. Consecutively, this led us to choose parameter *m=2,* for EMG, GRF and kinematic data as recommended by research (Castiglioni et al., 2008; Montesinos et al., 2018; Pincus et al., 1991b; Yentes et al., 2013).

∗ The criterion for similarity parameter: r

The criterion for similarity parameter specifies a fraction *r* times the standard deviation that is used in the distance vector for computing correlations. When entropy is calculated, the probability is determined that *m*-length segments are similar and will remain similar when the segment length is increased to (*m+1)* (i.e.: closer to each other than a given distance $r*\sigma$). In other words, *r* determines the tolerance for the algorithm to find these correlations. Fortunately, research discussed the choosing of *r* in human hormonal processes (Pincus et al., 1991b; Pincus et al., 1992), in ECG data (Castiglioni et al., 2008), in respiratory signals (Chen et al., 2018) and in gait data (Yentes et al., 2013). Typically, these authors suggest using an *r* value between 0.1-0.25. Most of these authors recommend a value of *r*=0.2 for these datatypes. It is important to mention that others speculate that the *r* that maximizes entropy outcomes, defined as r_{max}, is the best *r* value to choose. The value of entropy obtained by r_{max} then quantifies the highest information difference between segments of length *m* and (*m+1)*. Therefore, this method allows to account for more of the signal complexity than other values of *r* (Chen et al., 2018; Castiglioni et al., 2008). In the present research, we chose the *r* value in the range 0.1-0.25 that maximized entropy outcomes, as recommended by recent literature (*r*=0.1) (Chen et al., 2018).

∗ Dataset length parameter: N

The dataset length dependency of entropy algorithms is extensively reported in literature (Pincus et al., 1991b; Pincus et al., 2000; Pincus et al., 1992; Yentes et al., 2013). However, some studies do not account for the dataset length bias. These studies typically conduct entropy analysis in either original or coarser scales of time series data, while the number of samples are unequal between compared subjects (Bisi et al., 2016; Kang et al., 2016; McCrum et al., 2019; Monaco et al., 2009). Entropy results deviate with coarser time scales, when unequal sample lengths are used. This phenomenon is shown in the current appendix.

We review the effect of the number of samples on *SaEn* outcomes of a regular signal, a 5Hz sinusoid. The signal is generated for two different sample times and is plotted at a convenient eigenfrequency to display the effect of dataset length. We determined *coarse-grained time series* of the signal for two sample times and calculated *SaEn* values of the series.

The complexity of an ideal sinusoid function is zero. Subsequently, we generated a 5Hz sinusoid at f_s=*1000 Hz* in matlab *(Figure A.4).* The generated sinusoid is described with 200 datapoints per revolution. Due to small rounding errors in matlab, the output of the sinusoid does not reach 0.000 at the end of every revolution. In fact, the placement of datapoints varies over the repetitions, leading to a slightly increased complexity value from zero in the original temporal resolution. In the 20th temporal resolution of the signal, *scale 20,* the sinusoid is described with 10 datapoints per revolution. Moreover, the placement of these 10 samples does not vary over the repetitions. Therefore, all its revolutions are identical. Consecutively, the entropy algorithm detects complexity zero in this scale. In matlab, the entropy algorithm will yield exactly zero for any other sinusoid signal that is plotted for f_s, while its eigen frequency and temporal resolution satisfy:

$$\frac{f_{sample}}{temporal\ res.} * \frac{1}{f_{eig,sin}} = \frac{10\ datapoints}{rev}$$

SaEn outcomes of *coarse-grained time series 1-20* are plotted for the 5Hz sinusoid at two different sample times *(Figure A.5a).* Here, the difference in dataset length affects *SaEn* across the temporal resolutions. To elaborate on why *SaEn* values deviate in coarser scales of the signal, we review its Probability Density Function (PDF). The PDF of *scale 15* of the signal is plotted for the two sample times in *Figure A.5bc*. Here, the signal with small sample time (*T=2s)*, yields less certainty in the amplitude counts (high σ_{sig}) and leads to high complexity. In turn, the signal with the increased sample time *(T=20s),* yields more certainty in the amplitude counts (smaller σ_{sig}) and leads to a low complexity. Here, the *SaEn* outcomes differ, because the final outcome is derived with tolerance $r^*\sigma_{sig}$. This exposes the importance of analyzing data with an equal number of samples in research (Pincus et al., 1991b; Pincus et al., 2000; Pincus et al., 1992; Yentes et al., 2013).

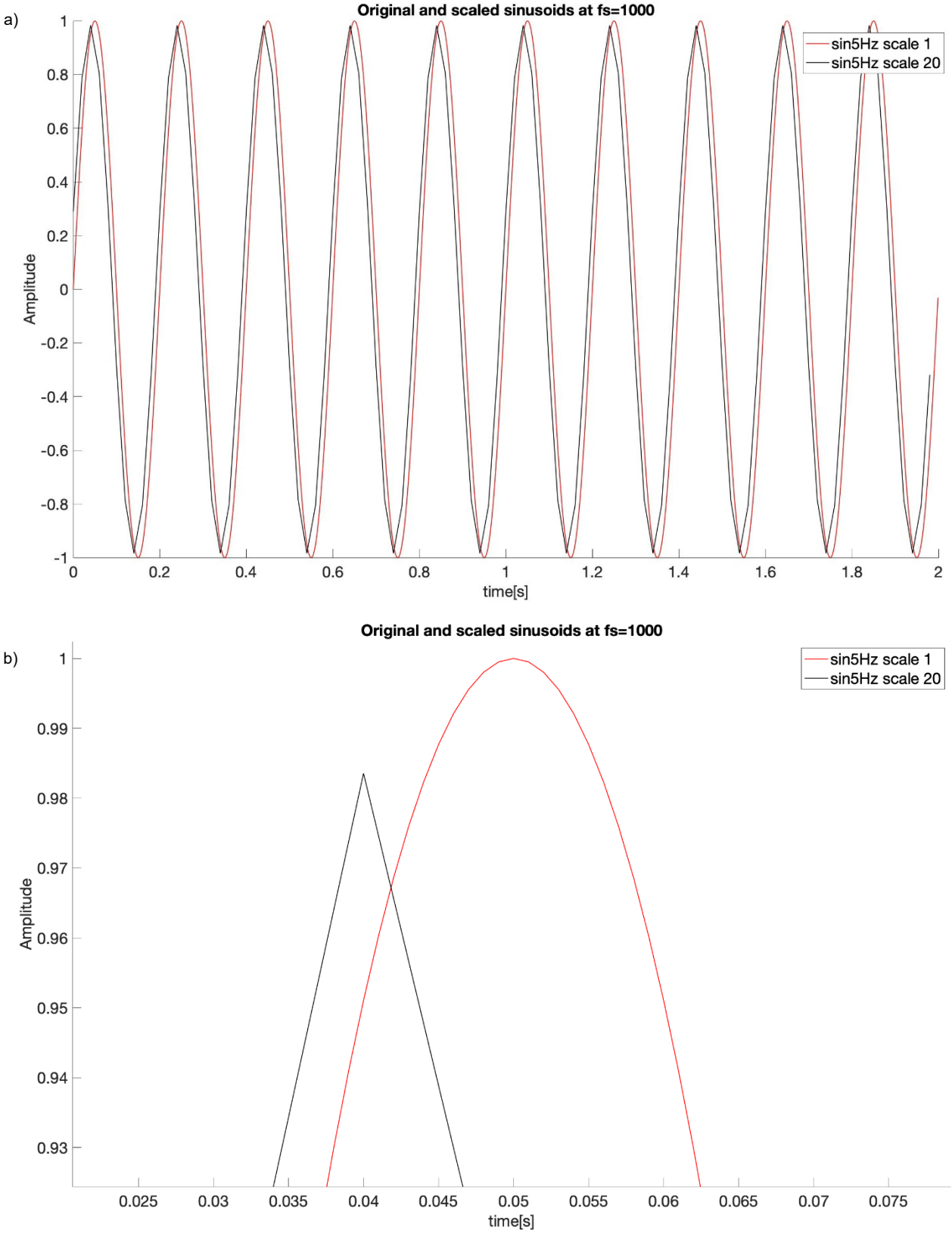

Figure A.4ab) Coarse-grained time series of a 5Hz sinusoid signal – **a)** The original temporal resolution and the 20th coarse-grained time series of a 5Hz sinusoid *(f_s=1000 Hz)* are displayed. In *scale 20*, the placement of datapoints does not vary over the repetitions. This leads to the entropy algorithm detecting a complexity of zero. **b)** Same as in a). The plot is zoomed in on the first peak of the sinusoids. In *scale 1*, the complexity slightly deviated from zero due to small rounding error in matlab. In *scale 20*, the complexity is zero. Coarse-grained time series were implemented in Matlab 2018a (Mathworks, Natick MA).

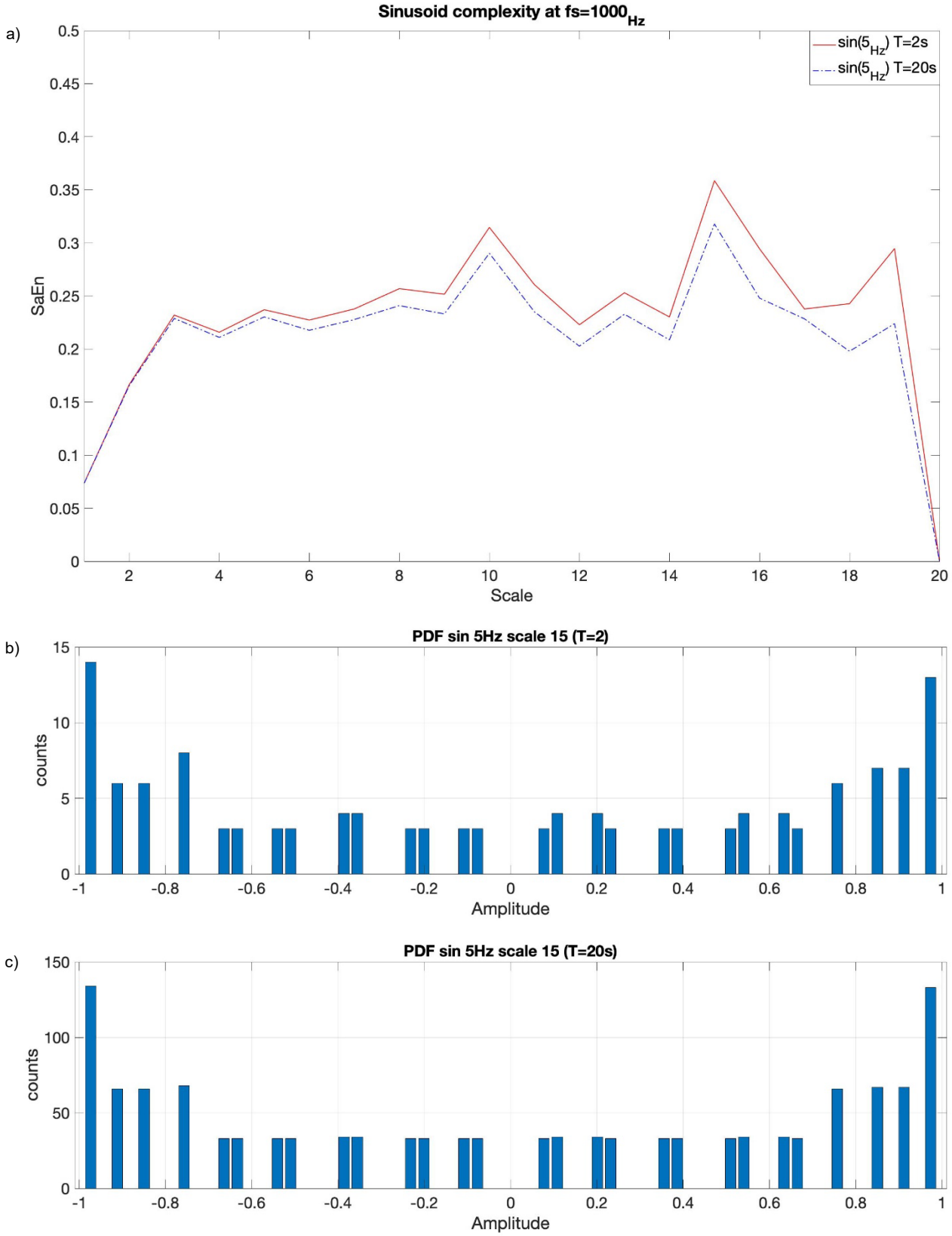

Figure A.5abc) MSE and PDF of 5Hz sinusoid – **a)** Displays the *SaEn* outomes for *scale 1-20* of the 5Hz sinusoid for two sample times. In coarser scales of the signal, a clear deviation can be detected in entropy outcomes. **b,c)** Displays the *PDF* of the 5Hz sinusoid in *scale 15*. Here, the signal with small sample time (*T=2s)*, yields less certainty in the amplitude counts (higher σ_{sig}), leading to a higher complexity. In turn, the signal with the increased sample time *(T=20s),* yields more certainty in the amplitude counts (smaller σ_{sig}), leading to a lower complexity.

Appendix B – Entropy in biological time series

The present appendix highlights studies that investigate complexity changes in human gait, ECG and EEG signals with the *Sample Entropy (SaEn)* algorithm *(Appendix B1)*. Secondly, we identified limitations in these studies (*Appendix B2)*. Lastly, we proposed a solution to these limitations (*Appendix B3)*.

B1) Examples of entropy in medical research

⋆ Signal complexity changes with age in human gait

Recent research assessed entropy changes in human gait as a result of age. An exemplar study assessed EMGs of young (23y +/- 2y) and old subjects (72y +/- 6y) during comfortable treadmill walking (Kang et al., 2016). Here, older adults exhibited increased *SaEn* of EMG activations in contrast with younger adults in the gastrocnemius. Subsequently, proximal muscles decreased in *SaEn* with age. These muscles included the vastus lateralis, biceps femoris and tibialis anterior muscle. This study concluded that the decrease in EMG complexity with aging may be limited to proximal leg muscles, and that slower walking attenuates this decrease in the original time scale of the data. These findings were likely correlated to the walking task.

Additionally, an interesting study by Bisi and colleagues assessed *SaEn* changes of vertical (VE) and anterior-posterior (AP) trunk accelerations from development till decline. In this study, toddlers with two weeks of walking experience till 84-year-olds were measured. Results showed that entropy decreased in VE and AP until the subject reached 15 years of age. Subsequently, entropy in VE and AP increased until the age of 84 years was reached (Bisi et al., 2016).

Lastly, a study was identified that assessed leg joint complexity during walking in young (25y +/- 5y) and old subjects (75y +/- 5y). Leg joint complexity was assessed for unperturbed and perturbed walking trials (Qiao et al., 2018). The study calculated *SaEn* in flexion-extension and abduction-adduction angels of the hip, knee and ankle. Interestingly, this study found that compared with young adults, older adults walked normally with on average 35% larger abduction-adduction hip joint complexity in unperturbed trials. No differences were found in the knee or ankle joint complexities. Subsequently, older adults were disproportionately susceptible to even the smallest amplitude of perturbation. In response to these perturbations, larger complexities were found in old subjects in the flexion-extension complexity of the hip, knee and ankle joint.

⋆ Signal complexity changes with walking velocity and with fall risk in human gait

A study by Masani and colleagues assessed optimization of the neuromuscular locomotor (NML) system for different walking velocities. The study evaluated the complexity of GRFs during treadmill walking of young subjects (29y +/- 5y) for walking velocities in the 3-8 km/h range (Masani et al., 2002). The main finding of the study was that walking velocity altered GRF complexity. Vertical GRF reflected a minimum complexity at PWS. Subsequently, when walking speeds were increased or decreased from PWS, complexity increased. This suggested that the NML system is most stabilized at PWS.

Successively, an elegant study was identified that assessed *SaEn* outcomes of GRF signals in 101 elderly subjects (67y +/- 9y). Subjects were classified to low, medium and high fall risk groups. The main goal of the study was to correlate *SaEn* outcomes of GRF signals to fall risk. Results of the study showed that *SaEn* of vertical GRFs correlated with the level of fall risk (Liang et al., 2016). This suggested that the complexity of GRF was an indicator for system instability of the NML system.

⁎ Signal complexity changes in ECGs and EEGs

We identified studies that applied the entropy algorithm in ECG and EEG data. In a study by Costa and colleagues, the complexity of cardiac interbeat interval time series was assessed of healthy subjects, subjects with congestive heart failure and subjects with atrial fibrillation. Here, *SaEn* values of healthy subjects were significantly higher in the coarser time scales of the data, when compared to pathologic function (Costa et al., 2005; Costa et al., 2002). The study suggested that *SaEn* could be used to identify subjects with heart failure in early stages of the disease.

Consecutively, a study by McIntosh and colleagues examined changes in EEG complexity from childhood to adulthood (McIntosh et al., 2010). In this work, a complexity increase was found in EEG signals with maturation, that correlated with more stable and accurate cognitive performance. Results from more recent work displayed that old adults at risk for cognitive decline do not show an increase at the original time scale of EEG data. Moreover, older subjects exhibited either similar or higher entropy at coarser time scales of the data, when compared to healthy subjects (McIntosh et al., 2018). Here, *SaEn* could potentially help identifying early onset of dementia. Other work added on these results and displayed that interpreting *SaEn* across temporal resolutions of the data could help identify early onset of cognitive decline (Bertrand et al., 2016; Maturana-Candelas et al., 2019; McIntosh et al., 2010; Yang et al., 2013).

B2) Limitations in current entropy research

* Introduction

We often have the capability to measure a variety of data types in patients, that can provide insight into diagnosis and treatment of health limitations. These limitations can range from aging, to dementia, to Parkinson's disease. Recent research explores topics that focus on how we identify these limitations and how they can be quantified in early stages. An interest for quantifying these limitations with entropy algorithms is reflected in research (Harbourne et al., 2009; Kang et al., 2009; Pincus et al., 2006; Smith et al., 2011; Srinivasan et al., 2012; Stergiou et al., 2006; Madeleine et al., 2009; Morrison et al., 2012). Axes of interest include entropy analysis of heart rate time series (Pincus et al., 2006), hormonal process dynamics (Pincus et al., 1996), EEGs (Bertrand et al., 2016) and EMGs (Kang et al., 2016). However, recent studies were identified that compare *SaEn* values of subject data that differed in number of samples. These studies violate the entropy algorithm requirement of dataset length equality. In the present appendix, we briefly go over these limitations. Consecutively, we display a suitable solution for these limitations in *Appendix B3*.

* Limitations: SaEn in gait analysis – EMG studies

An exemplar study that executed *SaEn* analysis in EMG signals is a study by Kang and colleagues (Kang et al., 2016). In their study, young and old subjects were measured during a normal walking task on a treadmill at different walking speeds. In their results subjects are compared that walked for 5 minutes. However, the amount of gait phases and the number of samples per gait phase were not normalized. Therefore, in their study, subjects are compared for an unequal amount of gait phases and an unequal number of samples per gait phase, leading to entropy deviations in coarser scales of the data.

Consecutively, limitations can be identified in a study by Toa and colleagues that investigated *SaEn* for different temporal resolutions of EMG data (Tao et al., 2015). In their study, the complexity of EMG patterns was studied in healthy children compared to children with cerebral palsy. Subjects walked across a straight walking trajectory. Here, subjects walked at different walking velocities. An equal amount of gait phases was analyzed, but no normalization was applied to account for the difference in the number of samples per gait phase. Consecutively, this leads to *SaEn* deviations.

* Limitations: SaEn in gait analysis – Accelerometry studies

A study by Bisi and colleagues applied *SaEn* to human trunk and leg acceleration signals. Here, subjects were asked to walk in a straight line across a corridor (Bisi et al., 2016). *SaEn* values were used to quantify complexity changes in trunk and ankle acceleration with age, across different temporal scales of the data. *SaEn* values were found significantly different across age categories. The study reported that ten consecutive strides were analyzed per subject. However, the number of samples varied between 1000 and 1500 between subjects. Of course, this violates the dataset length equality requirement of the *SaEn* algorithm, which will yield entropy deviations across different time scales of the data.

* Limitations: SaEn in human brain data – EEG studies

Lastly, studies of McIntosh and colleagues were identified that assessed EEG complexity changes with age (McIntosh et al., 2018; McIntosh et al., 2010). In the methods section, different measurement times per subjects were reported. Measurement times often differed in seconds, leading to biased *SaEn* results in coarser scales of the data. Additionally, we identified a study by Chung and colleagues that assessed EEG signals during different sleep states in healthy versus Parkinson's patients. *SaEn* values were compared across subjects per 30 second EEG epoch. Although, the number of included epochs per patient differed significantly. The latter caused a difference in the number of samples of datasets that were compared, causing *SaEn* deviations (Chung et al., 2013).

B3) Solution to the limitations: Normalizing the number of samples

We identified several *SaEn* studies that compared subjects with an unequal number of samples (Bisi et al., 2016; Ching et al., 2013; Kang et al., 2016; McIntosh et al., 2018; McIntosh et al., 2010; Tao et al., 2015). Subsequently, we propose a solution to the entropy dataset length bias. In our experiments we compared young and old subjects. Subject first walked at PWS in *trial 1 (ANS)*. Subsequently, subjects walked at 130%*PWS in *trial 2 (AFS)*. Mean PWS of young subjects was equal to 1.31+/- 0.17 m/s. Mean PWS of old subjects was equal to 1.22 +/- 0.18 m/s. As a result, the number of samples differed between the subjects for equal measurement times. Therefore, we extracted the same number of gait phases per datatype for all subjects. Consecutively, we identified the subject with the least number of samples and resampled subjects to this number of samples. Now, every subject included the same number of strides, described by the same number of samples. This procedure was repeated for *trial 3* and *trial 4*. The resampling algorithm was selected with respect to previous literature. We identified studies that resampled human movement data, EMG and EEG using shape preserving spline algorithms (in matlab: pchip). These studies showed the original frequency content of the data was preserved (Coutinho et al., 2017; Eng et al., 2007; Lencioni et al., 2017; Marateb et al., 2016; Unser et al., 1999).

To display the effect of resampling with a shape preserving spline algorithm on *SaEn* outcomes, we interpret a sinusoid. First, we display the change of shape of the signal using different resampling rates. The max resampling rate used in the experimental data was equal to:

$$\frac{Subject\ with\ min.nr.of\ samples}{Subject\ with\ max\ nr.of\ samples} \approx 50\%$$

Second, we plot *SaEn* outcomes with the resampling rates for the original temporal resolution of the signal. To assess these changes, we interpret the PDF of the signal. Lastly, we repeat these two steps for the experimental EMG data of an exemplar old subject.

∗ Effects of resampling with 'pchip' in regular data – sinusoid

We interpret a 5Hz sinusoid for one revolution (f_s*=1000 Hz, T=0.02s*). We plot the sinusoid and its complexity values for 5 resample rates: *[0.5, 0.6, 0.7, 0.8, 0.9]*$N_{original}$*. The shape of the original signal is preserved with 'pchip' for the resampling rates. For the resampling rate of 0.5*$N_{original}$, the amplitude and curvature of the resampled signal accurately resembles the original signal (*Figure A.6)*. We see that *SaEn* values increase the more datapoints are removed *(Figure A.7a)*. This is explained with the PDF for the original sinusoid and the sinusoid with 50% of the original number of samples *(Figure A.7bc)*. The resampled signal displays less certainty in the amplitude counts (σ increase), leading to a higher complexity.

∗ Effects of resampling with 'pchip' in erratic data – EMG response of VM

Consecutively, we interpret the experimental data of the VM muscle of one of the old subjects that was measured in *trial ANS*. The EMG activity is plotted for one stride, that is resampled for the same five resample rates as above *(Figure A.8a)*. High frequency content is preserved in the resampled signal. Entropy values of erratic data decrease with the resample rate *(Figure A.8b)*. This is explained by PDF of the EMG signal (*Figure A.9ab)*. More certainty is displayed in the amplitude counts for the resampled signal (σ increase), leading to lower complexity.

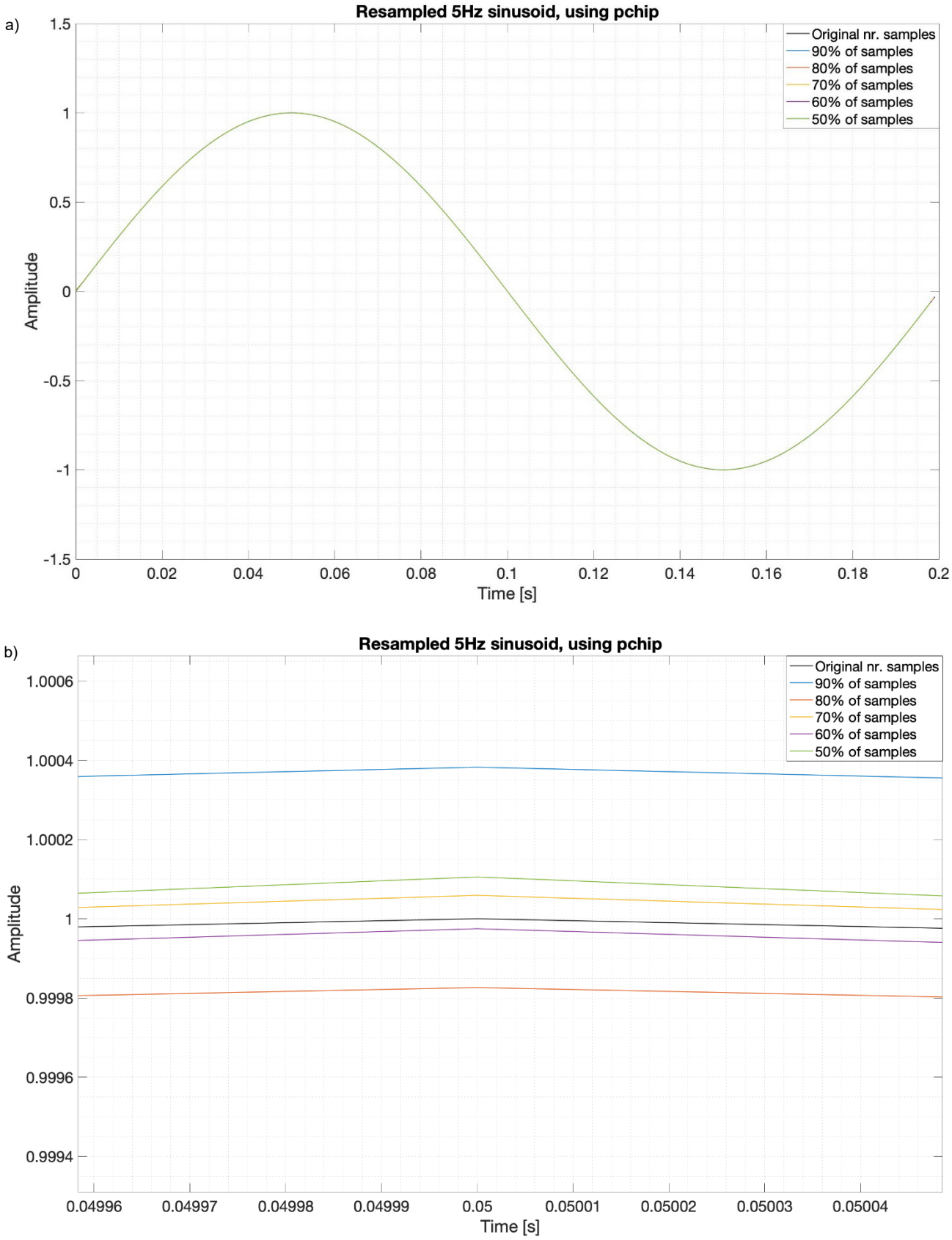

Figure A.6ab) Resampled sin(5Hz) using 'pchip' – **a)** The 5Hz sinusoid is plotted at f_s=*1000 Hz* for one resolution. The signal is resampled using function *resample* with a shape preserving spline algorithm. Resampling was conducted for 5 different rates: [*0.5, 0.6, 0.7, 0.8, 0.9*]*$N_{original}$. The shape of the original signal is preserved. **b)** Zoom in on the first peak of the sinusoid. Higher resample rates yield a fairly accurate representation of the original signal trajectory. Resampling procedures were implemented in Matlab 2018a (Mathworks, Natick MA).

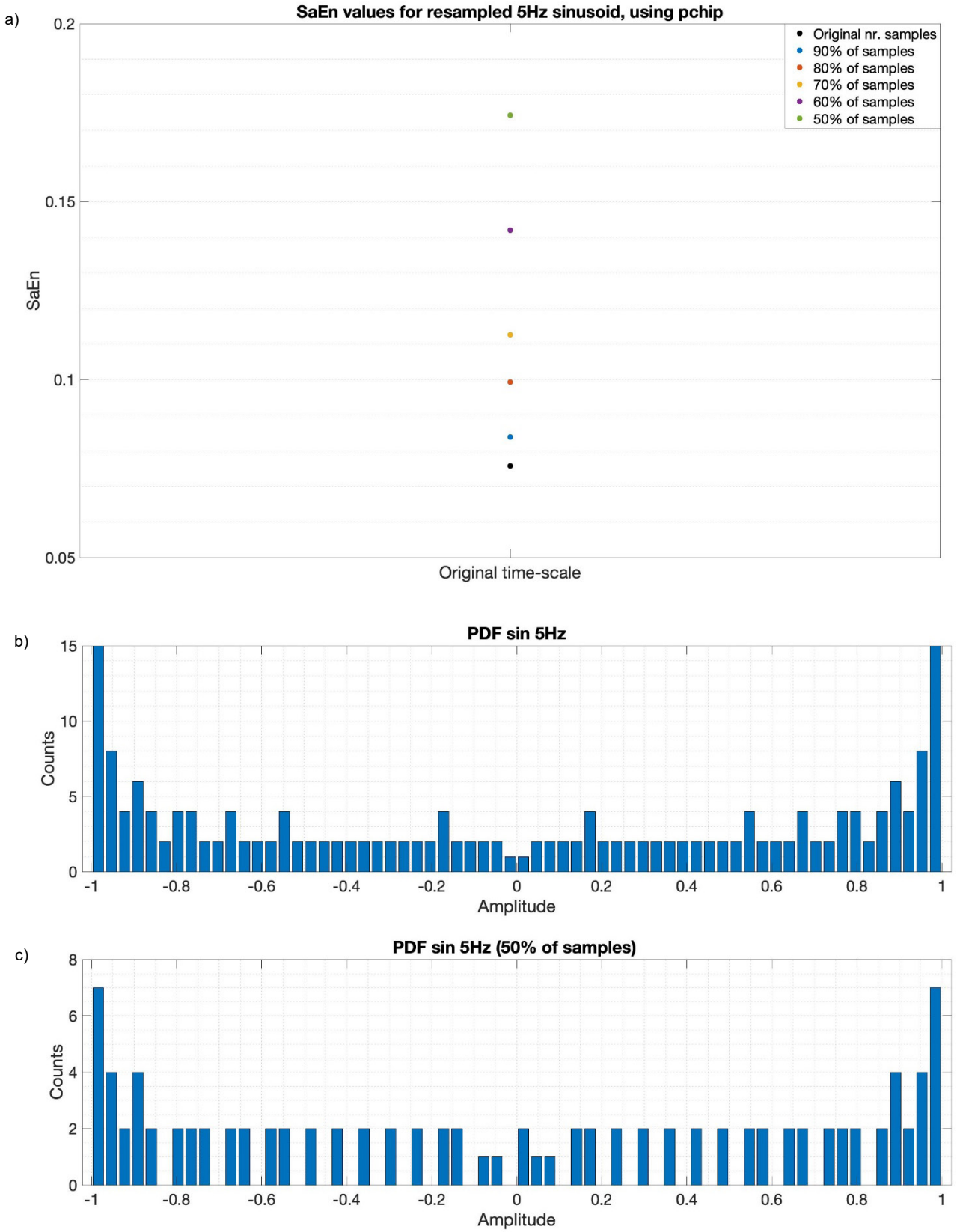

Figure A.7abc) SaEn values and PDF of resampled sin(5Hz) using 'pchip' – **a)** Displays *SaEn* values for the 5Hz sinusoid at f_s*=1000 Hz, T=0.02s*. The signal is resampled at resample rates [*0.5, 0.6, 0.7, 0.8, 0.9*]*$N_{original}$. *SaEn* values increase with the resample rate, that is explained with the PDF of the signal. **b)** PDF of the original sinusoid and the sinusoid with 50% of the original number of samples. The resampled signal displays less certainty in the amplitude counts (σ increase), leading to a higher complexity.

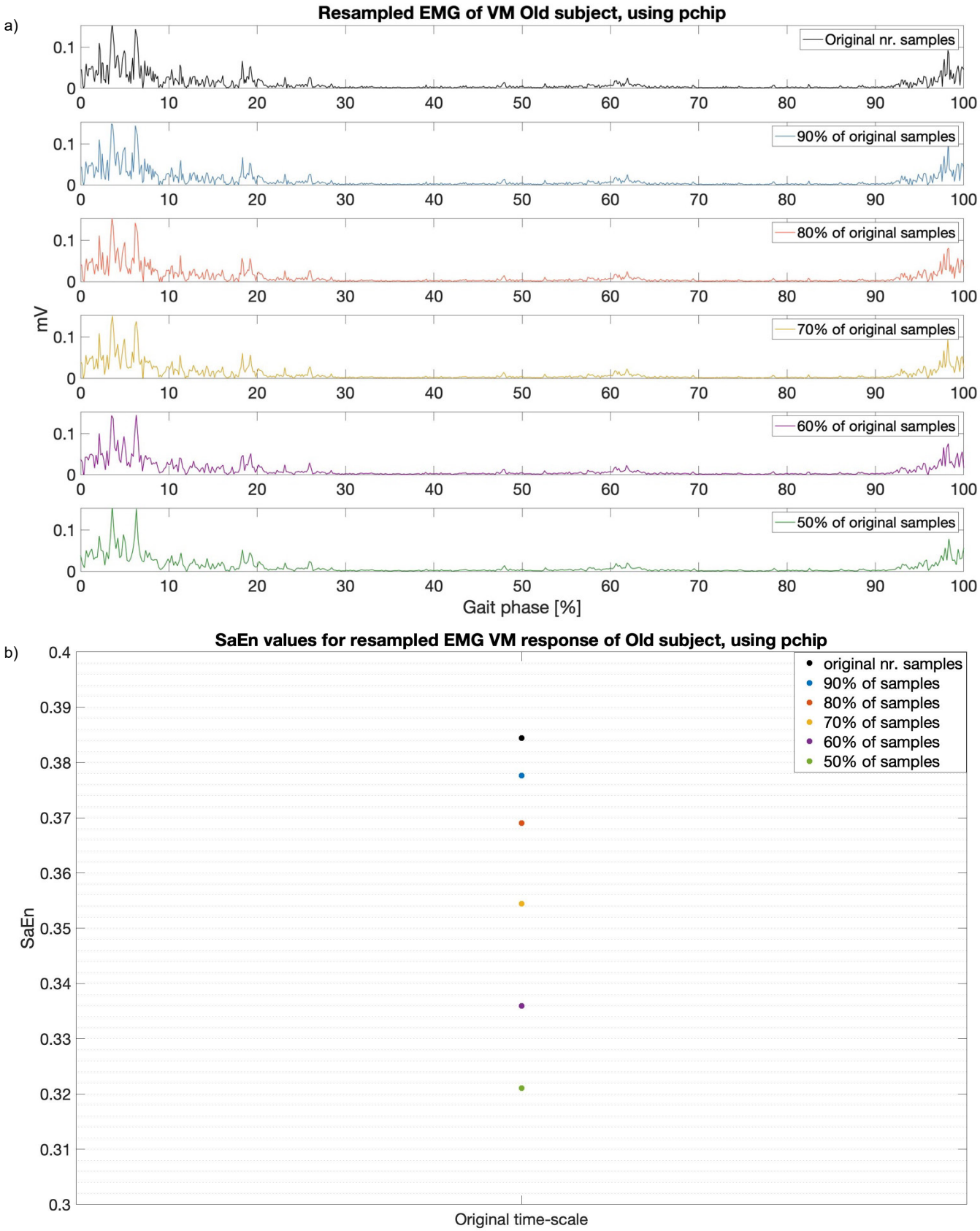

Figure A.8ab) Resampled EMG response of VM using 'pchip' and its SaEn values – **a)** Displays the EMG signal of the VM muscle of an exemplar old subject, measured in *trial 1*. The x-axis represents one gait phase, starting with the stance phase and ending with the swing phase. The erratic content is still preserved when resampling with the shape preserving spline algorithm. The signal is resampled at resample rates [*0.5, 0.6, 0.7, 0.8, 0.9*]*$N_{original}$. **b)** For erratic data, *SaEn* values decrease with the resample rate, that is explained with the PDF of the signal in *Figure A.9*.

a)

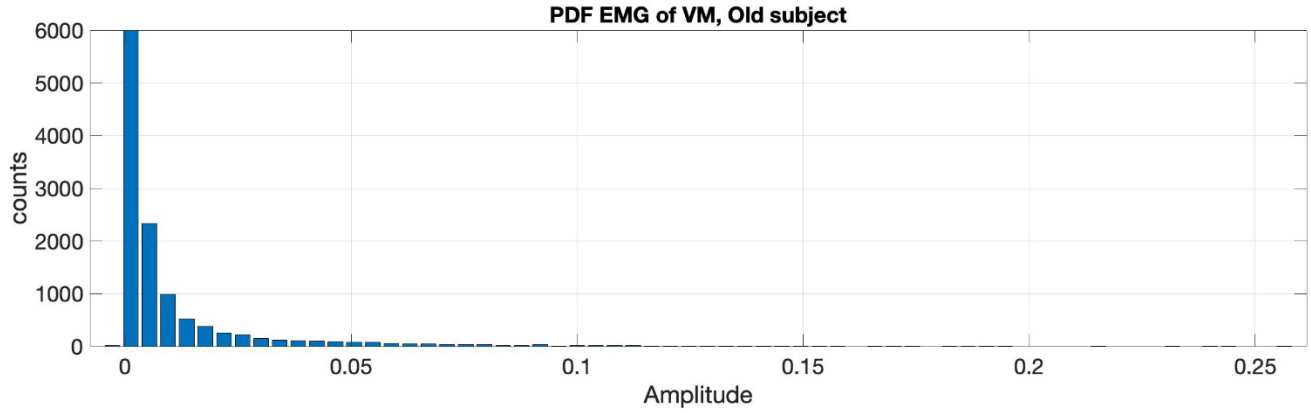

b)

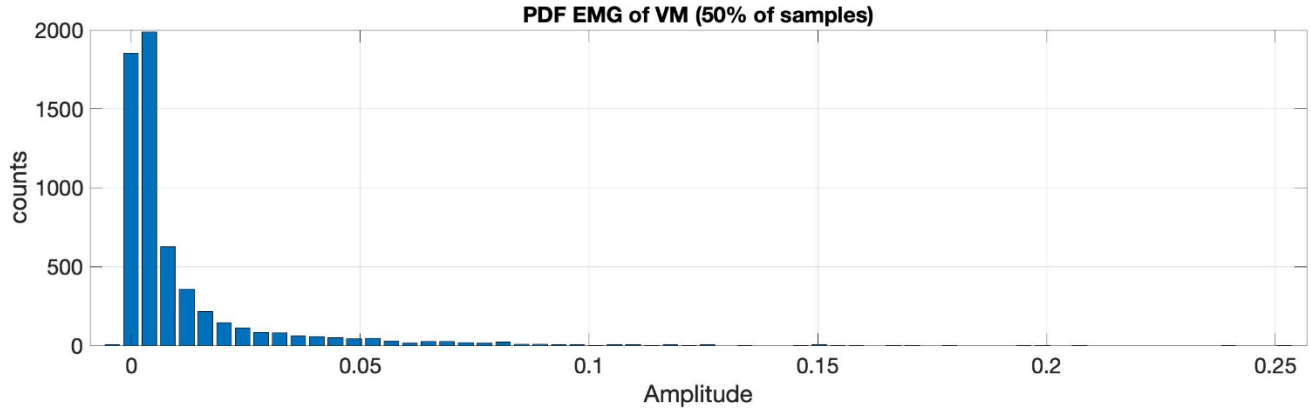

Figure A.9ab) PDF of resampled EMG response of VM using 'pchip' – Displays the PDF of the original and the resampled EMG response of the VM muscle of an exemplar old subject, measured in *trial 1.* The resampled signal with 50% of the original number of samples, displays more certainty in the amplitude counts (σ decrease), leading to a lower complexity.

Appendix C – Human Research Ethical Commission application

Delft University of Technology
ETHICS REVIEW CHECKLIST FOR HUMAN RESEARCH
(Version 22.01.2020)

I. Basic Data

Project title:	**Gait complexity changes with age and with walking velocity in human motion and electromyography signals**
Name(s) of researcher(s):	**Jeroen Vermeulen**
Research period (planning)	**March, April, May 2020**
E-mail contact person	**j.p.vermeulen@student.tudelft.nl**
Faculty/Dept.	**Biomedical Engineering, 3mE**
Position researcher(s):[1]	**MSc student**
Name of supervisor (if applicable):	**Alfred Schouten, Winfred Mugge**
Role of supervisor (if applicable):	**Associate professor, Assistant professor**

II. A) Summary Research

A major goal of many rehabilitative orthopedic treatments is the improvement of human gait. Gait complexity is suggested to increase with age and disease (Pincus et al., 1991; Pincus et al., 2006; Smith et al., 2011; Kang et al., 2016).

The present study aims to extract gait complexity measures. Healthy volunteers will be requested to walk across a lab (6m), on their preferred walking speed, a slower walking speed and a faster walking speed, while a motion capture system captures gait dynamics, an inertial measurement unit (IMU) captures trunk accelerations and surface electromyography (sEMG) electrodes capture muscle activity of leg muscles. Signal complexity of the recorded time series will be studied with entropy algorithms. Two entropy algorithms that assess signal complexity are displayed in 'Appendix 2'.

The experiment, including instruction, will take approximately 30 to 45 minutes.

[1] For example: student, PhD, post-doc

B) Risk assessment

Data collection

Measurement equipment
During the measurements, motion capture markers, sEMG sensors and an IMU will be attached to the participant. We do not expect potential risks for the subjects. Previous research displays that wearing these units while walking, does not introduce added risk for subjects (Hof et al., 2002; Tochi et al., 2012; Kang et al., 2016). The camera system (Qualysis) and the sEMG and IMU system (Delsys) both have European CE marks for medical devices and are applied for their intended use.

Personal data
Prior to the experiments, personal data (i.e.: weight, height, gender and age) will be asked of the participant on paper and will be stored in a secure location by the researcher, without access to others. Weight, height, gender and age information is used to assist in processing the experimental data and will only be kept for 12 months after the experiments. Only age, reflective marker movements, EMG recordings and trunk accelerations can be used for publication purposes. Here, important to note is that complexity differences in marker movements, EMG recordings and trunk accelerations will be displayed in an aggregated form, that is, per age group. We believe that these steps will maintain the confidentiality of the data.

Informed consent
As explained in the information letter in 'Appendix 4', to safeguard and maintain confidentiality of the collected personal data, necessary security steps are taken. All data will be processed confidentially and stored using a participant number only. The informed consent form will be stored on paper in a separate and secure location from the personal data, in the room of Dr.ir. Alfred Schouten (F-1-240). This way all personal details remain confidential. The participant number can only be coupled to the personal data by the researcher and will never be shared on publications about the research. We believe that these steps will maintain the confidentiality of the data. This way, we can make valuable research data available for validation and re-use purposes.

In the informed consent form, subjects are asked if they consent with the recording and use of their data. The informed consent form for data collection is displayed in 'Appendix 4'.

Participant recruitment
Subjects are recruited via e-mail. For the recruitment of subjects, the participant information letter is sent out to contacts of Jeroen Vermeulen. Data subjects invited for the study are not part of a specific focus group and are selected on their suitability for the present research only. In the present study, we enrolled subjects that reported that, to the best of their knowledge, they did not suffer from health issues that affect their movement in daily life activities. If individuals reported injuries, disabilities or taking medication that may influence gait, it was of utmost importance to not include them in the study. Recruited subjects are height, weight and age matched for the suitability of this research.

III. Checklist

Question	Yes	No
1. Does the study involve participants who are particularly vulnerable or unable to give informed consent? (e.g., children, people with learning difficulties, patients, people receiving counselling, people living in care or nursing homes, people recruited through self-help groups).		√
2. Are the participants, outside the context of the research, in a dependent or subordinate position to the investigator (such as own children or own students)?[2]		√
3. Will it be necessary for participants to take part in the study without their knowledge and consent at the time? (e.g., covert observation of people in non-public places).		√
4. Will the study involve actively deceiving the participants? (For example, will participants be deliberately falsely informed, will information be withheld from them or will they be misled in such a way that they are likely to object or show unease when debriefed about the study).		√
5. Sensitive personal data • Will the study involve discussion or collection of personal sensitive data (e.g., financial data, location data, data relating to children or other vulnerable groups)? Definitions of sensitive personal data, and special cases thereof are provided here.		√
6. Will drugs, placebos, or other substances (e.g., drinks, foods, food or drink constituents, dietary supplements) be administered to the study participants?		√
7. Will blood or tissue samples be obtained from participants?		√
8. Is pain or more than mild discomfort likely to result from the study?		√
9. Does the study risk causing psychological stress or anxiety or other harm or negative consequences beyond that normally encountered by the participants in their life outside research?		√
10. Will financial inducement (other than reasonable expenses and compensation for time) be offered to participants?		√
Important: if you answered 'yes' to any of the questions mentioned above, please submit a full application to HREC (see: website for forms or examples).		
11. Will the experiment collect and store videos, pictures, or other identifiable data of human subjects? [3]	√	

[2] **Important note concerning questions 1 and 2.** Some intended studies involve research subjects who are particularly vulnerable or unable to give informed consent .Research involving participants who are in a dependent or unequal relationship with the researcher or research supervisor (e.g., the researcher's or research supervisor's students or staff) may also be regarded as a vulnerable group . If your study involves such participants, it is essential that you safeguard against possible adverse consequences of this situation (e.g., allowing a student's failure to complete their participation to your satisfaction to affect your evaluation of their coursework). This can be achieved by ensuring that participants remain anonymous to the individuals concerned (e.g., you do not seek names of students taking part in your study). If such safeguards are in place, or the research does not involve other potentially vulnerable groups or individuals unable to give informed consent, it is appropriate to check the NO box for questions 1 and 2. Please describe corresponding safeguards in the summary field.

[3] Note: you have to ensure that collected data is safeguarded physically and will not be accessible to anyone outside the study. Furthermore, the data has to be de-identified if possible and has to be destroyed after a

Question	Yes	No
.		
12. Will the experiment involve the use of devices that are not 'CE' certified? *Only, if 'yes': continue with the following questions:*		√
➢ Was the device built in-house?	-	-
➢ Was it inspected by a safety expert at TU Delft? (*Please provide device report, see: HREC website)*	-	-
➢ If it was not built in house and not CE-certified, was it inspected by some other, qualified authority in safety and approved? *(Please provide records of the inspection).*	-	-
13. Has or will this research be submitted to a research ethics committee other than this one? (*if so, please provide details and a copy of the approval or submission).*		√

IV. Enclosures (tick if applicable)

- ~~Full proposal (if 'yes' to any of the questions 1 until 10)~~
- Informed consent form (if 'yes' to question 11)
- ~~Device report (if 'yes' to question 12)~~
- ~~Approval other HREC committee (if 'yes' to question 13)~~
- ~~Any other information which might be relevant for decision making by HREC~~
- Data management plan approved by a data steward (always)

V. Signature(s

Signature(s) of researcher(s)
Date:

Signature (or upload consent by mail) research supervisor (if applicable)
Date:

scientifically appropriate period of time. Also ask explicitly for consent if anonymised data will be published as open data.

A-Priori Power Analysis

Methods
To calculate the total number of participants needed to reach statistical significance, the software package 'G*Power 3.1' is used. To quantify the experimental effect in this research, a within-subject experiment design with independent variables is used: age, walking velocity. To study the main effects and interactions of age and walking velocity on gait complexity outcomes, a 'two-way fixed effects ANOVA' will be used.

Inputs
In G*Power, we select 'ANOVA: Fixed effects, special, main effects and interactions'. The parameters we use are:

Error probability: $\alpha = 0,05$
Degrees of freedom: df_1=2-1 (2 age groups); df_2=3-1 (3 velocity groups); $df=df_1*df_2=2$
Number of groups = 2
Effect size: $f^2 = (R_{AB}^2 - R_A^2)/(1-R_{AB}^2)$

Below, we calculated effect sizes for results found in previous pieces of research, to check the validity of our research set up.

Complexity difference in trunk accelerations with walking speed (Katonis et al., 2009)
f = 1.23: two groups of 7 subjects needed
EMG complexity of gastrocnemius in young and old adults (Kang et al., 2016)
f = 1.17: two groups of 8 subjects needed
EMG amplitude changes with walking speed in younger adults (Hof et al., 2002)
f = 0.9: two groups of 12 subjects needed
Complexity difference in gait angle at the knee with walking speed (Geerse et al., 2015)
f = 1.1: two groups of 9 subjects needed

Output
To give an estimation on our required effect size, we calculated effect sizes for previous complexity results in gait angle dynamics, trunk accelerations and EMG responses, that either displayed differences with age or walking speed. To reach significance in all domains, we need a total number of subjects of 26.

Group 1: 13 subjects aged around 60; Group 2: 13 subjects aged around 25.

Information letter & Informed Consent Form

Information letter for participants

Research Study
Gait complexity changes with walking velocity and with age in human motion and electromyography signals

This information letter is for individuals who are invited to participate in the TU Delft research study that investigates the effects of age and walking velocity on the complexity of human motion and electromyography signals.

Researchers:	Jeroen Vermeulen (contact), Winfred Mugge, Alfred Schouten, Jurriaan de Groot, Marjon Stijntjes
Supervisors:	Alfred Schouten, Winfred Mugge
Organization Name:	Delft University of Technology (TU Delft)
Faculty:	Biomedical Engineering – Mechanical, Materials and Maritime Engineering (3mE) Faculty, TU Delft

Below is a brief introduction to the study and your role in it. If you agree to participate after reading this information, please sign the certificate of consent at the end of this form.

Study information (25-02-2020)

Purpose of the research
A major goal of many rehabilitative orthopedic treatments is the improvement of human gait. In recent research, gait complexity is suggested to decrease with age and disease. The present study aims to extract gait complexity measures of young and old adults. For this purpose, you will be asked to walk across a 6m hallway on a 'preferred walking speed' a 'slower' and a 'faster' walking speed. Results of this study will help to understand if changes in gait complexity might serve as a useful biomarker for future orthopedic treatments.

Qualification
You are an adult of around 25 or 60 years old, who weighs between 50 and 100 kg. To the best of your knowledge, you do not suffer from health issues that affect your movement in daily life activities. To participate, you must be in Delft on the experiment day.

Your role and time commitment
Before starting the experiment, your weight, height, age and gender will be asked. Next, we will connect reflective markers, that will measure your leg dynamics, and surface electromyography (sEMG) electrodes, that will measure your leg muscle activity. Reflective markers and sEMG electrodes are only recording data, which is completely harmless to your body. A calibration procedure for the measurement set-up is performed next, in which you will be asked to walk back and forth in a 6m long hallway. After calibration, you will be asked to walk the same trajectory on 3 different walking speeds. You are advised to wear tight-fitting clothes in order to maintain accuracy for the motion tracking system. Important note: We can provide the appropriate clothing at the lab. The experiment is expected to take approximately 30 to 45 minutes.

Discomforts
When wearing the sEMG electrodes and motion tracking markers, you might experience slight discomfort, however, this will subside once you are accustomed to it.

Data acquisition
Reflective markers for 3D motion acquisition will be attached to your feet, knee, hip and back. EMG electrodes will be placed directly on the skin to measure muscle activity of your leg muscles. An acceleration sensor will be attached to your trunk. All sensors and electrodes can easily be removed after the data has been recorded.

Data Policy
Personal information, your weight, height, gender and age, will be asked prior to the experiments on paper and only the researcher has access to it. This information is used to assist in processing the experimental data and will only be kept for 12 months after the experiments. The experimental data, your motion data and EMG recordings, will be recorded during the experiments. Your informed consent form will be stored on paper at a separate location from the personal information and the recorded data. Important to note is that the consent form contains your signature and subject number and can only be linked to other data by the researchers. Only the reflective marker movements, EMG recordings, trunk accelerations and your age can be used for publication purposes. Here, important to note is that these data outputs will only be displayed in an aggregated form, that is, complexity outcomes of marker movements, EMG recordings and trunk accelerations displayed per age group. This way, all personal details remain confidential at all times.

Participants rights
Participation in this research study is voluntary. Even after you agree to participate and begin the study, you are free to withdraw at any time and for any reason. You have the right to ask that any data you have supplied can be withdrawn. You have the right to omit or refuse to answer or respond to any question that is asked. When there is no data being recorded, you may ask any questions to the researcher, unless answering these questions would interfere with the study outcome. If any questions arise as a result of reading this information sheet, you need to ask the investigators before start of the experiment.

Reimbursement and compensation:
Reimbursement or compensation is not applicable for this study, although, the researcher will have snacks available for the participant.

Location
The measurements for the present study are performed in the Biomechamotion lab, located in room 34 E-0-300 at the Mechanical Engineering department of the TUDelft.

For further information:
The investigators and supervisors listed above will gladly answer your questions about this study at any time. If you are interested in the final results of this study, you can contact the investigator:
Jeroen Vermeulen at j.p.vermeulen@student.tudelft.nl, +31612239363

Subject no.: ___

My gender: m / w

My age: ___ [y]

My weight: ___ [kg]

My height: ___ [m]

Consent Form for study: 'Gait complexity changes with walking velocity and with age in human motion and electromyography signals'

(Please tick the appropriate boxes)	**Yes**	**No**
Taking part in the study		
I have read and understood the study information dated 25/02/2020, or it has been read to me. I have been able to ask questions about the study and my questions have been answered to my satisfaction.	□	□
I consent voluntarily to be a participant in this study and understand that I can refuse to answer questions and I can withdraw from the study at any time, without having to give a reason.	□	□
I understand that taking part in this study involved the recording of passive markers for motion acquisition, the recording of EMG electrodes for measuring muscle activity and the recording of an acceleration sensor to measure trunk accelerations.	□	□
I understand that any personal data will only be accessible for the researchers, at all times.	□	□
Use of information in the study		
I understand that information I provide will be used for the master thesis research of Jeroen Vermeulen. Complexity outcomes of reflective marker movements, EMG recordings and trunk accelerations can be displayed in publications in an aggregated form, that is per age group.	□	□
I understand that personal information collected about me that can identify me, such as my signature, age and weight, is only accessible to the researchers. Additionally, this consent form can be linked to personal data by the researchers only. This way, I understand that all personal information remains confidential at all times	□	□
Future use and re-use of the information by others		
I give permission that the information I provide (i.e. reflective marker movements, EMG recordings, trunk accelerations and my age) can be archived in the TU Delft Biomechamotion lab project drive. All data will be processed confidentially and will only be accessible by the researcher.	□	□

Certificate of consent
I have read and understand the information above, and have had the opportunity to ask questions and my questions have been answered satisfactorily. By signing this form, I consent to participate as a research participant in this study.

_____ _____ _____
(Signature of Participant) Subject no. Date

_____
(Name of Researcher - BLOCK)

_____ _____
(Signature of Researcher) Date

If you would like a copy of the consent form, please ask the researcher.

Data management plan

Gait complexity changes with age and with walking velocity in human motion and electromyography signals

General TU Delft data management questions **1. Is TU Delft the lead institution for this project?**

Yes, leading the collaboration
Dr. Ir. Jurriaan de Groot (j.h.de_groot@lumc.nl) (TUDelft/LUMc), is involved.

2. If you leave TU Delft (or are unavailable), who is going to be responsible for the data resulting from this project?

Associate TU Professor (dept. 3mE): Alfred Schouten (a.c.schouten@tudelft.nl)

3. Where will the data (and code, if applicable) be stored and backed-up during the project lifetime?

Project Storage at TU Delft
Password protected: BME Gait lab, 3mE, TUDelft

4. How much data storage will you require during the project lifetime?

< 250 GB -

5. What data will be shared in a research data repository?

Not all data can be publicly shared - please explain below which data and why cannot be publicly shared
Only age, reflective marker movements, EMG recordings and trunk accelerations will be used for publication purposes, and can be shared to a research repository.

6. How much of your data will be shared in a research data repository?

< 100 GB -

7. How will you share your research data (and code)?

My data can't be shared in a repository, so the metadata will be registered in Pure instead and all research publications resulting from the project have a statement explaining what additional datasets/materials exists; why access is restricted; who can use the data and under what circumstances.
-

8. Does your research involve human subjects?

Yes -

9. Will you process any personal data? Tick all that apply

Gender, date of birth and/or age
Prior to the experiments, participants are asked for personal information on paper: age, weight, height and gender. This data will only be kept 12 months after the experiments.
Experimental data, that can be linked to the participant, motion data and EMG recordings, will be recorded during the experiments.
The informed consent form will be stored on paper at a separate location from the personal information and the recorded data. Important to note is that the consent form contains the participant's signature and subject number and can only be linked to other data by the researchers. This way all personal details remain confidential at all times. Age, weight, height and gender information is used for the correct processing of EMG and motion data only and only the researchers have access to it.

TU Delft questions about management of personal research data

1. Please detail what type of personal data you will collect, for what purpose, how you will store and protect that data, and who has access to the data.

Please provide your answer in the table below. Add an extra row for every new type of data processed:

Type of data	How will the data be collected?	Purpose of processing	Storage location	Who will have access to the data
Age	The participant will be asked in the information letter	Extract gait complexity measures with age and walking velocity	TU Delft Project Storage	Only Researcher
Height, Weight, Gender	The participant will be asked in the information letter	Extract gait complexity measures with age and walking velocity	TU Delft Project Storage	Only Researcher
EMG, Accelerations, Marker movements	Sensors collect the data	Extract gait complexity measures with age and walking velocity	TU Delft Project Storage	Only Researchers involved in the project (Guarded with password)
Signature	The participant will be asked on the Informed Consent form	Informed Consent	Dr.ir. Alfred Schouten's room - 3mE: F-1-240	Only Researcher

2. Will you be sharing personal data with individuals/organisations outside of the EEA (European Economic Area)?

No -

3. What is the legal ground for personal data processing?

Informed consent - please describe the informed consent procedures you will follow
As explained in the information letter in 'Appendix 4', to safeguard and maintain confidentiality of the collected personal data, necessary security steps are taken. The informed consent form will be stored on paper in a separate and secure location from the personal data, in the room of Dr.ir. Alfred Schouten (F- 1-240). This way all personal details remain confidential. The participant number can only be coupled to the personal data by the researcher and will never be shared on publications about the research. We believe that these steps will maintain the confidentiality of the data. This way, we can make valuable research data available for validation and re-use purposes.
In the informed consent form, participants are asked if they consent with the recording and use of their data. The informed consent form for data collection is displayed in 'Appendix 4'.

4. Will the personal data be shared with others after the end of the research project, and if so, how and for what purpose?

No.

5. Does the processing of the personal data results in a high risk to the data subjects?

None of the above apply -

- ***End of Appendix C***

Appendix D – Joint marker placement

Marker name	Marker location	Marker placement
C7	7th cervical vertebra	Bend head forward, most pronounced vertebra is Spinous Process of 7th cervical vertebra. Check: bring head back upright and then rotate head, C7 will move, 1st thoracic vertebra won't.
T10	10th thoracic vertebra	On the Spinous Process, at level of the bottom of the shoulder blades (with arms handing down). Make sure it is in the middle.
XIPH	Xiphoid process	Lower edge of sternum. Make sure it is in the middle
JN	Jugular notch	Upper edge of sternum. Make sure it is in the middle.
LASIS RASIS	Left/Right ASIS	Palpate from below the anterior superior iliac spine. Place marker on most pronounced part.
LPSIS RPSIS	Left/Right PSIS	Placed on the skin on most pronounced part on dimple (if visible).
LGTRO RGTRO	Left/Right greater trochanter	Technical marker only. Palpate from distal while pushing hip outward ('model pose') or rotate the leg.
LLTHI	Left lateral thigh	On the lateral side of thigh; ±1/3 in line LGTRO – LLEK just below the swing of the hand. The anterior/ posterior position critical for definition upper leg.
RLTHI	Right lateral thigh	On the lateral side of thigh; ±2/3 in line LGTRO – LLEK just below the swing of the hand. The anterior/ posterior position critical for definition upper leg.
LATHI	Left anterior thigh	Technical marker only. On the anterior side of thigh at same height as LLTHI. Exact location not relevant, but not in line with other markers.
RATHI	Right anterior thigh	Technical marker only. On the anterior side of thigh at same height as RLTHI. Exact location not relevant, but not in line with other markers.
LLEK RLEK	Left/Right lateral epicondyle knee	Placed on the lateral epicondyle of the left knee.
LMEK RMEK	Left/Right medial epicondyle knee	Placed on the medial epicondyle of the knee along an imaginary line that passes through the transfemoral axis.
LFH RFH	Left/Right fibula head	Most pronounced part, just underneath LEK. Palpate from distal direction
LTT RTT	Left/Right tibial tuberositas	In the medial/lateral most pronounced middle, underneath patellar tendon insertion. Palpate from distal direction.
LLSHA RLSHA	Left/Right lateral shank	On the lateral side of the shank. Halfway LEK and LM.
LLM RLM	Left/Right lateral malleolus ankle	Most pronouncing part along an imaginary line that passes through the transmalleolar axis
LMM RMM	Left/Right medial malleolus ankle	Most pronouncing part along an imaginary line that passes through the transmalleolar axis.
LHEE RHEE	Heel / dorsal calcaneus	Placed in the middle of the posterior aspect of the calcaneus at the same height above the plantar surface of the foot as MT2. MT2 and LHEE used to calculate line of the foot for progression.
LMT5 RMT5	Left/Right 5th metatarsal	On top of 5th metatarsal head.
LMT2 RMT2	Left/Right 2nd metatarsal	Placed on top of the distal ends of the caput of the 2nd metatarsal bone, on joint line midfoot/toes.
LMT1 RMT1	Left/Right 1st metatarsal	On top of 1st metatarsal head.
LTOE RTOE	Left/Right tip of toe	On top of tip of 1st toe.

Table 4) Kinematics: marker name, location and placement – The marker name, location and placement is displayed for capturing movement kinematics of the lower extremity. Markers of the upper extremity were not used for entropy analysis. For data extraction, all marker positions were linked to boney landmarks.

Appendix E – Detailed results

⁎ Overview

Here, we display power spectra plots for EMG, GRF an GA data of exemplar young subject data. Subsequently, we display *SaEn* outcomes of temporal resolutions *1-20* of the data for *trial 1-2: Asymmetric Normal Speed (ANS) – Asymmetric Fast Speed (AFS)* and for *trail 3-4: Slow fixed speed (F1) – Fast fixed speed (F2)*. Lastly, we display *SaEn* results of the temporal resolution that maximized complexity for *trial 1-4.*

Appendix E1: Power spectra

E1.1) Raw EMG power spectrum at PWS – trial (ANS)
E1.2) Raw GRF power spectrum at PWS – trial (ANS)
E1.3) Raw GA power spectrum at PWS – trial (ANS)

Appendix E2: Multiscale Entropy outcomes

E2.1)	*MSE EMG,*	*trial (ANS, AFS)*
E2.2)	*MSE EMG,*	*trial (F1, F2)*
E2.3)	*MSE GRF,*	*trial (ANS, AFS)*
E2.4)	*MSE GA,*	*trial (ANS, AFS)*

Appendix E3: Sample Entropy outcomes

E3.1)	*SaEn EMG,*	*trial (ANS, AFS),*	*scale 1*
E3.2)	*SaEn EMG,*	*trial (F1, F2),*	*scale 1*
E3.3)	*SaEn GRF,*	*trial (ANS, AFS),*	*scale 12*
E3.4)	*SaEn GA,*	*trial (ANS, AFS),*	*scale 14*

E1) Power spectra

* **E1.1) Raw EMG power spectrum at PWS (exemplar young subject – *trial ANS*)**

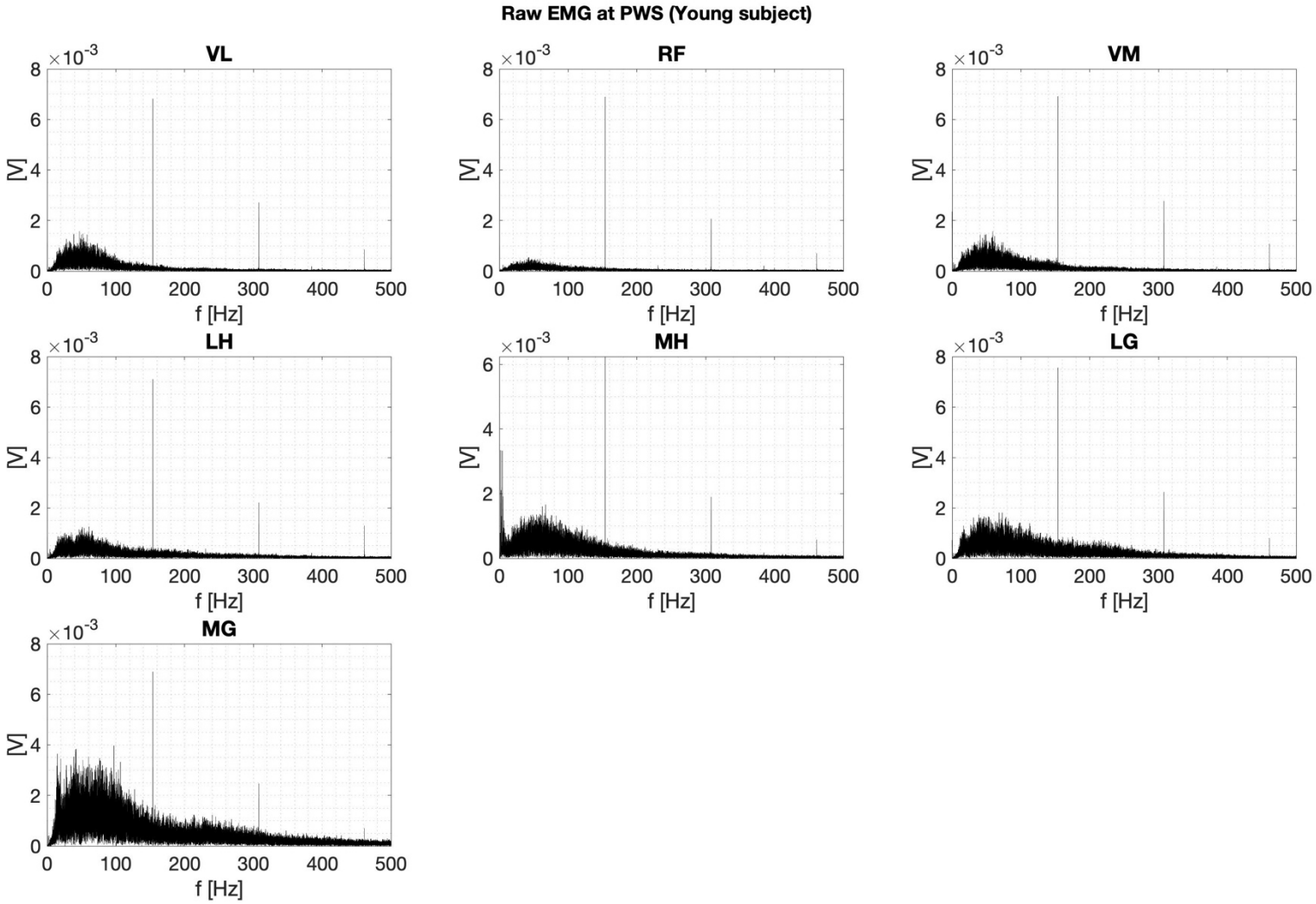

* **E1.2) Raw GRF power spectrum at PWS (exemplar young subject – *trial ANS*)**

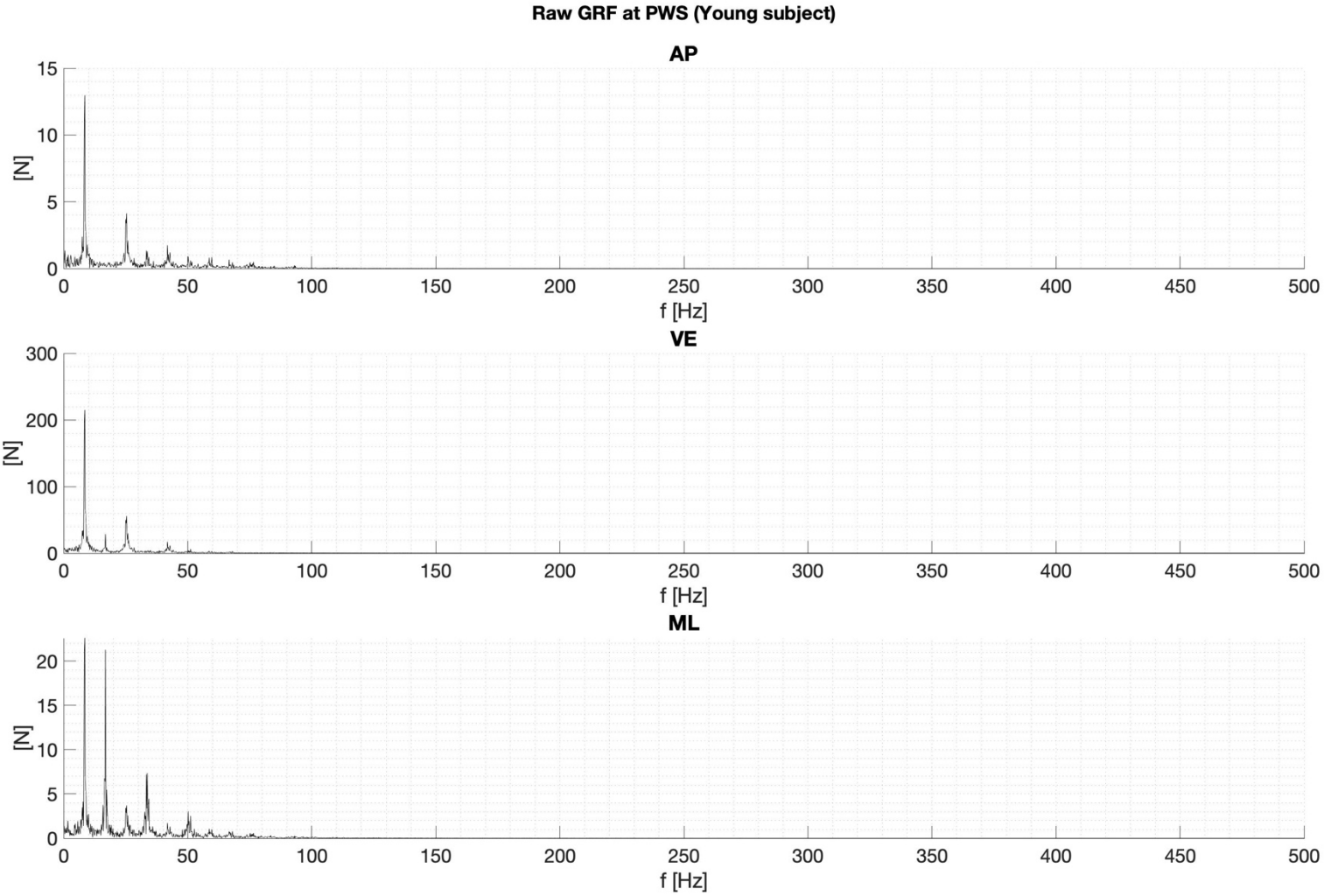

* **E1.3) Raw GA power spectrum at PWS (exemplar young subject – *trial ANS*)**

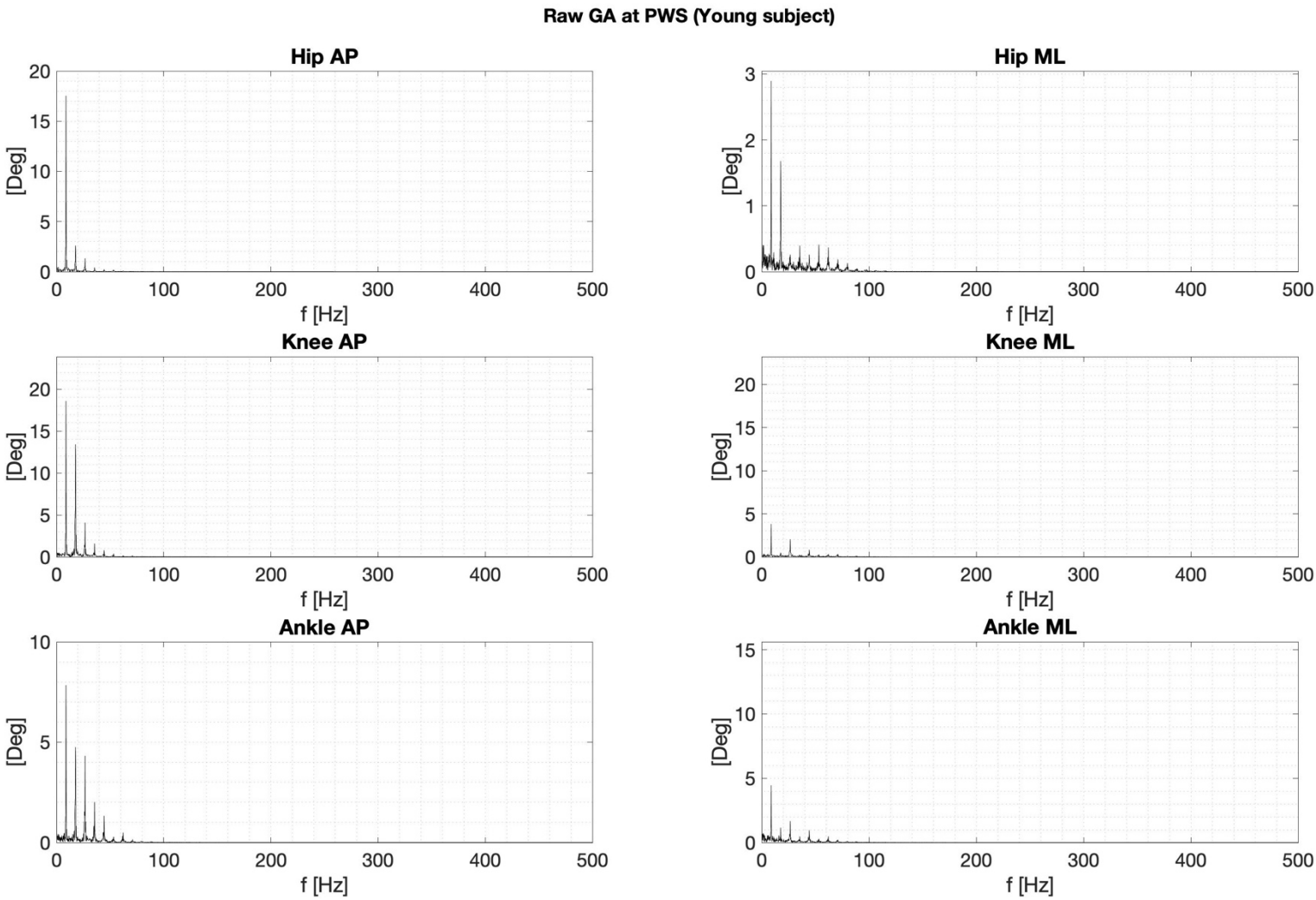

E2) Multiscale Entropy curves

* **E2.1) EMG complexity for short steps and for long steps (*trial ANS, AFS*)**
(N_{young} = 18, N_{old} = 19)

E2.1.1) Vastus Lateralis

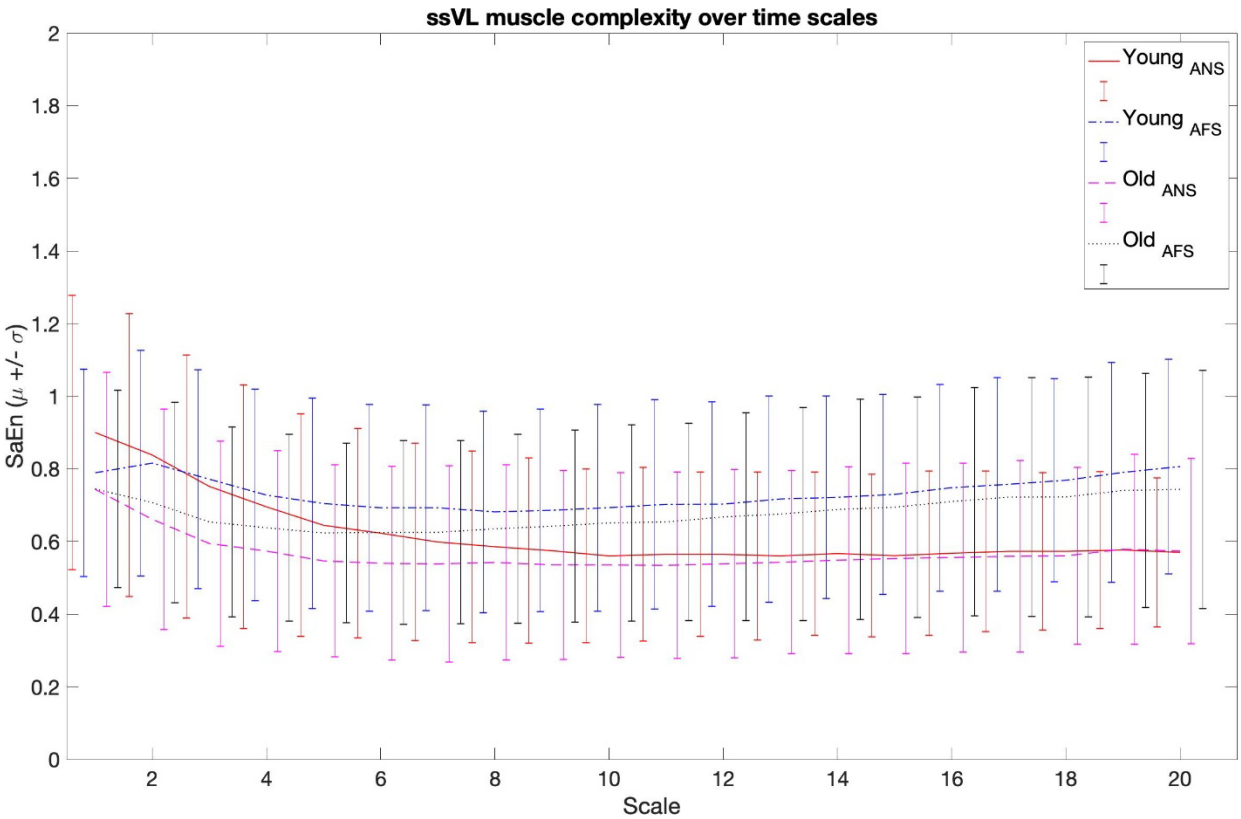

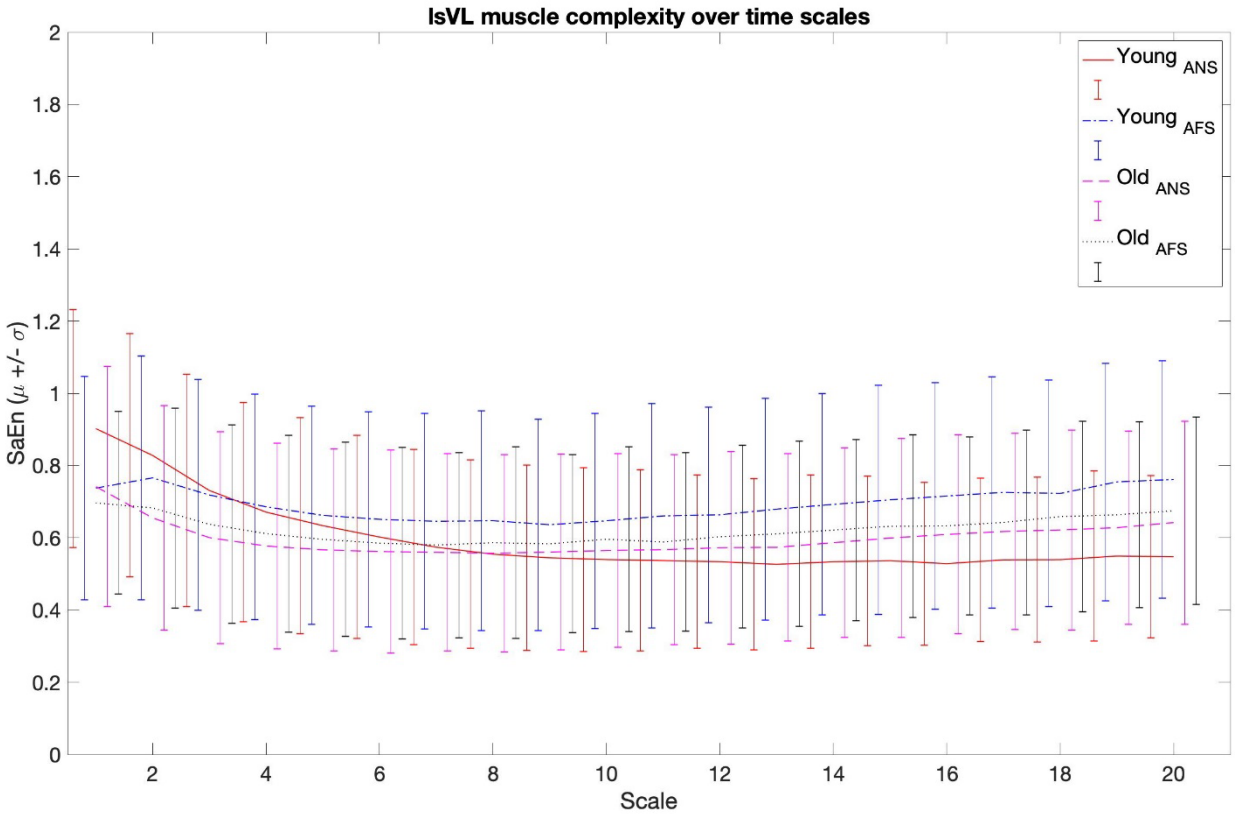

E2.1.2) Rectus Femoris

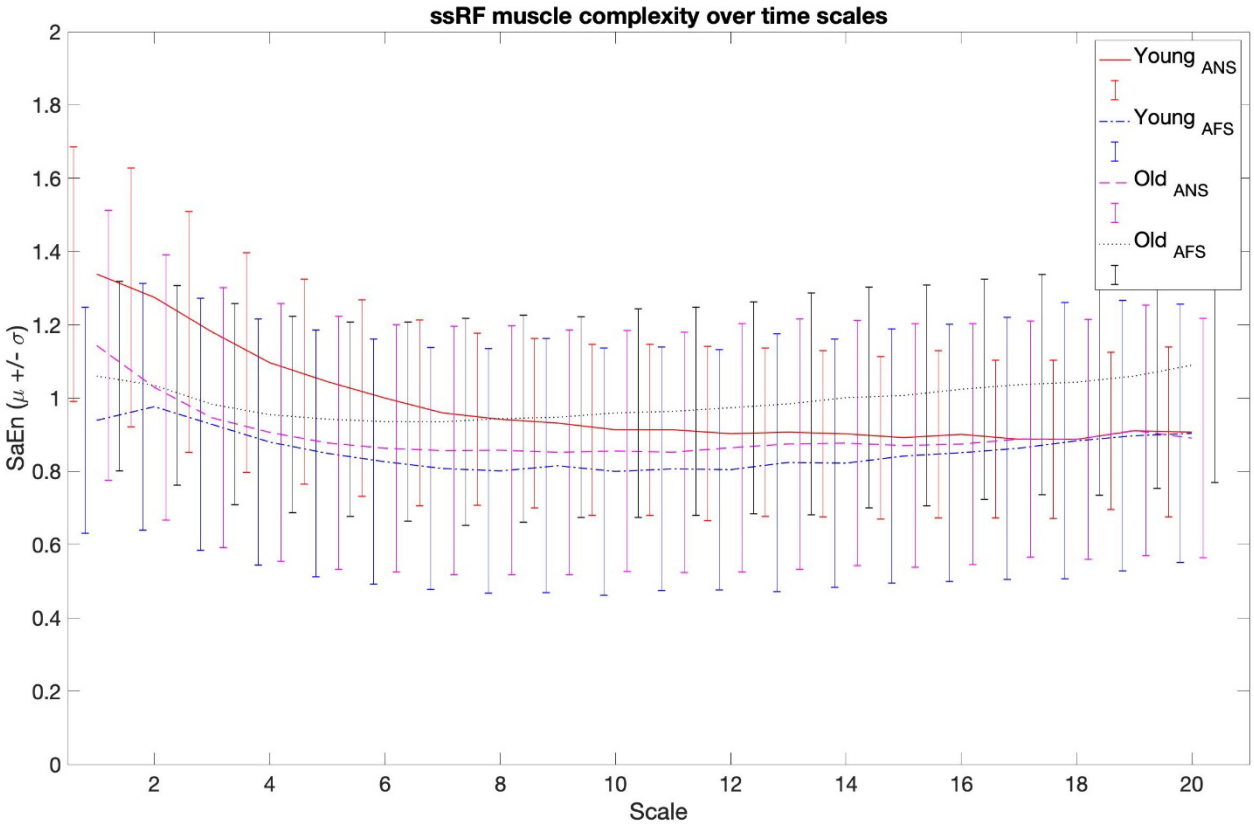

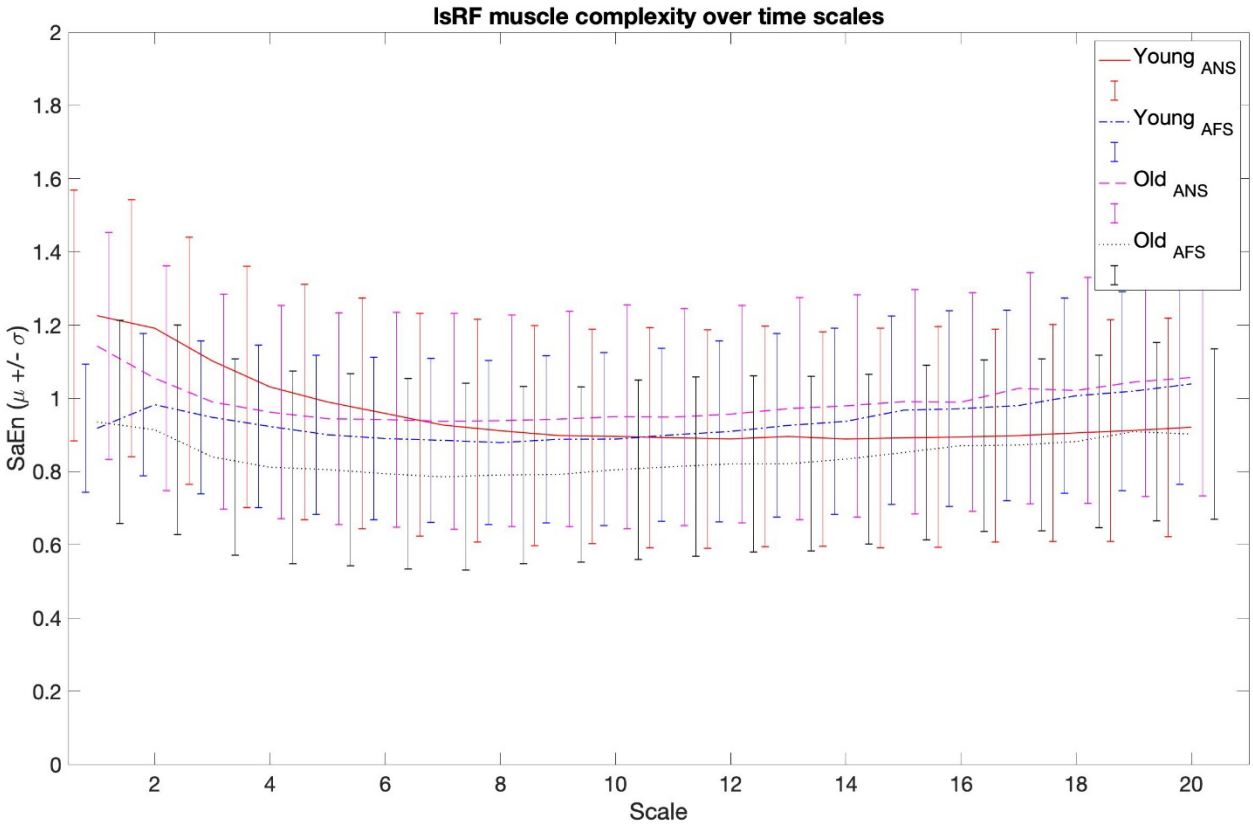

E2.1.3) Vastus Medialis

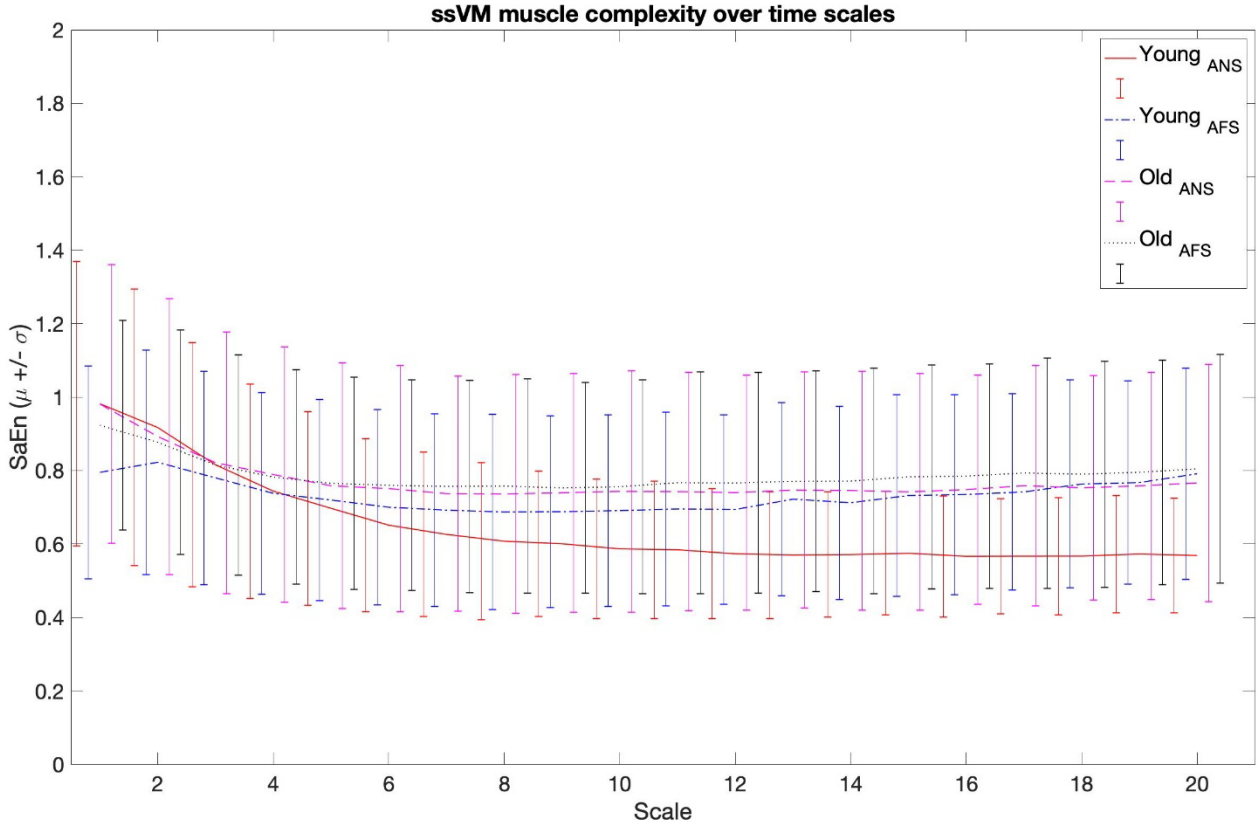

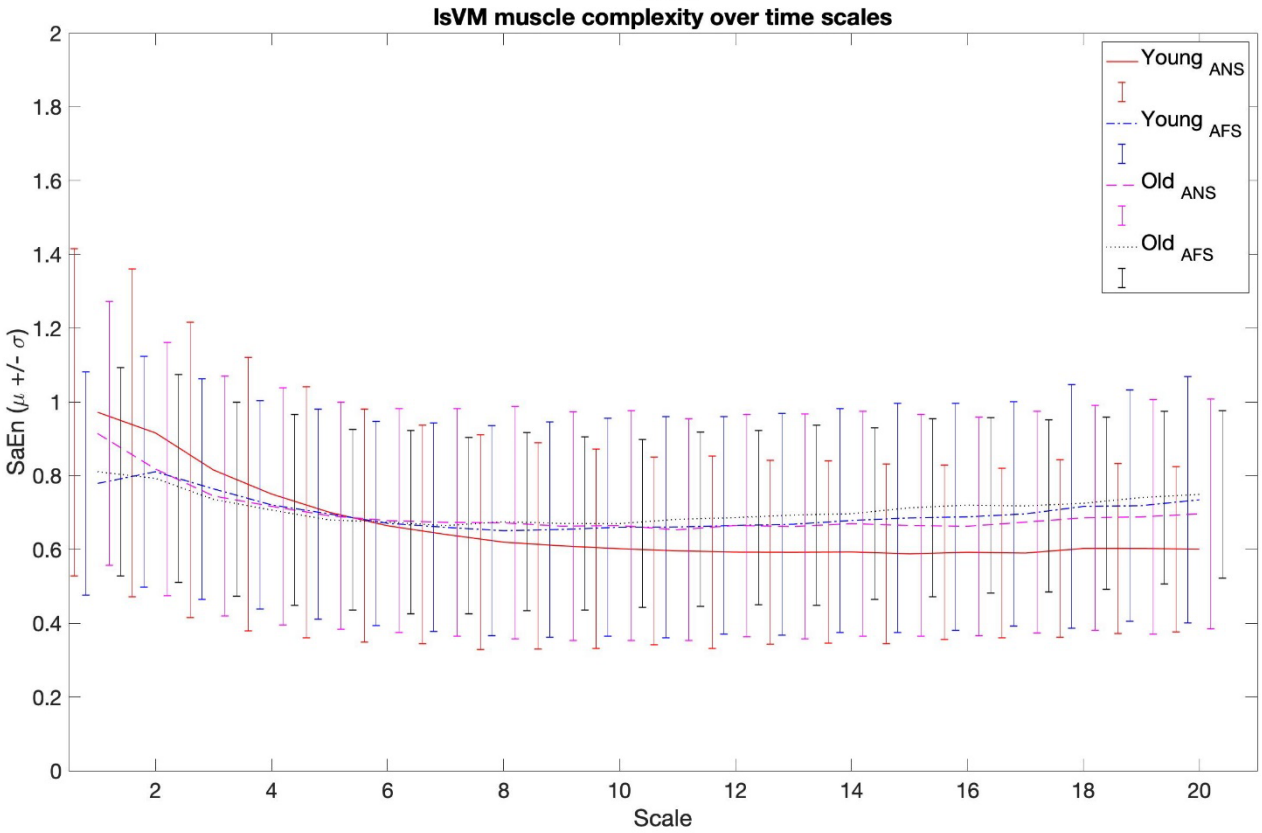

E2.1.4) Lateral Hamstrings (Biceps Femoris)

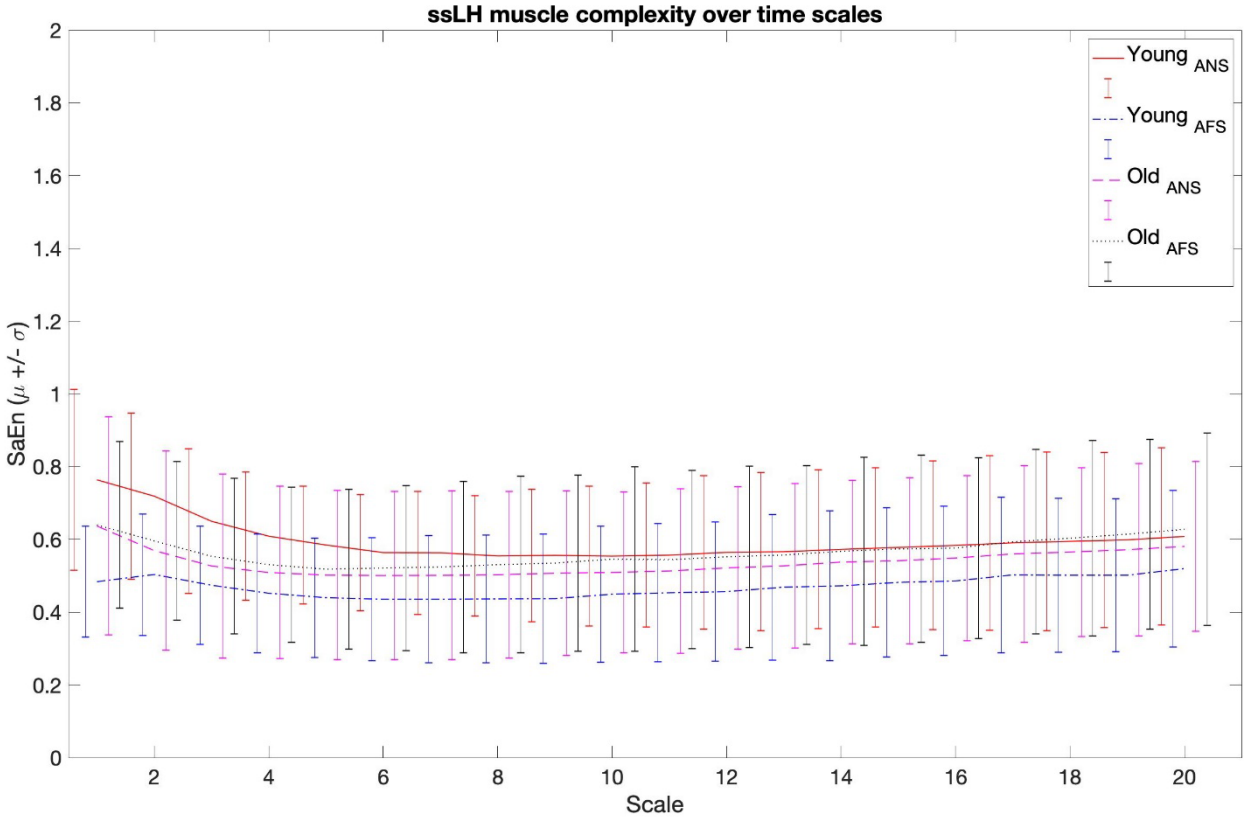

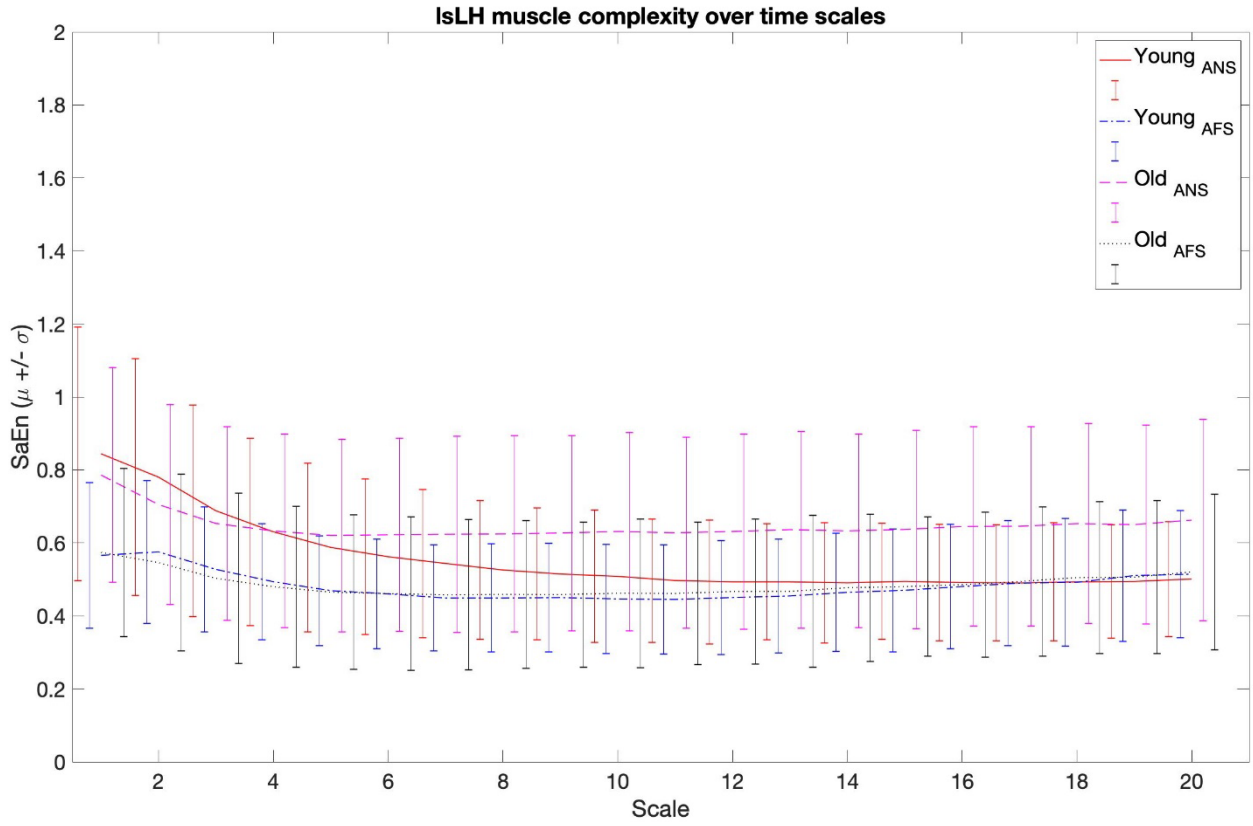

E2.1.5) Medial Hamstrings (Semimembranosus, Semitendinosus)

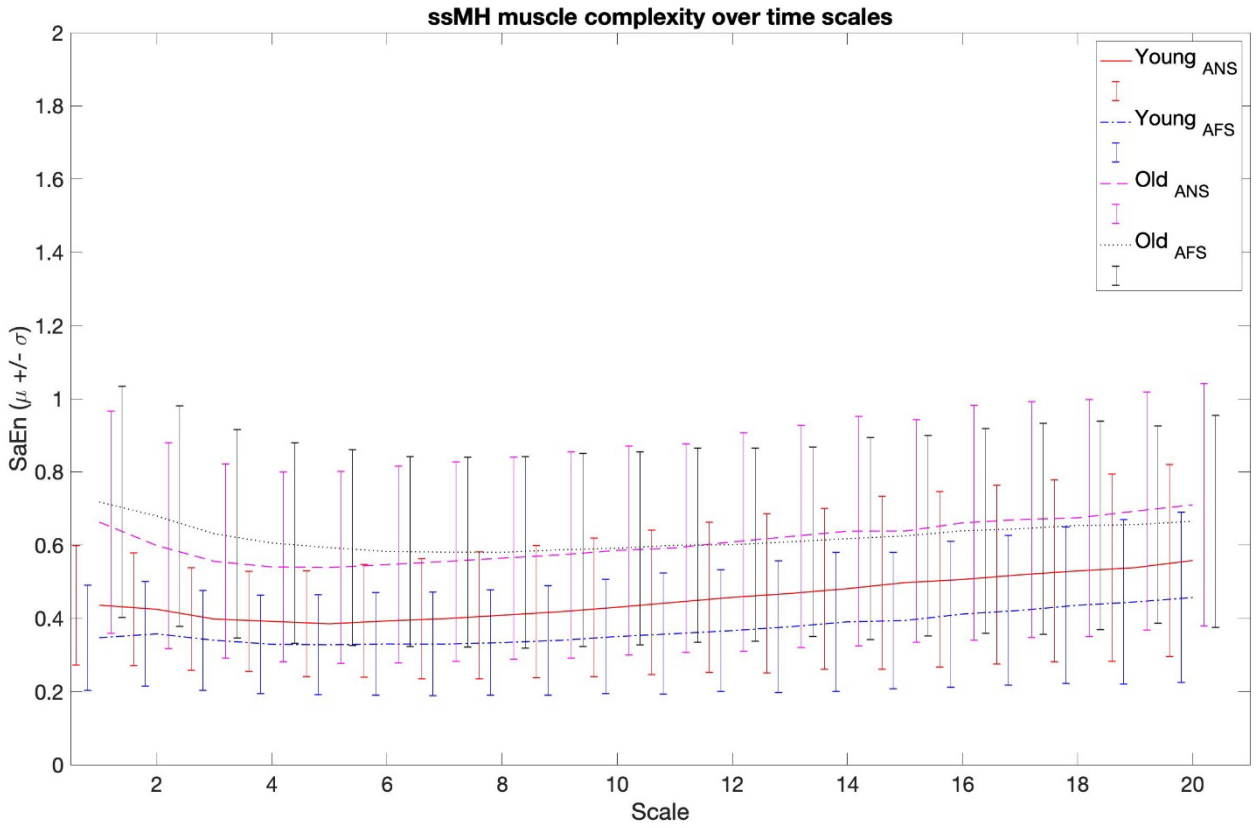

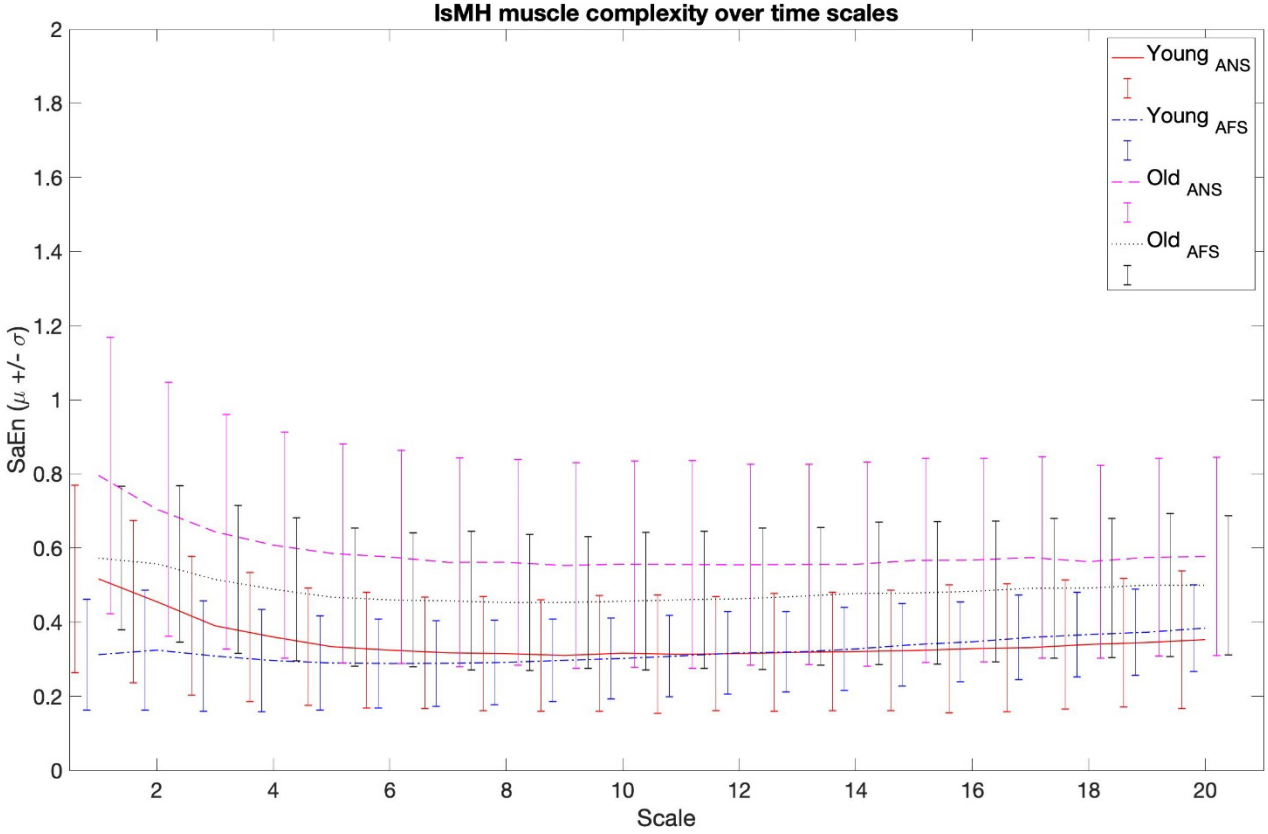

E2.1.6) Lateral Gastrocnemius

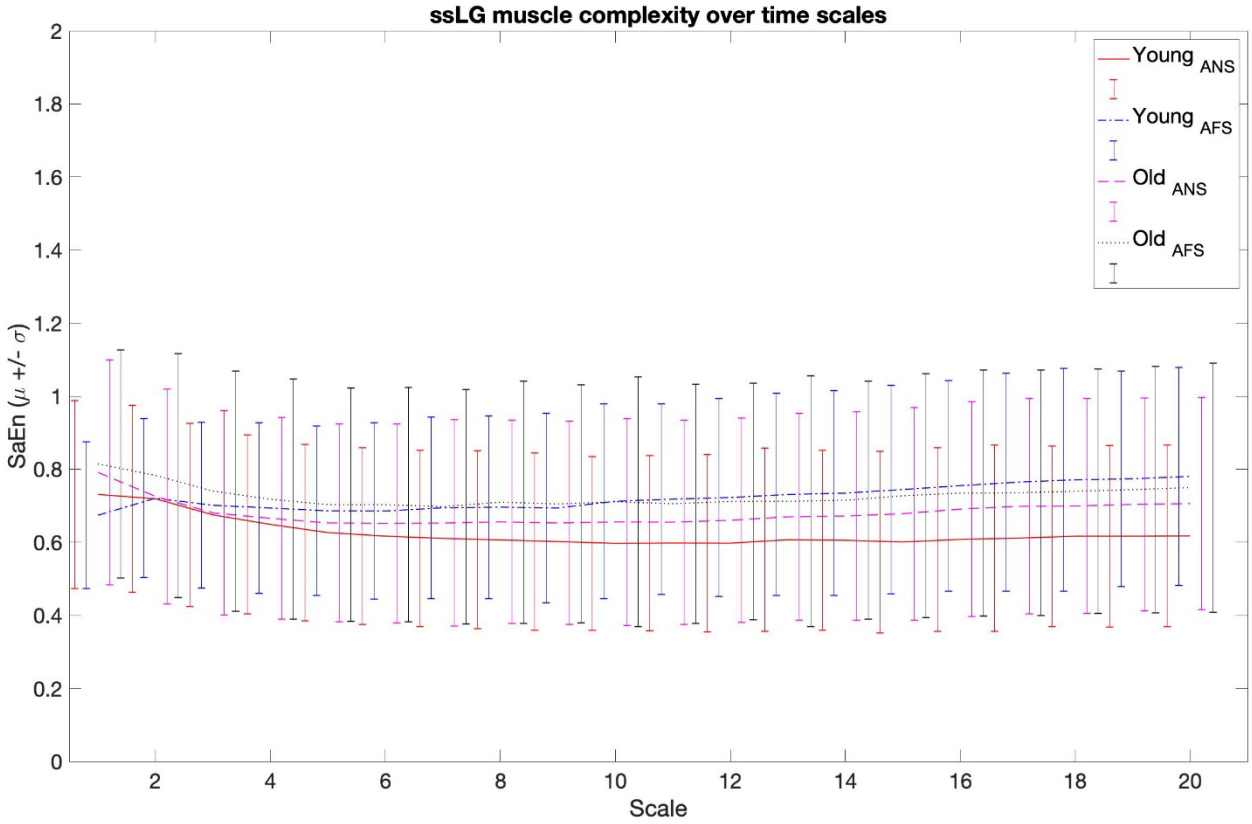

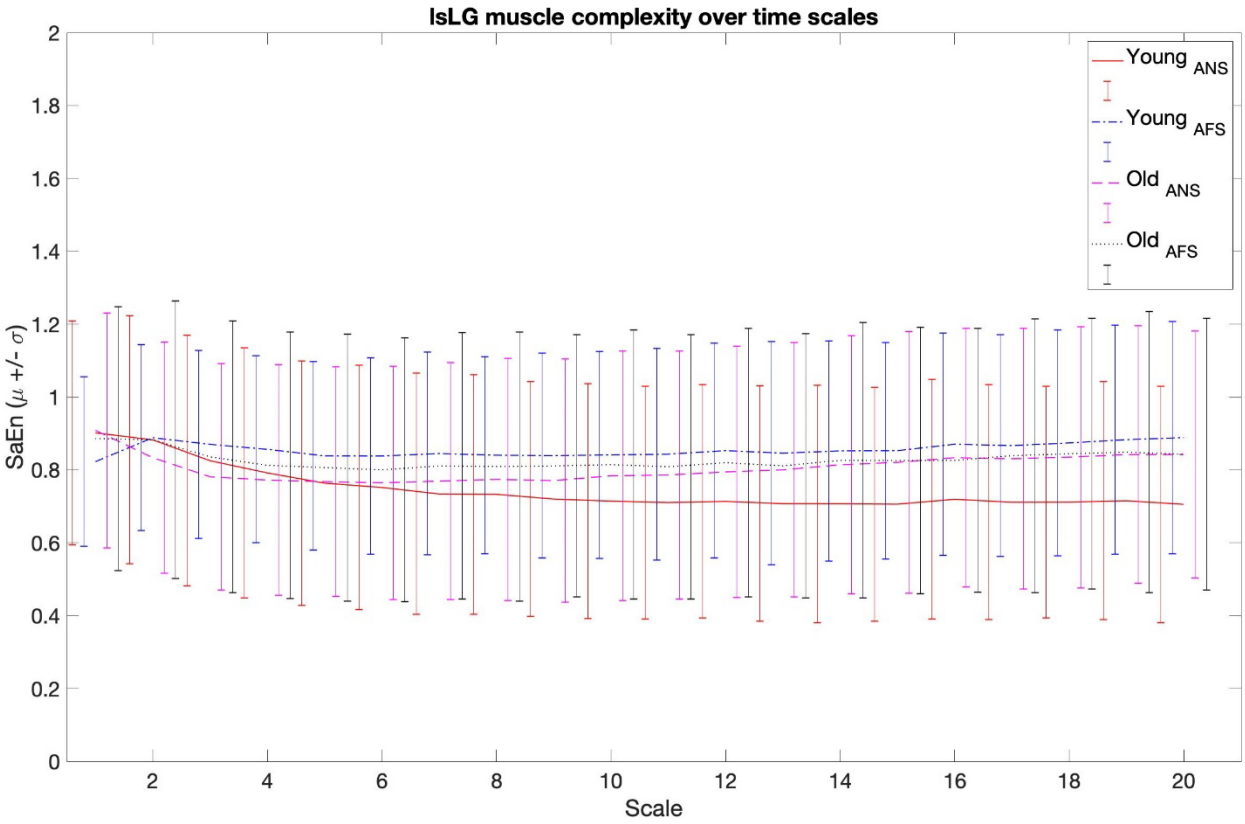

E2.1.7) Medial Gastrocnemius

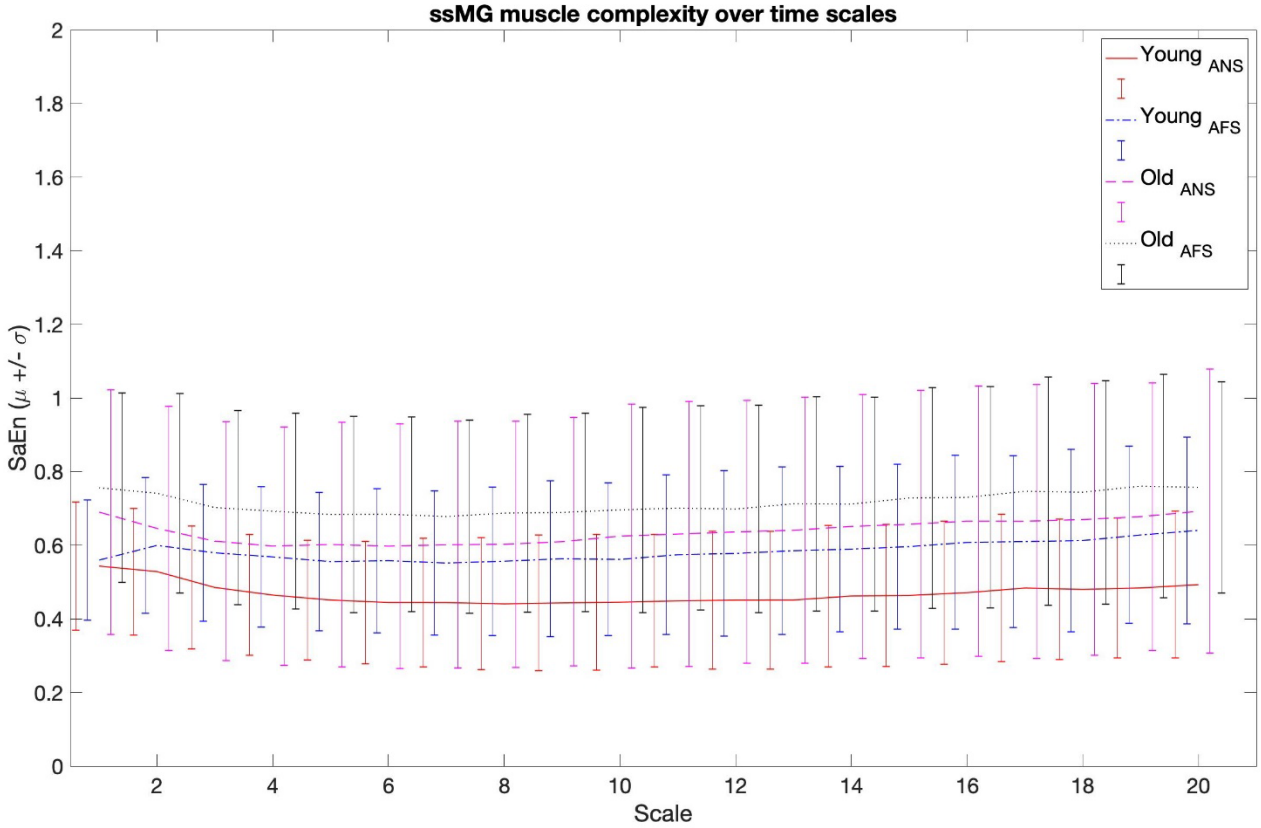

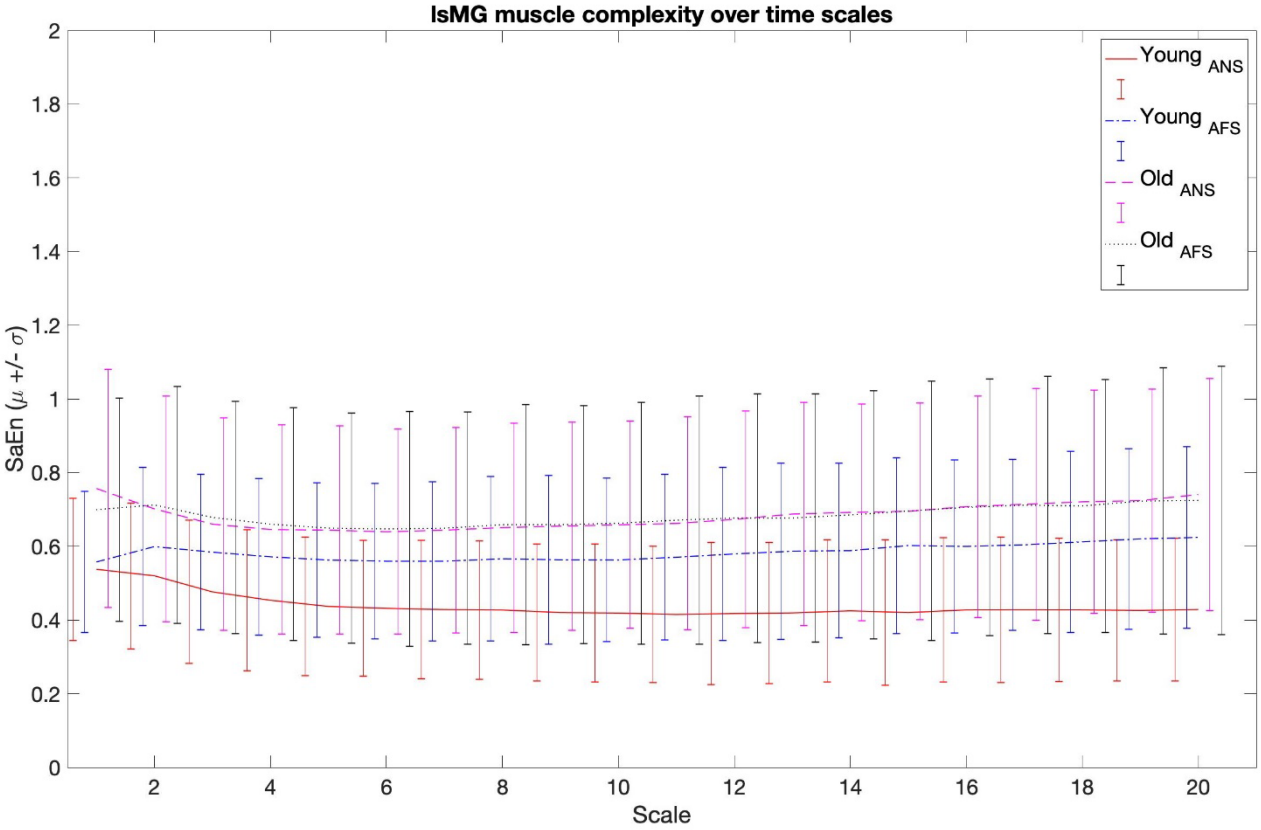

* **E2.2) EMG complexity for 0.7*PWS and for 1.6*PWS (*trial F1, F2*)**
(N_{old} = 17)

E2.2.1) Vastus Lateralis

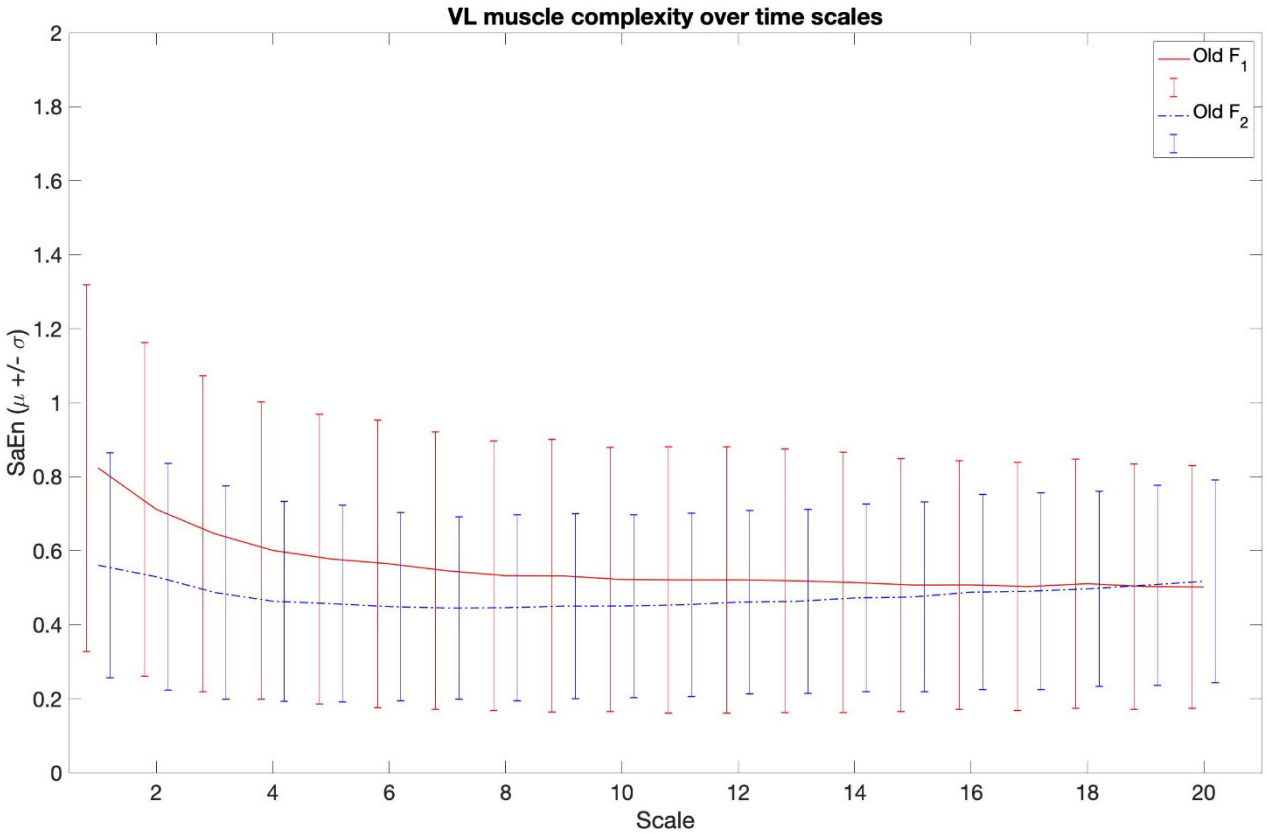

E2.2.2) Rectus Femoris

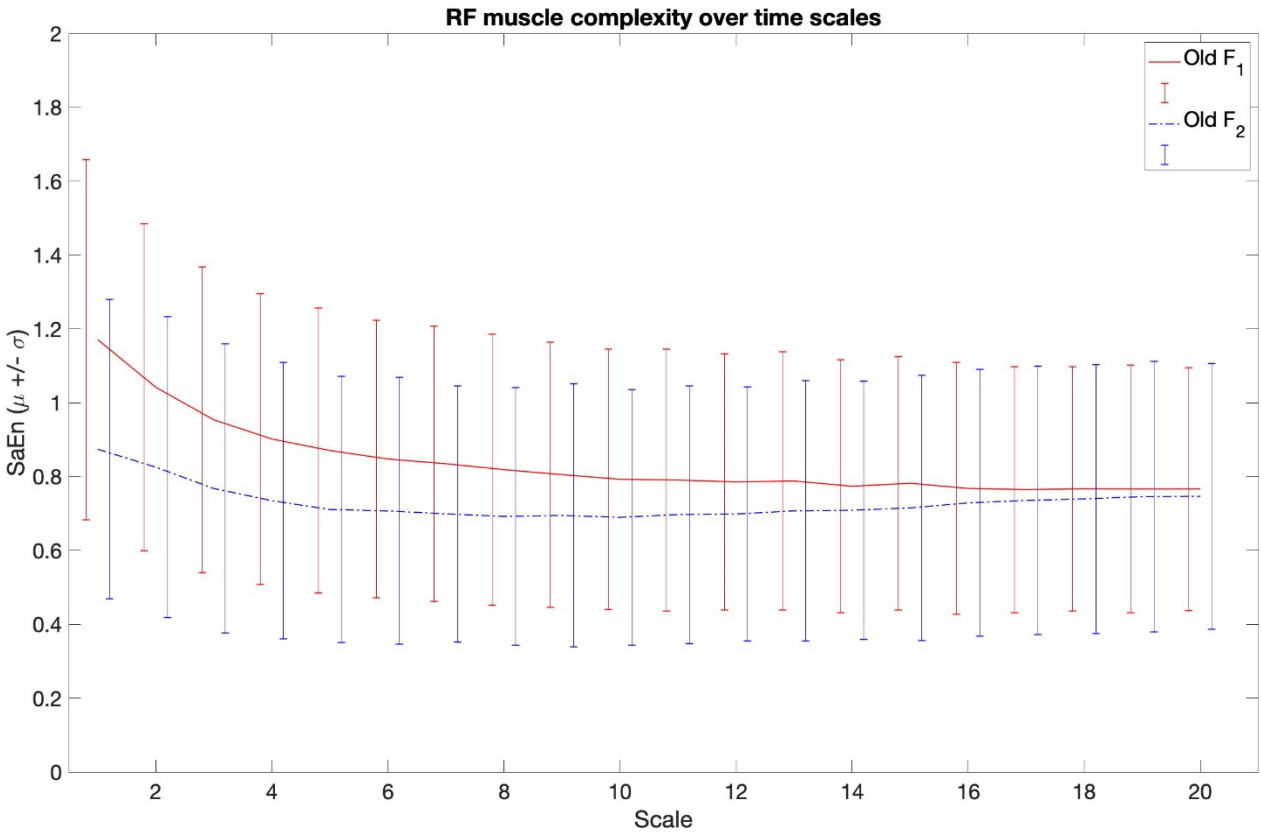

E2.2.3) Vastus Medialis

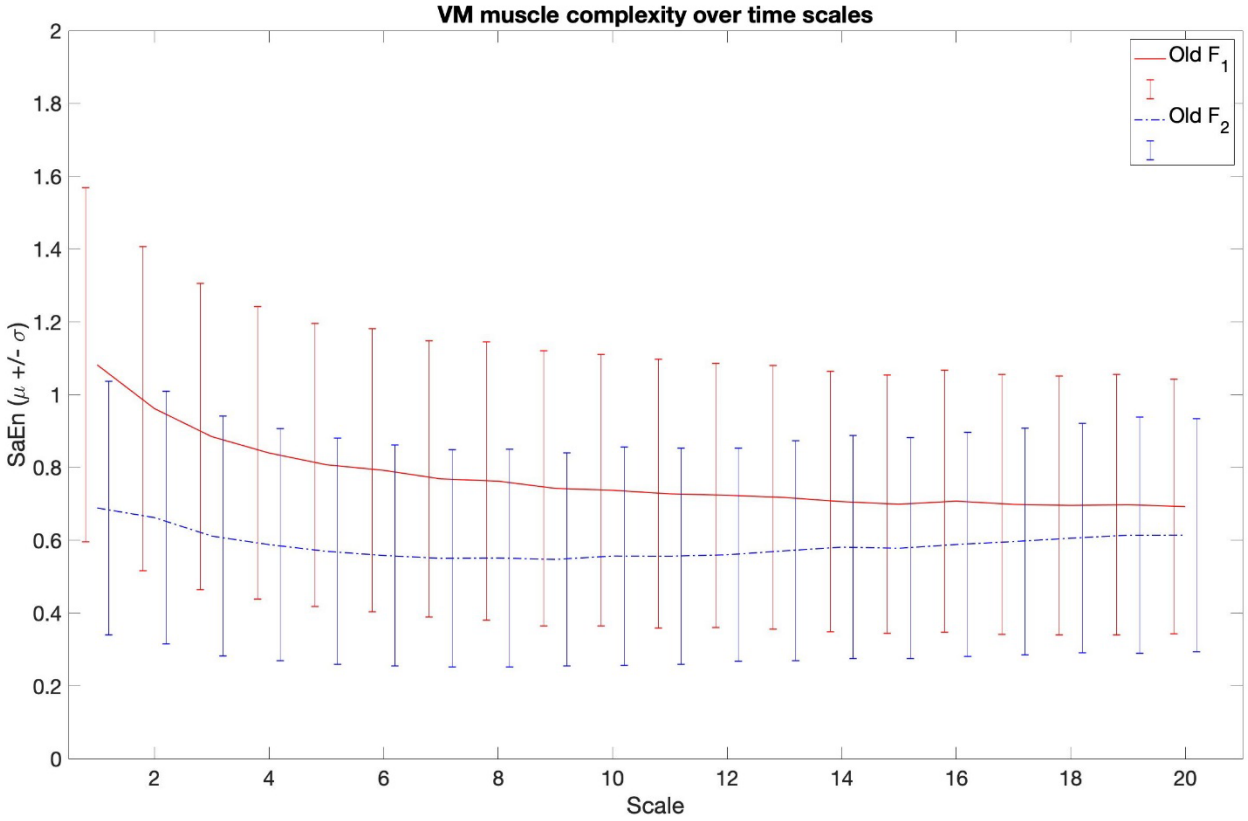

E2.2.4) Lateral Hamstrings (Biceps Femoris)

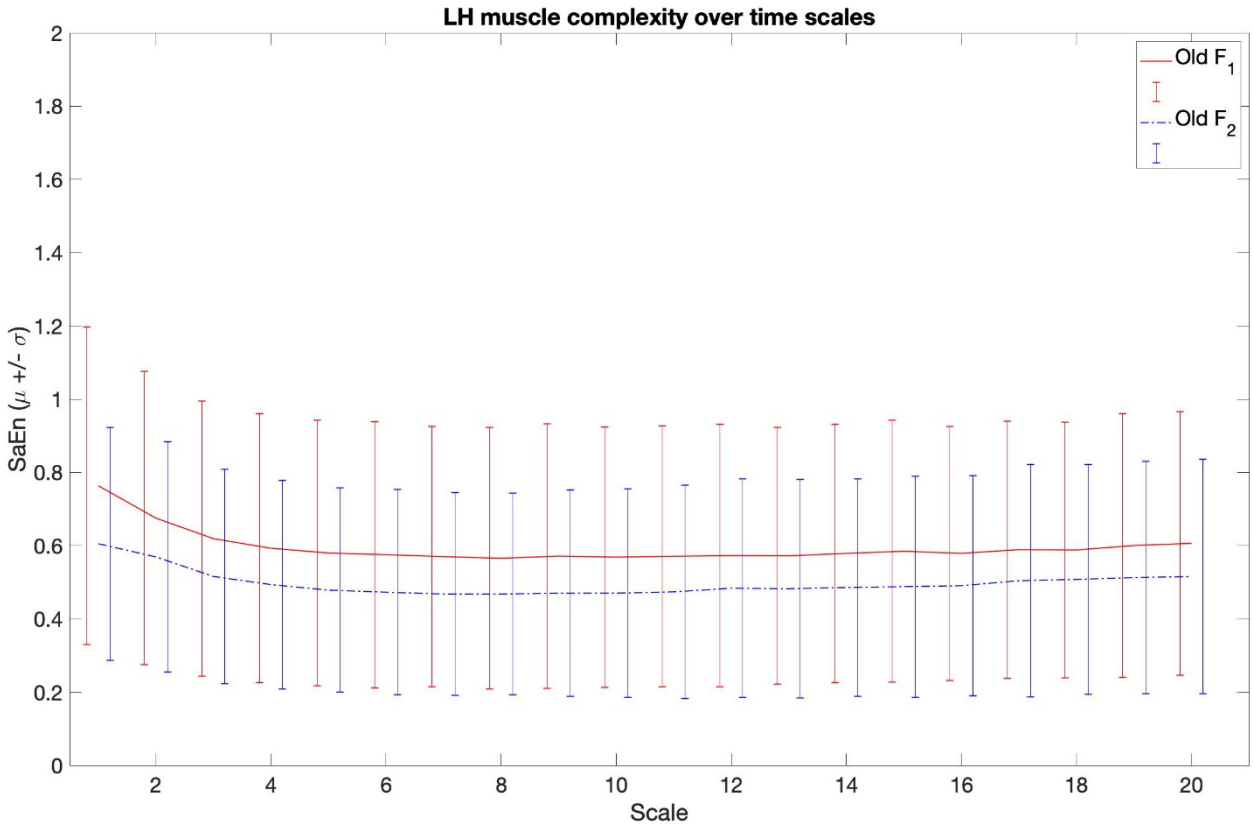

E2.2.5) Medial Hamstrings (Semimembranosus, Semitendinosus)

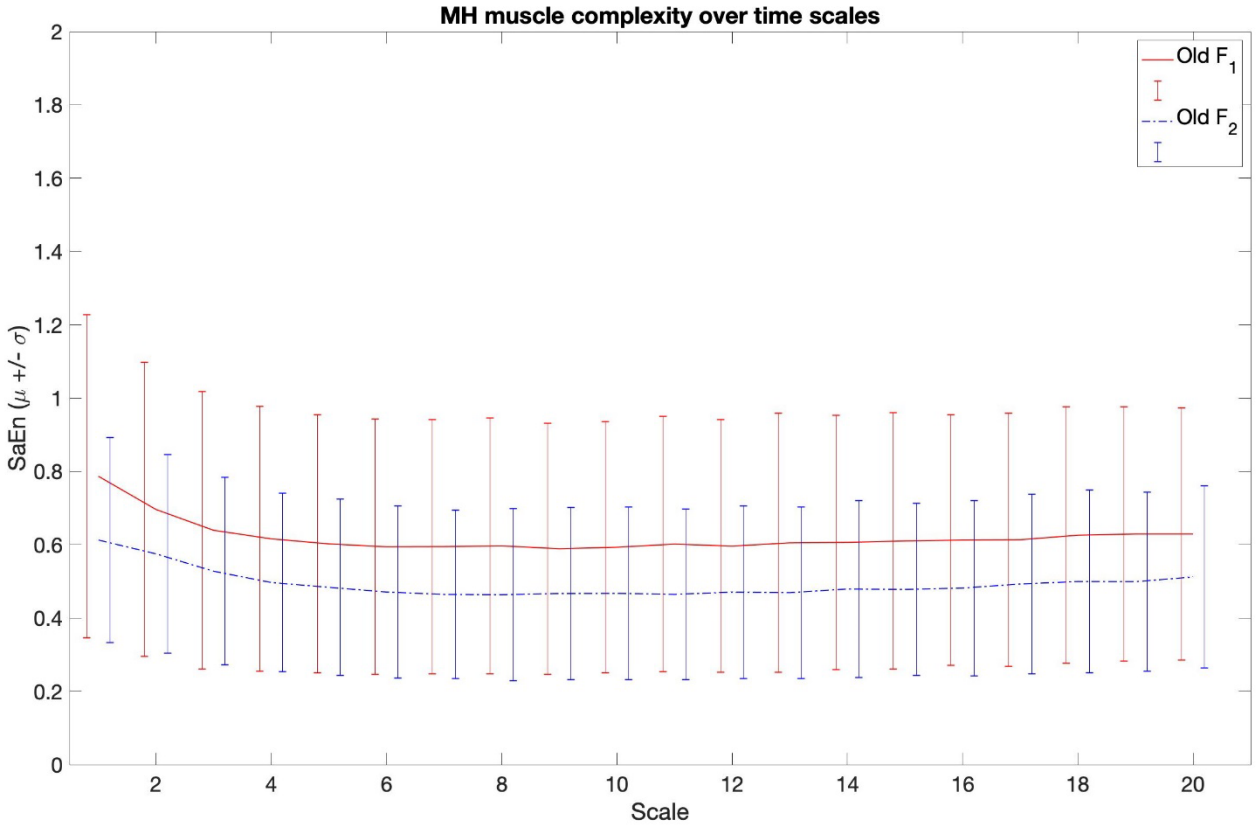

E2.2.6) Lateral Gastrocnemius

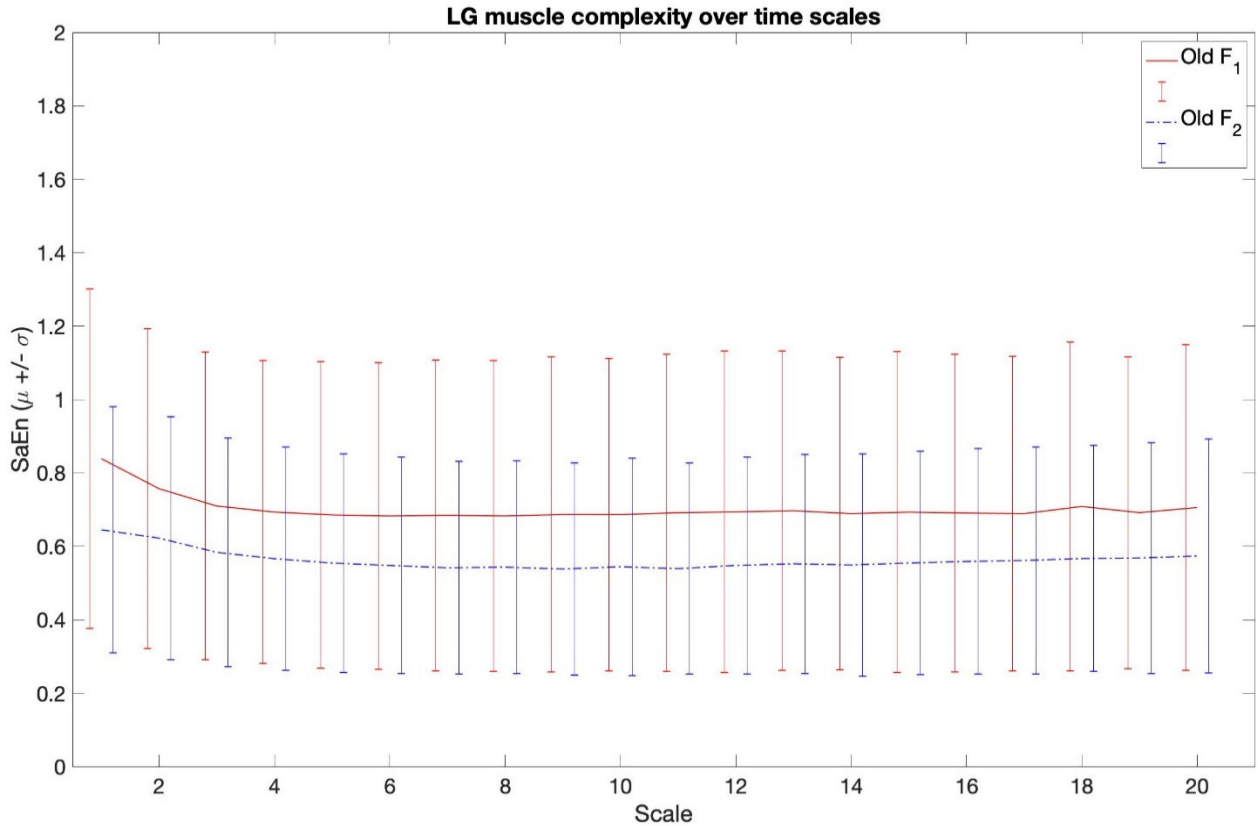

E2.2.7) Medial Gastrocnemius

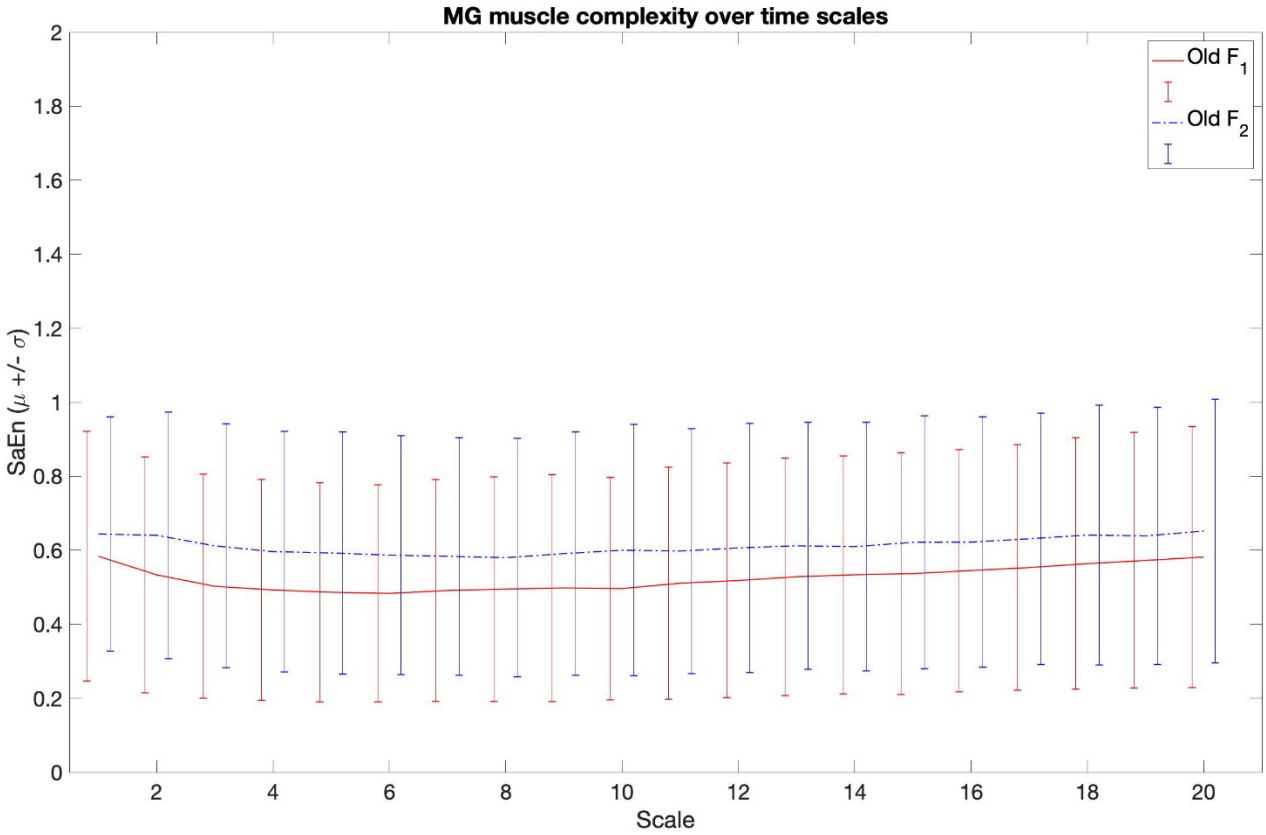

* **E2.3) GRF complexity for short steps and for long steps (*trial ANS, AFS*)** (N_{young} = 18, N_{old} = 18)

E2.3.1) Anterior-Posterior component

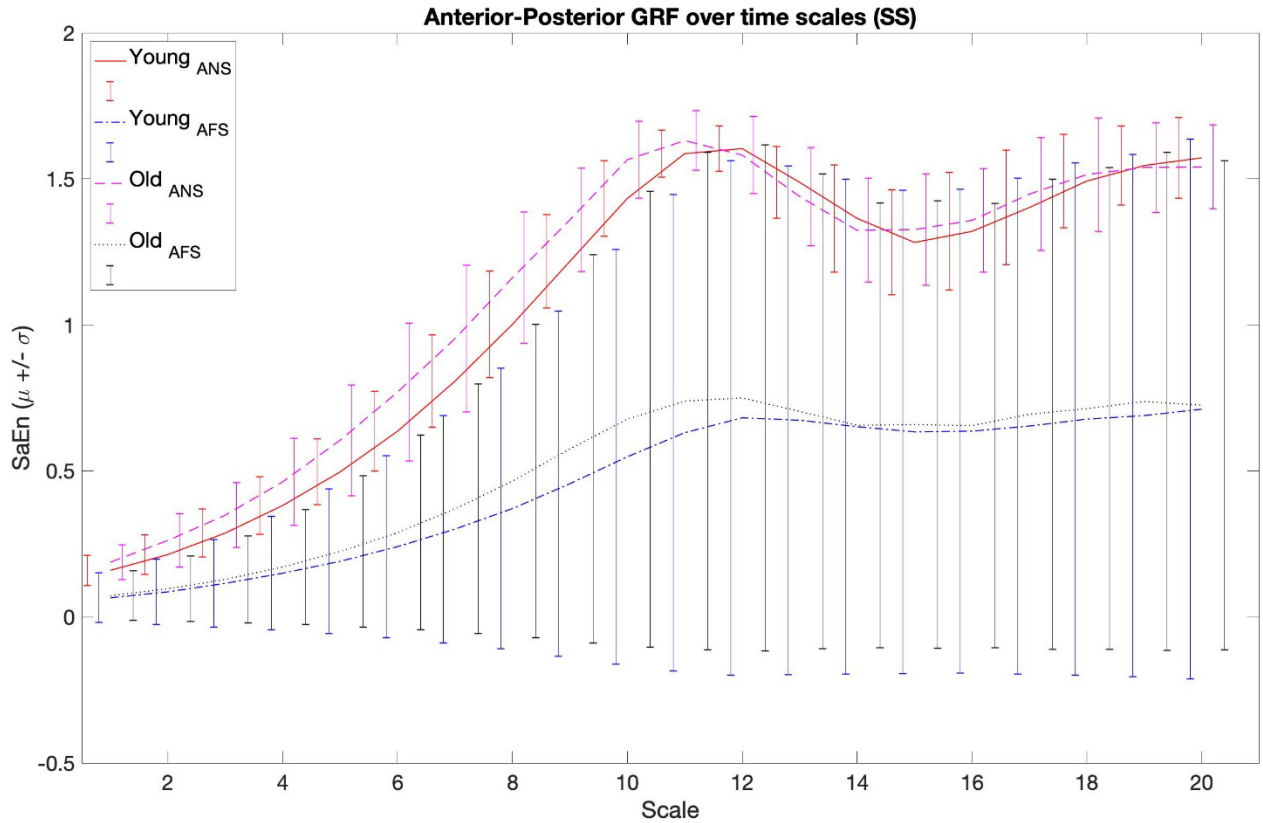

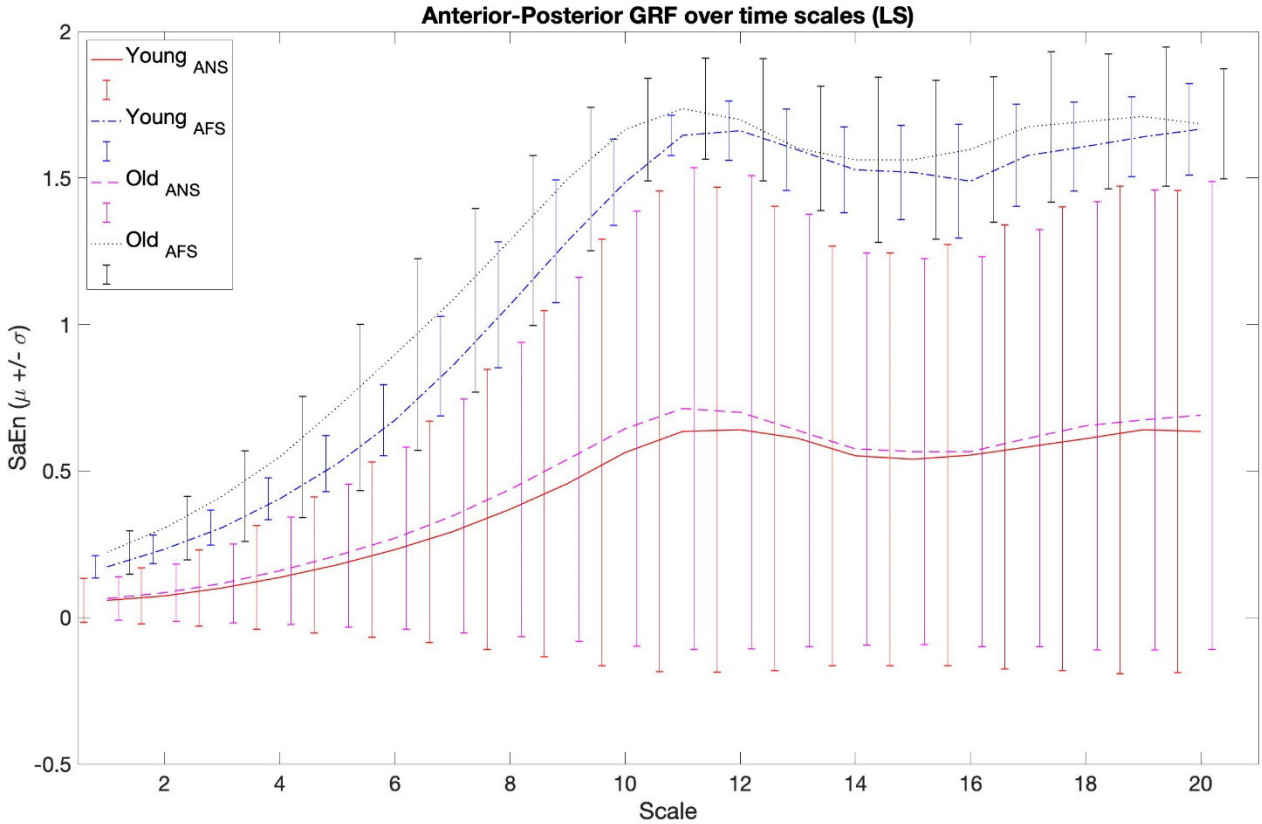

E2.3.2) Vertical component

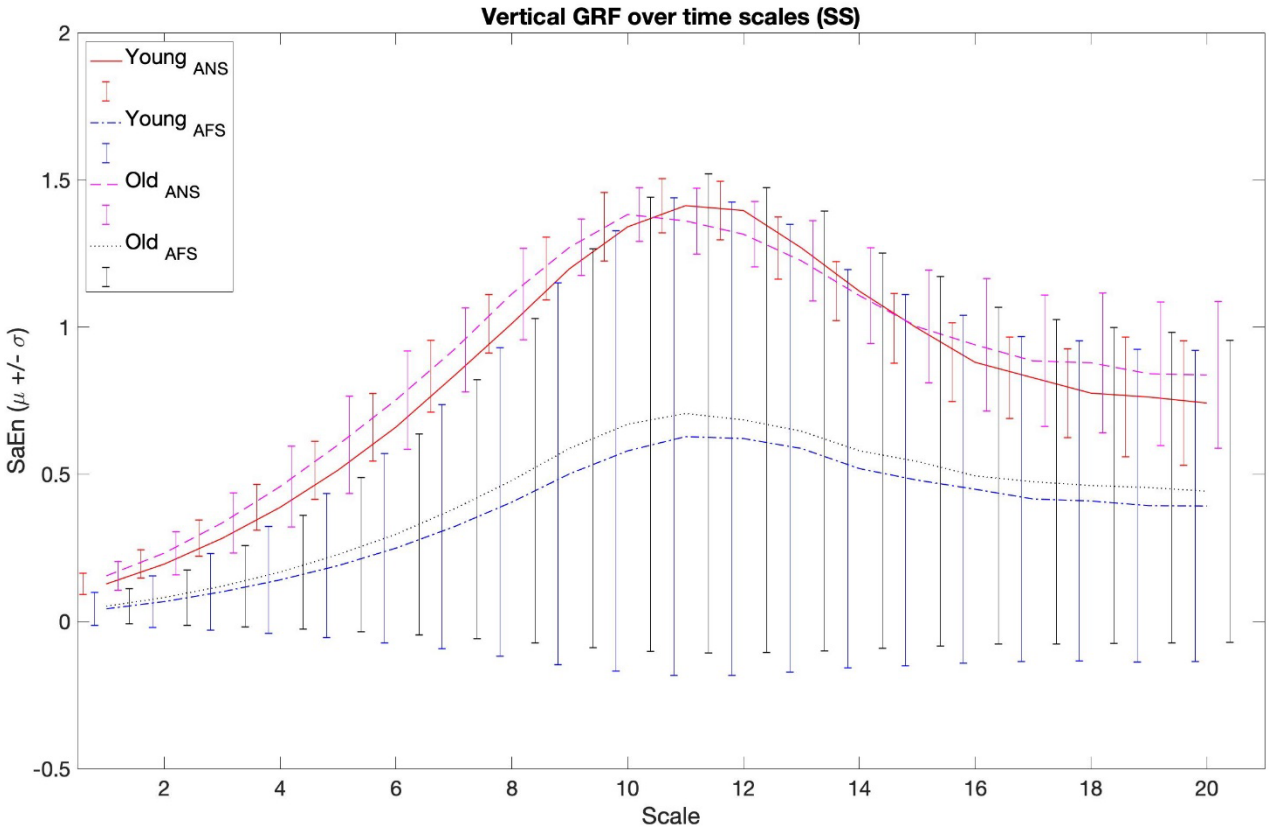

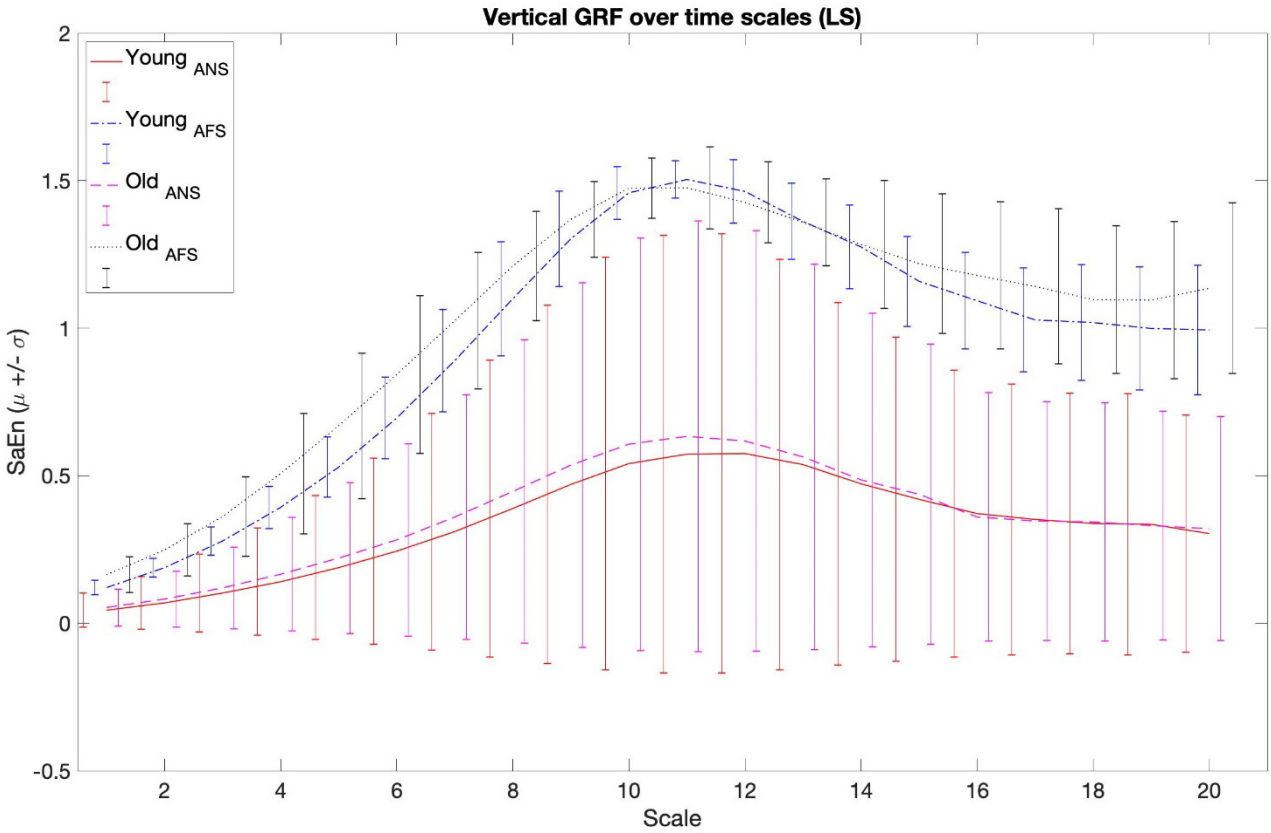

E2.3.3) Medial-Lateral component

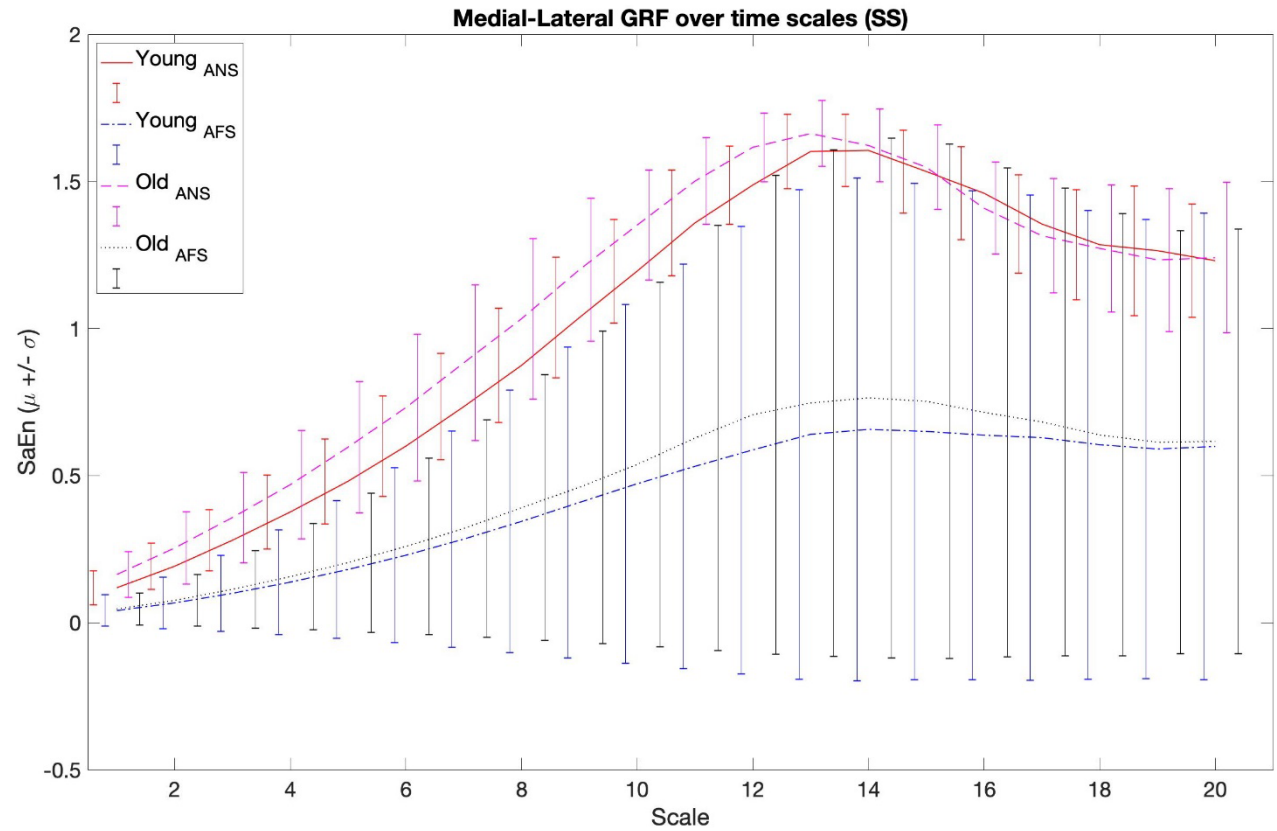

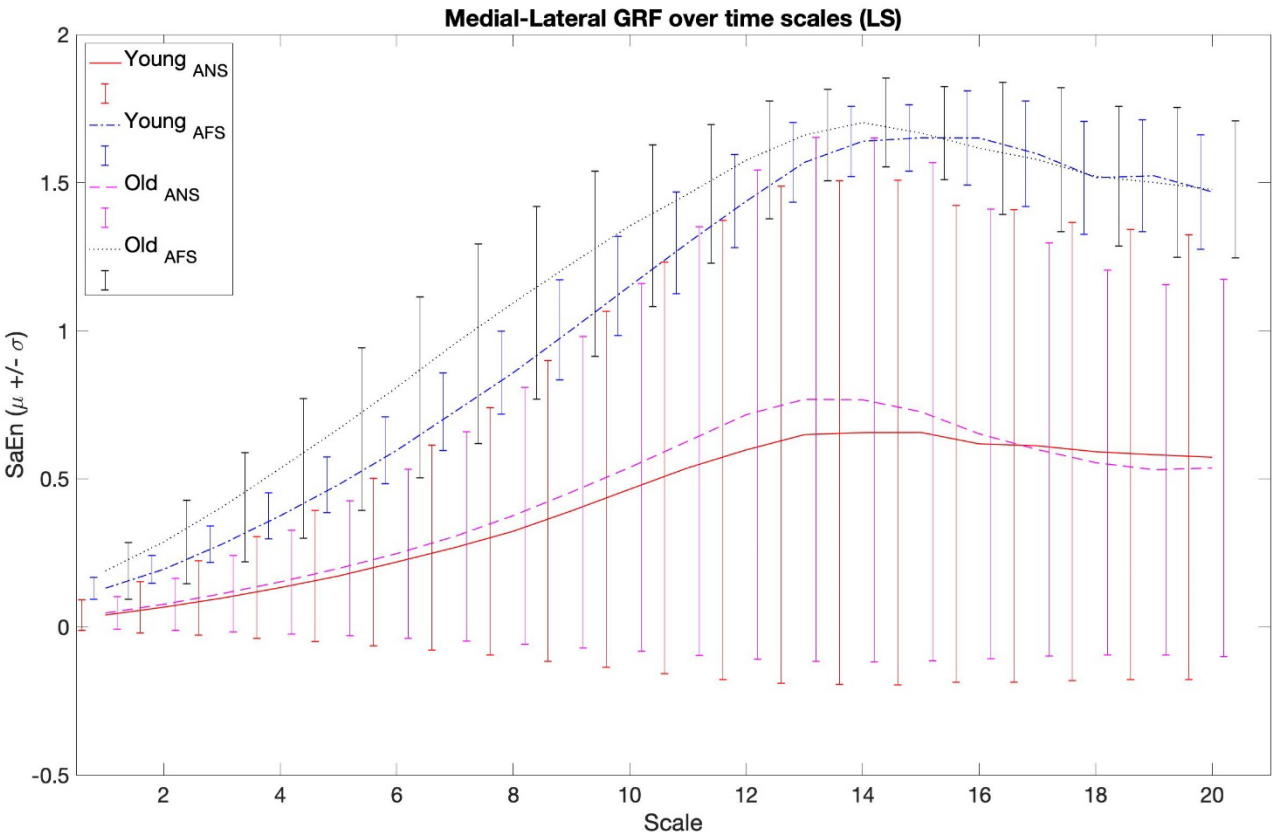

* **E2.4) GA complexity for short steps and for long steps (*trial ANS, AFS*)**
(N_{young} = 18, N_{old} = 18)

E2.4.1) Anterior-Posterior Hip component

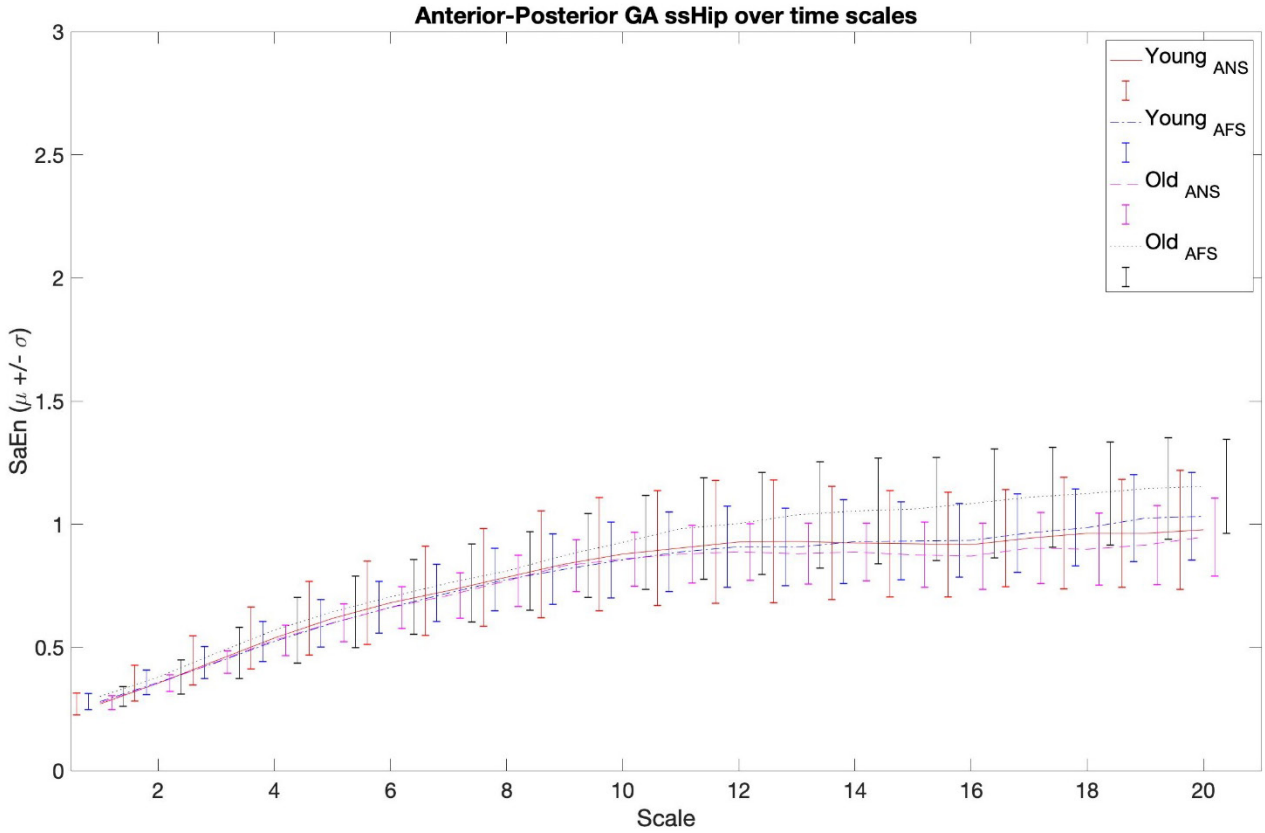

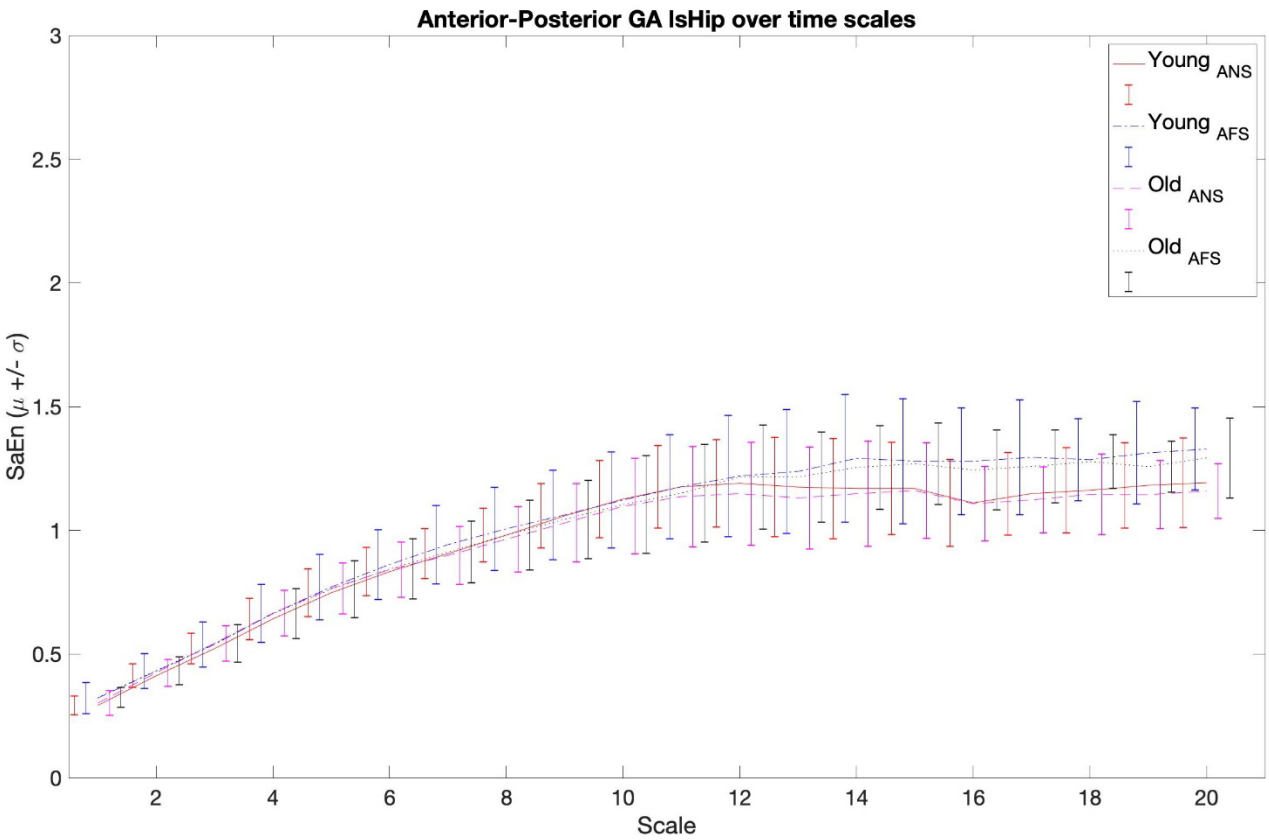

E2.4.2) Medial-Lateral Hip component

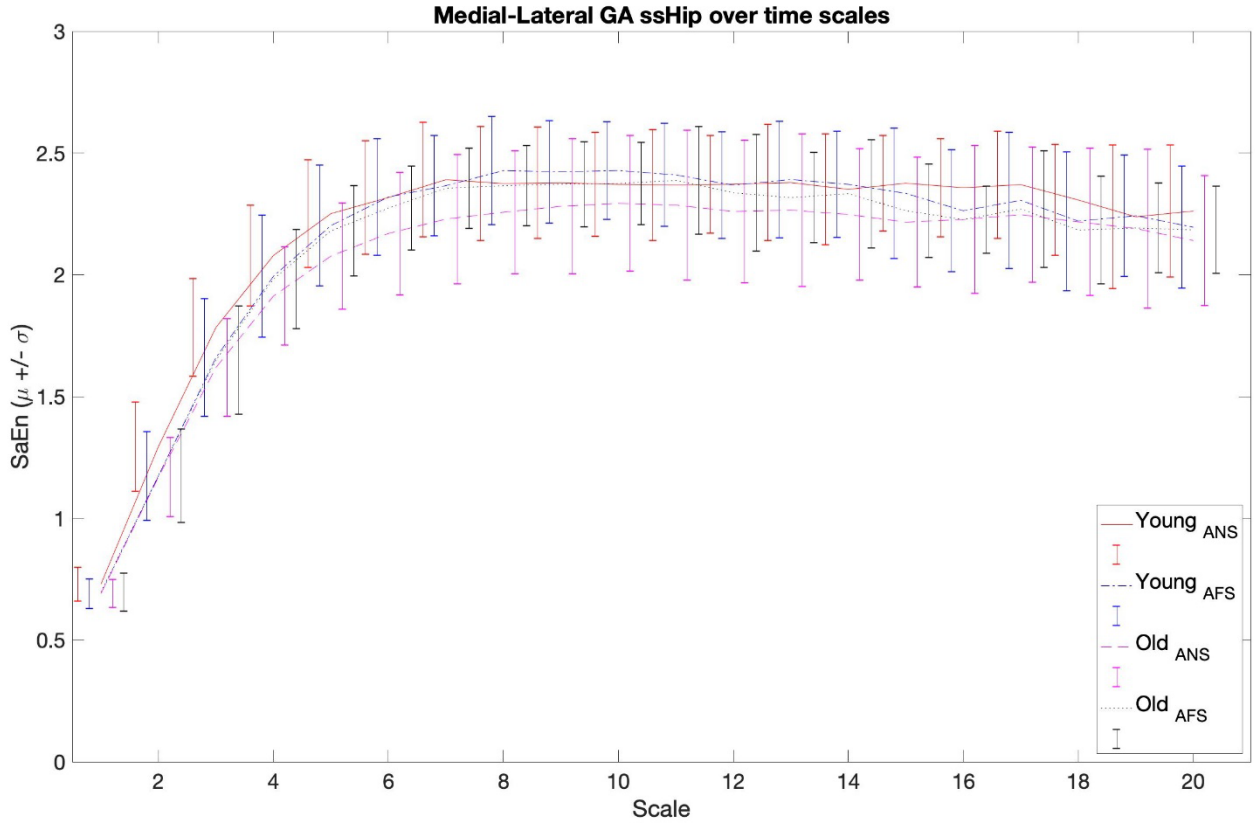

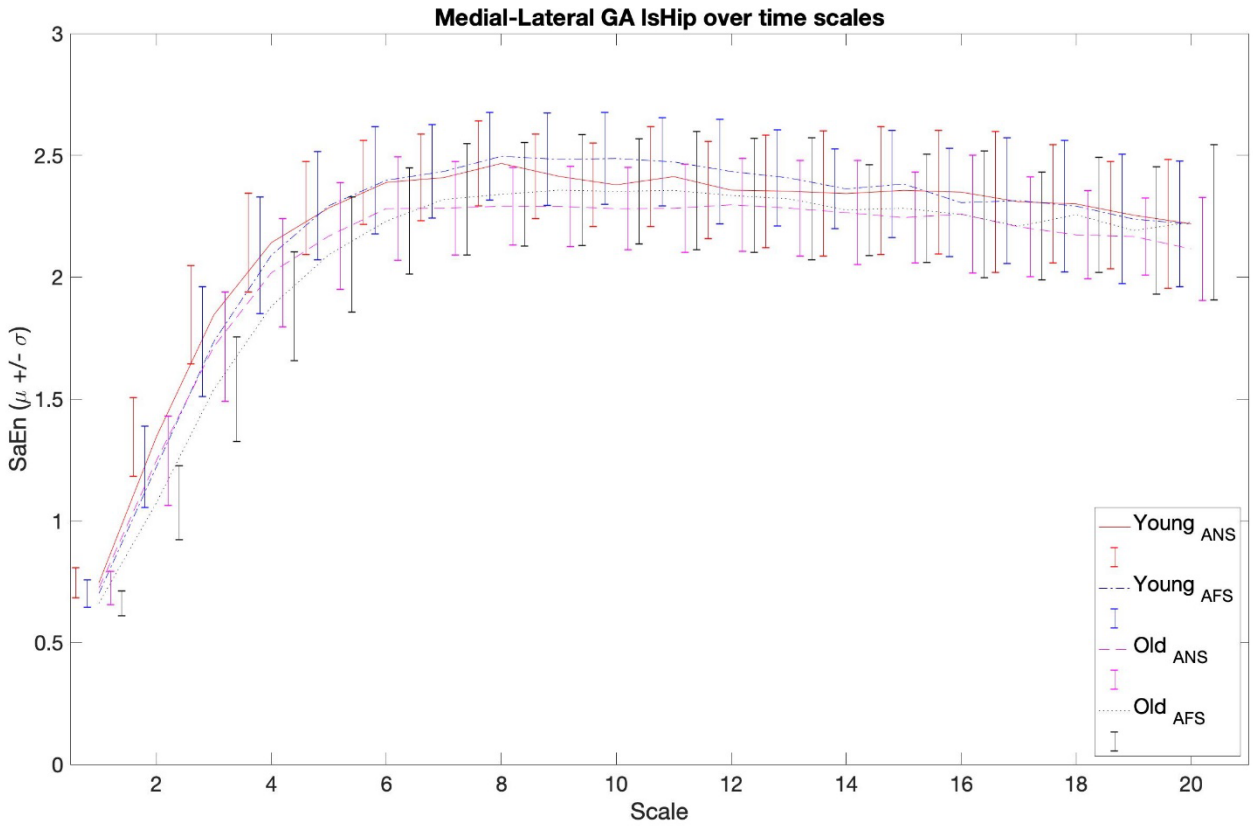

E2.4.3) Anterior-Posterior Knee component

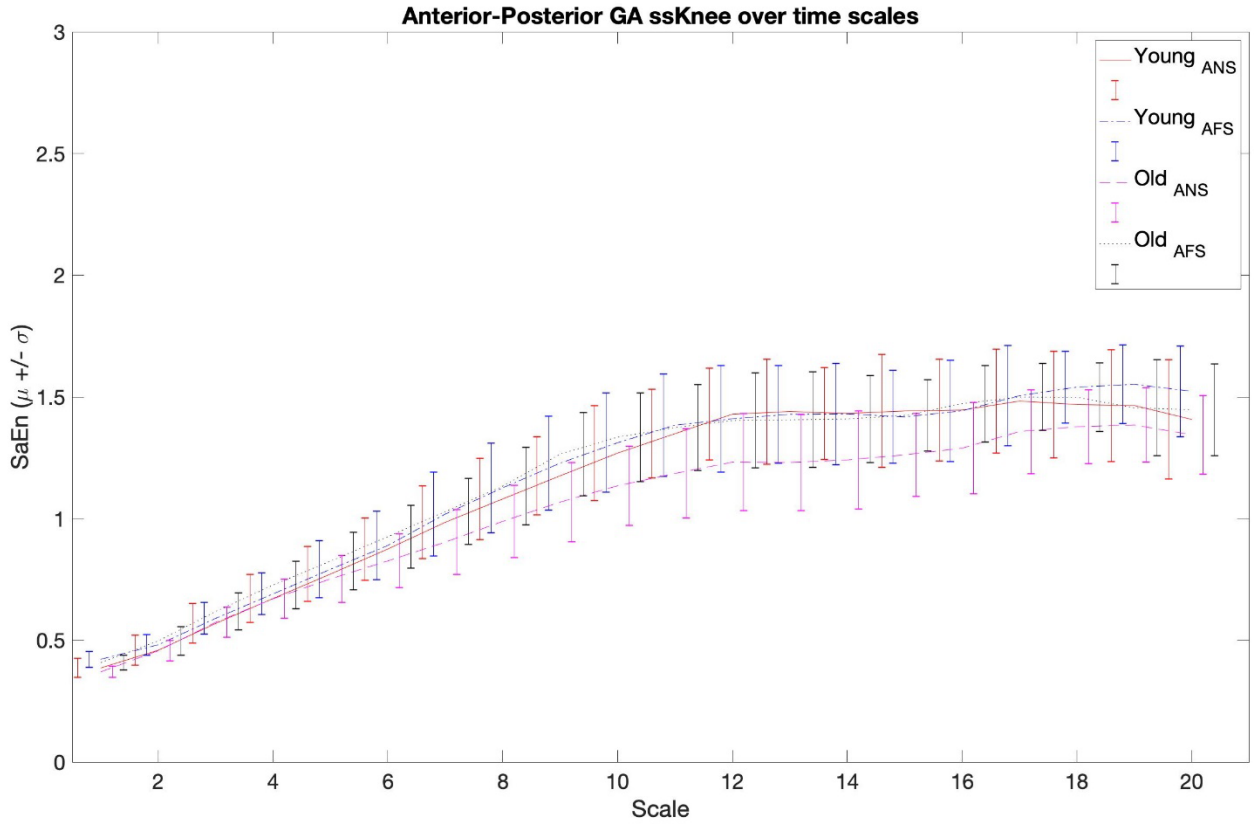

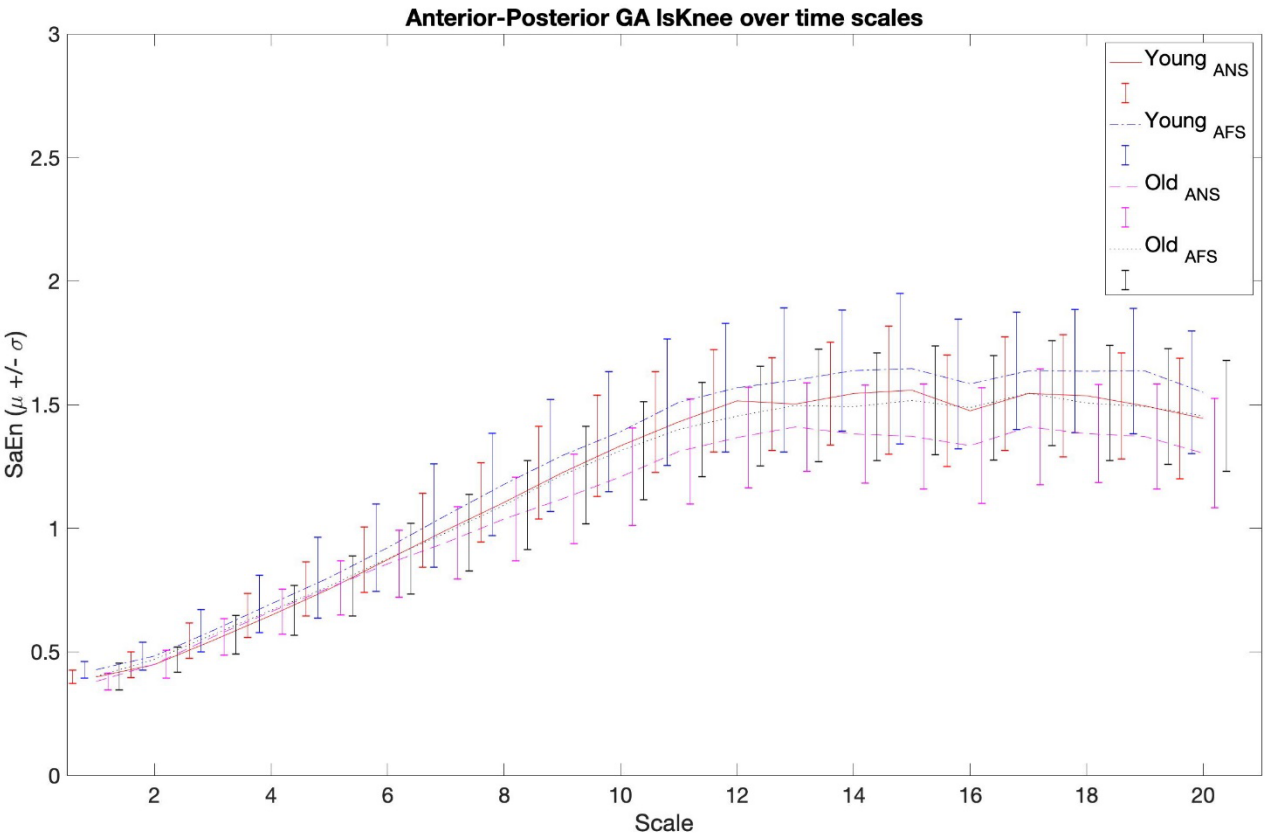

E2.4.4) Medial-Lateral Knee component

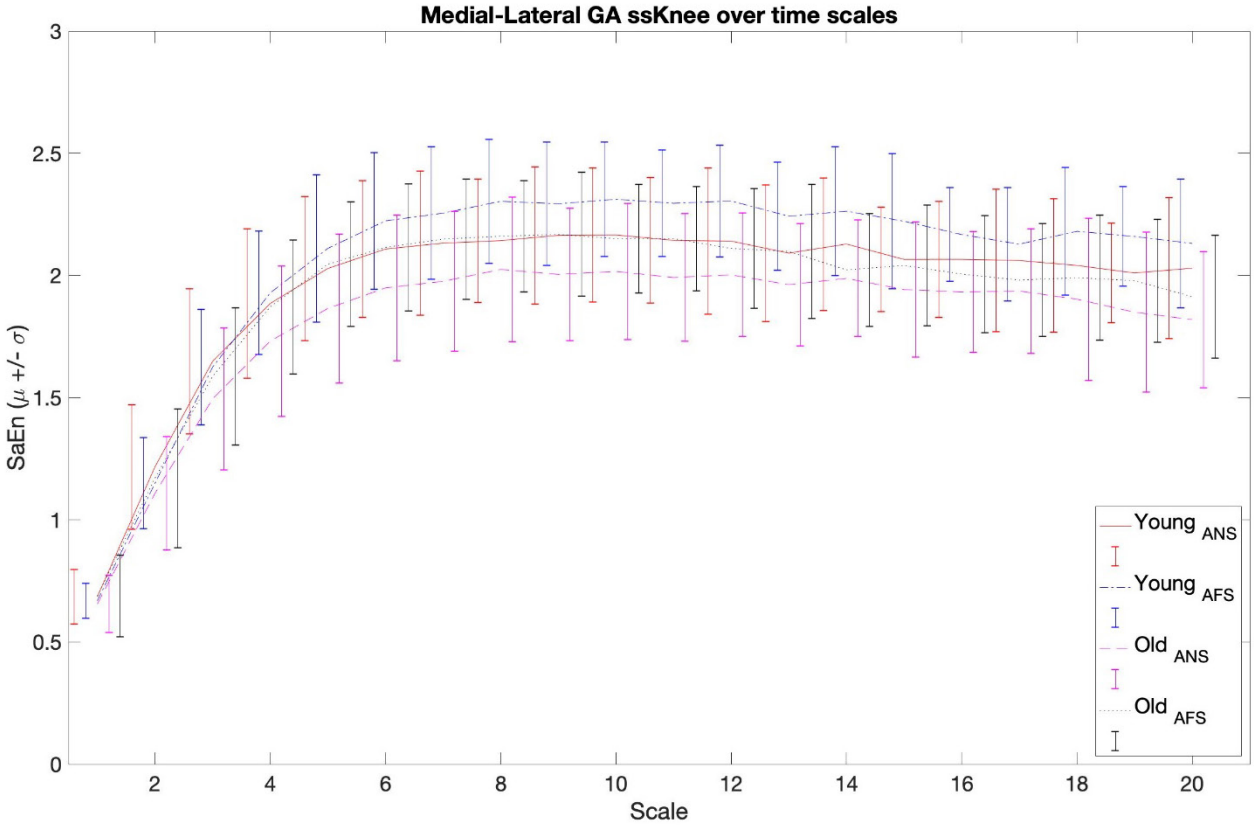

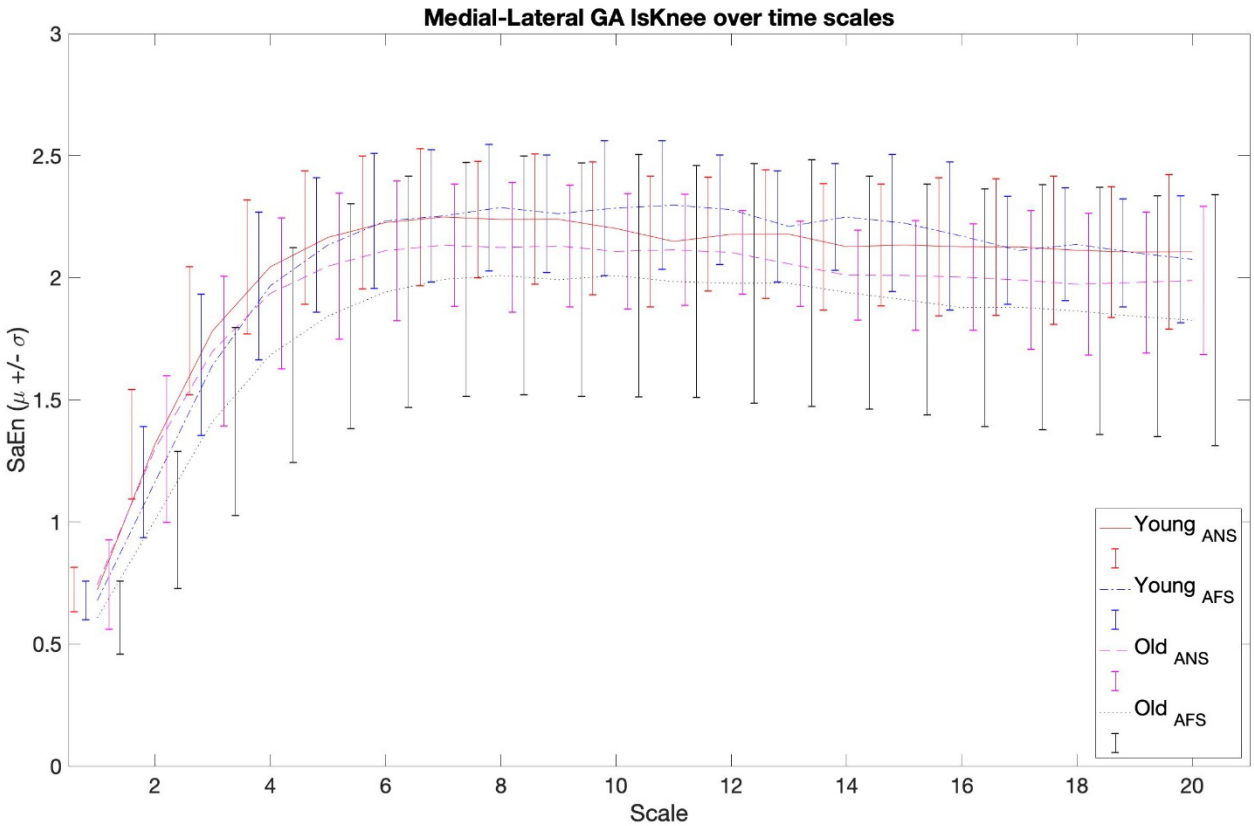

E2.4.5) Anterior-Posterior Ankle component

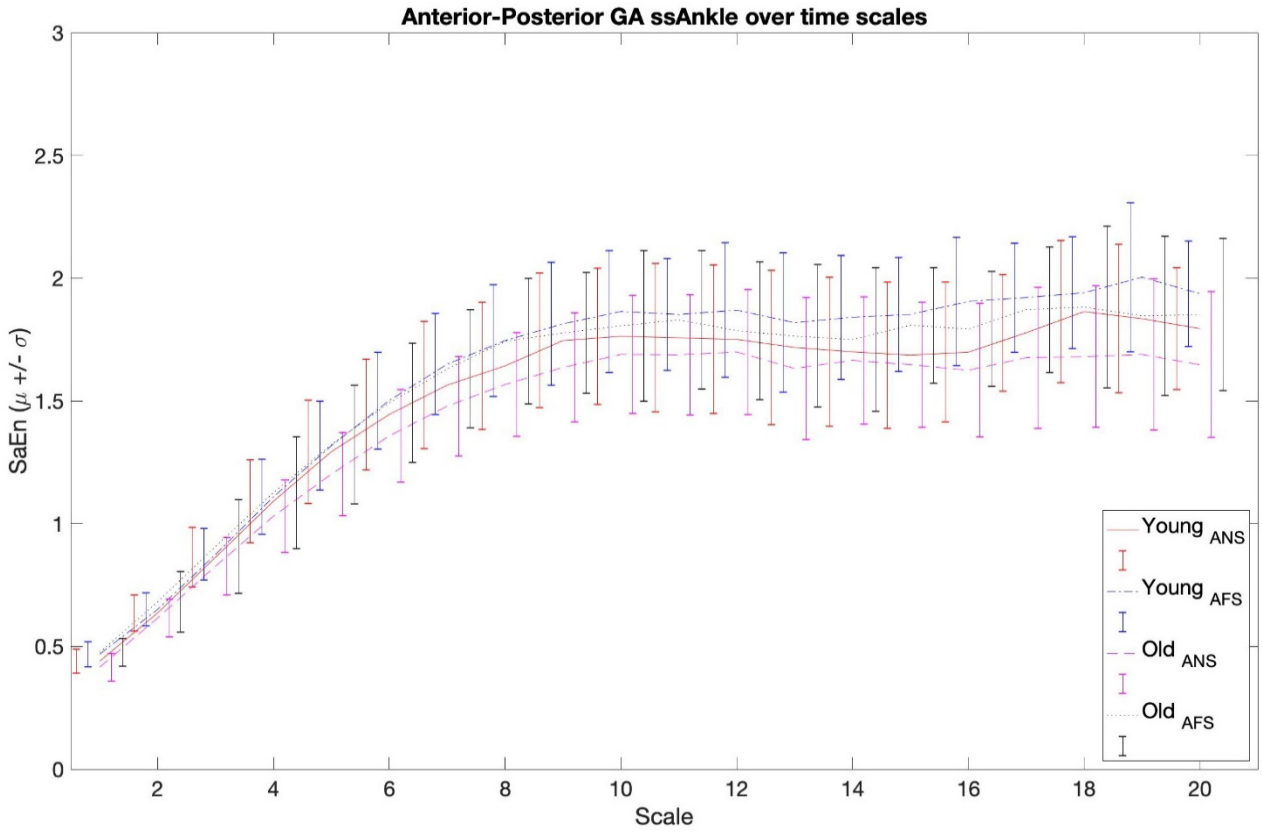

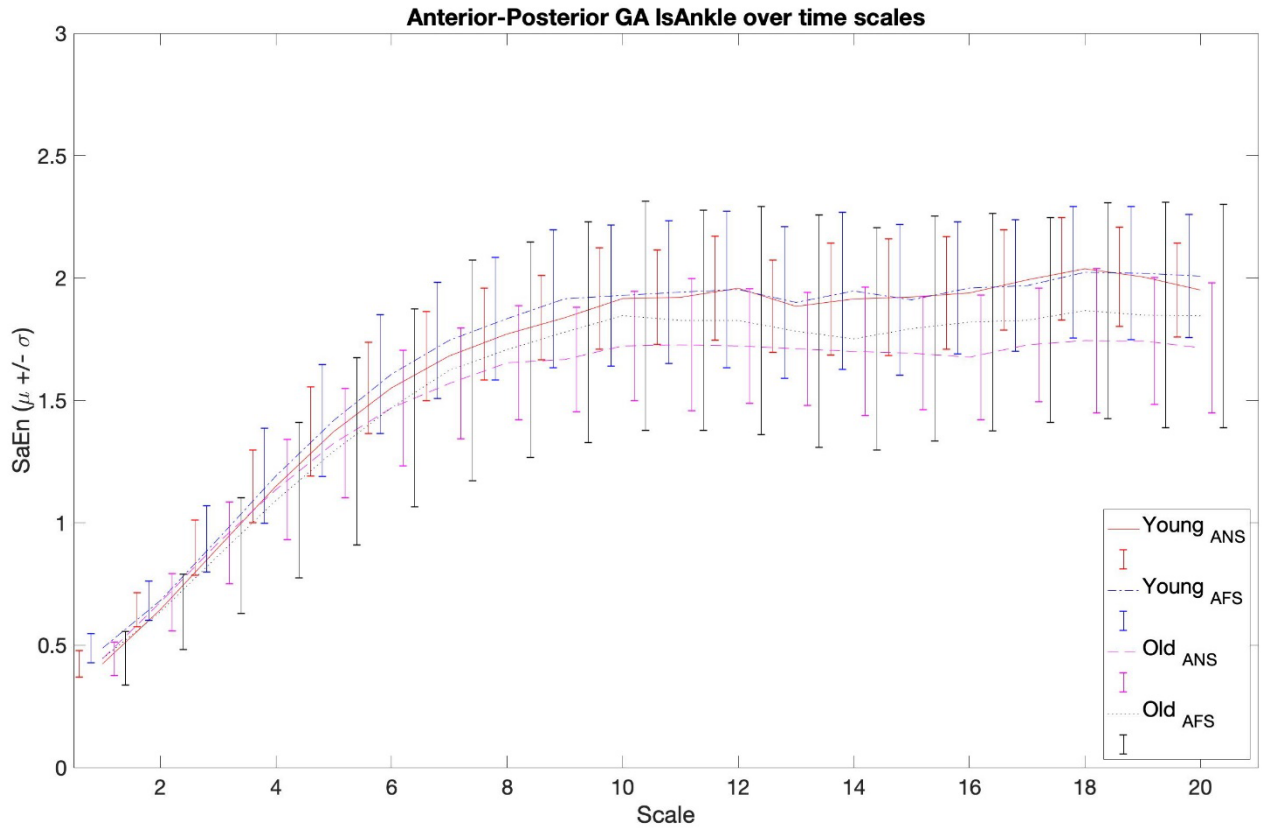

E2.4.6) Medial-Lateral Ankle component

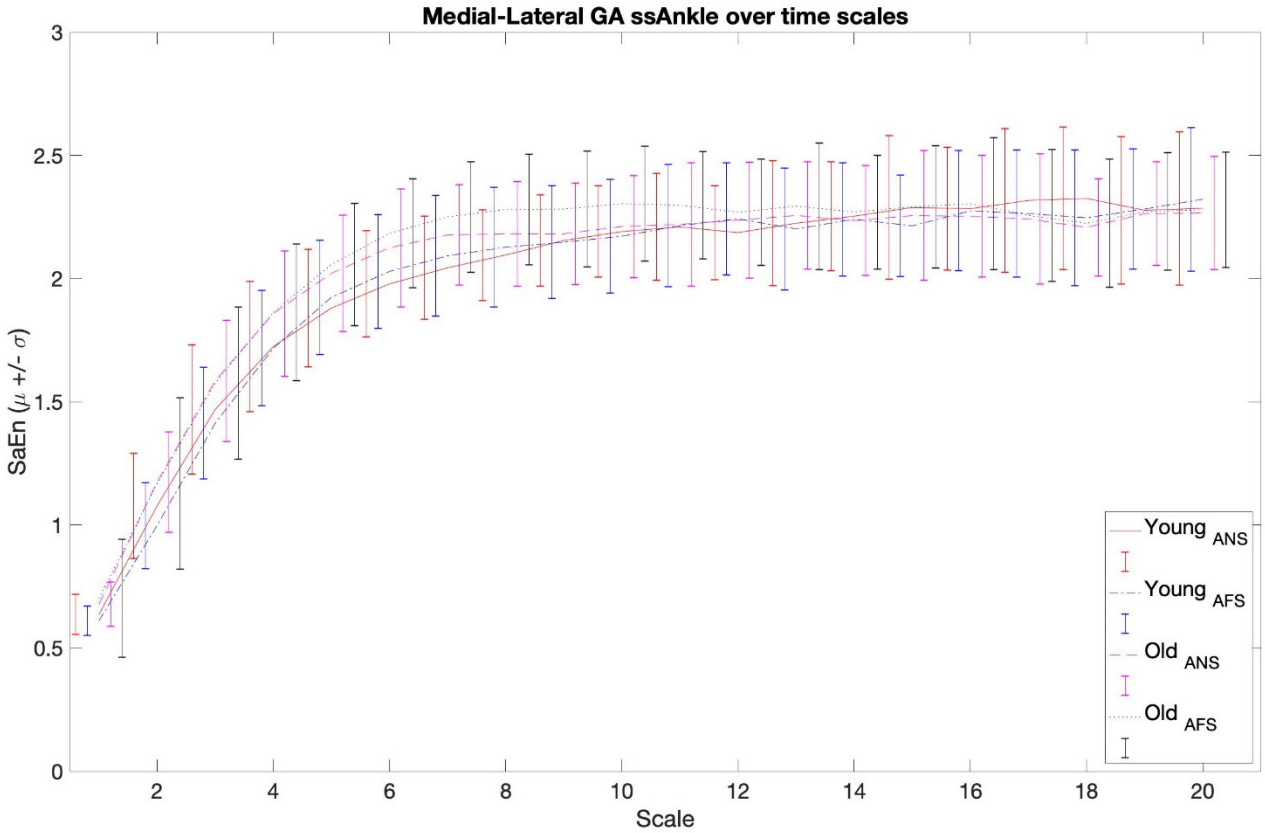

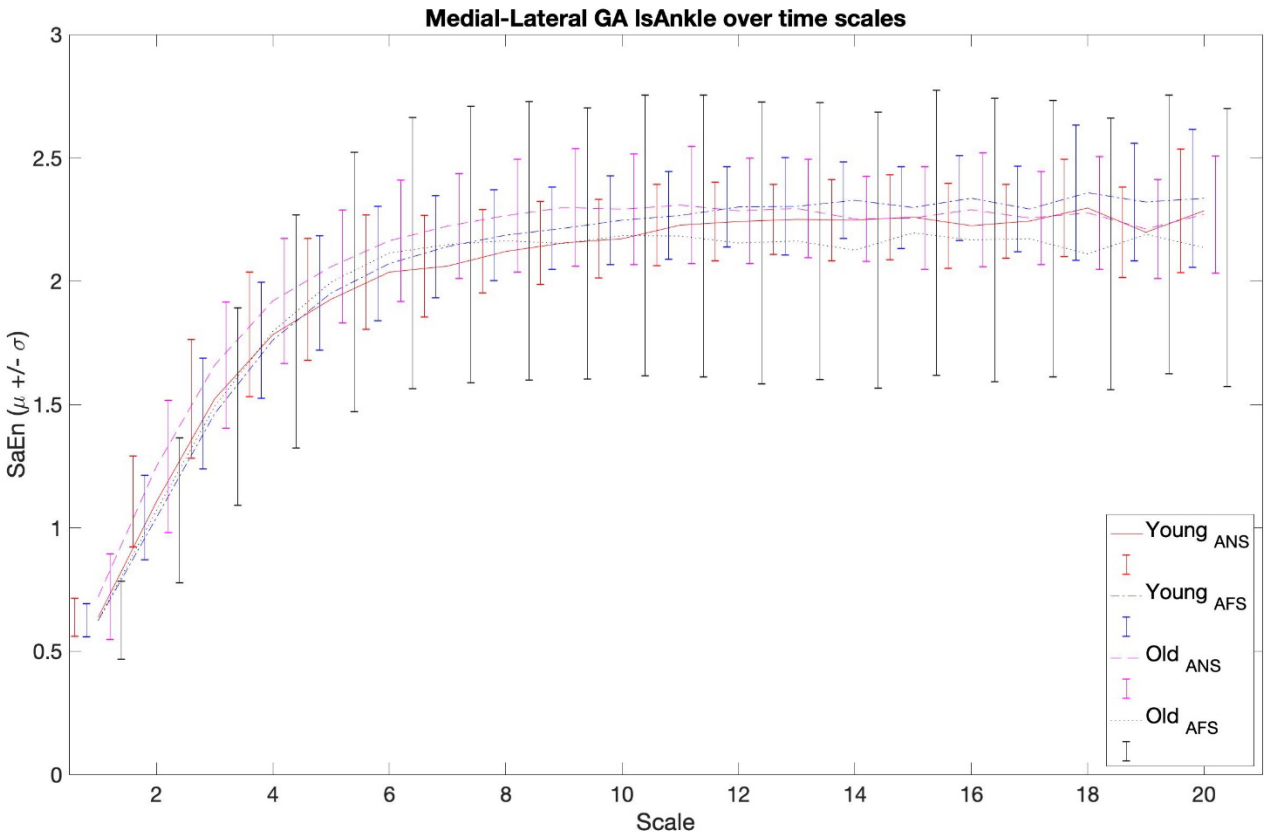

E3) Sample Entropy outcomes

* **E3.1) EMG complexity for short steps and for long steps (*trial ANS, AFS*)**
Scale 1 (N_{young} = 18, N_{old} = 19)

E3.1.1) Main effect 'velocity'

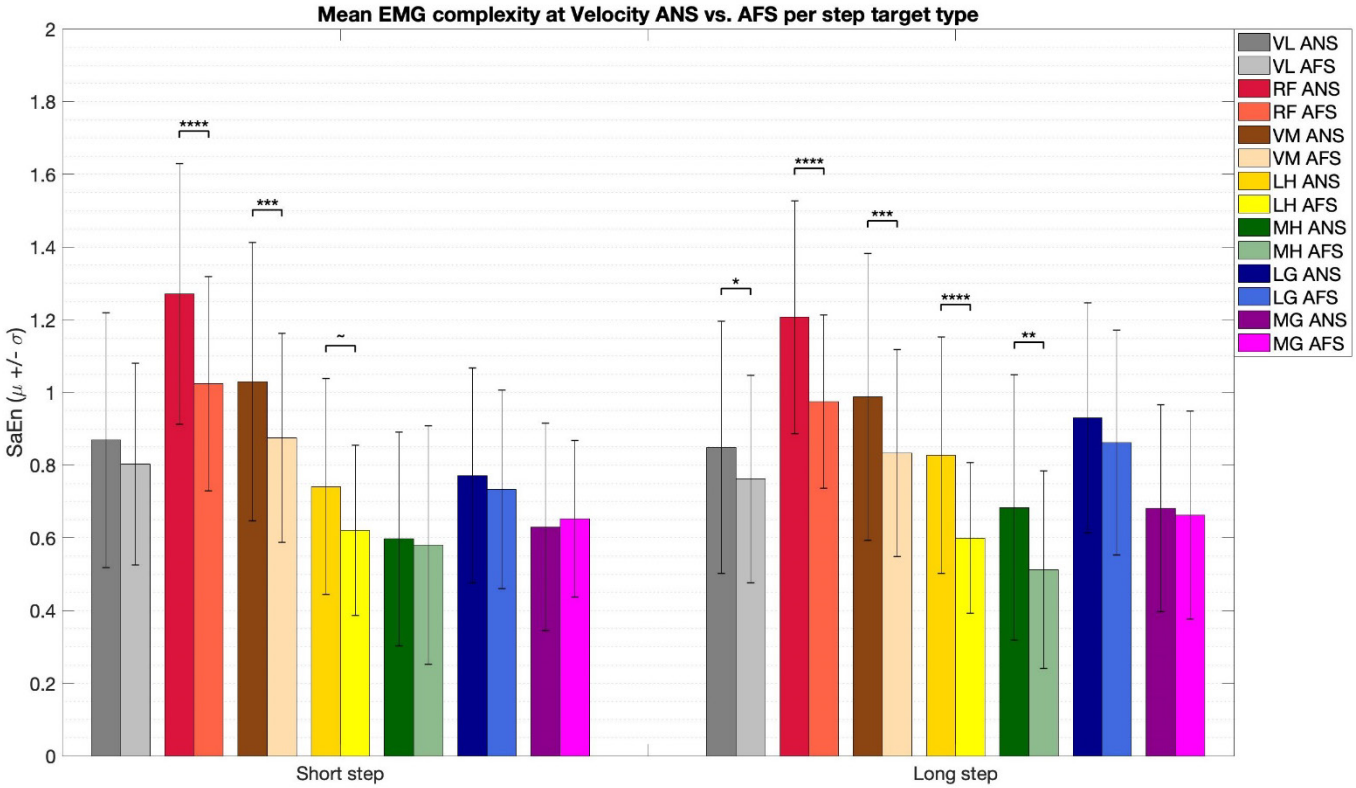

E3.1.2) Main effect 'age'

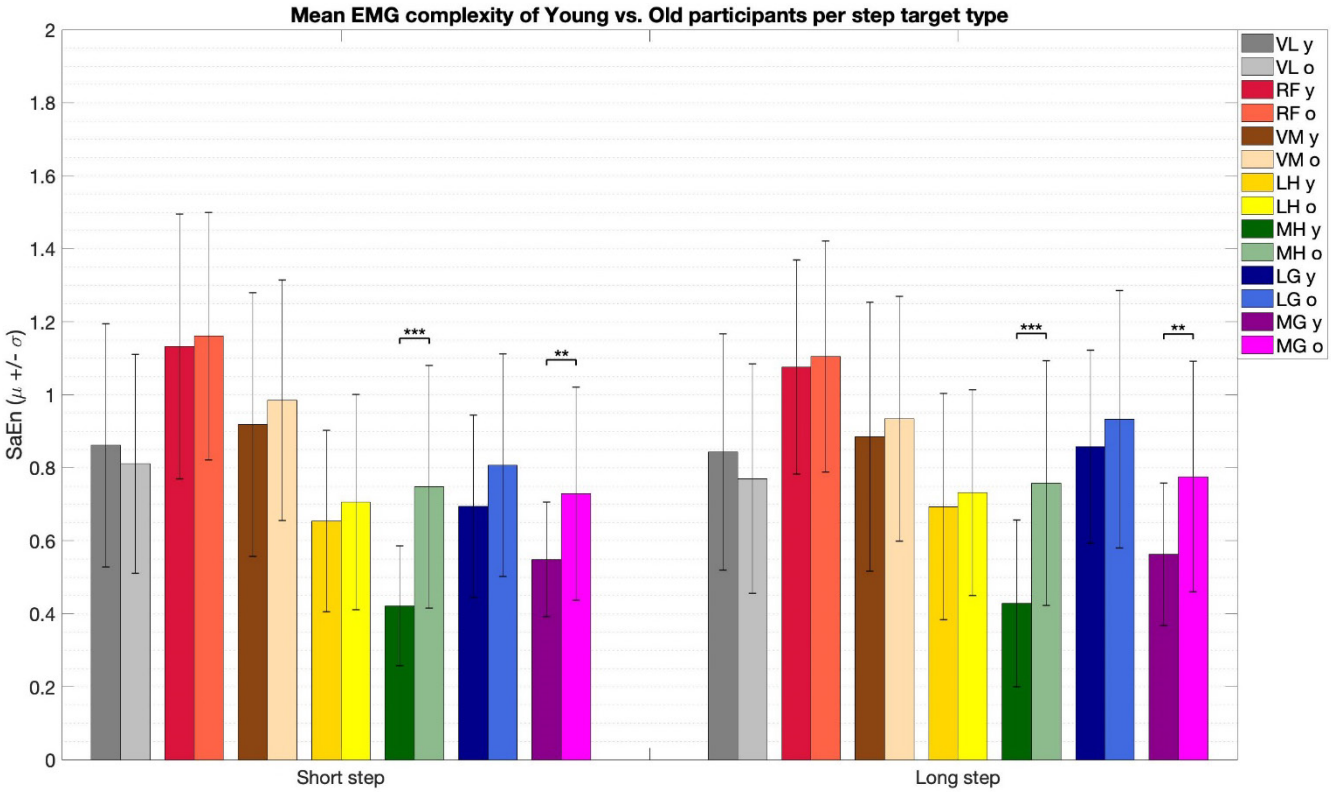

*E3.1.3) Interaction effect 'velocity*age'*

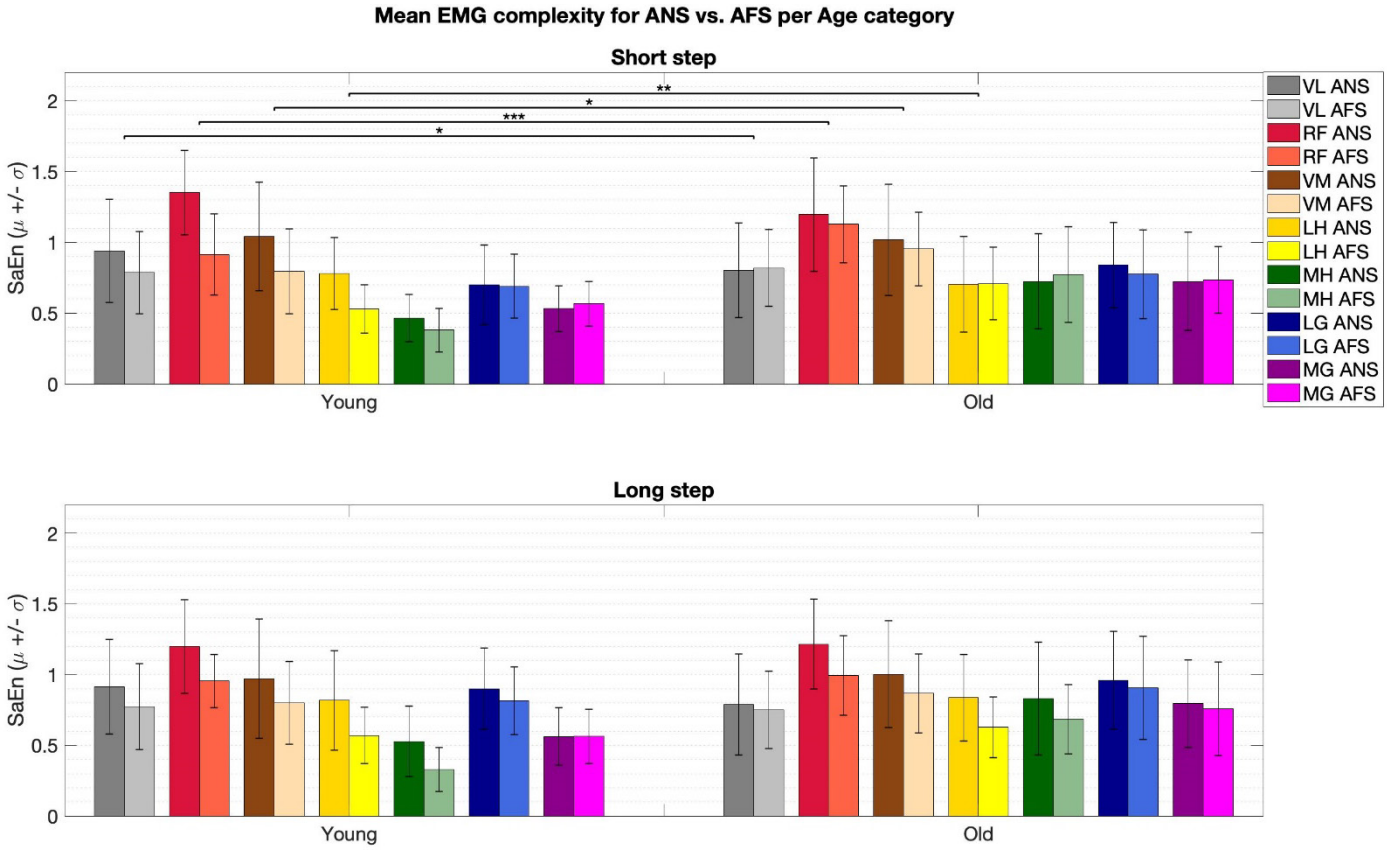

* **E3.2) EMG complexity for 0.7*PWS and for 1.6*PWS (*trial F1, F2*)**
Scale 1 (N_{old} = 17)

Main effect 'velocity'

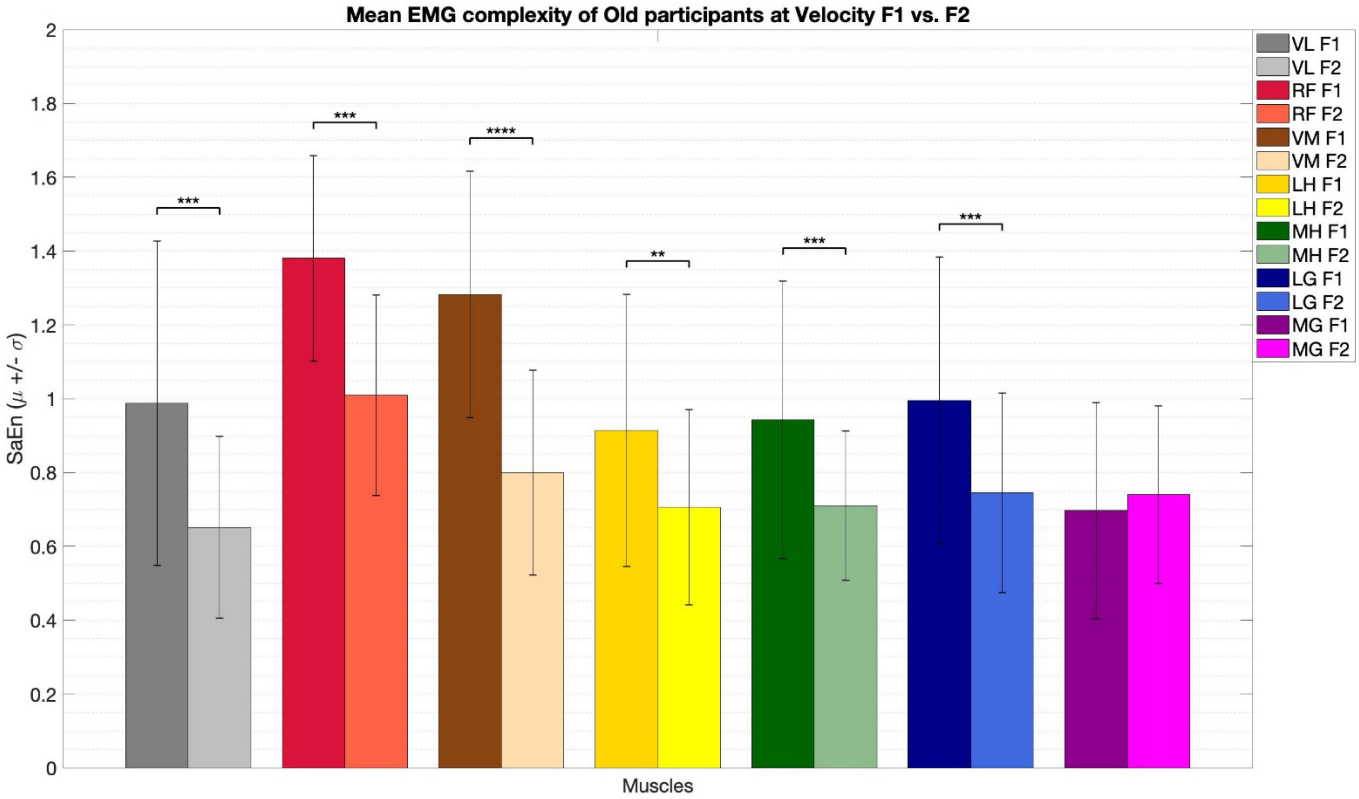

* **E3.3) GRF complexity for short steps and for long steps (*trial ANS, AFS*)**
Scale 12 (N_{young} = 18, N_{old} = 18)

E3.3.1) Main effect 'velocity'

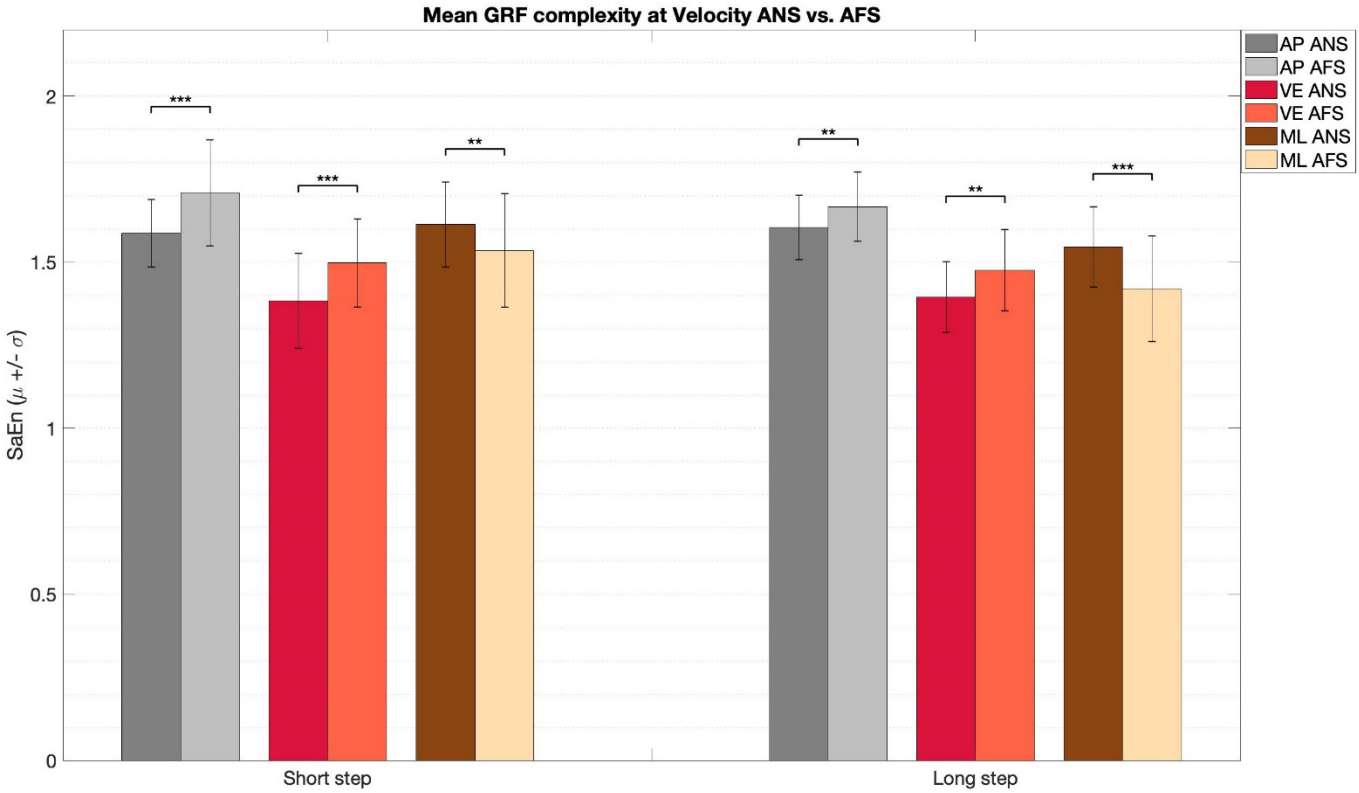

E3.3.2) Main effect 'age'

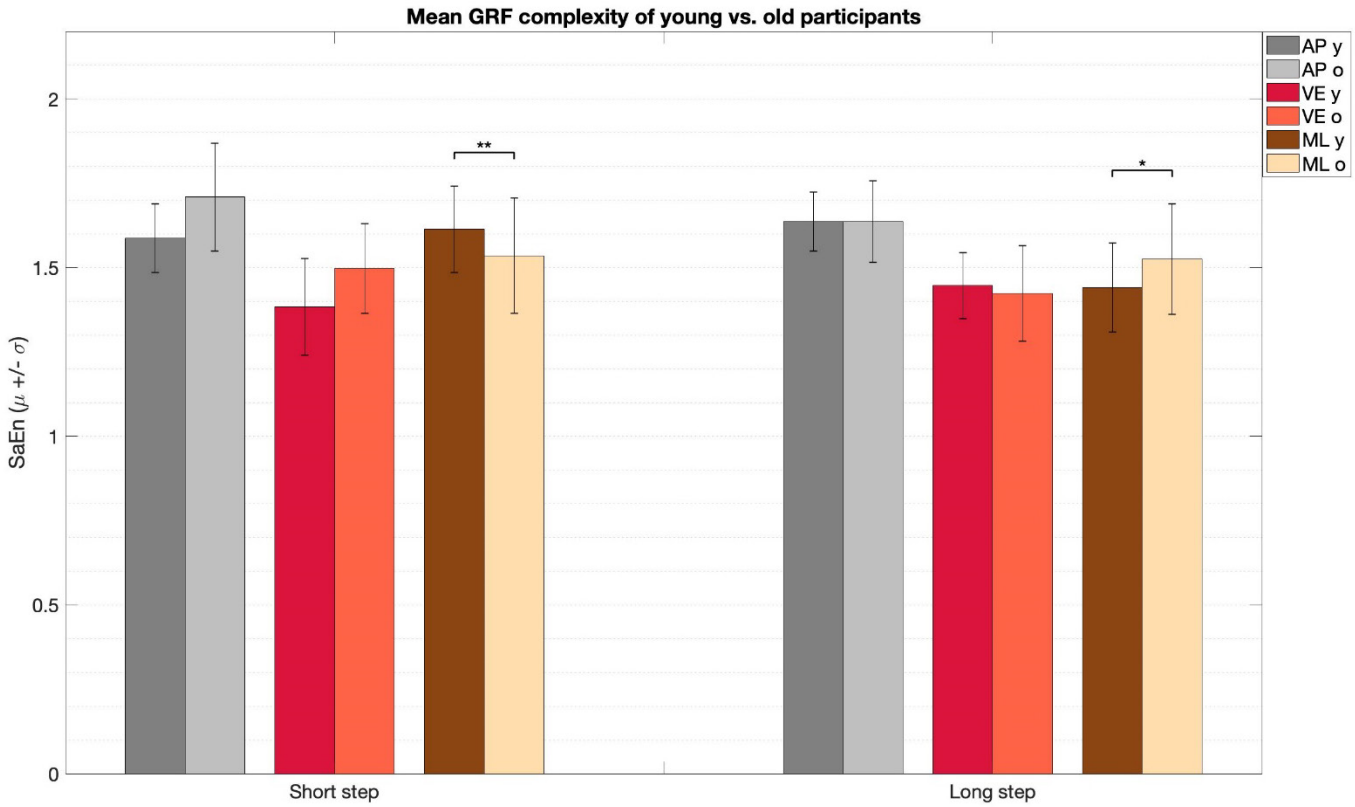

*E3.3.2) Interaction effect 'velocity*age'*

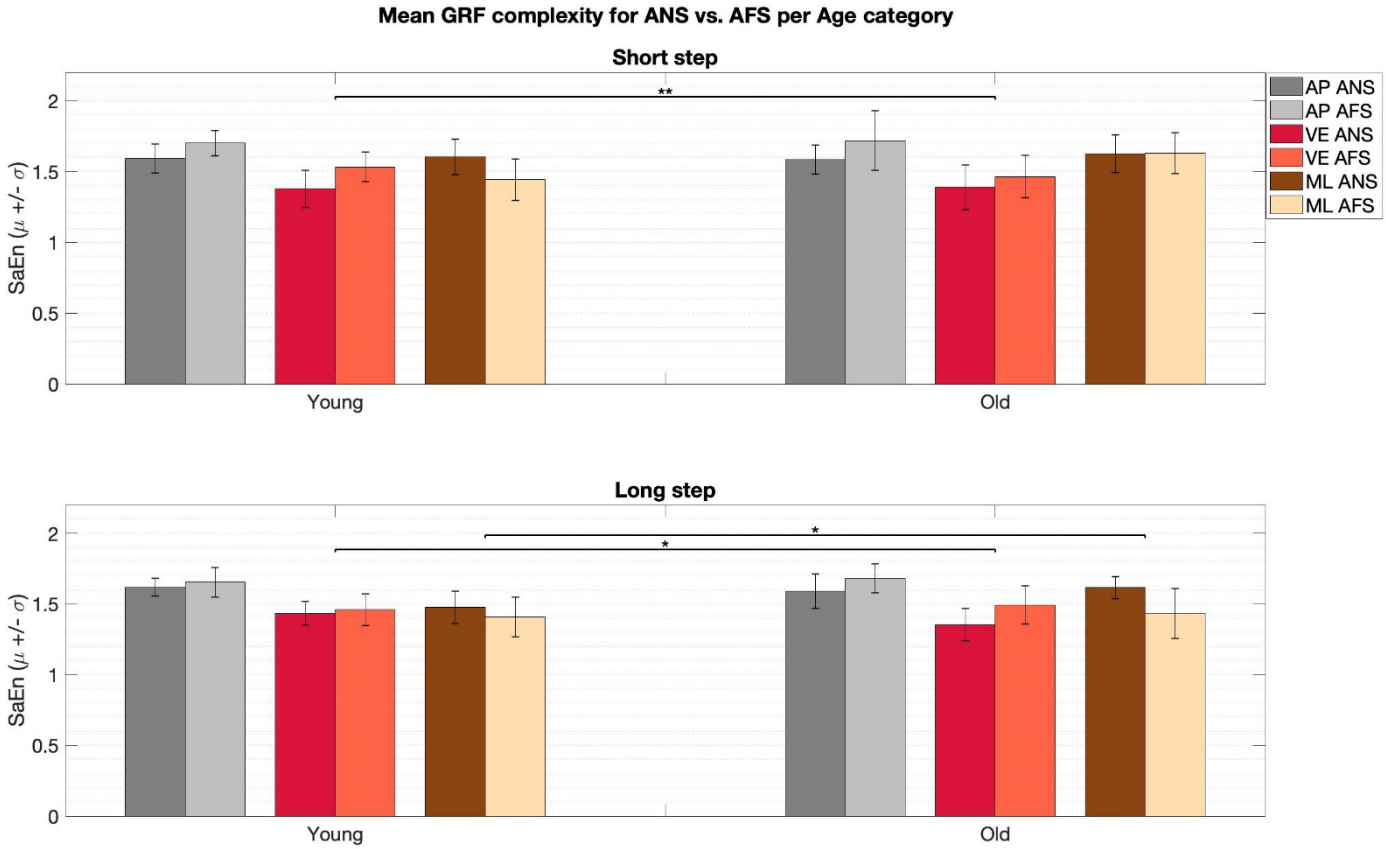

* **E3.4) GA complexity for short steps and for long steps (*trial ANS, AFS*)**
Scale 14 (N_{young} = 18, N_{old} = 18)

E3.4.1) Main effect 'velocity'

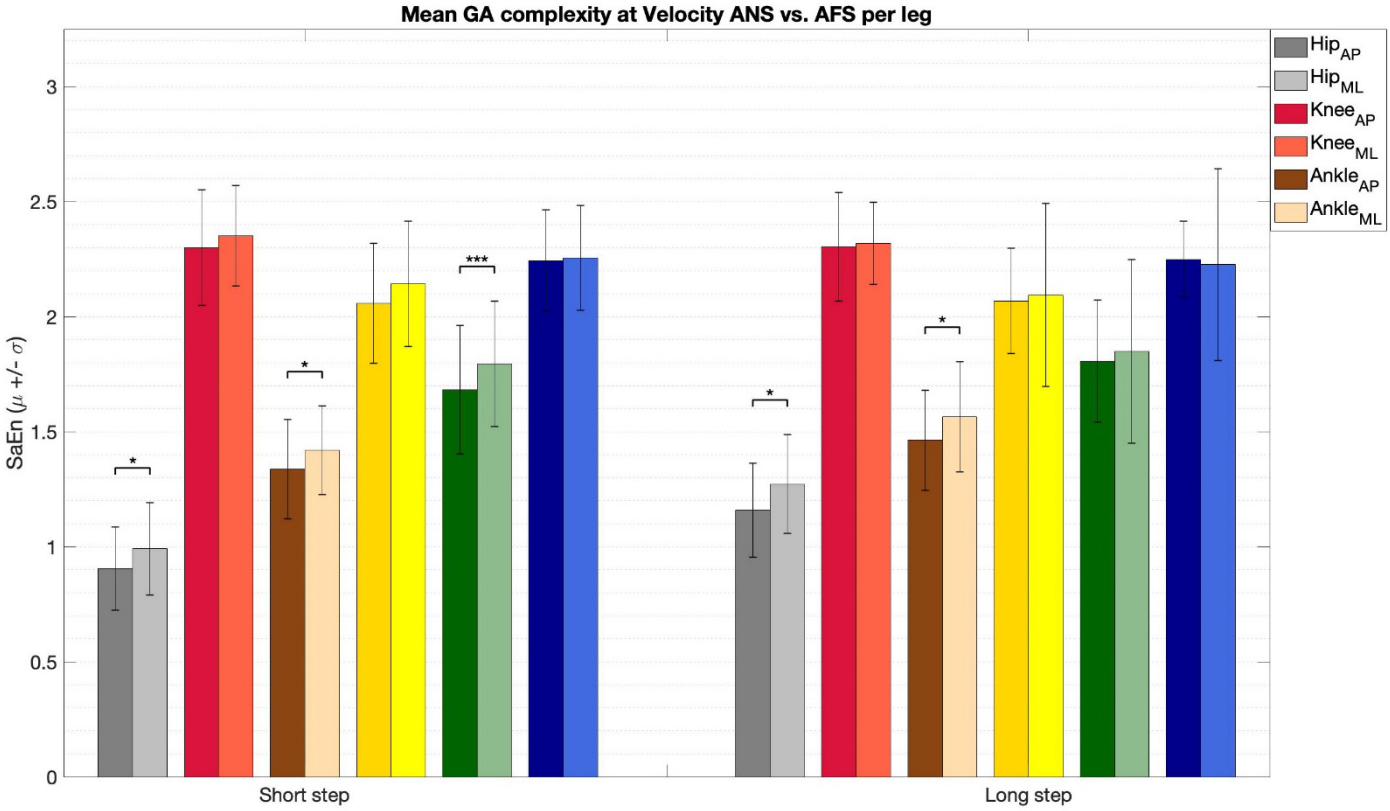

E3.4.2) Main effect 'age'

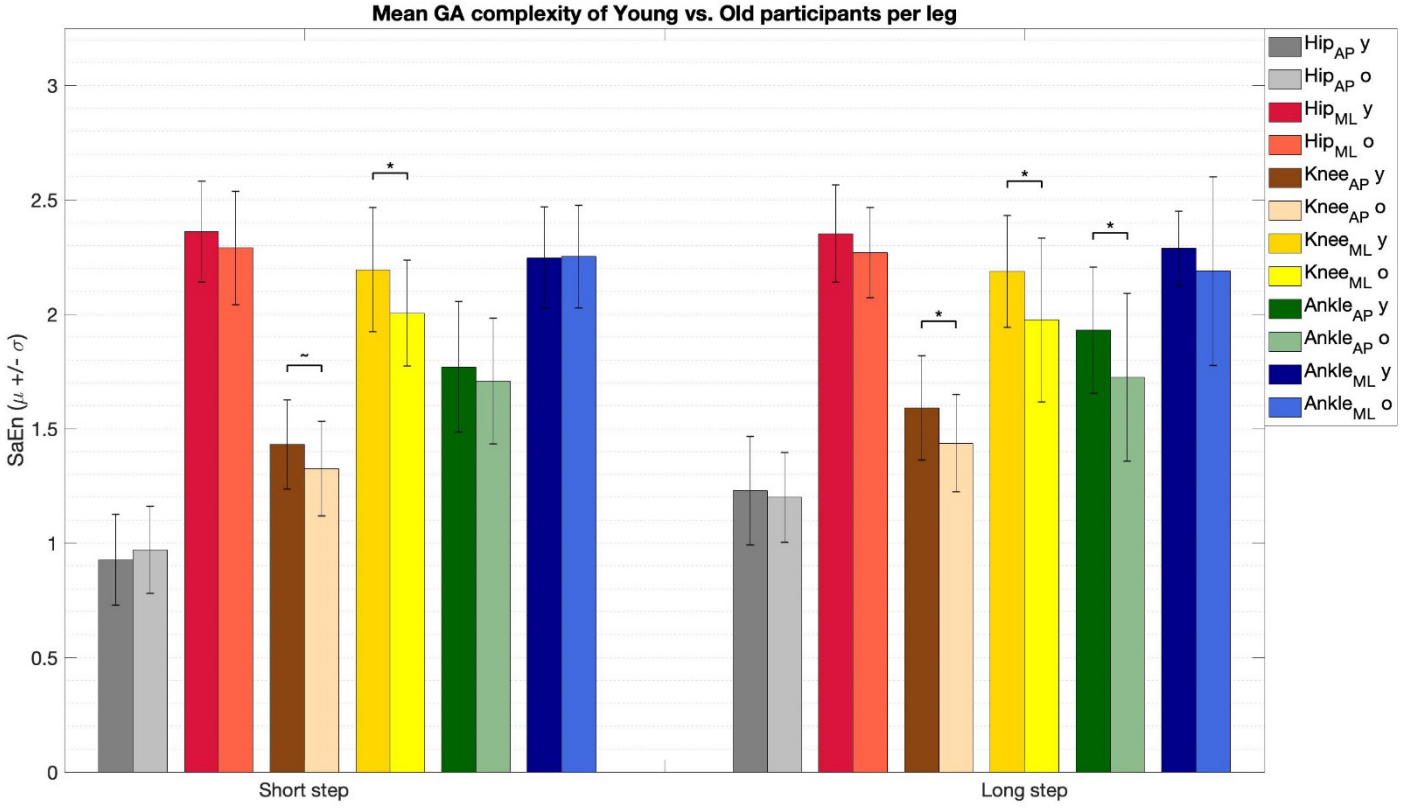

*E3.4.3) Interaction effect 'velocity*age'*

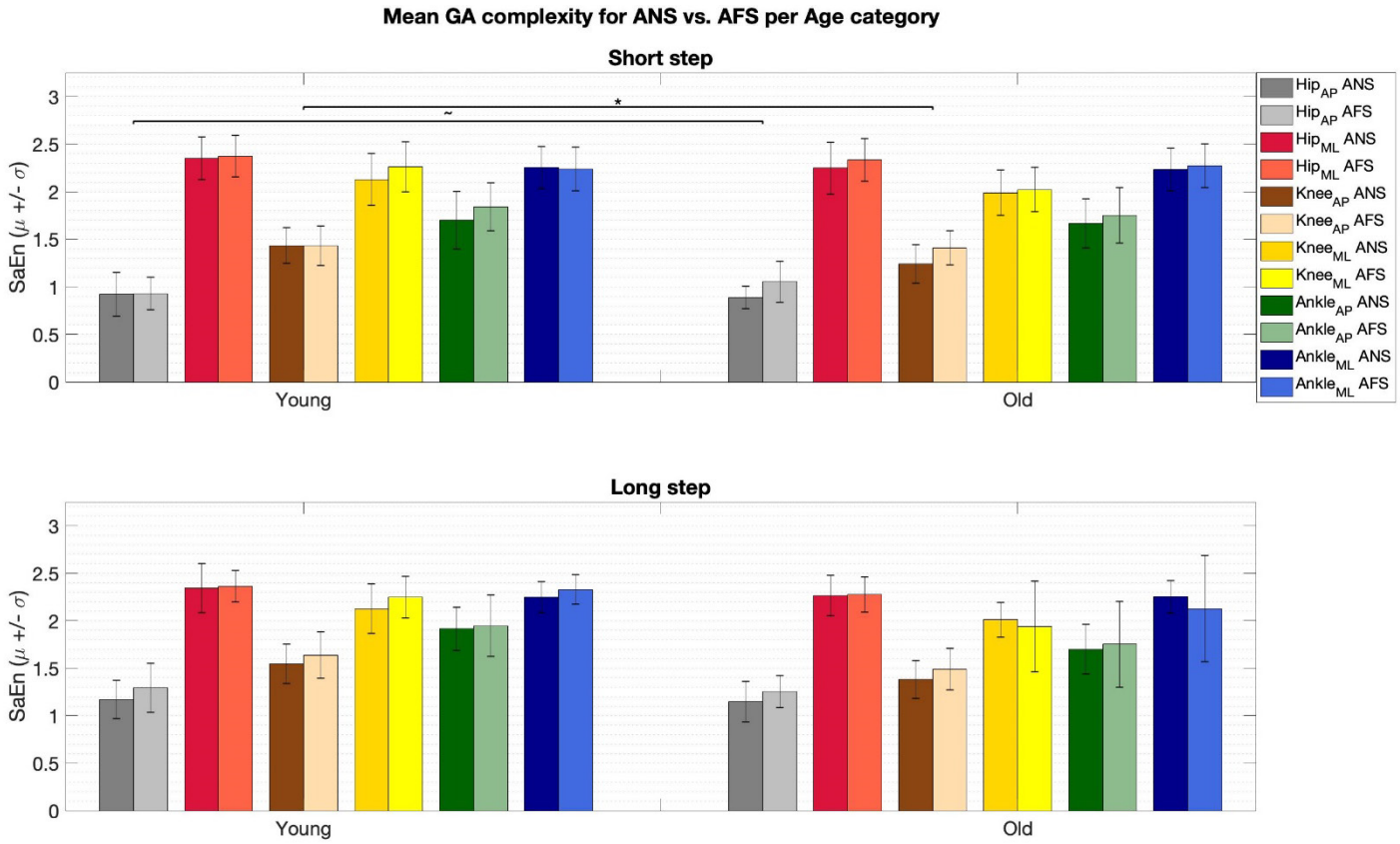

- ***End***